New Design of Polyphenylene Dendrimers

for Full-Color Light-Emitting Diodes

Dissertation

zur Erlangung des Grades

"Doktor der Naturwissenschaften"

dem Fachbereich Chemie und Pharmazie

der Johannes Gutenberg-Universität in Mainz

vorgelegt von

Tianshi Qin

geboren in Nanjing, P. R. China

Mainz, 2010

Table of contents

Index of Abbreviations

AFM	atomic force microscopy
Alq$_3$	8-hydroxyquinolinealuminum
ATRP	atom transfer radical polymerization
CAN	cerium ammonium nitrate
CBP	4-bis-(carbazol-9-yl)biphenyl
CIE	Commission Internationale de L'Eclairage
CV	cyclic voltammetry
DCM	dichloromethane
EL	electroluminescence
EQE	extern quantum yield
ETL	electron transporting layer
FD MS	field desorption mass spectroscopy
FRET	Förster resonance energy transfer
FWHM	full width of half maximum
GPC	Gel permeation chromatography
HBL	hole blocking layer
HOMO	highest occupied molecular orbital
Ir(btp)$_3$	*fac*-tris(2-benzo[b]thiophenylpyridyl) iridium(III)
Ir(piq)$_3$	*fac*-tris(1-phenylisoquinoline) iridium(III)
Ir(ppy)$_3$	fac-tris(2-phenylpyridinato) iridium(III)
ITO	indium tin oxide
I-V-L	current density and luminescence versus voltage
LC	ligand-centered
LEC	light-emitting electrochemical cell
LUMO	lowest unoccupied molecular orbital
MALDI-TOF	matrix-assisted laser desorption ionization – time of flight
MLCT	metal-to-ligand charge transfer

NTSC	National Television System Committee
OLED	organic light emitting diode
PDI	perylenetetracarboxydiimide
PEDOT	poly(3,4-ethylenedioxythiophene)
PF	polyfluorene
PhOLED	phosphorescent organic light emitting diode
PL	photoluminescence
PLQY	photoluminescence quantum yield
PMI	perylenemonoimide
PPV	poly(para-phenylene vinylene)
PSS	poly(styrenesulfonate)
RGB	red, green, and blue
SMS	single molecule spectroscopy
TBAF	tetrabutylammonium fluoride
TCCz	N-(4-[9,3';6',9'']tercarbazol-9'-yl)phenylcarbazole
TCTA	4,4',4''-tri(carbozol-9-yl)-triphenylamine
TDI	terrylenetetracarboxydiimide
TGA	thermogravimetric analysis
THF	tetrahydrofuran
TiPS	triisopropylsilyl
TMS	trimethysilyl
TPBI	1,3,5-tris(2-N-phenylbenzimidazolyl)-benzene
WAXS	wide-angle X-ray scattering

Chapter 1

Introduction:

A mini-review of functionalized polyphenylene dendrimers

Dendrimer research was initially created in the mid 1980s and has exploded during past two decades.[1] After pioneering works concerning synthesis, the interest in dendrimers is now mainly driven by their properties and applications. For example, dendrimers have been studied for use as host-guest sensitive and selective sensors,[2] as catalysts,[3] as templates for the growth of encapsulated metal nanoparticles,[4] and in biological applications,[5] including biomarkers,[6] magnetic resonance imaging,[7] and drug delivery.[8] However, it has only been more recently that such macromolecular structures have been explored in terms of their optoelectronic properties,[9] which is the focus of this thesis. In the following pages, the design, synthesis, and functionalization of a series of full-color light-emitting dendrimers and their photophysical properties as well as device performances will be shortly overviewed.

1.1 Dendrimer chemistry - a short overview

Traditional polymers, according to Staudinger, can be classically divided into three major macromolecular architectures: linear, cross-linked and branched polymers. Recently, a fourth class of polymer topologies has been dedicated to dendrimers.[10]

The term "dendrimer" was first offered by Tomalia in 1984.[11] The word "dendrimer" derives from the Greek (dendron = tree, meros = part). As the name implies, these "tree-shaped" macromolecules consist of three parts: a core, scaffolds, and surfaces (Figure 1-1). The latter two parts are sometimes called dendrons, which extensively branch in three dimensional architecture, and generally possess excellent solubility as well as a high degree of surface functionality and versatility. The natures of the peripheral functional groups are the important factors that determine the chemical and

1

physical properties of these dendritic molecules. Unlike traditional polymers, dendrimers are monodisperse macromolecules, and their molecular sizes and masses can be specifically controlled during the step-wise generation growth.[12]
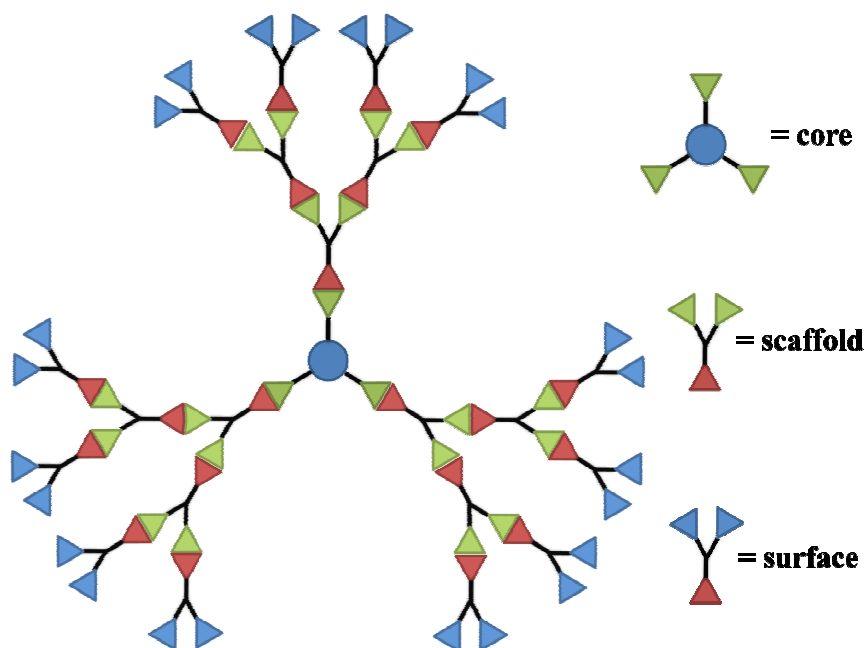
Figure 1-1: Schematic structure of a dendrimer.

Since Vögtle et al. synthesized the first basic dendrimer structure in 1978,[13] dendrimers can be generally achieved by using either a divergent method or a convergent method (Scheme 1-1). There is a fundamental difference between these two construction concepts.

1.1.1 Divergent synthesis

In the divergent methods, the dendrimer grows outwards from a multifunctional core molecule. The core molecule reacts with monomer molecules containing one reactive and two dormant groups giving the first generation dendrimer. Then the new periphery of the molecule is activated for reactions with more monomers. The process is repeated for several generations and a dendrimer is built layer after layer. The divergent approach is successful for the production of large quantities of dendrimers. Problems

occur from side reactions and incomplete reactions of the end groups that lead to structural defects. To prevent side reactions and to force reactions to completion a large excess of reagents is required. It causes some difficulties in the purification of the final product.
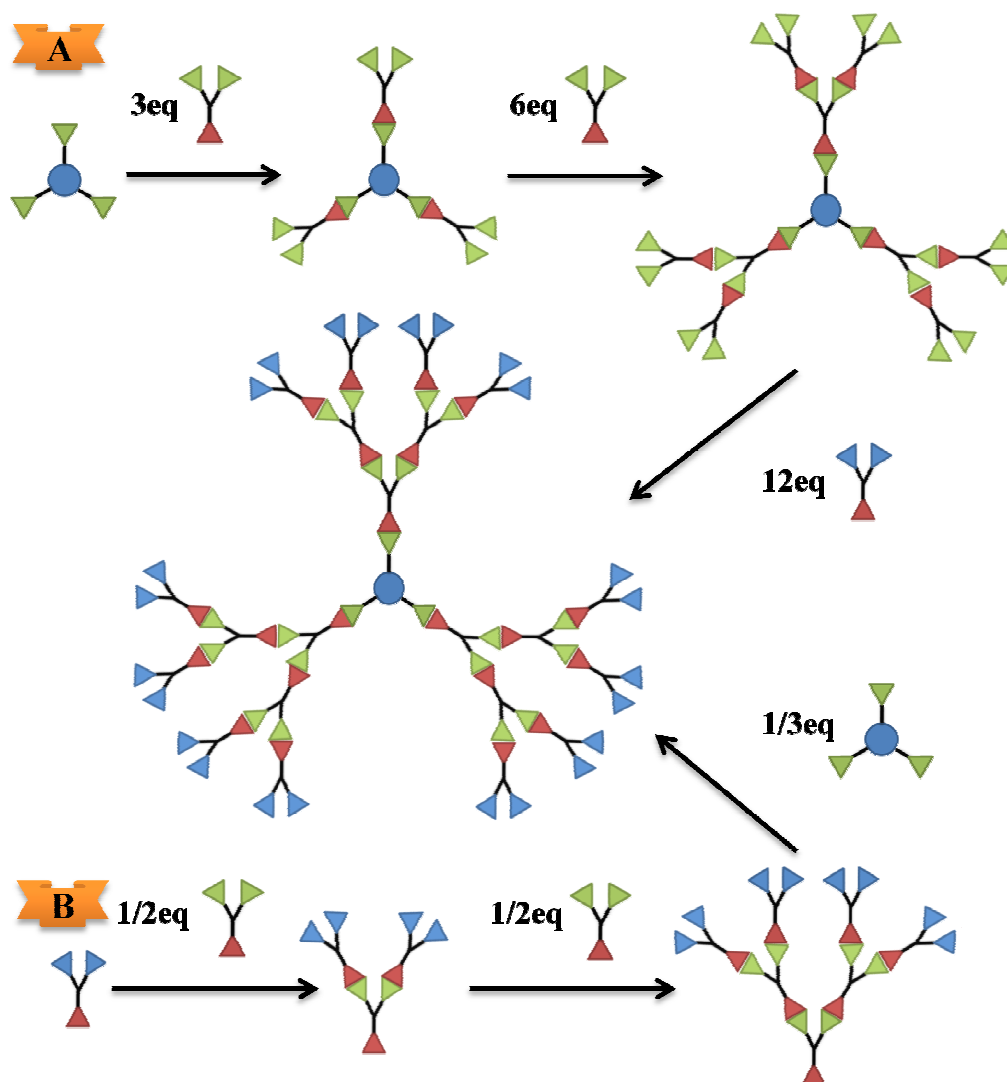
Scheme 1-1: Synthesis of dendritic macromolecules: A) divergent method; the synthesis starts at the polyfunctional core and follows a step by step growth. B) convergent method; construction of dendrons and final reaction with the core molecule.

1.1.2 Convergent synthesis

The convergent methods were developed as a response to the weaknesses of the divergent synthesis. In the convergent approach, the dendrimer is constructed stepwise, starting from the end groups and progressing inwards. When the growing branched polymeric arms, called dendrons, are large enough, they are attached to a multifunctional core molecule. The convergent growth method has several advantages. It is relatively easy to purify the desired product and the occurrence of defects in the final structure is minimized. It becomes possible to introduce subtle engineering into the dendritic structure by precise placement of functional groups at the periphery of the macromolecule. The convergent approach does not allow the formation of high generations because steric problems occur in the reactions of the dendrons and the core molecule.

Both assembly approaches have been adopted by researchers. The divergent dendrimer synthesis have been reported by Vögtle, Denkewalter, Meijer, Mülhaupt, Tomalia, and Newkome, and the convergent approach to dendrimer synthesis can be found in the work of Fréchet, Miller, and Moore.

1.2 Polyphenylene dendrimers

Different from the flexible dendrimers based on mobile alkyl chains, the shape-persistent dendrimers demonstrated a more stable structure and their own properties.[14] Hart et al. introduced nanometer sized dendrimers in which benzene units were bound to each other via two σ bonds (**1-1**, Scheme 1-2).[15] These dendrimers, based on extended iptycenes, turned out to be extremely stiff and shape persistent as they did not allow any rotational movement, but showed difficulties to introduce further functionalities at desired positions by demand. Branched bicyclopropylidenes such as **1-2** were published by de Meijere et al., not yet allowing further extension of generations of this rigid and shape-persistent dendrimer.[16] Moore et al. connected the

branching points with inherently stiff chains, affording dendrimers constructed from phenylacetylene units (**1-3**);[17] Miller et al. introduced dendrimers consisting of 1,3,5-substituted benzenes (**1-4**).[18] Both these kinds of dendrimers **1-3** and **1-4** were synthesized by the convergent method, because the metal catalyzed coupling reactions led to side products and incomplete reactions rendering a divergent synthesis not practicable. Therefore a new strategy based on non catalytic Diels-Alder cycloaddition reaction was developed, allowing the divergent growth and synthesis of high generation polyphenylene dendrimers in quantitatively yields (**1-5**).[19]
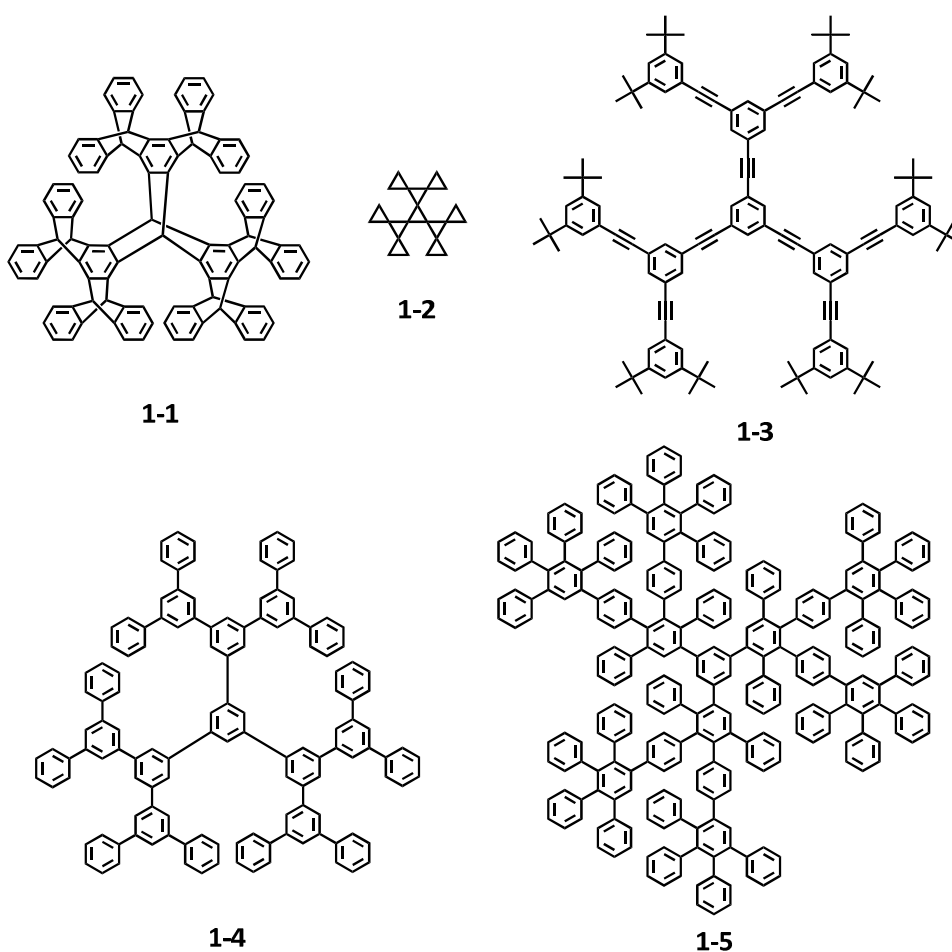
Scheme 1-2: Shape persistent polyphenylene dendrimers: **1-1** iptycene dendrimer by Hart et al., **1-2** triangulene dendrimer by de Meijere et al., **1-3** poly(phenylenevinylene)dendrimers by Moore et al., **1-4** polyphenylene dendrimers by Miller et al., and **1-5** polyphenylene dendrimers by Müllen et al.

Furthermore, it is immediately clear from the structures in Scheme 2-1, that many more phenylene units can be incorporated in **1-5** compared to **1-3** and **1-4**. Additionally it turned out that dendrimers **1-3** and **1-4** based on 1,3,5-substitituted benzene rings, led to conformational isomers.

1.3 Synthesis of polyphenylene dendrimers

In our group, the synthesis of polyphenylene dendrimers, firstly reported in 1997,[20] was based on two reactions with nearly no side products and quantitative yields: i) a "growth" step – the Diels-Alder cycloaddition of tetraphenylcyclopentadienones to ethynes, and ii) a "deprotection" step – the desilylation of triisopropylsilyl substituted alkynes. In order to use the [4+2] Diels-Alder cycloaddition for dendrimer synthesis, we introduced the AB$_2$ building unit 2,5-diphenyl-3,4-bis[4-(tri-isopropylsilylethynyl)-phenyl]cyclopentadienone (**1-6**, Scheme 1-3) which was synthesized via the double Knoevenagel condensation of 1,3-diphenylacetone (**1-7**) and 4,4'-bis(tri-isopropylsilylethynyl)benzil (**1-8**) on a large scale with yields up to 85%.
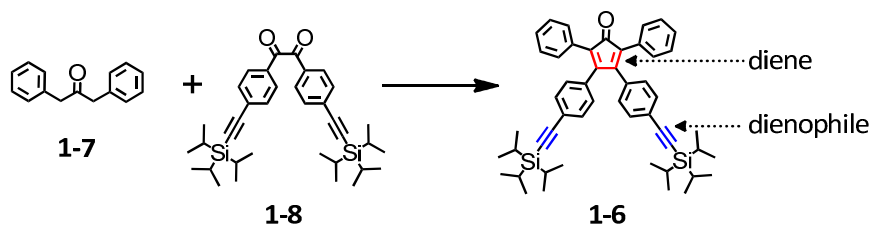
Scheme 1-3: The synthesis of AB$_2$ building unit **1-6**.

This building unit **1-5** consists of a diene subunit for the Diels-Alder cycloaddition and two protected ethynes as the dienophile. The bulky triisopropylsilyl (TiPS) substituents serve to protect the building unit from self-cycloaddition. After isolation of the TiPS-ethynyl substituted dendrimer, the protecting groups (TiPS) can easily be removed by fluoride salt, such as tetrabutylammonium fluoride (TABF), to give the "free" ethynyl

substituted dendrimer, which allow continuing the Diels-Alder cycloaddition again to achieve high generations.
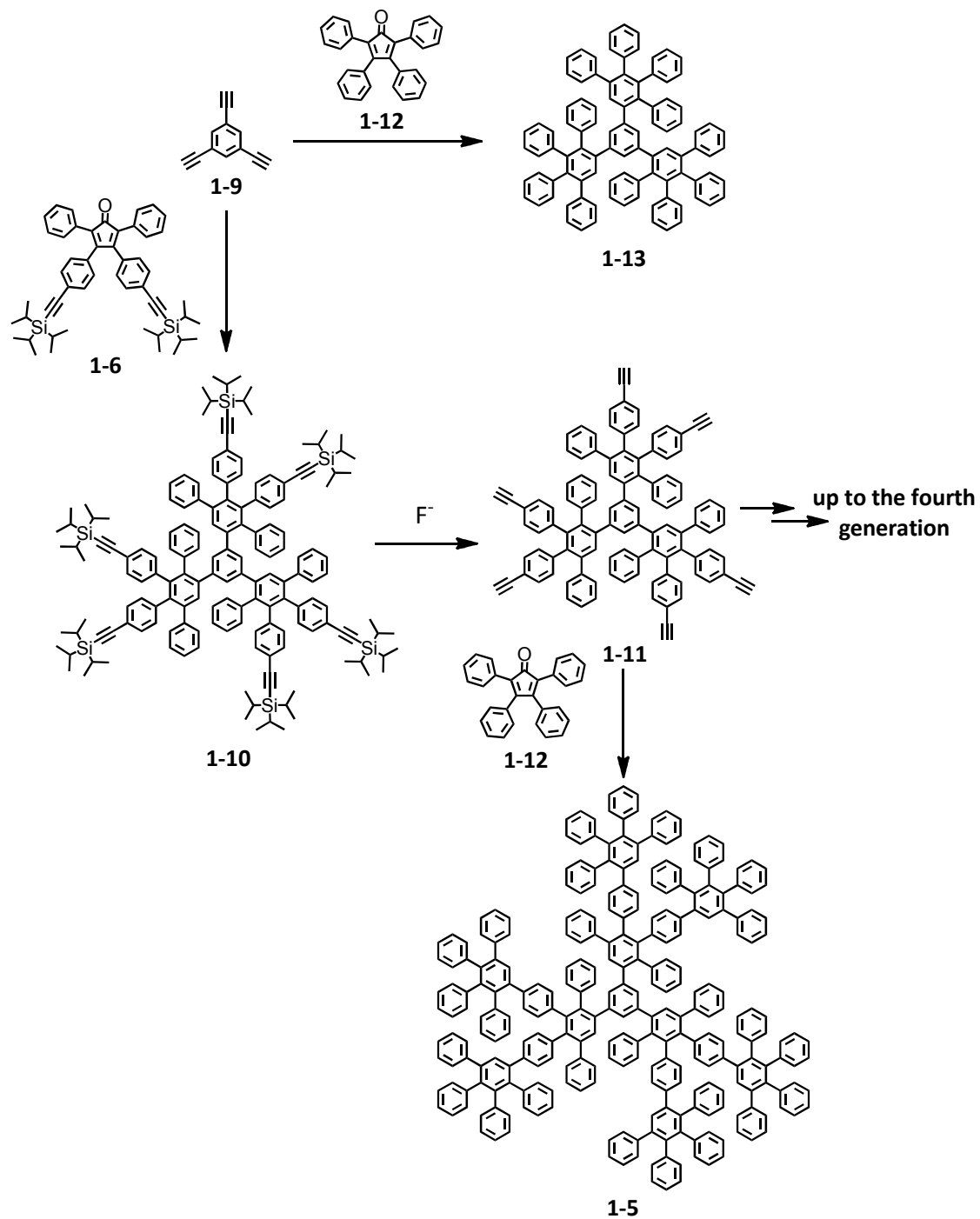
Scheme 1-4: Divergent synthesis of the polyphenylene dendrimers starting from the 1,3,5-triethynylbenzene core

The synthesis of polyphenylene dendrimers via the divergent method starts with a "growth" step (Scheme 1-4), the [4+2] Diels-Alder cycloaddition of the building units to a core with multi-ethynyl substituents, e.g., 1,3,5-triethynylbenzene (**1-9**), in refluxing o-xylene, affording the first generation dendrimer with TiPS-substituted ethynes (**1-10**). After a "deprotection" step with TBAF, the corresponding "free" ethynyl substituted first generation dendrimer (**1-11**) is obtained, which allows the growth to the next generation. When unsubstituted tetraphenylcyclopentadienone **1-12** is used as the termination agent for **1-9** and **1-11**, the unfunctionalized first and second generation dendrimers **1-13** and **1-5** are obtained, respectively. By repeating the cycloaddition and the deprotection, we can synthesize the monodisperse polyphenylene dendrimers up to the fourth generation, in which the steric density is sufficiently high to prohibit further generation growth.

In 1999, our group developed a convergent method for the synthesis of polyphenylene dendrimers based on a pentaphenylbenzene repeating unit.[21] The synthesis of the required repeating unit takes part in two steps: i) the Diels-Alder cycloaddition of tetraphenylcyclopentadienone with benzil-substituted ethynyl to give the dendronized benzil, and ii) the double Knoevenagel condensation of the dendronized benzil with 1,3-diphenylacetone to cyclopentadienone, as the building units. The starting point of the convergent synthesis is the 4,4'-diethynylbenzil (**1-14**, Scheme 1-5), which contains two ethynylic dienophile units and one ethanedione function which can react in a Knoevenagel condensation. The two-fold Diels-Alder cycloaddition of an excess of tetraphenylcyclopentadienone (**1-9**), which is regarded as the first generation dendron, with **1-14** leads to the dendronized benzil **1-15** and the Knoevenagel condensation of the benzil with 1,3-diphenylacetone (**1-6**) to give the second generation dendron **1-16**. The synthesis of a third generation dendron has not been realized up to now, since the dendronized benzil with larger tails exists exclusively in the trans conformation, making the double Knoevenagel condensation impossible. In the final step, the Diels-Alder

cycloaddition of an excess of the second generation dendron **1-16** with a multi-ethynyl substituted core can provide the second generation polyphenylene dendrimer **1-13**.
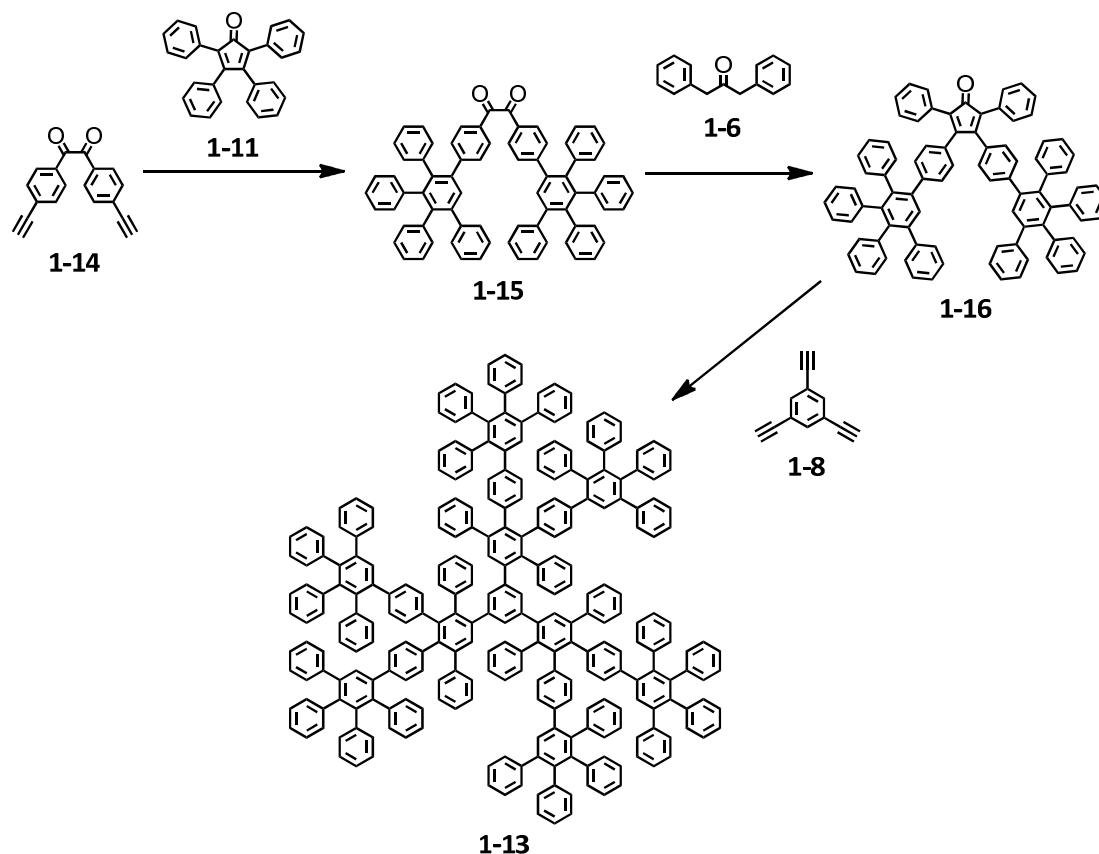
Scheme 1-5: Convergent synthesis of the second generation polyphenylene dendrimer (**1-13**) based on dendronized buliding units (**1-16**).

Compared to the divergent approach, the convergent method at first glance affords the same monodisperse products with similarly high yield. The convergent approach provides a fast access to second generation dendrimers but cannot be used to synthesize higher generation dendrimers. However, this method opens a pathway to import multi-type functionalized dendrons on an asymmetric core. In contrast, the divergent approach can be used up to the higher generations, but it only allows the ordered attachment of one type of functional group.

1.4 Functionalization of polyphenylene dendrimers

In contrast to flexible dendrimers, the polyphenylene dendrimers exist as shape persistent nanoparticles as we have demonstrated above. The preparation of functionalized dendrimers is the key step towards various applications. As can be seen from Figure 1-1, the functional groups can be introduced into the polyphenylene dendrimer at three places – the core, scaffolds, and surfaces.[22] We will consider the functionalization in each part respectively in the following chapters.

1.4.1 Functionalization in the Core

The variation of the dendrimer core can strongly influence the dendrimer architecture of whole dendrimers. We have previously reported that a wide variety of hydrocarbon cores (Scheme 1-6), e.g. triethynylbenzene (**1-8**), 3,3',5,5'-tetraethynylbiphenyl (**1-17**), tetrakis(4-ethynylphenyl)methane (**1-18**) and hexakis(4-ethynylphenyl)benzene, can be used to synthesize differently shaped dendrimers.[19]

According to the simulations of Bredas et al. the dendrimer with core **1-8** adopts a false-propeller structure without rotational symmetry,[23] whereas the dendrimer with core **1-19** shows a true-propeller shape. They are different in the orientation of the branches around the center of the molecule. The biphenyl core **1-17** leads to a growth that results in a kind of dumbbell shape of dendrimers; while the tetrahedral core **1-18** induces a globular shape. Recently, in our group, Haberecht et al. firstly introduced a central positively charged transition-metal complex, tris(2,2'-bipyridyl)ruthenium(II) (**1-20**), as the core of polyphenylene dendrimers based on an octahedral symmetry.[24] Therefore, the geometry of core, a simple core functionalization, can influence the overall shape of the resulting dendrimers.

1-8   **1-17**   **1-18**   **1-19**   **1-20**
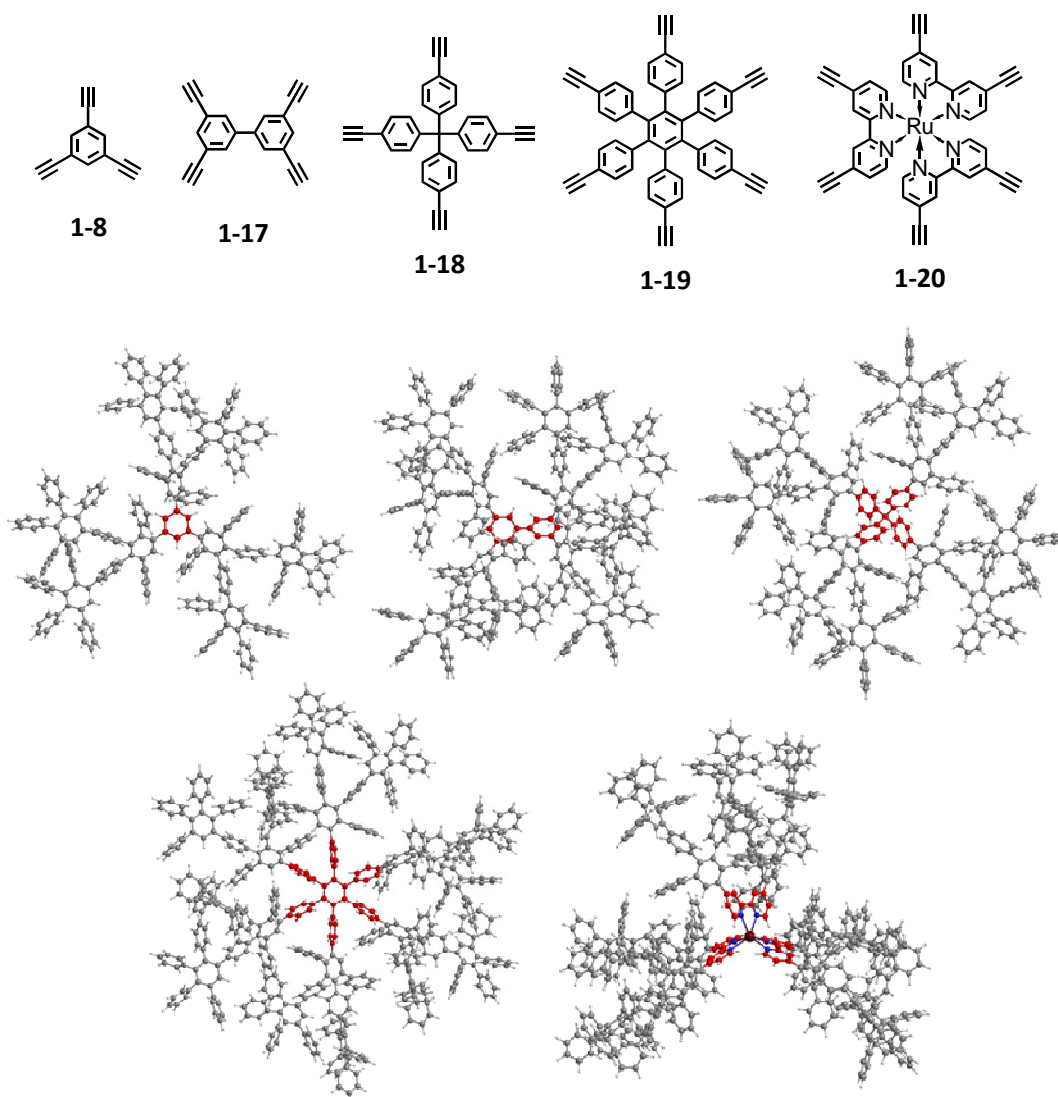
Scheme 1-6: Different ethynyl carrying cores and the 3D structures of the corresponding second generation dendrimers based on this core.

As well as controlling the symmetry of dendrimers it is also possible to incorporate a chromophore in the center of a shape persistent dendrimer. Such a spatial isolation of a photostable chromophore in a discrete and inert nanoenvironment is highly interesting for a variety of applications such as for organic light emitting diodes (OLEDs)[25] or single molecule spectroscopy (SMS).[26] The outstanding chemical and photophysical properties of rylene chromophores make them attractive for these purposes. Therefore, the pyrene[27] (**1-21**, Scheme 1-7) and perylenetetracarboxydiimide (PDI)[28] (**1-22**, **1-23**)

functionalized with four ethynyl groups can be used as cores for polyphenylene dendrimers.

In general, pyrene and perylene dyes show a strong aggregation tendency,[29] which induces a luminescence quenching and a bathochromic shift in solid state. However, by means of the covalent encapsulation of such a chromophore in a polyphenylene dendritic shell this aggregation can be avoided. Furthermore, the polyphenylene dendrons also serve as solubilizing groups shielding the chromophore from atmospheric degradation.[27] They further show good solution processing abilities and hindered migration in polymer films. These properties implicate dendritic macromolecules as highly interesting candidates for luminescent layers in OLEDs.[25] In addition, a chromophore surrounded by a perfectly defined environment might be regarded as a potential candidate for SMS, allowing study of the interactions of a fluorophore with the surrounding matrix by high spatial resolution, which is currently under investigation.

1-21

1-22

1-23
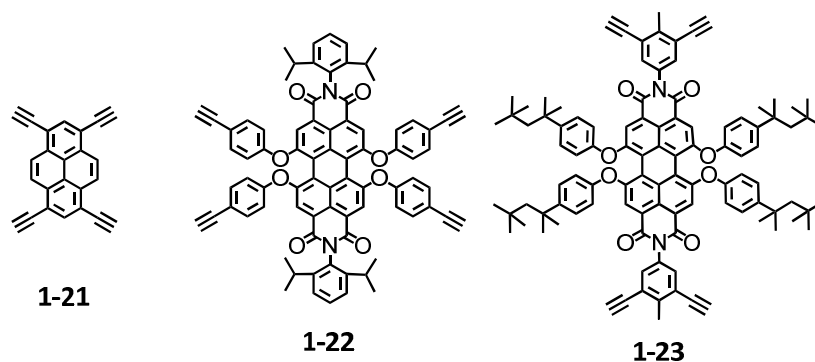
Scheme 1-7: Functional cores for extension of dendrimers.

Moreover, the repeating units of conjugated polymers, such as 2,7-dibromo-9,9-bis(4-ethynylphenyl)fluorene (**1-24**, Scheme 1-8), can also be dendronized with polyphenylene side chains before their polymerization.[30] The shape-persistent polyphenylene dendronized side chains can not only improve the polymer solubility, but also prevent the coiling and aggregation of conjugated polymer chains, thus improve

their photophysical properties, such as a change in the dynamics of singlet excitions in the solid state, an increase in triplet lifetime and a reduction in diffusion of triplet excitions.
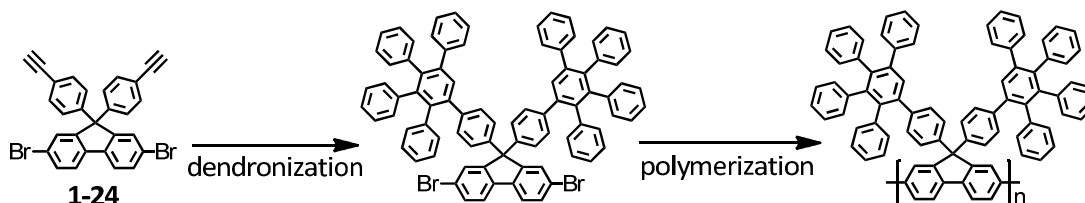
Scheme 1-8: Polyfluorene with dendronized polyphenylene side chain.

1.4.2 Functionalization on the scaffold

In comparison with the uniqueness of the core variation, which is restricted to one functional group, the functionalization on the numerous dendritic scaffolds can import multiple functionalities. In order to functionalize these scaffolds, the synthesis of stably functionalized cyclopentadienones (**1-25**, Scheme 1-9), which carry both desired functions (F_1 and F_2) at α-position and/or β-position and dendrimer growing groups (TiPS-ethynyl), is the key component.[22]   Such cyclopentadienones are prepared by Knoevenagel double condensation of functionalized benzyls (**1-26**) with 1,3-disubstituted acetones (**1-27**). Unfortunately this often comes together with a high synthetic effort as for every desired function the according cyclopentadienone has to be synthesized.
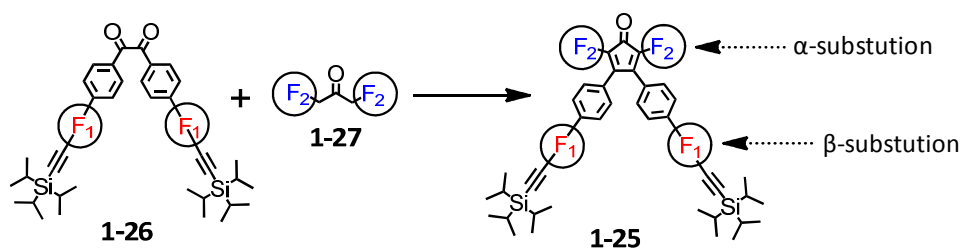
Scheme 1-9: Functionalized CP units **1-25** with functions in α-position (F_1) and β-position (F_2).

As the bis-dioxaborolane substituted cyclopentadienone (**1-28**, Scheme 1-10) can be synthesized from commercially available precursors in high yield, it is often used as the starting point for the synthesis of β-position functionalized building units, e.g. the terphenyl extended tetraphenylcyclopentadienone (**1-29**),[31] the 1,3-dithiolanes substituted cyclopentadienone (**1-30**)[32] and the PDI containing cyclopentadienone (**1-31**).[33] By covalent linkage of these functionalities it is possible to obtain materials with various novel properties that are different from those of the parent compounds.
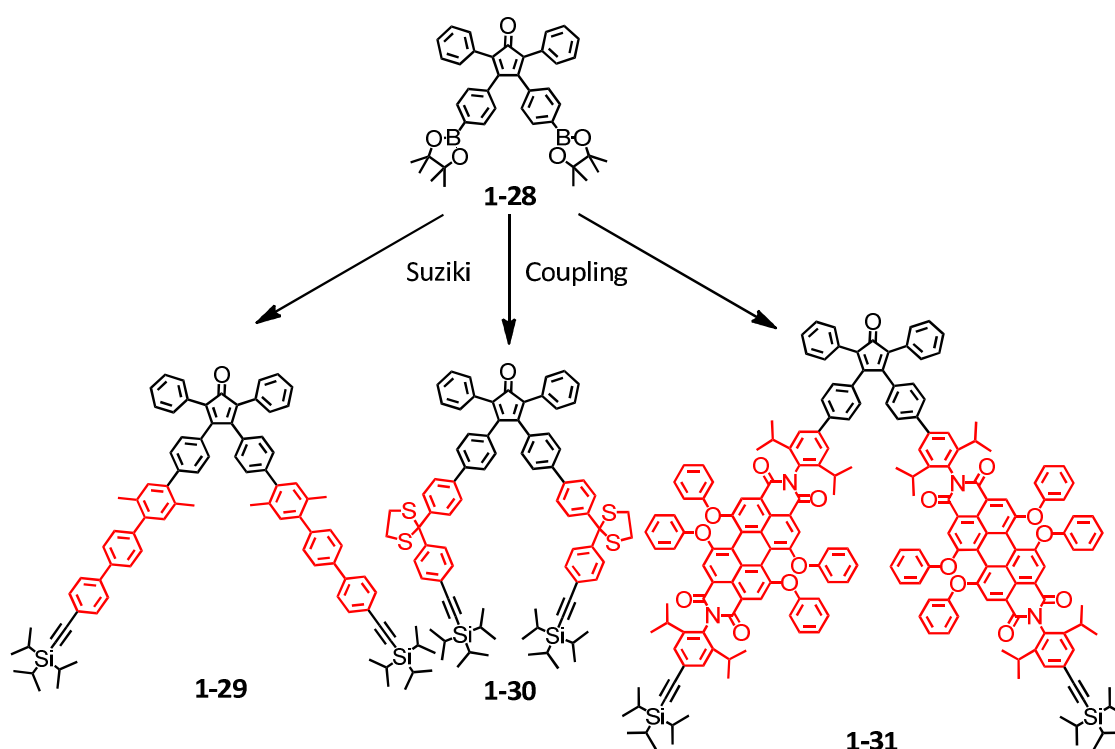
Scheme 1-10: Further substituted CP units with extra functions in β-positions for scaffold functionalization.

To the best of our knowledge, the synthesis of polyphenylene dendrimers around a tetraphenylmethane core has thus far been limited to the fourth generation because of incomplete conversion at higher generations, presumably the prohibitive result of steric crowding at the chain ends. In light of this observation, by using terphenyl extended tetraphenylcyclopentadienone (**1-29**), a spacer was introduced into each arm of the

branching unit to decrease the congestion of the chain ends at higher generations (Figure 1-2).[31] Since the connectivity of the branching points in the dendrimers with extended arms is the same as for the parent polyphenylene dendrimers, their molecular sizes should be much larger than the comparable sizes of the parent cases. This situation would enable the stepwise synthesis of a structurally perfect dendrimer up to sixth generation with a diameter of 27 nm, which well exceeds the dimension of the narrowly disperse but not monodisperse particles that have been synthesized by self-assembly or multiphase approaches.
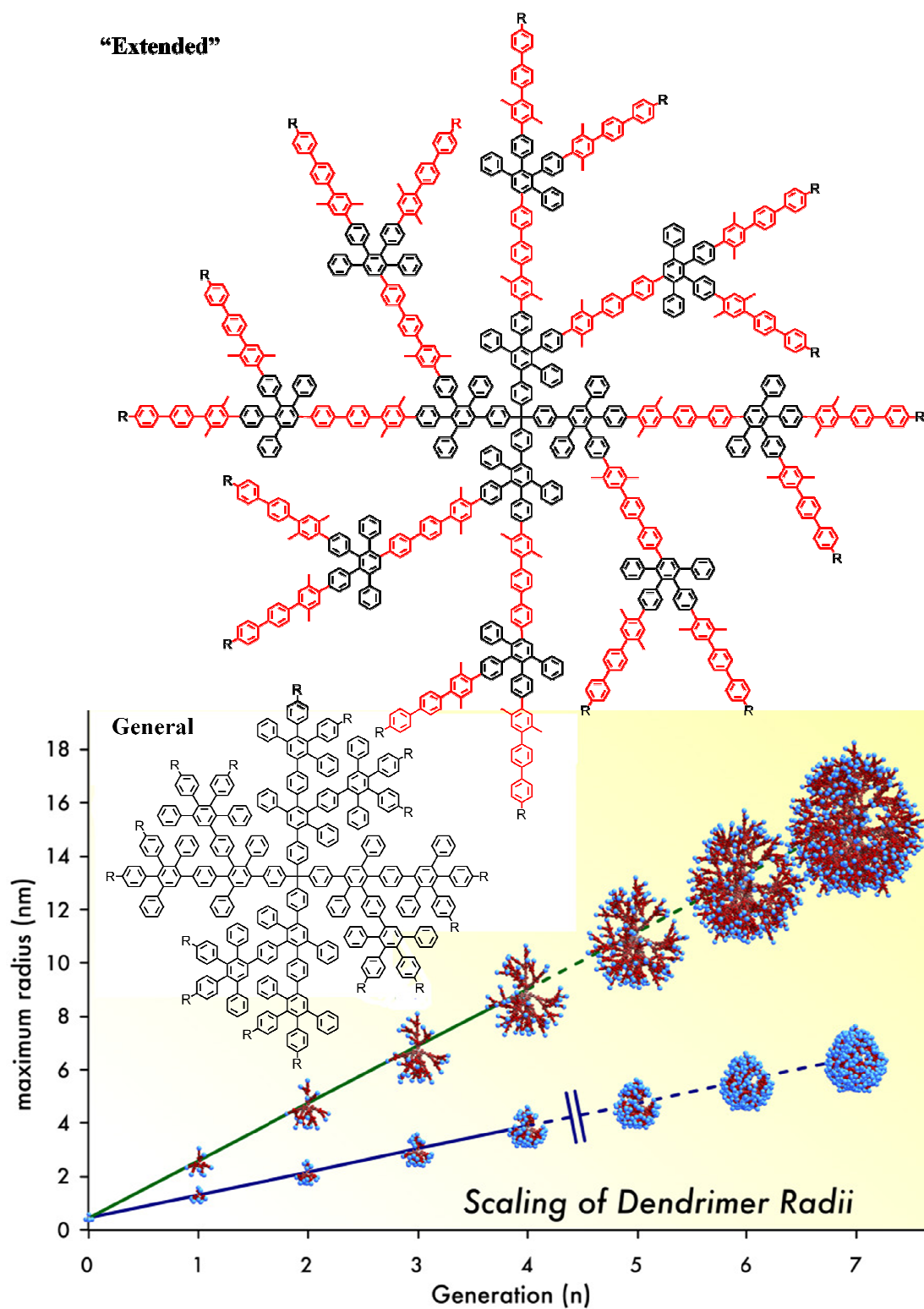
Figure 1-2: Comparison between extended polyphenylene dendrimers with terphenyl-spacer and traditional polyphenylene dendrimers.

The 1,3-dithiolanes substituted tetraphenylcyclopentadienone (**1-30**) is used to synthesize polyphenylene dendrimers, bearing a defined number of keto groups in their scaffolds (**1-32**, Scheme 1-11).[32] These dendrimers turn out to be suitable substrates for a perfect postsynthetic functionalization of the inner dendrimer using organolithium reagents. Even large reaction partners such as pyrene can be introduced quantitatively (**1-33**), allowing the easy and versatile modification of the dendritic scaffold. This postsynthetic procedure provides a pathway of introducing functionalities, which are not stable under the conditions of the Diels-Alder cycloaddition, into the periphery of dendrimers.
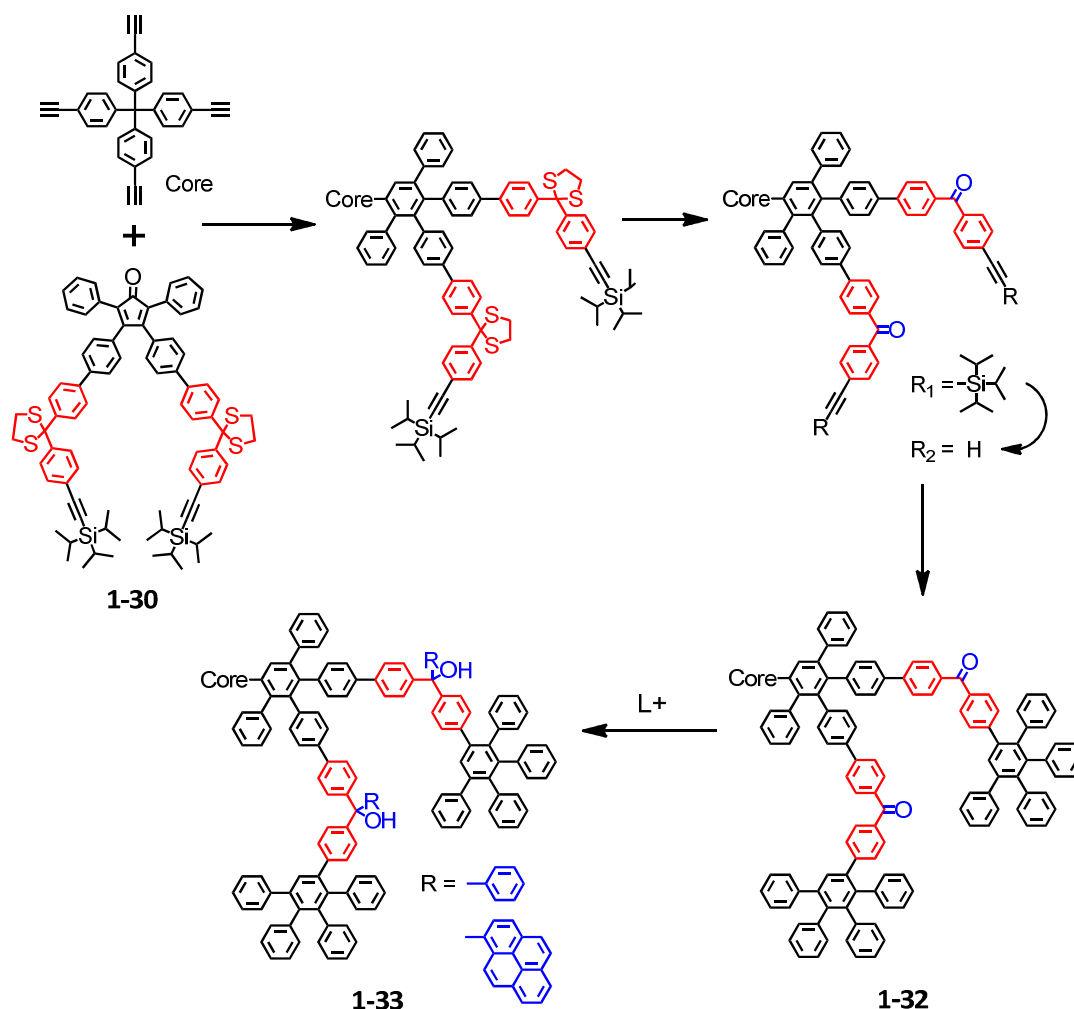
Scheme 1-11: The synthesis of second-generation polyphenylene dendrimer **1-32** carrying eight benzophenones in its scaffold and its postsynthetic hydroxyl functionalization via Li reagents.

Single-molecule spectroscopy of well-chosen dendritic multichromophoric systems allows investigation of fundamental photophysical processes such as energy or electron transfer in much greater detail than the respective ensemble measurements. Therefore, the PDI containing tetraphenylcyclopentadienone (**1-31**) are chosen to build up these dendritic multichromophoric systems (**1-34**, Scheme 1-12),[33] since the PDI derivative dyes possess large molar extinction coefficients in the visible region of the spectrum, a high quantum yield of fluorescence and excellent photostability . In these systems, the PDI dyes are all located in scaffolds, and their relative positions and orientations are fixed in space and determined by the synthetic route.

1-34
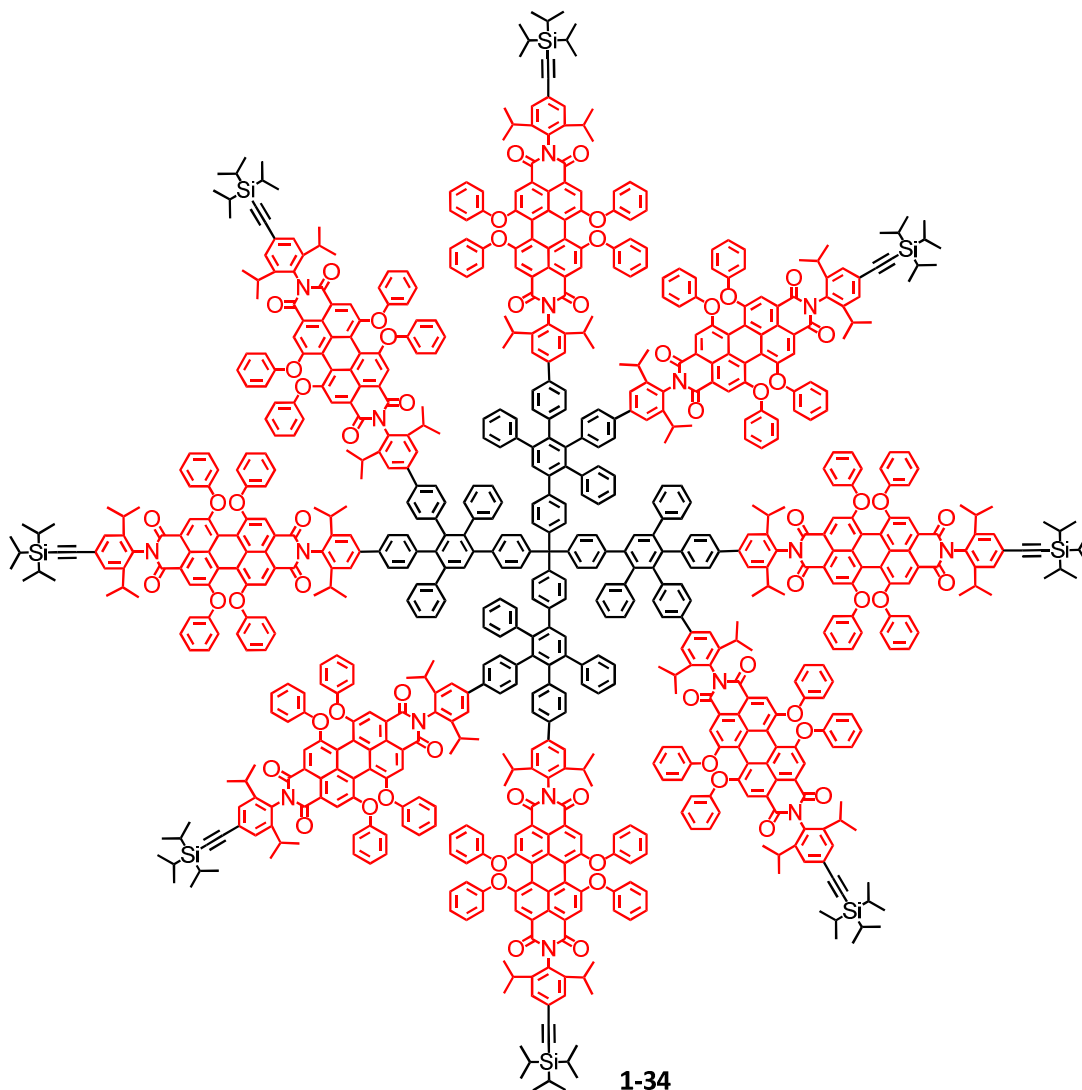
Scheme 1-12: Multichromophoric dendrimer **1-34** carrying eight PDIs in its scaffold.

The functional groups can also be added into the α-positions of cyclopentadienones by using 1,3-functionalized acetones (Scheme 1-13), e.g. 2,5-methylformate-3,4-bis[4-(tri-isopropylsilylethynyl)-phenyl]cyclopentadienone (**1-35**)[34] and 2,5-di(2-pyridinyl)-3,4-bis[4-(tri-isopropylsilylethynyl)-phenyl]cyclopentadienone (**1-36**).[35] The substituents in the α-position allow introducing functionality within the scaffolds, which may enable to affect the internal density of the dendrimer and the chemical properties of the cavities without influencing the possible number of branches or the number of potential functional groups on the surface. Thus by using the building unit **1-35**, up to 24 ester groups can be incorporated within a second generation dendrimer (**1-37**). These ester groups then hydrolyze to carboxylates (**1-38**), and thus produce a multiple negatively charged host macromolecule which can attract guest molecules with positive charges as a chemical sensor.[34] The polyphenylene dendrimers can also carry pyridine units (**1-36**) into the scaffolds. Since the pyridine groups are able to efficiently adsorb metal ions, these pyridine-containing polyphenylene dendrimers (**1-39**) can be regarded as nanosized macromolecular templates for the preparation of metal-containing hybrid catalytic materials.[35]

1-35

1-36

1-37

1-38

1-39

R =
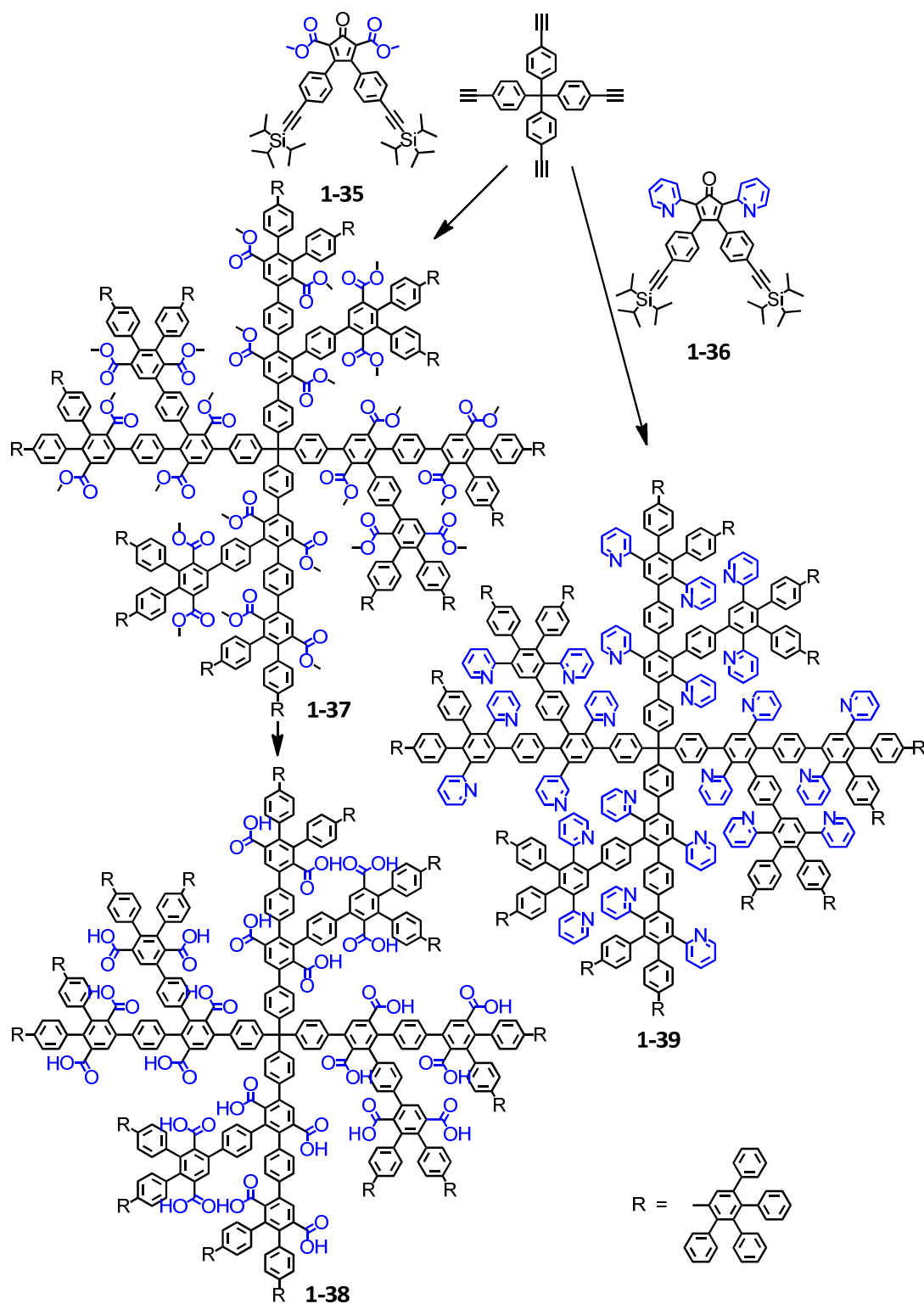
Scheme 1-13: Dendrimers with carboxylic (**1-38**) and pyridine (**1-39**) functions in the scaffold.

1.4.3 Functionalization on the surface

Functional groups on the surface do not change the shape and density of the polyphenylene dendrimers, but they can influence the chemical and physical properties of whole dendrimers. Moreover, functionalization at the periphery is the simplest but most effective method of functionalizing dendrimers with various possibilities for controlling the type, number and position of the substituents. We functionalized the surface of polyphenylene dendrimers via two different methods: i) the priori group introduction, which is achieved by using functionalized cyclopentadienones during the synthesis of dendrimers, and ii) the posteriori group introduction, which converts the existing substituents into the desired functional groups directly in the periphery of dendrimers.[22]

1.4.3.1 The priori group introduction

The introduction of the functional group in the course of the dendrimer synthesis presents an elegant way to obtain topologically well defined monodisperse products. In this case the numbers of functions as well as their geometrical arrangement are well known. The only requirement of this approach is that the desired function has to be chemically and thermally stable under the conditions of the Diels-Alder cycloaddition (Scheme 1-14), often requiring protecting group chemistry. With this approach, the polyphenylene dendrimers can possess photonic and electronic properties by using the building units with chromophores, e.g. perylenemonoimide (PMI) (**1-40**),[36] electron conductors, e.g. terthiophene (**1-41**),[37] and hole-transporting materials, e.g. triphenylamine (**1-42**).[38] Nevertheless, the dendrimer solubilities, the intermolecular interactions, the self-assembly behaviors, and the surface affinity can be controlled by introducing hydrophobic and hydrophilic substitutes on the dendrimer surface, e.g. fully fluoride substituents (**1-43**),[39] alkyl chains (**1-44**)[40] and ethylene oxide chains (**1-45**).[41]
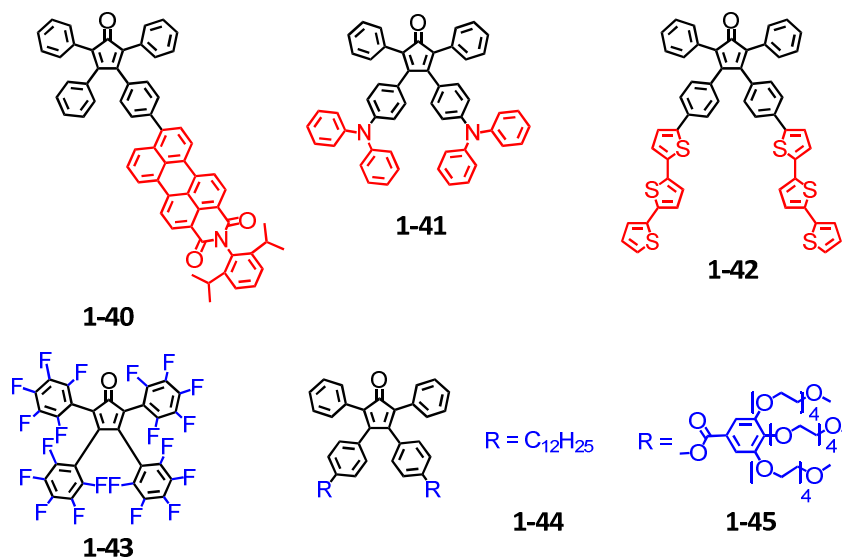
Scheme 1-14: Functional CPs for surface activation.

Moreover, by using both chromophore functionalized core and building units, we can introduce more than one type of chromophores into one dendrimer. For example, the dendrimer **1-46** consists of a single terrylenetetracarboxydiimide (TDI) core and multiple PMI groups in the periphery (Scheme 1-15). It is a nice model for light-harvesting system in which there are energy transfers from PMI as donors to TDI as an acceptor.[42]
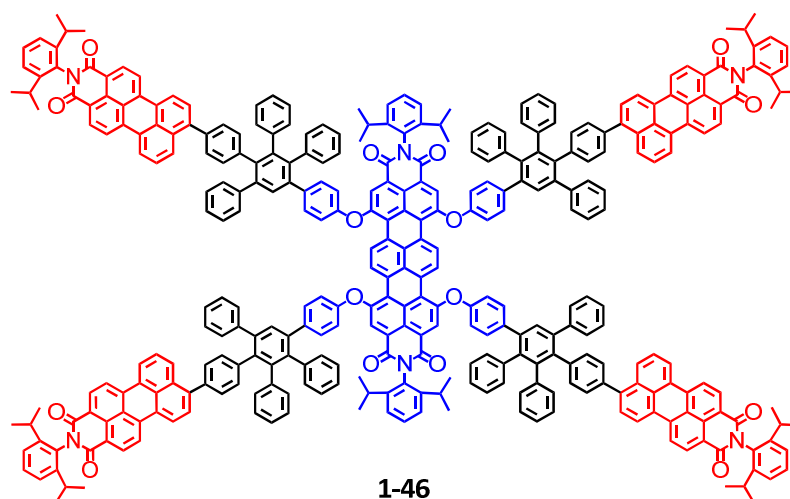
Scheme 1-15: Light-harvesting dendrimer **1-46** consists of PMI and TDI.

1.4.3.2 The posteriori group introduction

The generation of functional groups after the completed synthesis of the dendrimer constitutes a quick and variable way to get access to a large number of functionalized dendrimers. To apply multiple reactions on the surface of dendrimers, the already existing functional groups must exhibit a high reactivity as well as a high selectivity. The conversion of an already existing group A on the dendrimer into a substituent B by a subsequent reaction has been accomplished. In the ideal case, this reaction should be quantitative, but the possibility of incomplete conversions or side products must always be considered. The side products such as unreacted reagents can normally not be separated from the desired product. Up to now, we are able to functionalize polyphenylene dendrimers with carboxyl, hydroxyl, amide, and lithium groups in the periphery via this method (Scheme 1-16).

A	B
CN	COOH
OMe	OH
NH$_2$	NHCOR
Br	Li
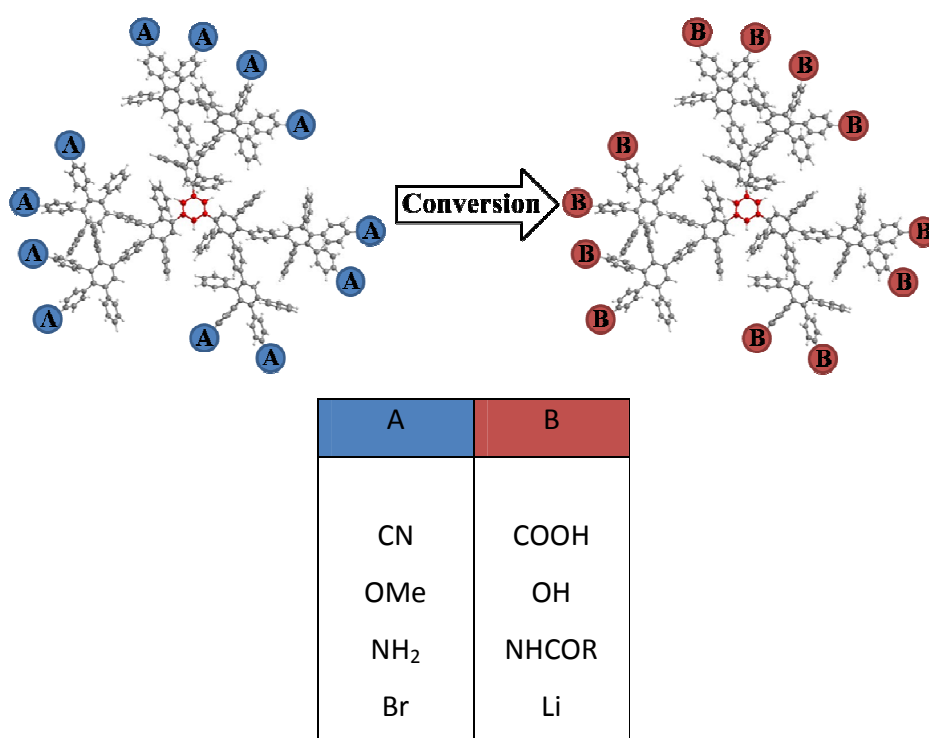
Scheme 1-16: Posteriori reactive group transformation.

Furthermore, the hydroxyl groups are able to yield to 2-bromo-2-methylpropionic ester groups (**1-47**, Scheme 1-17), which are the macroinitiators for atom transfer radical polymerization (ATRP) of *tert*-butyl acrylate.[43] The amine groups can also further link to the maleimide groups (**1-48**), which are the precursors for reacting with the thiol groups of peptides. Both of these water soluble core-shell structures based on dendrimer surface functionalization are highly interesting in the biological application.[44]
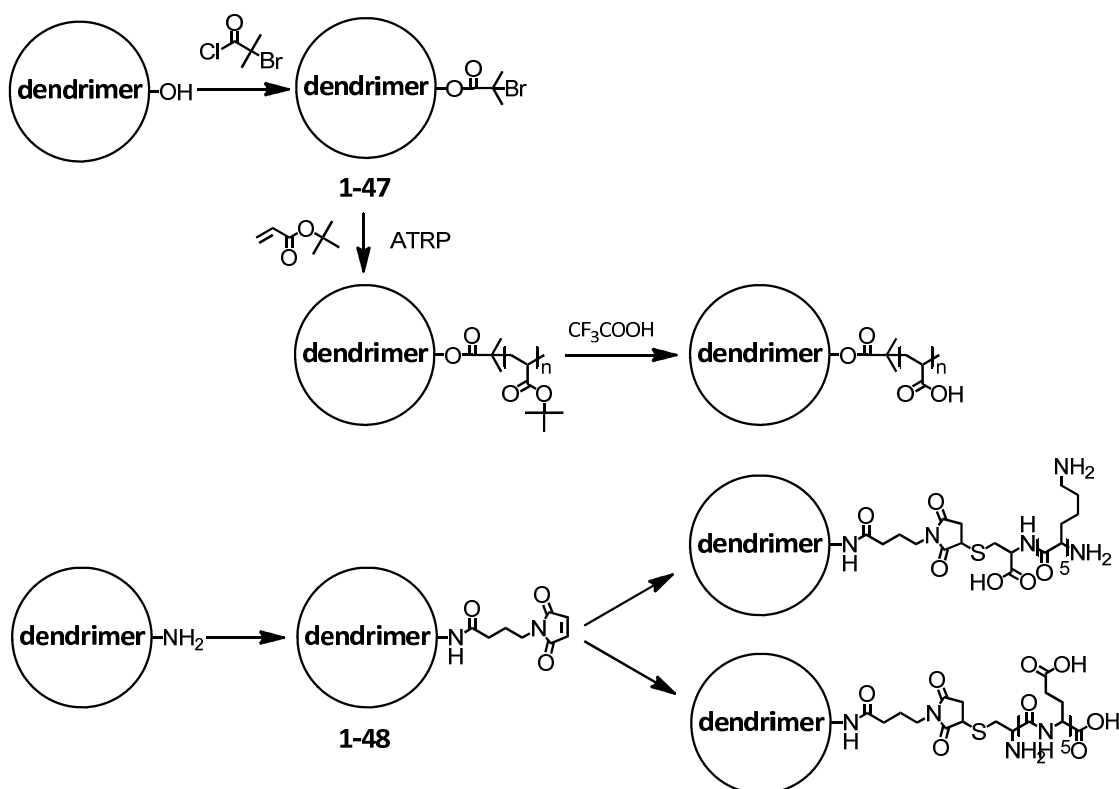
Scheme 1-17: Surface functionalized water-soluble polyphenylene dendrimers.

1.5 Dendritic macromolecules for organic light-emitting diodes (OLEDs)

A new term of "organic semiconductor", which is commonly used today, led to the award of the Nobel Prize in Chemistry in 2000 to Heeger,[45] MacDiarmid[46] and Shirakawa[47] for their contributions in conducting polymers. Meanwhile, an epoch of using organic semiconductors in the application of organic light-emitting diodes (OLEDs)

has begun since 1986, when Tang et al. demonstrated that a double-layer device consisting of a hole-transporting layer of aromatic diamine and an emissive layer of 8-hydroxyquinolinealuminum (Alq$_3$) could generate high efficiency organic electroluminescence (EL).[48] This double-layer design has become a landmark achievement and a prototypical structure for OLED devices. The demonstration of EL in conjugated polymers by Burroughes et al. in 1990 further highlighted the interest of research and development in organic electroluminescence.[49]

In the last two decades, organic electroluminescent materials are generally categorized into two classes, small molecules [50] or conjugated polymers.[49, 51] Whereas small molecules such as Alq$_3$ are conventionally deposited under high-vacuum conditions by evaporation,[52] high molecular weight polymeric materials such as poly(p-phenylene)vinylenes (PPVs)[53] or polyfluorenes (PFs)[54] can be processed under ambient conditions from solution[55] and can even be printed using ink-jet techniques.[56] However, either rather low or extremely high molecular weight materials have their own limitations. Therefore, between these two classes of materials a natural intermediate with monodisperse dendritic molecules containing repeating units was developed. These dendritic materials can combine the benefits of both previous classes.[57] The high molecular weights of these dendritic macromolecules, as well as the surface groups often attached to the distal (outer) ends of the dendrons, can improve the solution processability, and thus can be deposited from solution by simple processes such as spin-coating and ink-jet printing. The latter method allows the deposition of different colors side by side, enabling color displays to be printed. Moreover, even better than the traditional polymeric light-emitting materials, the well-defined monodisperse distributed dendrimers possess a high purity comparable to that of small molecules, and as such can be fabricated into high performance OLEDs. Most importantly, the emissive chromophores can be located at the core of the dendrimer, within the dendrons, and/or at the surface of the dendrimers because of their unique dendritic architectures. The different parts of the macromolecule can be selected to give the desired optoelectronic and processing properties.

The first light-emitting dendrimers were fluorescent but more recently highly efficient phosphorescent dendrimers have been developed.[25] All these dendrimers have been investigated that the most successful approach being the one found, when the core is the light-emitting component. Light-emitting dendrimers can be roughly divided into those with conjugated dendrons and those with saturated dendrons. In the latter case, the emissive moieties are covalently connected but with non-conjugated links. For conjugated dendrons and dendrimers, the branching points mean that while they may be fully conjugated, they are not necessarily fully delocalized, such as in meta-phenylene units. However, by using appropriate connectivity between the conjugated moieties, both classes of dendrimers can be considered as macromolecules comprised of molecular chromophores. This construction indicates that dendrimers are the natural structural design for solution processable fluorescent and phosphorescent emitters.

The molecular design outlined above gives light-emitting dendrimers many attractive features:

i)   It provides a means of making a light-emitting chromophore solution-processable. This opens up the possibility of ink-jet printing the materials, with its associated scope for simple manufacture and for the patterning of large-area displays.

ii) The molecular design is modular so that different parts of the molecule have different functions. This therefore allows independent optimization of the electronic and processing properties, for example, by selecting a core to give the desired color, and surface groups to give the desired solubility.

iii) The modular synthetic strategy means that dendron and core libraries can be developed making structural variations simpler. For instance, the same dendrons and surface groups can be used with different cores to give materials with different emission colors.

iv) The dendrimer generation can be used to control intermolecular interactions, which have a major effect on the photophysical and charge-transporting properties of organic materials. In particular, interactions between emissive chromophores can

lead to quenching of the luminescence, but dendrons can be used to keep the chromophores apart and so avoid this problem.

v)   The dendritic architecture can give rise to thermally stable amorphous thin films with high glass-transition temperatures.

As will be seen later, the advantages of the dendrimer architecture for luminescent emitters and the way the structure can be varied to enhance materials performance as well as the device design are illustrated.

1.6 Motivation

As reviewed above, the polyphenylene dendrimers show excellent properties, such as high chemical stability, strict monodispersity and shape persistent structure.[10] Furthermore, due to the unique dendritic architectures, by introducing functional groups into the core, scaffolds and surface, these functionalized polyphenylene dendrimers demonstrate novel chemical and physical properties. Especially the chromophoric dendrimers exhibit outstanding photophysical properties and potential application in organic light emitting diodes (OLEDs).[27-28] From the molecular design and material application points of view, some more improvements are desirable:

i)   The full-color light emission is brought by the presence of chemically and thermally stable chromophores with high photoluminescence quantum yields (PLQYs), such as polycyclic aromatic hydrocarbon (PAH) units and transition metal-complexes.

ii)   The chromophores are incorporated into a rigid dendritic polyphenylene scaffold; they thus adopt sterically defined positions and avoid inter- and intra-molecular chromophore-chromophore quenching interactions.

iii) Amorphous films for promising the solution process are obtained as a result of the lack of intermolecular interactions.

iv)   The amount of extraneous substituents effecting on solubility, such as alkyl chains, is kept at a minimum.

In this thesis work, the new molecular design, the new synthetic protocol and a series of new blue, green, red light emitting materials will be presented as the following:

i)   In chapter 2, a unique design for blue light emitting materials is presented. Starting from a new type of building units, diphenylcyclopentaphenanthrenone derivatives (1-49, Scheme 1-18), polytriphenylene dendrimers (1-50) were synthesized with promising performances in OLED devices.
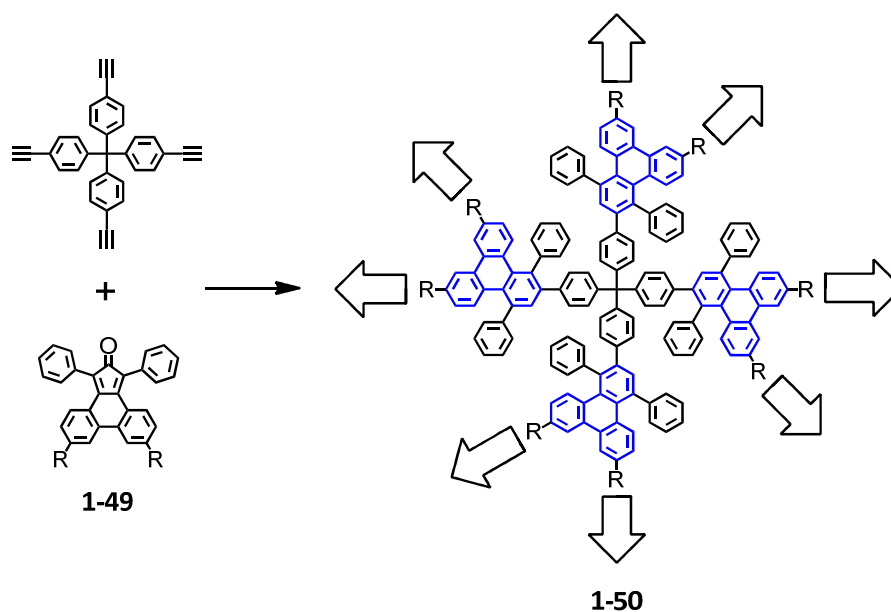
Scheme 1-18: Synthesis of blue fluorescent polytriphenylene dendrimers.

ii) In chapter 3, a new divergent synthesis of green triplet emitting polyphenylene dendrimers based on iridium(III) (Ir(III)) complex core (**1-51**, Scheme 1-19) is presented. A series of Ir(III) complex polyphenylene dendrimers up to fourth generation, which, up to now, is the largest Ir(III) dendrimer, were synthesized and their high efficient phosphorescent organic light emitting diode (PhOLED) devices were prepared.
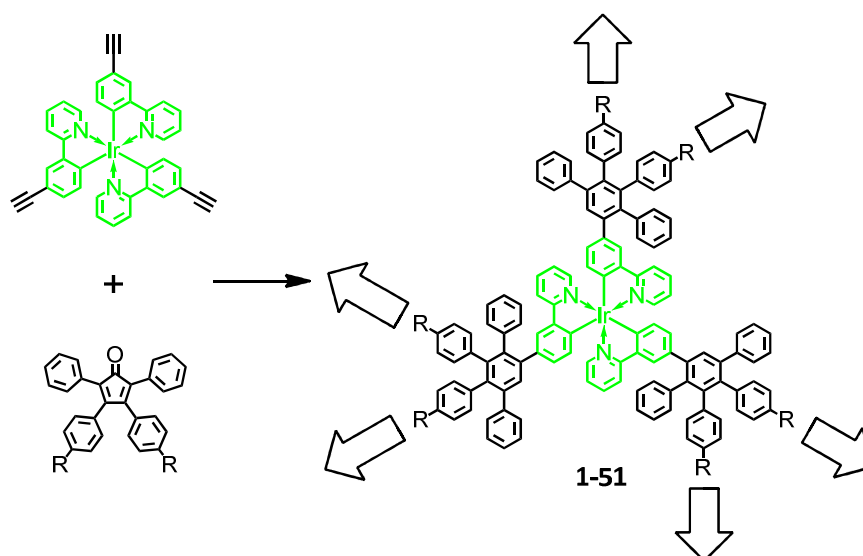
Scheme 1-19: Synthesis of green phosphorescent polyphenylene dendrimers.

iii) In chapter 4, a modification of the Ir(III) complex core is described, yielding a series of red phosphorescent polyphenylene dendrimers (**1-52**, Scheme 1-20). After a functionalization of hole-transporting materials on the dendrimer surface, these self host-guest systems demonstrate very promising performances in non-doped PhOLED devices.
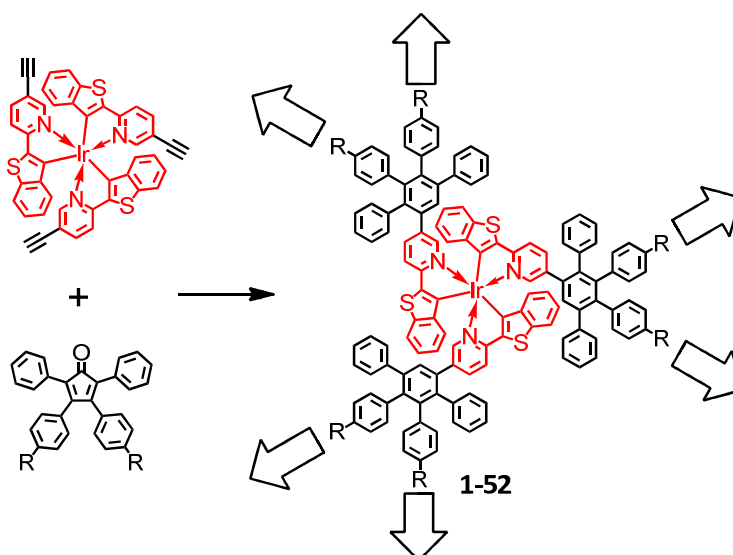
Scheme 1-20: Synthesis of red phosphorescent polyphenylene dendrimers.

References

[1]   a)Tomalia, D. A., Baker, H., Dewald, J., Hall, M., Kallos, G., Martin, S., Roeck, J., Ryder, J., Smith, P., *Polym. J.* **1985**, *17*, 117; b)Tomalia, D. A., Baker, H., Dewald, J., Hall, M., Kallos, G., Martin, S., Roeck, J., Ryder, J., Smith, P., *Macromolecules* **1986**, *19*, 2466; c)Vogtle, F., Gestermann, S., Hesse, R., Schwierz, H., Windisch, B., *Prog. Polym. Sci.* **2000**, *25*, 987; d)Grayson, S. M., Frechet, J. M. J., *Chem. Rev.* **2001**, *101*, 3819; e)Frechet, J. M. J., *Science* **1994**, *263*, 1710; f)Hawker, C. J., Frechet, J. M. J., *J. Am. Chem. Soc.* **1990**, *112*, 7638; g)Matthews, O. A., Shipway, A. N., Stoddart, J. F., *Prog. Polym. Sci.* **1998**, *23*, 1.

[2]   a)Krasteva, N., Besnard, I., Guse, B., Bauer, R. E., Mullen, K., Yasuda, A., Vossmeyer, T., *Nano Lett.* **2002**, *2*, 551; b)Schlupp, M., Weil, T., Berresheim, A. J., Wiesler, U. M., Bargon, J., Mullen, K., *Angew. Chem. Int. Ed.* **2001**, *40*, 4011; c)Pistolis, G., Malliaris, A., Tsiourvas, D., Paleos, C. M., *Chem. Eur. J.* **1999**, *5*, 1440.

[3]   a)Kreiter, R., Kleij, A. W., Gebbink, R., van Koten, G., *Dendrimers Iv* **2001**, *217*, 163; b)Rahim, E. H., Kamounah, F. S., Frederiksen, J., Christensen, J. B., *Nano Lett.* **2001**, *1*, 499.

[4]   a)Scott, R. W. J., Wilson, O. M., Crooks, R. M., *J. Phys. Chem. B* **2005**, *109*, 692; b)Crooks, R. M., Zhao, M. Q., Sun, L., Chechik, V., Yeung, L. K., *Acc. Chem. Res.* **2001**, *34*, 181; c)Grohn, F., Bauer, B. J., Akpalu, Y. A., Jackson, C. L., Amis, E. J., *Macromolecules* **2000**, *33*, 6042.

[5]   a)Hawker, C. J., Wooley, K. L., *Science* **2005**, *309*, 1200; b)Lee, C. C., MacKay, J. A., Frechet, J. M. J., Szoka, F. C., *Nat. Biotechnol.* **2005**, *23*, 1517; c)Cloninger, M. J., *Curr. Opin. Chem. Biol.* **2002**, *6*, 742.

[6]   Lesniak, W., Bielinska, A. U., Sun, K., Janczak, K. W., Shi, X. Y., Baker, J. R., Balogh, L. P., *Nano Lett.* **2005**, *5*, 2123.

[7]   Stiriba, S. E., Frey, H., Haag, R., *Angew. Chem. Int. Ed.* **2002**, *41*, 1329.

[8]   a)Luo, D., Saltzman, W. M., *Nat. Biotechnol.* **2000**, *18*, 33; b)Tang, M. X., Redemann, C. T., Szoka, F. C., *Bioconjugate Chem.* **1996**, *7*, 703.

[9]   a)Hecht, S., Frechet, J. M. J., *Angew. Chem. Int. Ed.* **2001**, *40*, 74; b)Adronov, A., Frechet, J. M. J., *Chem. Commun.* **2000**, 1701; c)Halim, M., Pillow, J. N. G., Samuel, I. D. W., Burn, P. L., *Adv. Mater.* **1999**, *11*, 371; d)Wang, P. W., Liu, Y. J., Devadoss, C., Bharathi, P., Moore, J. S., *Adv. Mater.* **1996**, *8*, 237; e)Lupton, J. M., Samuel, I. D. W., Beavington, R.,

Burn, P. L., Bassler, H., *Adv. Mater.* **2001**, *13*, 258; f)Freeman, A. W., Koene, S. C., Malenfant, P. R. L., Thompson, M. E., Frechet, J. M. J., *J. Am. Chem. Soc.* **2000**, *122*, 12385.

[10]   a)Grimsdale, A. C., Mullen, K., *Angew. Chem. Int. Ed.* **2005**, *44*, 5592; b)Berresheim, A. J., Muller, M., Mullen, K., *Chem. Rev.* **1999**, *99*, 1747; c)Bosman, A. W., Janssen, H. M., Meijer, E. W., *Chem. Rev.* **1999**, *99*, 1665; d)Zeng, F. W., Zimmerman, S. C., *Chem. Rev.* **1997**, *97*, 1681; e)Tomalia, D. A., Naylor, A. M., Goddard, W. A., *Angew. Chem. Int. Ed. Engl.* **1990**, *29*, 138.

[11]   Tomalia, D. A., *Adv. Mater.* **1994**, *6*, 529.

[12]   Mourey, T. H., Turner, S. R., Rubinstein, M., Frechet, J. M. J., Hawker, C. J., Wooley, K. L., *Macromolecules* **1992**, *25*, 2401.

[13]   Buhleier, E., Wehner, W., Vogtle, F., *Synthesis-Stuttgart* **1978**, 155.

[14]   a)Frauenrath, H., *Prog. Polym. Sci.* **2005**, *30*, 325; b)Weil, T., Reuther, E., Mullen, K., *Angew. Chem. Int. Ed.* **2002**, *41*, 1900; c)Moore, J. S., *Acc. Chem. Res.* **1997**, *30*, 402.

[15]   Hart, H., Bashirhashemi, A., Luo, J., Meador, M. A., *Tetrahedron* **1986**, *42*, 1641.

[16]   Demeijere, A., Kozhushkov, S. I., Spaeth, T., Zefirov, N. S., *J. Org. Chem.* **1993**, *58*, 502.

[17]   Xu, Z. F., Kahr, M., Walker, K. L., Wilkins, C. L., Moore, J. S., *J. Am. Chem. Soc.* **1994**, *116*, 4537.

[18]   Miller, T. M., Neenan, T. X., Zayas, R., Bair, H. E., *J. Am. Chem. Soc.* **1992**, *114*, 1018.

[19]   Wiesler, U. M., Berresheim, A. J., Morgenroth, F., Lieser, G., Mullen, K., *Macromolecules* **2001**, *34*, 187.

[20]   Morgenroth, F., Mullen, K., *Tetrahedron* **1997**, *53*, 15349.

[21]   Wiesler, U. M., Mullen, K., *Chem. Commun.* **1999**, 2293.

[22]   a)Wiesler, U. M., Weil, T., Mullen, K., *Top. Curr. Chem.* **2001**, *212*, 1; b)Bauer, R. E., Grimsdale, A. C., Mullen, K., *Top. Curr. Chem.* **2005**, *245*, 253.

[23]   Brocorens, P., Zojer, E., Cornil, J., Shuai, Z., Leising, G., Mullen, K., Bredas, J. L., *Synth. Met.* **1999**, *100*, 141.

[24]   Haberecht, M. C., Schnorr, J. M., Andreitchenko, E. V., Christopher, C. G., Wagner, M., Mullen, K., *Angew. Chem. Int. Ed.* **2008**, *47*, 1662.

[25]   a)Hwang, S. H., Moorefield, C. N., Newkome, G. R., *Chem. Soc. Rev.* **2008**, *37*, 2543; b)Burn, P. L., Lo, S. C., Samuel, I. D. W., *Adv. Mater.* **2007**, *19*, 1675; c)Lo, S. C., Burn, P. L., *Chem. Rev.* **2007**, *107*, 1097.

[26]   a)De Schryver, F. C., Vosch, T., Cotlet, M., Van der Auweraer, M., Mullen, K., Hofkens, J., *Acc. Chem. Res.* **2005**, *38*, 514; b)Hofkens, J., Maus, M., Gensch, T., Vosch, T., Cotlet, M., Kohn, F., Herrmann, A., Mullen, K., De Schryver, F., *J. Am. Chem. Soc.* **2000**, *122*, 9278; c)Gensch, T., Hofkens, J., Heirmann, A., Tsuda, K., Verheijen, W., Vosch, T., Christ, T., Basche, T., Mullen, K., De Schryver, F. C., *Angew. Chem. Int. Ed.* **1999**, *38*, 3752.

[27]   Bernhardt, S., Kastler, M., Enkelmann, V., Baumgarten, M., Mullen, K., *Chem. Eur. J.* **2006**, *12*, 6117.

[28]   Herrmann, A., Weil, T., Sinigersky, V., Wiesler, U. M., Vosch, T., Hofkens, J., De Schryver, F. C., Mullen, K., *Chem. Eur. J.* **2001**, *7*, 4844.

[29]   Rapacioli, M., Calvo, F., Spiegelman, F., Joblin, C., Wales, D. J., *J. Phys. Chem. A* **2005**, *109*, 2487.

[30]   Setayesh, S., Grimsdale, A. C., Weil, T., Enkelmann, V., Mullen, K., Meghdadi, F., List, E. J. W., Leising, G., *J. Am. Chem. Soc.* **2001**, *123*, 946.

[31]   Andreitchenko, E. V., Clark, C. G., Bauer, R. E., Lieser, G., Mullen, K., *Angew. Chem. Int. Ed.* **2005**, *44*, 6348.

[32]   Bernhardt, S., Baumgarten, M., Wagner, M., Mullen, K., *J. Am. Chem. Soc.* **2005**, *127*, 12392.

[33]   Oesterling, I., Mullen, K., *J. Am. Chem. Soc.* **2007**, *129*, 4595.

[34]   Bauer, R. E., Clark, C. G., Mullen, K., *New J. Chem.* **2007**, *31*, 1275.

[35]   Shifrina, Z. B., Rajadurai, M. S., Firsova, N. V., Bronstein, L. M., Huang, X. L., Rusanov, A. L., Muellen, K., *Macromolecules* **2005**, *38*, 9920.

[36]   a)Weil, T., Wiesler, U. M., Herrmann, A., Bauer, R., Hofkens, J., De Schryver, F. C., Mullen, K., *J. Am. Chem. Soc.* **2001**, *123*, 8101; b)Maus, M., De, R., Lor, M., Weil, T., Mitra, S., Wiesler, U. M., Herrmann, A., Hofkens, J., Vosch, T., Mullen, K., De Schryver, F. C., *J. Am. Chem. Soc.* **2001**, *123*, 7668.

[37]   John, H., Bauer, R., Espindola, P., Sonar, P., Heinze, J., Mullen, K., *Angew. Chem. Int. Ed.* **2005**, *44*, 2447.

[38]   Qu, J. Q., Pschirer, N. G., Liu, D. J., Stefan, A., De Schryver, F. C., Mullen, K., *Chem. Eur. J.* **2004**, *10*, 528.

[39]   Bauer, R., Liu, D., Heyen, A. V., De Schryver, F., De Feyter, S., Mullen, K., *Macromolecules* **2007**, *40*, 4753.

[40]   a)Loi, S., Wiesler, U. M., Butt, H. J., Mullen, K., *Macromolecules* **2001**, *34*, 3661; b)Loi, S.,
          Wiesler, U. M., Butt, H. J., Mullen, K., *Chem. Commun.* **2000**, 1169.

[41]   Kohl, C., Weil, T., Qu, J. Q., Mullen, K., *Chem. Eur. J.* **2004**, *10*, 5297.

[42]   a)Lor, M., Thielemans, J., Viaene, L., Cotlet, M., Hofkens, J., Weil, T., Hampel, C., Mullen,
          K., Verhoeven, J. W., Van der Auweraer, M., De Schryver, F. C., *J. Am. Chem. Soc.* **2002**,
          124, 9918; b)Gronheid, R., Hofkens, J., Kohn, F., Weil, T., Reuther, E., Mullen, K., De
          Schryver, F. C., *J. Am. Chem. Soc.* **2002**, *124*, 2418.

[43]   a)Yin, M. Z., Cheng, Y. J., Liu, M. Y., Gutmann, J. S., Mullen, K., *Angew. Chem. Int. Ed.*
          2008, *47*, 8400; b)Yin, M., Shen, J., Pflugfelder, G. O., Mullen, K., *J. Am. Chem. Soc.* **2008**,
          130, 7806.

[44]   a)Mihov, G., Grebel-Koehler, D., Lubbert, A., Vandermeulen, G. W. M., Herrmann, A.,
          Klok, H. A., Mullen, K., *Bioconjugate Chem.* **2005**, *16*, 283; b)Herrmann, A., Mihov, G.,
          Vandermeulen, G. W. M., Klok, H. A., Mullen, K., *Tetrahedron* **2003**, *59*, 3925.

[45]   a)Yu, G., Gao, J., Hummelen, J. C., Wudl, F., Heeger, A. J., *Science* **1995**, *270*, 1789;
          b)Sariciftci, N. S., Smilowitz, L., Heeger, A. J., Wudl, F., *Science* **1992**, *258*, 1474;
          c)Gustafsson, G., Cao, Y., Treacy, G. M., Klavetter, F., Colaneri, N., Heeger, A. J., *Nature*
          1992, *357*, 477.

[46]   a)Huang, W. S., Humphrey, B. D., Macdiarmid, A. G., *Journal of the Chemical Society-
          Faraday Transactions I* **1986**, *82*, 2385; b)Chiang, C. K., Fincher, C. R., Park, Y. W., Heeger,
          A. J., Shirakawa, H., Louis, E. J., Gau, S. C., Macdiarmid, A. G., *Phys. Rev. Lett.* **1977**, *39*,
          1098.

[47]   a)MacDiarmid, A. G., *Angew. Chem. Int. Ed.* **2001**, *40*, 2581; b)Shirakawa, T., Enomoto, T.,
          Shimazu, S., Hopkin, J. M., *Science* **1997**, *275*, 77; c)Shirakawa, H., Louis, E. J.,
          Macdiarmid, A. G., Chiang, C. K., Heeger, A. J., *J. Chem. Soc., Chem. Commun.* **1977**, 578.

[48]   a)Tang, C. W., *Appl. Phys. Lett.* **1986**, *48*, 183; b)Tang, C. W., Vanslyke, S. A., *Appl. Phys.
          Lett.* **1987**, *51*, 913; c)Tang, C. W., Vanslyke, S. A., Chen, C. H., *J. Appl. Phys.* **1989**, *65*,
          3610.

[49]   Burroughes, J. H., Bradley, D. D. C., Brown, A. R., Marks, R. N., Mackay, K., Friend, R. H.,
          Burns, P. L., Holmes, A. B., *Nature* **1990**, *347*, 539.

[50]   a)Shen, Z. L., Burrows, P. E., Bulovic, V., Forrest, S. R., Thompson, M. E., *Science* **1997**,
          276, 2009; b)Baldo, M. A., Thompson, M. E., Forrest, S. R., *Nature* **2000**, *403*, 750;
          c)Baldo, M. A., O'Brien, D. F., You, Y., Shoustikov, A., Sibley, S., Thompson, M. E., Forrest,

S. R., *Nature* **1998**, *395*, 151; d)Sheats, J. R., Antoniadis, H., Hueschen, M., Leonard, W., Miller, J., Moon, R., Roitman, D., Stocking, A., *Science* **1996**, *273*, 884.

[51]   a)Friend, R. H., Gymer, R. W., Holmes, A. B., Burroughes, J. H., Marks, R. N., Taliani, C., Bradley, D. D. C., Dos Santos, D. A., Bredas, J. L., Logdlund, M., Salaneck, W. R., *Nature* **1999**, *397*, 121; b)Ho, P. K. H., Kim, J. S., Burroughes, J. H., Becker, H., Li, S. F. Y., Brown, T. M., Cacialli, F., Friend, R. H., *Nature* **2000**, *404*, 481; c)Cao, Y., Parker, I. D., Yu, G., Zhang, C., Heeger, A. J., *Nature* **1999**, *397*, 414; d)Gross, M., Muller, D. C., Nothofer, H. G., Scherf, U., Neher, D., Brauchle, C., Meerholz, K., *Nature* **2000**, *405*, 661; e)Burn, P. L., Holmes, A. B., Kraft, A., Bradley, D. D. C., Brown, A. R., Friend, R. H., Gymer, R. W., *Nature* **1992**, *356*, 47; f)Greenham, N. C., Moratti, S. C., Bradley, D. D. C., Friend, R. H., Holmes, A. B., *Nature* **1993**, *365*, 628.

[52]   Kim, H., Gilmore, C. M., Pique, A., Horwitz, J. S., Mattoussi, H., Murata, H., Kafafi, Z. H., Chrisey, D. B., *J. Appl. Phys.* **1999**, *86*, 6451.

[53]   Hsieh, B. R., Yu, Y., Forsythe, E. W., Schaaf, G. M., Feld, W. A., *J. Am. Chem. Soc.* **1998**, *120*, 231.

[54]   Ranger, M., Rondeau, D., Leclerc, M., *Macromolecules* **1997**, *30*, 7686.

[55]   Muller, C. D., Falcou, A., Reckefuss, N., Rojahn, M., Wiederhirn, V., Rudati, P., Frohne, H., Nuyken, O., Becker, H., Meerholz, K., *Nature* **2003**, *421*, 829.

[56]   Hebner, T. R., Wu, C. C., Marcy, D., Lu, M. H., Sturm, J. C., *Appl. Phys. Lett.* **1998**, *72*, 519.

[57]   a)Markham, J. P. J., Lo, S. C., Magennis, S. W., Burn, P. L., Samuel, I. D. W., *Appl. Phys. Lett.* **2002**, *80*, 2645; b)Lo, S. C., Male, N. A. H., Markham, J. P. J., Magennis, S. W., Burn, P. L., Salata, O. V., Samuel, I. D. W., *Adv. Mater.* **2002**, *14*, 975; c)Sooklal, K., Hanus, L. H., Ploehn, H. J., Murphy, C. J., *Adv. Mater.* **1998**, *10*, 1083; d)Lupton, J. M., Hemingway, L. R., Samuel, I. D. W., Burn, P. L., *J. Mater. Chem.* **2000**, *10*, 867.

Chapter 2

Polytriphenylene dendrimers:

A unique design for blue light-emitting materials

In this chapter, a novel synthetic concept to design multi-chromophoric dendrimers for blue OLEDs will be presented. Different generation polytriphenylene dendrimers were synthesized in a divergent method. A series of solution processable, chemical and thermal stable blue light-emitting materials were obtained in high yields. Their photophysical properties and device performances were studied.

2.1 Motivation in design of blue fluorescent dendrimers

Full color OLED display may be constructed in different ways such as i) filtering white light for a specific color,[1] ii) applying different bias potentials to OLEDs,[2] iii) using efficient dyes to convert colors,[3] or iv) patterning pixels for the three principle colors red, green, and blue (RGB) independently.[4] Color filtering of white light is simple but wastes energy due to the generation of unwanted colors. The voltage dependent multicolor emitting materials cannot control the light intensity and the emission color at the same time.[2a, 5] For the last two methods, the blue light-emitting diodes are still the most challengeable one in RGB OLED display for the following reasons. There are very efficient dyes for converting colors, but the energy can most easily be transferred from the absorption of short wavelength light to the emission of a longer one, which means a blue OLED alone may generate all colors, while green or red are more difficult to be converted to blue color (Figure 2-1).[6] Moreover, although most colors have been demonstrated in OLEDs, only green and orange OLEDs currently are available for commercial use. Blue light-emitting materials for commercial use are still under development, and red light-emitting materials must be further improved.[7]

Figure 2-1: Mechanism of color converting dyes.

Traditionally, the blue emitters as all others light-emitting materials have fallen into two main classes, small molecules and polymers. These materials and their individual advantages were covered in detail in the previously introduction chapter. The repeating units for blue light emission in linear polymers include phenylene vinylenes,[8] phenylenes,[9] thiophenes,[10] pyridines[11] and fluorenes.[12] Small molecules such as anthracene,[13] pyrene[14] and triphenylene[15] are also promising as blue light-emitting fluorophores. Most of these blue light-emitting fluorophores possess high chemical and thermal stability and good solubility in organic solvents.[16] However, both small molecules and linear polymers possess planar or partially planar molecular structures (Figure 2-2), and tend to exhibit low quantum efficiencies and excimer emissions due to the π-π stacking of individual chromophores in the solid state.[17] Although by introducing the spacing or solubilizing substituents, such as alkyl, alkoxy, phenyl and phenoxy chains,[18] or even polyphenylene dendrons,[19] the intermolecular interactions can be reduced or hindered, thereby preventing aggregation. Such "extraneous" substituents have no benefits for emission, complicate the synthetic route and increase the producing cost, while still cannot completely prevent the aggregation. These aggregations and π-π stackings can be totally eliminated by introducing the chromophores into a dendritic architecture (Figure 2-2). The dendritic shell can also isolate the emissive excitation from environment, thus decreasing parasitic perturbations, such as solvation effects in the condensed phase or luminescence quenching, through interaction with the environment or surrounding chromophores in the solid film.[20] Therefore, the dendrimer-based light-emitting materials have been considered as an attractive candidate for OLEDs.

(a) small molecule

(b) linear polymer

(c) dendrimer
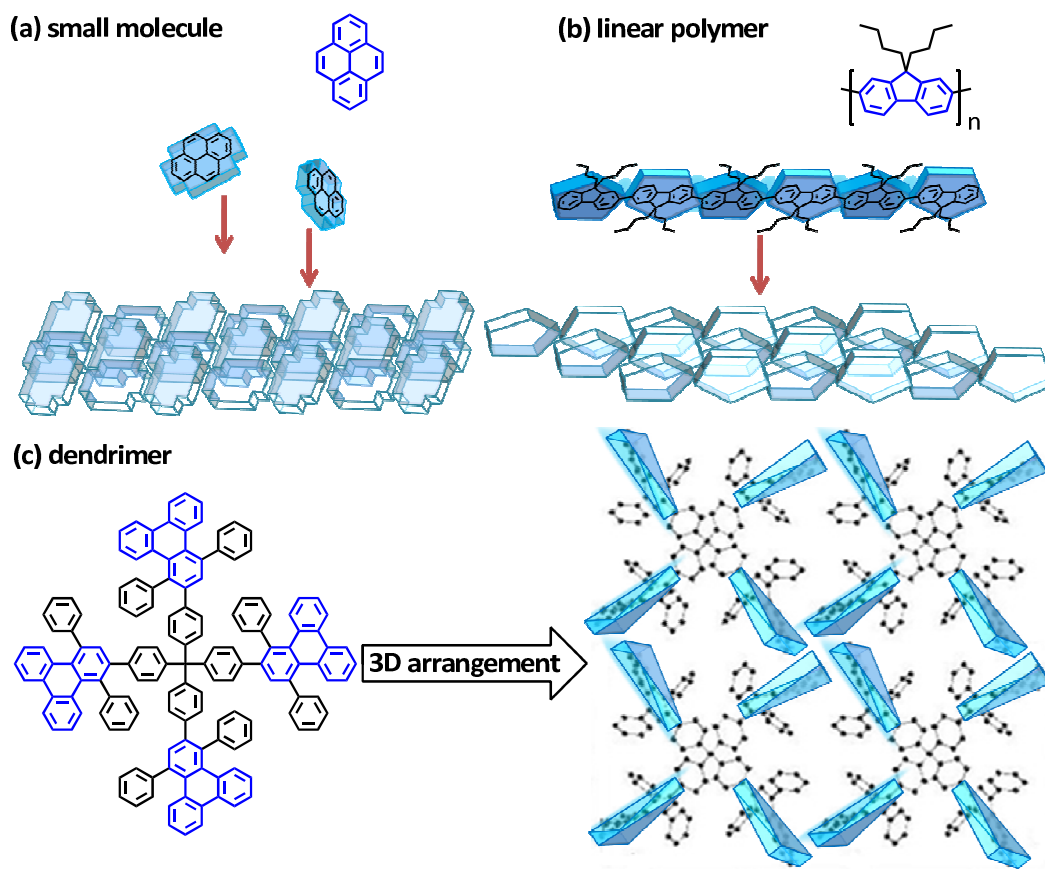
3D arrangement

Figure 2-2: Intermolecular arrangements of three types of chromophores: (a) small molecule, (b) linear polymer, and (c) dendrimer.

The blue fluorescent dendrimers are divided into two types as the result of placing emitters into different locations (Scheme 2-1): i) a single blue chromophore located in the center of the dendrimer and isolated by dendrons in the periphery, such as anthracene (**2-1**),[21] pyrene (**2-2**),[22] distyrylstilbene (**2-3**),[23] etc.; and ii) blue light-emitting oligomers situated in the scaffold as repeating units, such as stilbene (**2-4**),[24] phenylacetylene (**2-5**),[25] truxene (**2-6**),[26] etc., which can not only produce emission, but also prevent chromophore aggregation.
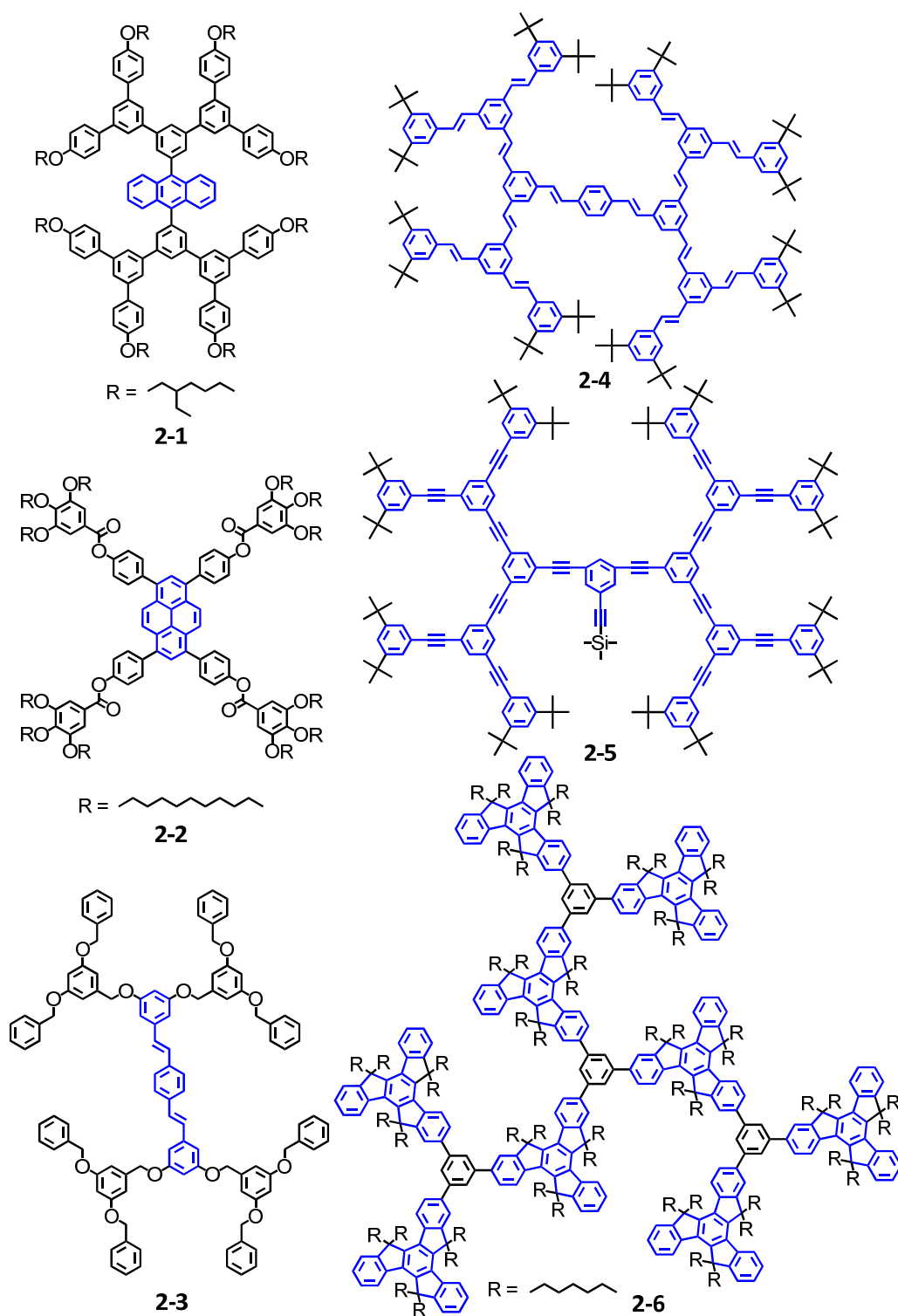
Scheme 2-**1:** Blue fluorescent dendrimers with various emitting cores, such as anthracene (**2-1**), pyrene (**2-2**), distyrylstilbene (**2-3**) or repeating units in the scaffold, such as stilbene (**2-4**), phenylacetylene (**2-5**), truxene (**2-6**).

In contrast to the first type of dendrimers, which contain only one blue emissive core and exhibits relatively low quantum efficiency, the second type of dendrimers have multiple chromophores and possesses high quantum efficiency. However, the syntheses of these multi-chromophoric dendrimers still restrict and challenge their application in OLEDs. Up to now, most blue fluorescent dendrimers with multi-chromophores have been prepared in a convergent strategy by metal-catalytic cross-coupling reactions, which limited these dendrimers to low generations and in low yield.),[24-26] These blue light-emitting materials with low molecular weights show poor thermal stability and worse morphology in solid film, thus degrade the device performance. Nevertheless, the minimum metal catalyst residues, which cannot be removed from the products, will result in poor device performance.[27] Therefore, it was necessary to design a new non-catalytic and high yield synthesis route to achieve high generation dendrimers with chromophores as building units.

2.2 Blue fluorescent polytriphenylene dendrimers

Most recently, triphenylene derivatives[28] and their linear[29] and hyperbranched[30] polymers were reported as promising candidates for blue OLEDs for the following considerations:

i)   Triphenylene based π-conjugated systems are known to exhibit longer excited state lifetimes than their phenyl analogs, and should therefore foster through-bond energy migration.

ii) Triphenylene derivatives are one of the most common discotic mesogens which have a tendency to form discotic liquid crystalline phases that facilitate charge transport, but which leads to bathochromically shifted emission. The nature of shape-persistent dendrimers may prevent intra- and inter-dendrimer π-stacking, enabling blue emission.

iii) Triphenylene derivatives, as polycyclic aromatic hydrocarbons, demonstrate very high chemical and thermal stability. Their full aromatic ring structures avoid the

tendency for oxidation which leads to the appearance of a long wavelength emission band and the deterioration of device.

A number of triphenylene-based small molecules and polymers have been designed and investigated, the high tendency towards self-association of triphenylene often led to a dramatic decrease in fluorescence intensity due to their strong π-π stacking.[28] To the best of our knowledge, dendrimers based exclusively on interlinked triphenylene units have not been realized. This is most probably due to the challenges associated with functionalized triphenylene derivatives serving as branching reagents in dendrimer synthesis. Herein we will present a novel divergent synthetic concept to achieve triphenylene units along with the growth of dendrimer generations. In this contribution, triphenylene is introduced as building block for the dendritic systems. Though bearing a higher risk of intramolecular triphenylene-triphenylene chromophore interaction, this allows for a higher density of emitting units in the active layer. Therefore, the amount of electro-inactive material contained in dendrimer films can be kept at a minimum. Chemical, photophysical and optoelectronic characterizations show that the new triphenylene based dendritic materials are promising candidates for blue light emitting devices.

2.2.1 Design of cyclopentaphenanthrenone derivative AB$_2$-type building unit

Since Sasaki et al. firstly found that phencyclone possessed a high reactive diene moiety in Diels-Alder [4+2] cycloaddition reactions with ethynyl units in 1976,[31] phencyclone and its derivatives have been used to synthesize various polycyclic aromatic hydrocarbons (PAHs),[32] especially the triphenylene units.[33] Herein, we planned to use a phencyclone derivative **2-7** (Scheme 2-2) as the building unit, leading to AB$_2$-type diphenyltriphenylene repeating units **2-8** via the [4+2] Diels-Alder cycloaddition with ethynyl groups.
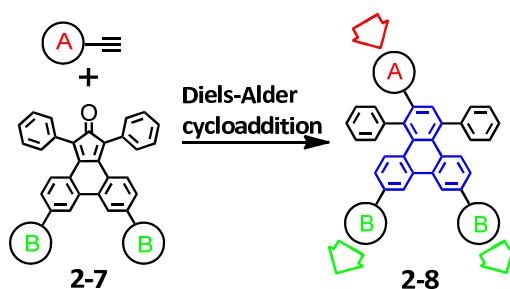
Scheme 2-2: Synthesis of AB$_2$-type diphenyltriphenylene repeating units (**2-8**) from phencyclone derivative (**2-7)** via Diels-Alder cycloaddition.

The key step was the utilization of a novel AB$_2$-type building unit, 1,3-diphenyl-6,9-bis(triisopropylsilylethynyl)-cyclopentaphenanthrenone **2-9** (Scheme 2-3), which combined a diene and two protected ethynyl functions in the same molecule. Compared to the tetraphenylcyclopentadienone derivatives being used in the synthesis of already known polyphenylene dendrimers,[34] building unit **2-9** contained one additional bond in the ortho-positions between two neighboring phenyl rings. This led to triphenylene units after Diels-Alder [4+2] reaction.
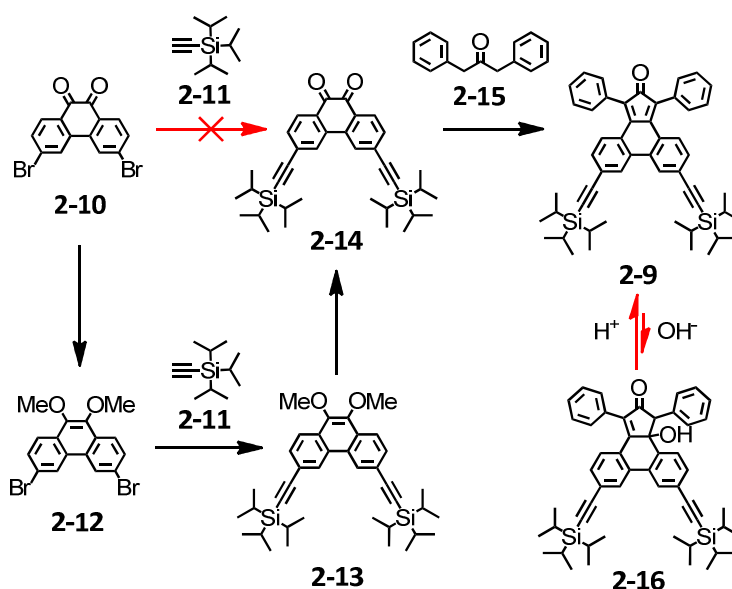
Scheme 2-3: Synthesis of AB$_2$-type building unit, 1,3-diphenyl-6,9-bis((triisopropylsilyl)ethynyl)-cyclopentaphenanthrenone **2-9**.

The synthesis of the key intermediate **2-9** began from the commercially available 3,6-dibromo-9,10-phenanthroquinone (**2-10**), which was readily obtained by bromination of 9,10-phenanthroquinone according to a literature procedure.[35] Recrystallization from nitrobenzene gave **2-10** as a dark yellow solid in almost quantitative yield. In the next step, the direct Hagihara-Sonogashira coupling reaction of the triisopropylsilylacetylene (**2-11**) with **2-10** was unsuccessful due to the side reaction which occurred between the diketone and the ethynyl group. Therefore, compound **2-10** had to be reacted with dimethyl sulfate at room temperature, and then intermediately converted to 3,6-dibromo-9,10-dimethoxyphenanthrene (**2-12**), in which the diketone group could be protected, in 92% yield. The introduction of the ethynyl groups in 3,6-bis(triisopropylsilylethynyl)-9,10-dimethoxyphenanthrene (**2-13**) was obtained in 84% yield by Hagihara-Sonogashira coupling reaction between triisopropylsilylacetyleneand **2-12** by using dichloro-bis(triphenylphosphine)palladium(II), copper(I)iodide, and triphenylphosphine as catalysts in toluene/triethylamine solution. The dimethoxy group in **2-13** converted back to the diketone group and achieved 3,6-bis(triisopropylsilylethynyl)-9,10-phenanthroquinone **2-14** via an efficient oxidation using cerium ammonium nitrate (CAN) aqueous solution in 84% yield. Subsequent double Knoevenagel condensation of **2-12** with 1,3-diphenylacetone (**2-15**) in K_2CO_3/ethanol system could provide the building unit, 1,3-diphenyl-6,9-bis((triisopropylsilyl)ethynyl)-cyclopentaphenanthrenone (**2-13**) in 61% yield as dark green color solid. The building unit **2-13** was unstable in basic environment tending to a side product **2-16** with hydroxy cyclopentenone structure. The side reaction could be avoided by using 1M HCl-methanol solution to neutralize the pH value immediately after the Knoevenagel condensation reaction finished.

2.2.2 Synthesis of first- to third-generation polytriphenylene dendrimers

The preparation of the structurally defined monodisperse polytriphenylene dendrimers has been realized by a divergent protocol.[36] The unfunctionalized first-generation

dendrimer **TPG1** (Scheme 2-4) with 4 triphenylene units was synthesized from Diels-Alder cycloaddition by heating the tetra(4-ethynylphenyl)methane (**2-17**) and commercially available phencyclone (**2-18**) in refluxing o-xylene. Since the first-generation dendrimer **TPG1** was poorly soluble in common organic solvents, the pure dendrimer **TPG1** was achieved by repetitive precipitation in methanol as light yellow solid in 97% yield.

It should be mentioned that compared with the traditional Diels-Alder cycloaddition condition, which took about 12-16 hours heating in an oil bath, the microwave reaction at higher temperature and under microwave power could dramatically accelerate the reaction time to 30 minutes.[1] This new reaction performing type has often been applied for the Diels-Alder cycloaddition reaction in my thesis work, since it always showed comparable yield and much shorter reaction time.
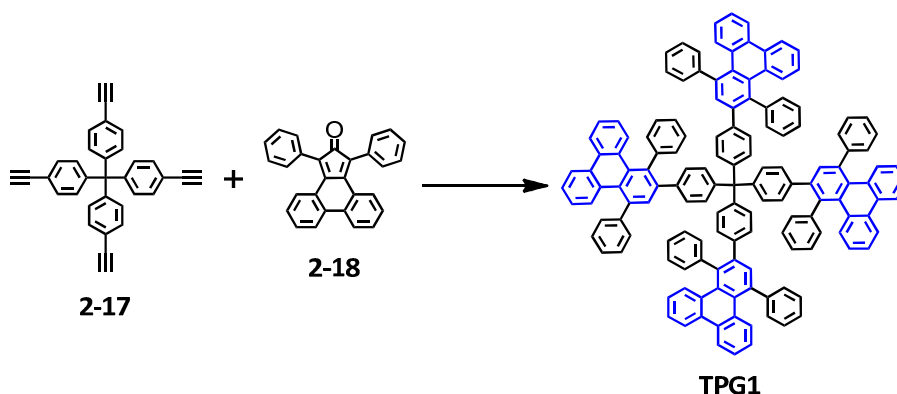
Scheme 2-4: Synthesis of first-generation polytriphenylene dendrimer (**TPG1**)

The synthesis of the higher-generation polytriphenylene dendrimers **TPG2** and **TPG3** with 12 and 28 triphenylene units, respectively, was carried out following the divergent synthetic protocol (Scheme 2-5). The reaction of AB$_2$-type building unit **2-9** and tetra(4-ethynylphenyl)methane (**2-17**) gave the first-generation dendrimer **2-19**, decorated with 8 triisopropylsiyl (TiPS) protected ethynyl groups in 81% yield. The desilylation of the

---

[1] Temperature: 170 °C, Pressure: 5 bar, Power: 300 W, Solvent: o-xylene, CEM Discover.

TiPS protecting groups with tetrabutylammonium fluroride (TBAF) yielded the first-generation dendrimer **2-20** with 8 activated ethynyl groups for further dendrimer growth in 90% yield. The subsequent Diels-Alder cycloaddition between dendrimer **2-20** and either the termination agent **2-18** or the AB_2 building unit **2-9** provided the unfunctionalized second-generation dendrimer **TPG2** in 94% yield or second-generation dendrimer **2-21** with 16 TiPS protected ethynyl groups in 88% yield, respectively. All TiPS units in dendrimer **2-21** were cleaved by TBAF, affording the second-generation dendrimer **2-22** with 16 activated ethynyl groups in 94% yield. Finally, the unfunctionalized third-generation dendrimer **TPG3** was obtained in 90% yield by continuing the Diels-Alder cycloaddition between dendrimer **2-22** and the end-capping unit **2-18**. The purification of higher generation dendrimers was achieved by either GPC column chromatography to remove unreacted building units after the cycloaddition reaction or precipitation in methanol after the TiPS deprotection step.
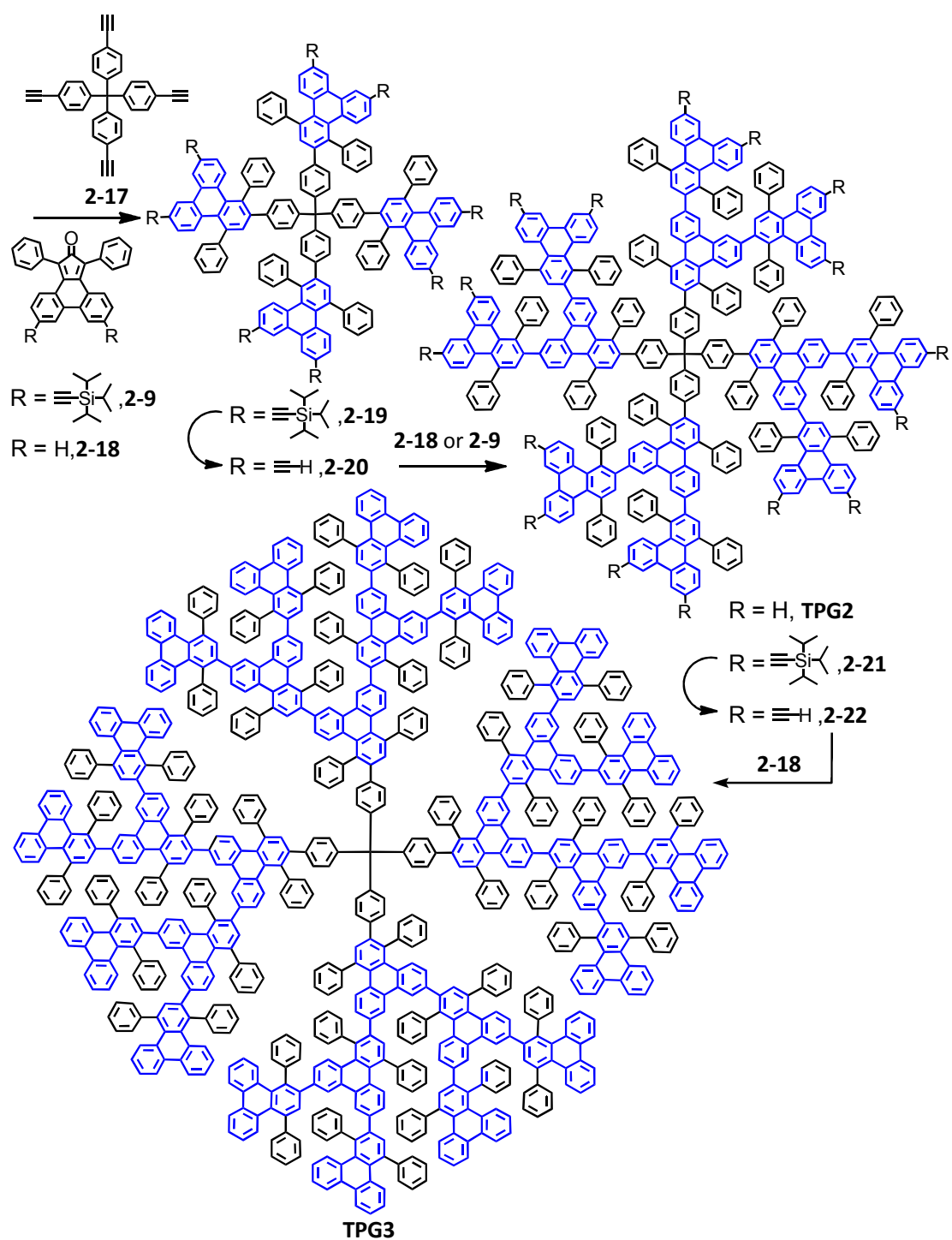
Scheme 2-5: Synthesis of second and third generation polyphenylene dendrimers (**TPG2** and **TPG3**).

For comparison, a model compound 1,2,4-triphenyltriphenylene **TTP** (Scheme 2-6) containing the triphenylene repeat unit was synthesized by the Diels-Alder cycloaddition reaction between ethynylbenzene and phencyclone **2-18**, checking the distortion of the triphenylene unit by the phenyl substitution and using it as monomeric unit for quantum yield determination. Furthermore, **a**nother second generation dendrimer **TPG2'** (Scheme 2-6) with peripheral pentaphenyl end-groups was prepared via the Diels-Alder cycloaddition reaction between the dendrimer **2-20** and tetraphenylcyclopentadienone **2-23** for comparison with **TPG2**. Here the scaffold containing triphenylenes were shielded by the phenylene shell completely, hindering intermolecular triphenylene aggregation.
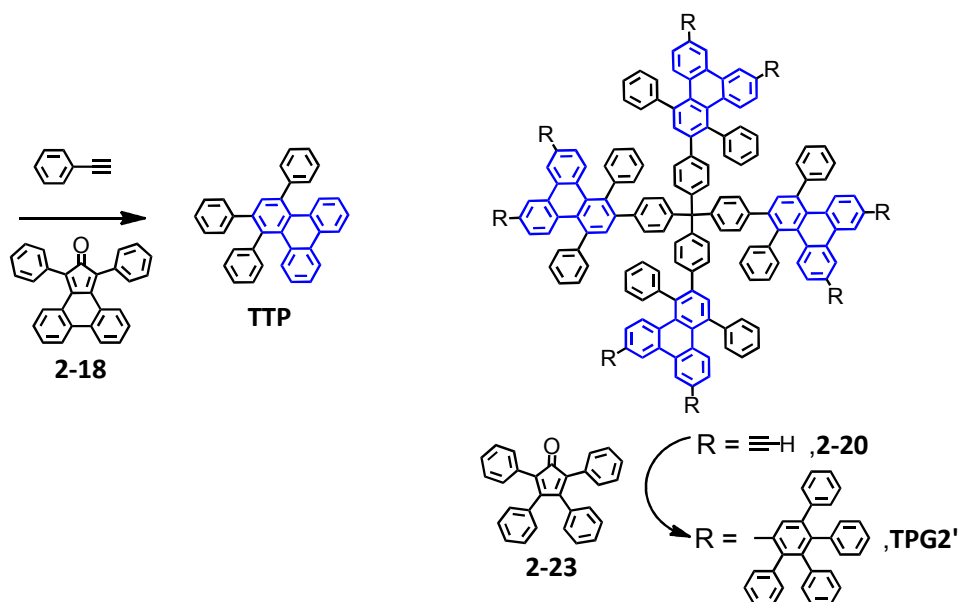
Scheme 2-6: Synthesis of model compound 1,2,4-triphenyltriphenylene **TTP** and peripheral pentaphenyl polytriphenylene dendrimer **TPG2'**

2.2.3 Characterization of the polytriphenylene dendrimers

The monodispersity of the described dendrimers could easily be verified by applying MALDI-TOF mass spectrometry. The MALDI-TOF mass spectra revealed a single intense signal corresponding to the calculated m/z ratio of dendrimers **TPG1**, **TPG2** and **TPG3**, as illustrated in Figure 2-3.
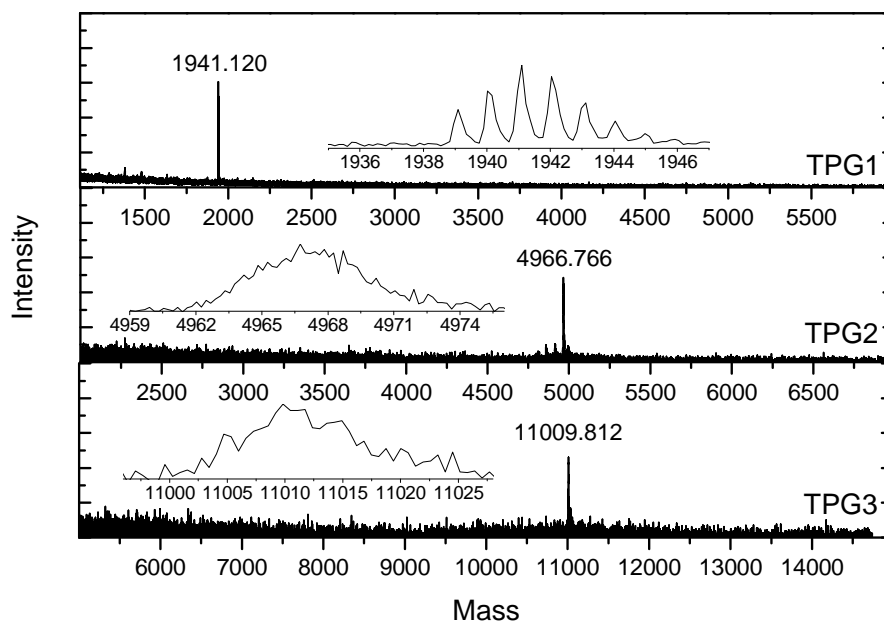
Figure 2-3: MALDI-TOF mass spectra of first to third generation polytriphenylene dendrimers **TPG1**, **TPG2** and **TPG3**.

The samples of all three generation polytriphenylene dendrimers (**TPG1**, **TPG2** and **TPG3)** for MALDI-TOF mass spectrometry were prepared by mixing the analytes with matrix which dissolved silver trifluoroacetate in dichloromethane in a ratio of 1/250. For the first-generation dendrimers **TPG1**, the experimentally determined m/z ratio was a single signal at 1941.120 $g \cdot mol^{-1}$, perfectly agreeing with the calculated value of 1940.628 $g \cdot mol^{-1}$ $(M+Ag)^+$, with an additional silver ion. For second- and third-generation dendrimers **TPG2** and **TPG3**, the MALDI-TOF mass spectra displayed a single intense signal at 4966.766 and 11009.812 $g \cdot mol^{-1}$, respectively, both in accord with their calculated m/z ratios. These three different generation samples indicated that MALDI-TOF mass spectrometry was probably the most efficient and powerful method for proving the structural perfection of polytriphenylene dendrimers with high molecular weights. Moreover, all generation dendrimers possessed enough solubilities in common organic solvent such as DCM, THF, and toluene, thus allowing their full characterization by standard analysis techniques such as NMR spectroscopy. Characterization by ^{1}H NMR spectroscopy showed well-separated and clearly assignable signals for the aromatic

triphenylene protons as well as for the ethynyl or TiPS protons. Figure 2-4 demonstrated the ^{1}H NMR of **2-20** as an example.
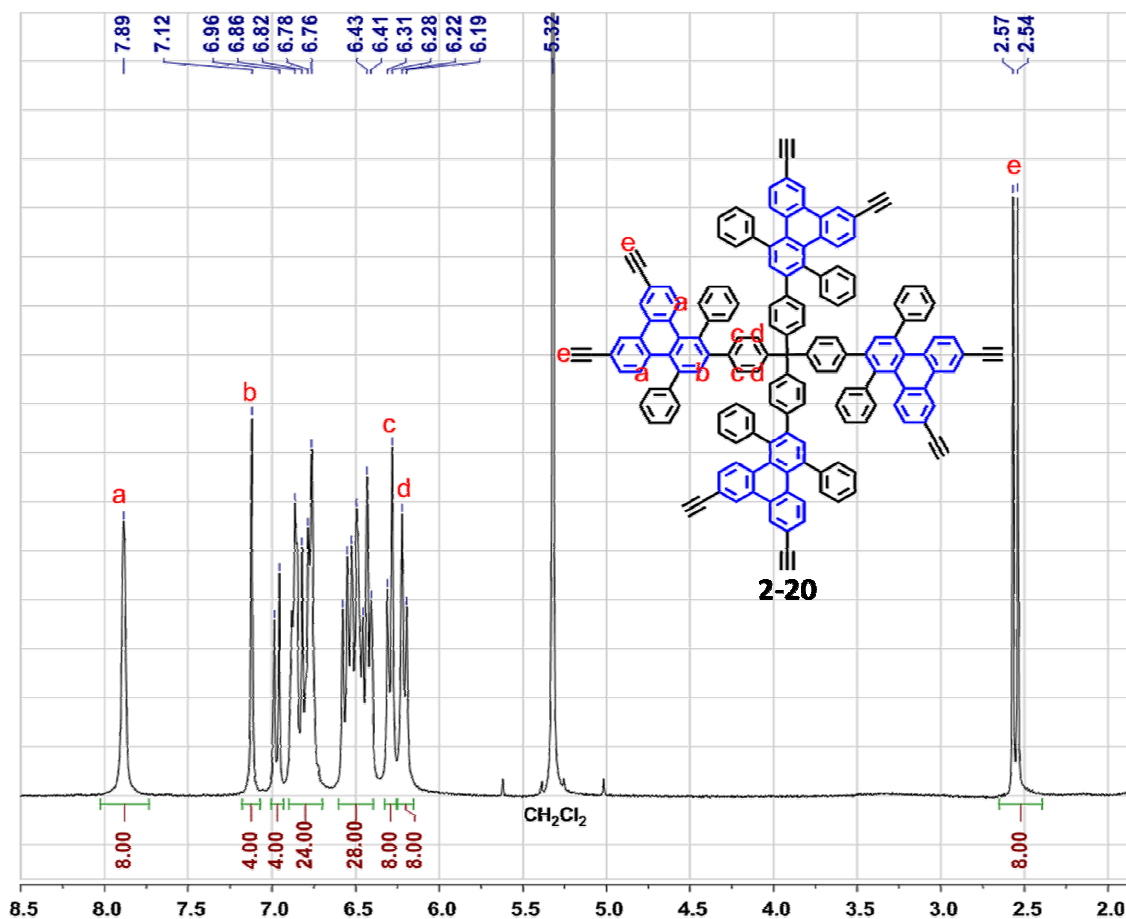
Figure 2-4: ^{1}H NMR spectrum of ethynyl substituted polytriphenylene dendrimer **2-20**.

The ethynyl protons (H$_e$) appeared like a doublet but in reality could be treated as two singlets with similar intensity and chemical shifts around 2.5 ppm. This was due to the co-excistence of different rotational conformers in equilibrated distribution. During the Diels-Alder cycloaddition, two rotational conformers were obtained, where the ethynyl groups were located in two different positions as para- or meta-substituents in respect to the newly formed triphenylene unit. In the aromatic region, only some protons on the triphenylene units and the tetraphenylmethane core could be assigned unambiguously. The proton H$_a$ of the triphenylene units appeared as a singlet at low field (7.89 ppm), and the proton H$_b$ also showed a singlet but with a down-field shift at

7.12 ppm, due to the deshielding effect of the adjacent phenyl ring. Moreover, the protons H_c and H_d of the tetraphenylmethane core demonstrated doublets respectively at high field (6.31-6.28 and 6.22-6.19 ppm). The other aromatic protons could not be distinguished due to strong signal overlaps. For the higher generation dendrimers, these aromatic protons displayed unresolved signals thereby reflecting more complicated chemical shifts on different generation dendrons. In the case of the other ethynyl or TiPS-ethynyl substituted dendrimers, the intensity ratios between aromatic and aliphatic signals were all corresponding to the expected values.

2.3 Visualization and simulation

2.3.1 Crystal structure of the first generation polytriphenylene dendrimer

To investigate the spatial arrangements of polytriphenylene dendrimers and their optimum tetrahedral geometry, single crystal X-ray analysis was performed as most direct method to investigate the spatial arrangements of polytriphenylene dendrimers and their structural features.[37] The single crystal of **TPG1** suitable for structure determination was obtained from a mixture of tetrachloroethane and hexane at room temperature by slow evaporation as colorless, tiny, needle-shaped crystals. The X-ray single crystal measurements were performed by Dr. Christopher Anson at the Forschungszentrum Karlsruhe. The pertinent crystallographic data, such as cell parameters, interplanar angles, and assignment of the planes as well as measuring conditions are provided in Table 2-1.

The projections of the crystal structure from different views are shown in Figure 2-5a. The **TPG1** molecule is located on a center of symmetry in a monoclinic cell (space group C2/c), with the cell parameters as a = 17.46 Å, b = 10.81 Å, c = 35.86 Å and β = 91.0°, and the single crystal contains two well ordered hexane (red marked) and two linked tetrachloroethane (yellow and green marked) molecules per dendrimer unit.

Table 2-1: X-ray data for **TPG1**, experiment details, structure solutions and refinements.

Compound	TPG1
Formula	$C_{171}H_{148}Cl_4$
Formula Weight M	2344.69
Crystal System	monoclinic
Space group	P 2/c
a (Å)	17.464(4)
b (Å)	10.811(2)
c (Å)	35.858(8)
α (º)	90.00
β (º)	91.005(4)
γ (º)	90.00
V (Å^3)	6769(3)
Z	2
ρ_{calc} (g×cm^{-3})	1.150
μ (MoKα) (mm^{-1})	0.141
F(000)	2484
R-Factor (%)	12.84
Color	Colorless
Shape	Needles
Temperature (K)	150(2)
Radiation, λ(Å)	MoKα, 0.80024
ϑ Min-Max (º)	2.48-21.39
Total data	12980
Unique data	5335
Observed data	2484

The four central phenyl rings of the tetraphenylmethane substituents are oriented with approximately tetrahedral symmetry, which suggests that all triphenylene subunits are separated by the tetraphenylmethane core and the angles between them are 86.4°, 84.5° and 83.5°. Moreover, the angle of torsion between two closest intermolecular

triphenylene subunits is 89.7° and the shortest distance is 3.73 Å. This suggests that all triphenylene subunits in **TPG1** possess inter- and intra-molecularly nearly perpendicular arrangement with minimum packing effect.[38]
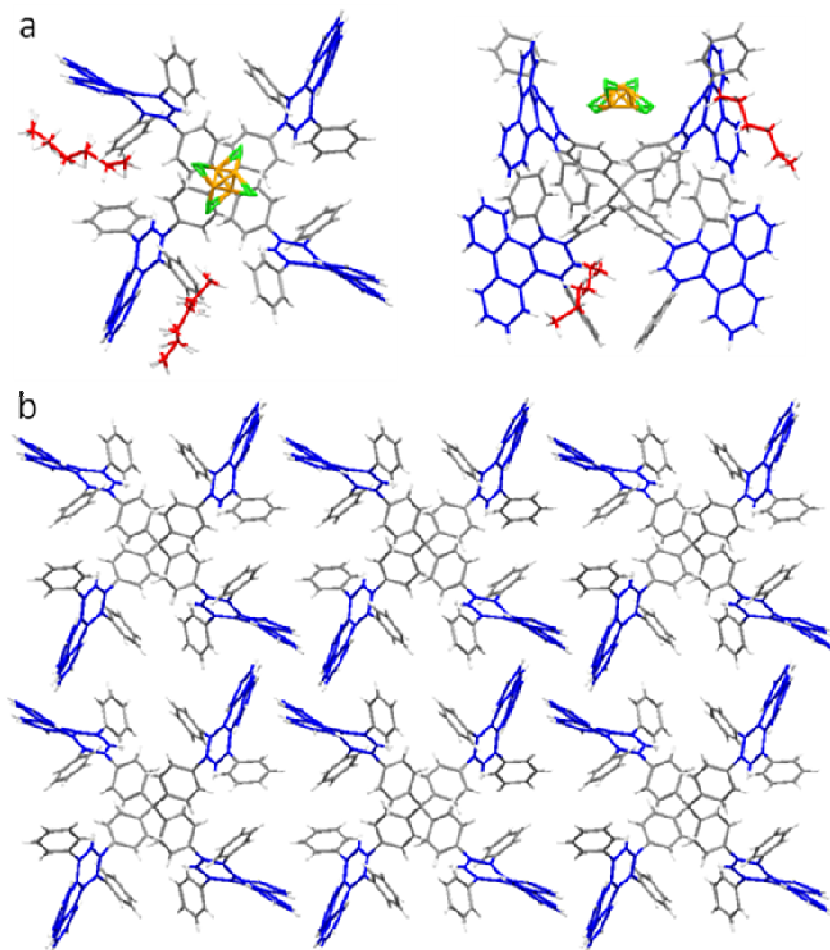
Figure 2-5: Crystallographic structures of **TPG1** (a) single crystal structure from *a*-axis view (left) and *c*-axis view (right), (b) packing diagram of crystals.

The crystal structure of the first-generation dendrimer **TPG1** displays that the attached phenyl rings produce a high steric shield and torsion of triphenylene subunits. Because of the rotation between triphenylene repeating units and the shape persistence of substituted phenyl rings, the triphenylene repeating units in higher generation dendrimers can be expected in even more twisted arrangement and with more pronounced shielding. [39]

The packing diagram reveals that these dendritic molecules exhibit a high perturbation of the packing within each triphenylene owing to the steric hindrance between the dendrimers (Figure 2-5b). This demonstrates that in polytriphenylene dendrimers the conformation of each triphenylene groups is highly twisted so that they cannot undergo π-stacking. The distance between two closest twisted triphenylene units in two neighboring dendrimer crystals is ca. 3.2 Å. In contrast to most other triphenylene derivatives the inter-dendrimer chromophore-chromophore quenching is thus much reduced.

2.3.2 Molecular modeling

Due to their large number of possible conformations, crystals of higher generation polytriphenylene dendrimers suitable for structure determination have never been obtained. In order to investigate the size, shape and structure of higher generation dendrimers, it was useful and could be performed in a molecular modeling force field (MMFF) method, because of the large number of atoms in these dendritic molecules.[40] The obtained structure for the first-generation dendrimer **TPG1** is depicted in Figure 2-6, which displays an almost perfect similarity to the single crystal structure of **TPG1**. This suggests that molecular modeling is a relatively reliable method to determine the structure of high generation polytriphenylene dendrimers. Table 2-2 lists the molecular weights and the radii of the unfunctionalized dendrimers **TPG1**, **TPG2**, and **TPG3**, obtained from MMFF simulation.

Table 2-2: Number of triphenylene units, molecular weights and radii of dendrimers **TPG1**, **TPG2**, and **TPG3**

	TPG1	TPG2	TPG3
no. of triphenylene units	4	12	28
molecular weight	1833	4858	10908
radius / nm	1.40	2.29	3.11
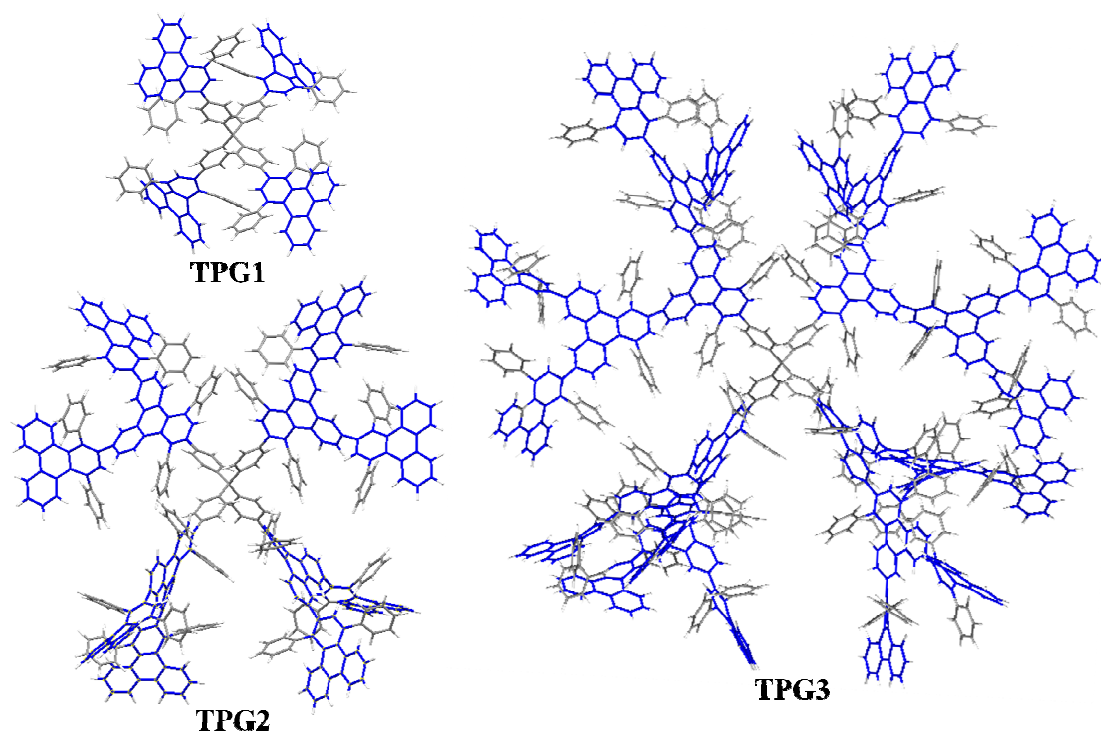
Figure 2-6: Three-dimensional structures of dendrimers **TPG1**, **TPG2**, and **TPG3**, obtained by molecular modeling using the MMFF method.

An almost linear increase of the radius can be found along with the increasing dendrimer generations from 1.40 nm for **TPG1** to 3.11 nm for **TPG3**; whereas the number of triphenylene chromophores increases exponentially. When the number of triphenylene chromophores is plotted against the radius of the corresponding dendrimer, their bilinear relationship (Figure 2-7a) demonstrates that the dendrimer shell becomes more and more dense along with increasing dendrimer generation. These polytriphenylene dendrimers exhibit a molecular structure that can be described by the "dense-shell" model,[41] which will increase the charge injection abilities in the periphery of dendrimers.[42] However, a linear trend appears when the number of triphenylene chromophores is plotted against the volume of the dendrimer (Figure 2-7b), indicating that the density of the chromophores was constant irrespective of the generation. These relationships indicated that the growing dendrimer generation will not deteriorate the distribution and separations of chromophores thus reducing the photoluminescence quantum yield (PLQY) in solid film. Moreover, higher generation

dendrimers possess more conjugating chromophoric units, which is a more important issue to increase the PLQY.[43] Therefore, the syntheses of high generation polytriphenylene dendrimers are necessary to investigate high performance blue OLEDs.
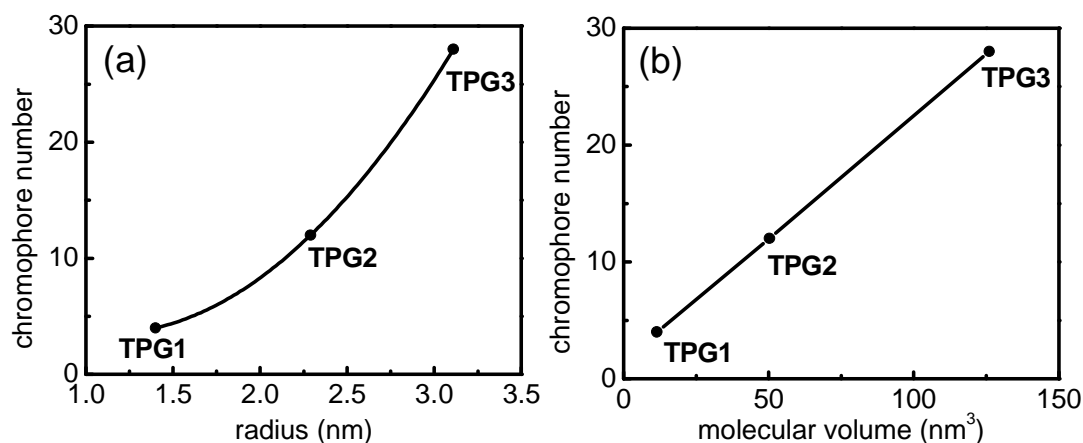
Figure 2-7: Numbers of triphenylene units versus dendrimer radius (a) and volume (b) $V = 4/3\pi r^3$.

2.4 Physical properties of polytriphenylene dendrimers

The dendritic architecture and different generation number provide a unique target for investigating the effect of chromophore spacing on the emission and transport properties of OLEDs. As shown in Table 2-2, the number of triphenylene chromophores in the dendrimers increases as $4 \times (2^G - 1)$ with generation number (G). Most importantly, as a new type of blue fluorescent materials, the photophysical properties of our polytriphenylene dendrimers will be investigated in the following paragraphs.

2.4.1 Photophysical properties in solution

Figure 2-8 shows the absorption and PL spectra of three generations of polytriphenylene dendrimers (**TPG1**, **TPG2**, and **TPG3**) and two comparable compounds (**TTP** and **TPG2'**) in toluene solutions (10^{-3} g/L).
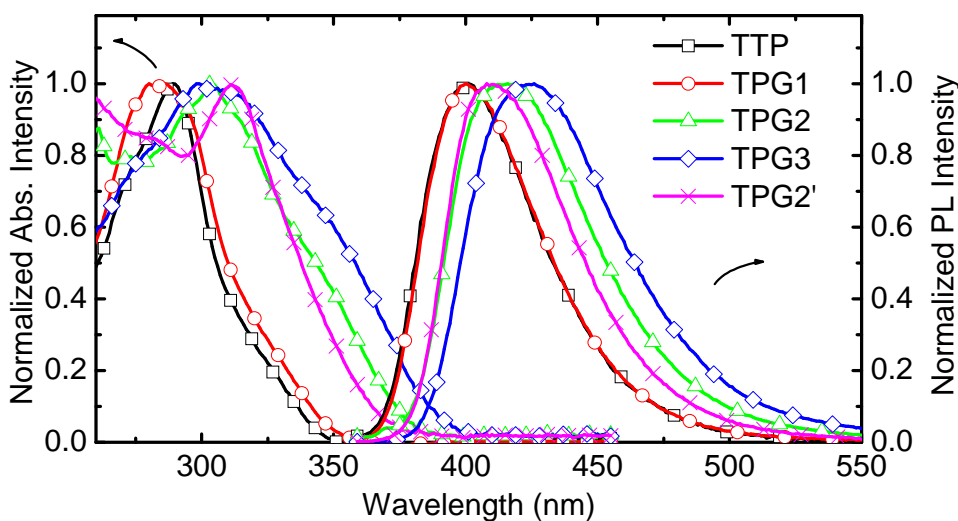
Figure 2-8: Normalized absorption and PL spectra of dendrimers (**TPG1**, **TPG2**, and **TPG3**) and two comparable compounds (**TTP** and **TPG2'**) in toluene solutions (10^{-3} g/L).

In the absorption spectra, samples **TTP** and **TPG1** demonstrate nearly identical curves, since the 4 **TTP** units in **TPG1** are connected through a sp3 carbon and therefore they both have the same chromophores. With the elongation of the longest conjugated oligotriphenylene segments going from **TPG1** to **TPG3**, the long-wavelength feature displays a substantial increase with growing generation, whereas the short-wavelength feature remains virtually unchanged. The effect is even more pronounced in solutions of the material, where quantum-chemical calculations could clearly demonstrate that the short-wavelength feature arises solely from the single triphenylene chromophore and the long-wavelength absorption is attributed to the effective conjugation in oligotriphenylene dendrons.[44] Indeed, besides providing a real space visualization of the molecular electronic modes involved in absorption, semi-empirical calculations can also explain the increase in the long-wavelength absorption strength with generation. The fact that the absorption features of the dendrimer showed bathochromic shifts with increasing molecular size can be taken as evidence for excitonic localization at the center of the molecule.[45] The broadening of absorption peaks are assigned to the asymmetry caused by the attached phenyl rings, thus increasing the oscillator strength of the symmetry forbidden $S_0 \rightarrow S_1$ and $S_0 \rightarrow S_2$ transitions.[46]

In the PL spectra, the emission maxima of different generation dendrimers show a bathochromic-shift from **TPG1** to **TPG3** since the effective conjugation length in triphenylene repeating units extends along with increasing generation. Therein, dendrimer **TPG2'**, which is an end capped version of the first generation dendrimer, has its peak positions situated between **TPG1** and **TPG2**. In fact, a closer look at the chemical structures reveals that the end caps resemble almost a second generation dendrimer, only lacking the connection at the outmost phenyl rings. Therefore it consists of longer segments than the **TPG1**, but is supposed to be more twisted than **TPG2**. Thus dendrimer **TPG2'** can be understood as a "link" between **TPG1** and **TPG2**.

The full widths at half maximum (FWHMs) of dendrimers broaden from 53 nm of **TPG1** to 66 nm of **TPG3** (Table 2-3), since the molecular sizes and conformation distributions of the dendrimers increase along with the growth of generations.[47] Nevertheless, the very large Stokes shifts ($\approx$ 110 nm) of all dendrimers are caused by the fact that absorption happens mainly from $S_0 \rightarrow S_4$ and emission from $S_1 \rightarrow S_0$.[48] The emitted photon has less energy than the absorbed photon, in which the losing energy part is used to twist triphenylene units with highly steric hindrance and causing various isomeric conformations.

The intermolecular interactions and aggregations of dendrimers **TPG1**, **TPG2** and **TPG3** were investigated by measuring the absorption and PL spectra of their toluene solutions at different concentrations (10^{-4}, 10^{-3}, and 10^{-2} g/L), but no bathochromic-shift and excimer emissions could be observed. This concentration independence suggested that the dendritic branches in each dendrimer effectively suppressed the intermolecular interactions and prevented the formation of aggregates.[49] The absence of aggregation was also evidenced by the rather high photoluminescence quantum yields (PLQYs) of these dendrimers (Table 2-3). With quinine sulfate as a standard,[50] the quantum yields of dendrimers **TPG1**, **TPG2** and **TPG3** in dilute toluene solutions (10^{-6} M) were measured as 6.6, 27.0, and 35.2%, respectively. These values revealed an increasing PLQY scaling with the size of the molecules. This could be ascribed to the reduced branch rotation in higher generations which decreases the vibrational relaxation and the intersystem

crossing in the excited state. Another plausible explanation for the higher PLQY in higher generations is the interactions between the chromophores and environment. With increasing dendritic generation, the central chromophores in the larger molecules are more effectively self-encapsulated,[51] which depresses the interactions among the chromophore themselves or between the chromophores and solvent molecules and therefore fluorescence quenching.

Table 2-3: photoluminescence quantum yields (Φ_P) of dendrimers (TPGx) and compound (TTP) in chloroform solution, relative to quinine sulfate dehydrate, and the full widths of half maximum (FWHMs) of their PL spectra in toluene with a concentration of 10^{-3} g/L.

	TTP	TPG1	TPG2	TPG3	TPG2'
Φ_P (%)	3.8	6.6	27.0	35.2	14.8
FWHM (nm)	53	53	62	66	55

2.4.2 Photophysical properties in thin film

Figure 2-9 shows the absorption and PL spectra of all samples in solid states. The thin films of all samples were prepared by spin coating on quartz substrate from toluene solution. The maxima of absorption from bulk films showed slight bathochromic shifts ($\approx$10 nm) for all dendrimers according to intermolecular aggregates in thin films. The most remarkable fact is that the absorption happens mainly from $S_0 \rightarrow S_3$ and $S_0 \rightarrow S_4$, since $S_0 \rightarrow S_1$ and $S_0 \rightarrow S_2$ are symmetry forbidden in isolated triphenylene molecules and only unresolved shoulder peaks could be observed around 350 nm.[48] The broadening of the high-wavelength flank of absorption peaks could be due to reduced symmetry caused by the non-planarity, attached phenyl rings and the neighboring triphenylene units, thus increasing the oscillator strength of the $S_0 \rightarrow S_1$ and $S_0 \rightarrow S_2$ transitions.[45]
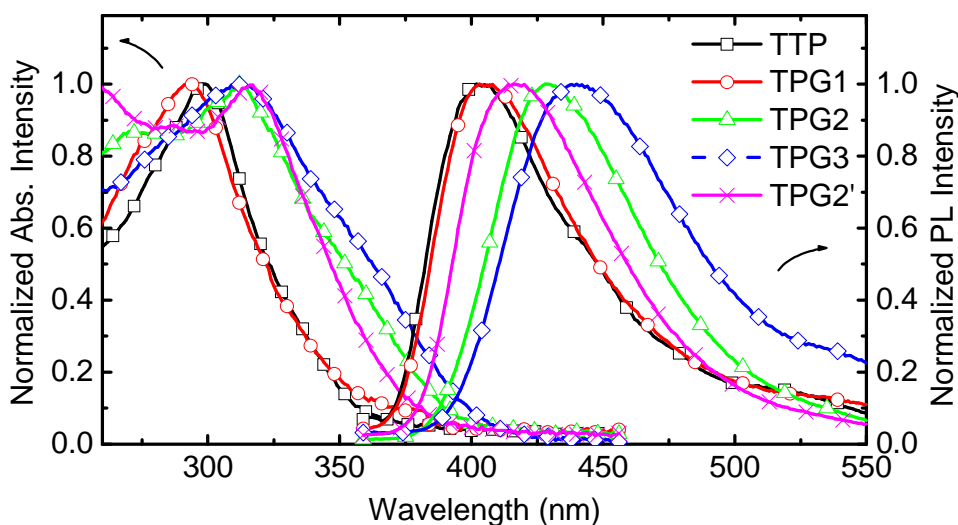
Figure 2-9: Normalized absorption and PL spectra of dendrimers (**TPG1**, **TPG2**, and **TPG3**) and two comparable compounds (**TTP** and **TPG2'**) in thin film.

Moreover, in the PL spectra of **TTP** and **G1**, a bathochromic shift of 1 and 6 nm at emission maximum, respectively, was observed compared to those of the solutions; whereas dendrimers **G2** and **G3** displayed a more pronounced bathochromic shift of 17 to 18 nm, respectively, compared to their corresponding solution spectra. We attribute this bathochromic shift to the solid state packing which leads to increased coupling of individual **TTP** units with increasing generations.[52] Like observed before, the behavior of the end capped dendrimer **TPG2'** is between **TPG1** and **TPG2** with a peak shift of approximately 10 nm.

2.4.3 Stability of polytriphenylene dendrimers

A critical criterion for emissive materials for blue OLEDs is their stability, which determines the device lifetime.[53] The major problem is the susceptibility of extended conjugated systems to be attacked by oxygen and/or water, which cannot be totally excluded even by the best device encapsulation techniques provided by dendritic architecture. In most emissive dendrimers, such as poly(para-phenylene vinylene) (PPV) dendrimers,[24, 54] the most vulnerable sites are the vinylene moieties. These could be protected by direct attachment of electron-withdrawing groups to them, but this is not

always possible and may have undesirable effects upon the emission color.[55] In polyarylenes, electron-rich units such as thiophenes appear to be susceptible to direct attack by oxygen,[56] while in bridged polyphenylenes such as polyfluorenes the main problem is oxidation at the bridgeheads to produce emissive ketones that act as traps and so bathochromic-shift the emission.[57]
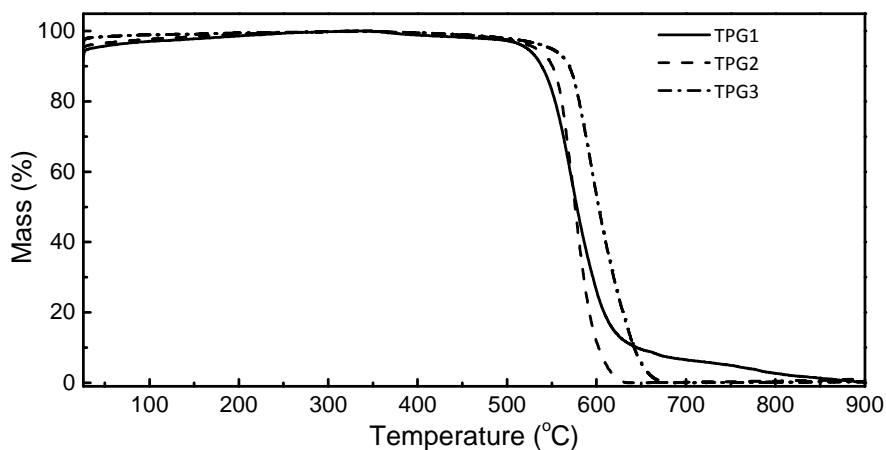
Figure 2-10: Thermogravimetric analysis of dendrimers **TPG1**, **TPG2** and **TPG3.**

Polytriphenylene, one kind of PAH, shows very high thermal and chemical stability.[58] The thermal properties of polytriphenylene dendrimers **TPG1**, **TPG2** and **TPG3** were studied by thermogravimetric analysis (TGA) and shown in Figure 2-10. In an N_2 atmosphere, they exhibited degradation above 450 °C, which was similar to other reported polyphenylene dendrimers, revealing the long life-time potential of these polytriphenylene dendrimers in OLEDs.

To investigate the oxygen sensitivity and emission stability, thermal degradation experiments of devices were examined. All dendrimers and small molecule **TTP** were quite stable up to 100 °C in air. After temperature increasing, **TTP** started to degrade at 150 °C and was almost totally destroyed after the 200 °C. **TPG1** and **TPG3** displayed a slight increase of the long wavelength tail at 200°C, whereas **TPG2** and **TPG2'** remained stable throughout the whole procedure, even after annealing at 200 °C in air for 2 hours (Figure 2-11). The emission were still stable in blue light range at 440 nm for **TPG2** and

420 nm for **TPG2'**, respectively. These thermal and chemical stability measurements indicated that **TPG2** and **TPG2'** would be processable in OLED fabricating.
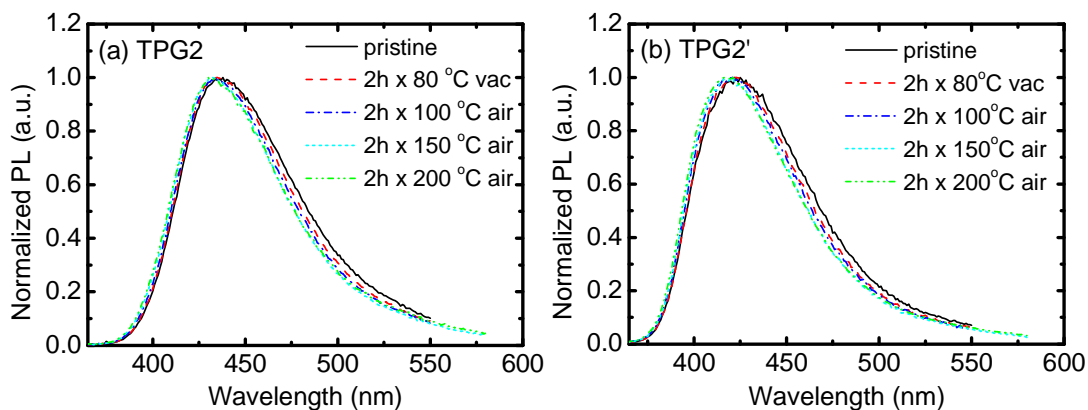

Figure 2-11: Thermal degradation of dendrimer **TPG2** (a) and **TPG2'** (b).

2.5 Blue OLEDs based on polytriphenylene dendrimers

2.5.1 Stability of polytriphenylene dendrimer based OLEDs

In order to find the most promising candidates for blue OLEDs, the EL color stability of OLED devices based on all dendrimers were measured at various voltages and operation times. Figure 2-12 shows voltage and time dependent EL spectra of all samples. Compared to solid state PL spectra, all dendrimer devices displayed bathochromic shifts of EL maxima along with the increase of driving voltage and delay of time. Since the dendrimers possessed a strong Stokes shift, self absorption within the emitting layer should not be responsible for these shifts. All dendrimers showed an additional peak at 680 nm, especially significant for **TTP** and **TPG1**, during long-term operation, due to the oxidation.[59] Moreover, dendrimer **TPG1** and **TPG3** also had another peak around 550 nm. The peak shifts and additional features are not fully understood yet, but they have to be overcome in order to achieve stable blue emission. Herein, compared to other generation dendrimers, second generation dendrimer **TPG2** and **TPG2'** possessed much higher voltage and time stabilities as the most promising candidates with suitable molecular sizes for long life-time blue OLEDs.
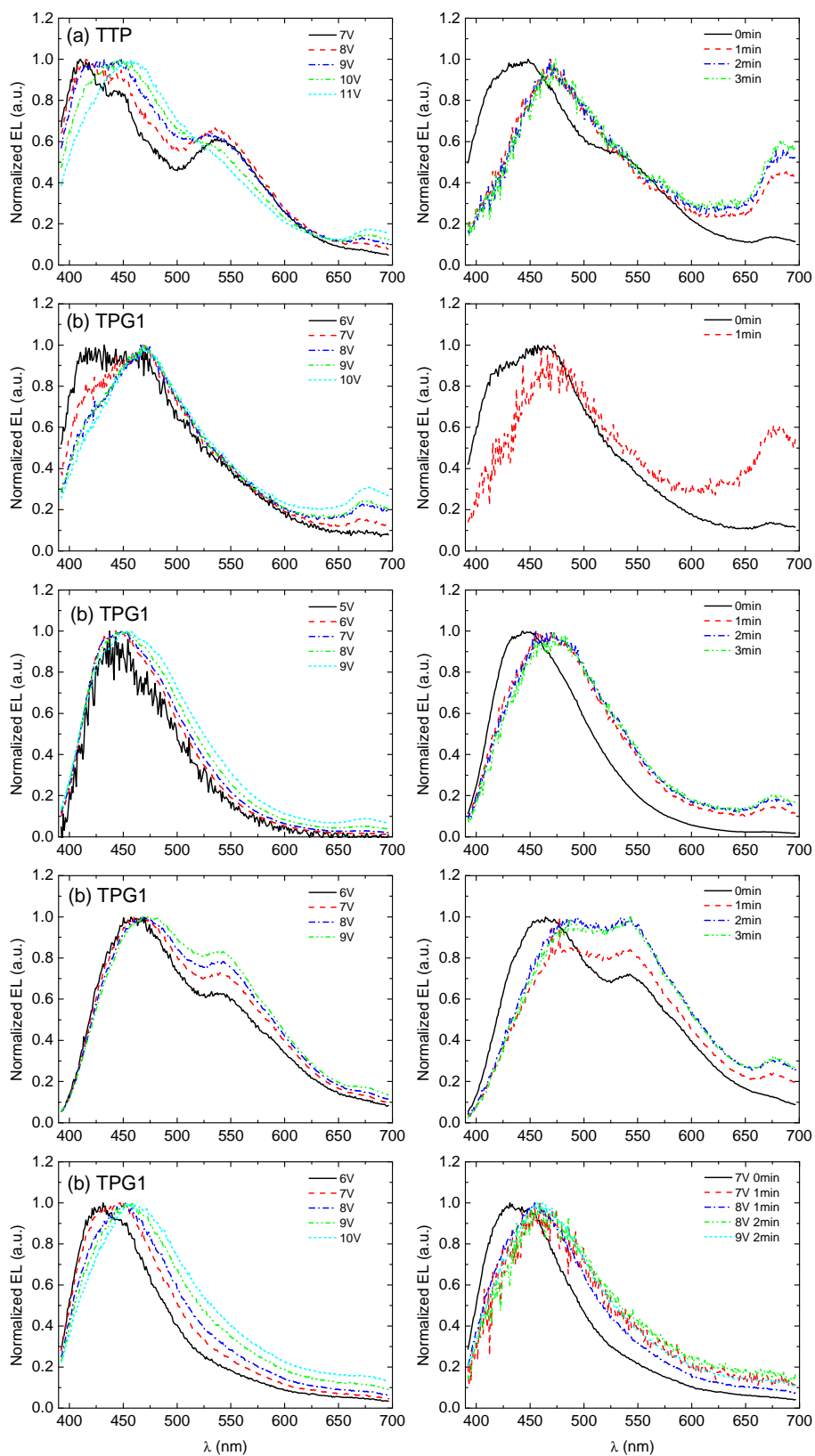
Figure 2-12: Voltage (left) and time dependent (right) EL spectra of triphenylene based OLEDs.

2.5.2 Fabrication of polytriphenylene dendrimer based OLEDs

The polytriphenylene dendrimer based OLED devices were processed and characterized by our corporate partners, Horst Scheiber, Wolfgang Wiedemair, and Prof. Emil List at Graz University of Technology.

As the most promising candidate, **TPG2** was firstly fabricated into an OLED device with a standard sandwich geometry: indium tin oxide (ITO)/poly(3,4-ethylenedioxythiophene) doped with poly(styrene sulfonate) (PEDOT:PSS)/**TPG2**/Ca/Al. Figure 2-13 shows the scheme of the structure of these dendrimer based blue OLED devices. The ITO covered glass substrates were firstly etched using oxygen plasma. Then a PEDOT/PSS layer was applied by spin coating at a speed of 3000rpm x 20s and heated for 15min in vacuum at 150 °C. The dendrimer emissive layer was spin-coated (1500rpm x 12s plus 3000rpm x 30s) afterwards from a toluene solution with concentration of 10 g/L and subsequently heated for 2 hours in vacuum at 80 °C. The electrodes were evaporated in an argon box (10 nm Ca and 100 nm Al).
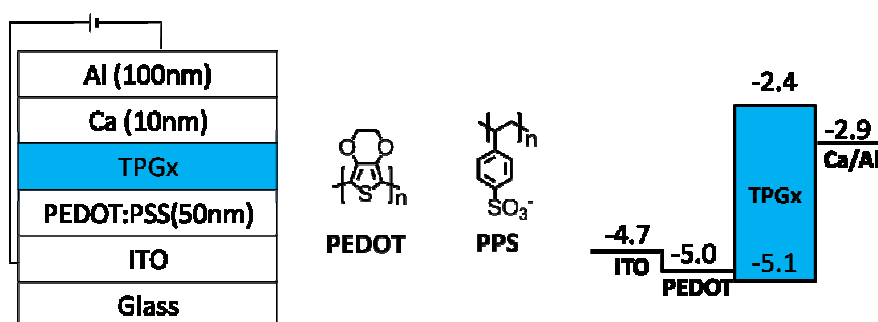
Figure 2-13: Schematic diagram of polytriphenylene dendrimer based electroluminescence (EL) device configurations (left), structures of poly(3,4-ethylenedioxythiophene) (PEDOT), and poly(styrenesulfonate) (PSS) (middle), and energy levels of EL devices (right).

2.5.3 Performance of polytriphenylene dendrimer based OLEDs

Figure 2-14 shows the current density and luminescence versus voltage (I-V-L) characteristics of OLED with dendrimer **TPG2** as the emitting layer. The device emits a deep-blue electroluminescence with a maximum brightness of 100 cd/m^2 at a bias voltage of 9 V, but the stability is low and moreover, efficiencies are extremely low with

less than 0.02 cd/A. This suggests that morphological issues (holes in the active layer),[60] crystallinity[61] or a highly imbalanced charge injection or transportation occurs in the device which prevents effective charge carrier recombination.[62]
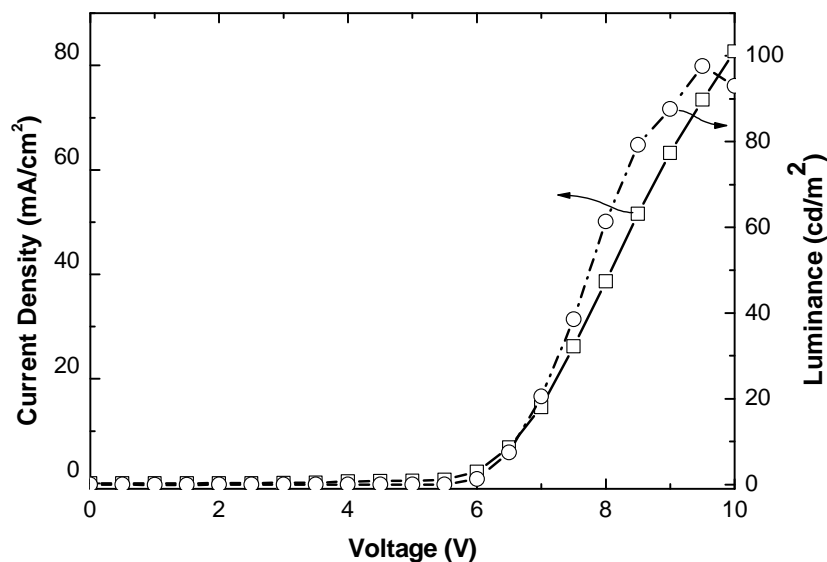
Figure 2-14: I-V-L characteristics of an ITO/PEDOT/**TPG2**/Ca/Al device.

The morphology of **TPG2** on the substrate has been investigated by atomic force microscopy (AFM) in order to confirm the reason of low device performance (Figure 2-15). The AFM image displayed that the morphology of an approximately 50 nm thick film revealed a rather flat surface without pinholes or other major irregularities. Over a 10 x 10 µm scanning area a mean roughness of less than 1 nm was found, which would be sufficient for device fabrication.
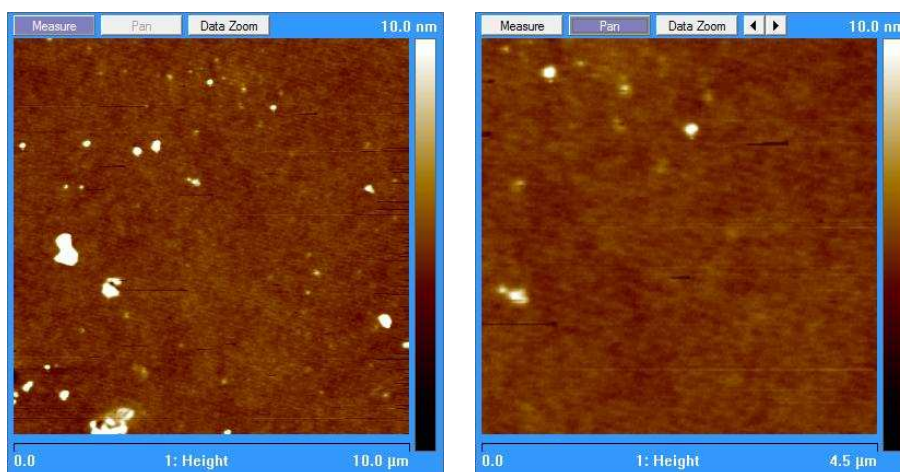
Figure 2-15: AFM height images at 10 µm (left) and 4.5 µm (right) scan sizes on the surface of a 50 nm thick **TPG2** film.

The crystallinity of dendrimer **TPG2** has been determined by wide-angle X-ray scattering (WAXS) measurements. Figure 2-16 shows WAXS patterns of an ITO substrate, a pristine **TPG2** film and an annealed **TPG2** film (both approximately 50 nm thick). Except for the ITO peaks there are no additional textures visible on either film and therefore crystalline structures are also very unlikely to be responsible for the bad device performance.
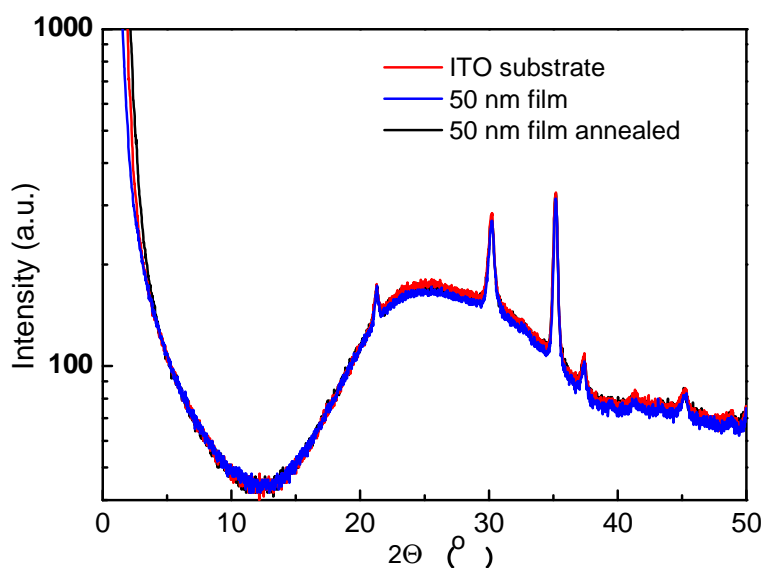
Figure 2-16: WAXS patterns of the ITO substrate, pristine **TPG2** film and annealed **TPG2** film.

If imbalanced charge carrier mobility is responsible for the unsatisfying performance, an additional electron transporting / hole blocking layer (ETL/HBL) could improve the performance of the fabricated OLEDs.[63] We were unable to determine the redox potentials of 1,3,5-tris(2-N-phenylbenzimidazolyl)-benzene (TPBI) (Figure 2-17) by cyclic voltammetry, but its highest occupied molecular orbital (HOMO) level has been reported to be 6.2 eV and lowest unoccupied molecular orbital (LUMO) 2.7 eV.[64] Therefore, the electrons and holes would be expected to recombine in the emissive dendrimer layer. Moreover, the Ca cathode was replaced to CsF/Al electrode in order to enhancing the electron injection ability.[65]
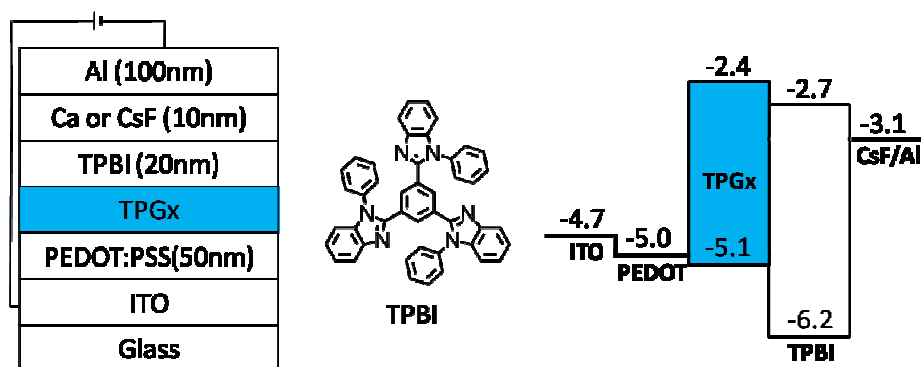
Figure 2-17: Schematic diagram of electroluminescence (EL) device configurations containing a ETL/HBL layer (left), structure of 1,3,5-tris(2-N-phenylbenzimidazolyl)-benzene (TPBI) (middle), and energy levels of EL devices (right).

We firstly tried to blend dendrimer **TPG2** with TPBI as the emissive layer, but did not get any improvements, except the blend emissive layer displayed a better color stability with almost no red-shift at lower voltages and higher efficiencies (0.07 cd/A). Unfortunately, the overall luminescence intensity was not improved (Figure 2-18) which could be explained by the fact that a blend improves electron transport, but is not able to block holes effectively from reaching the cathode.
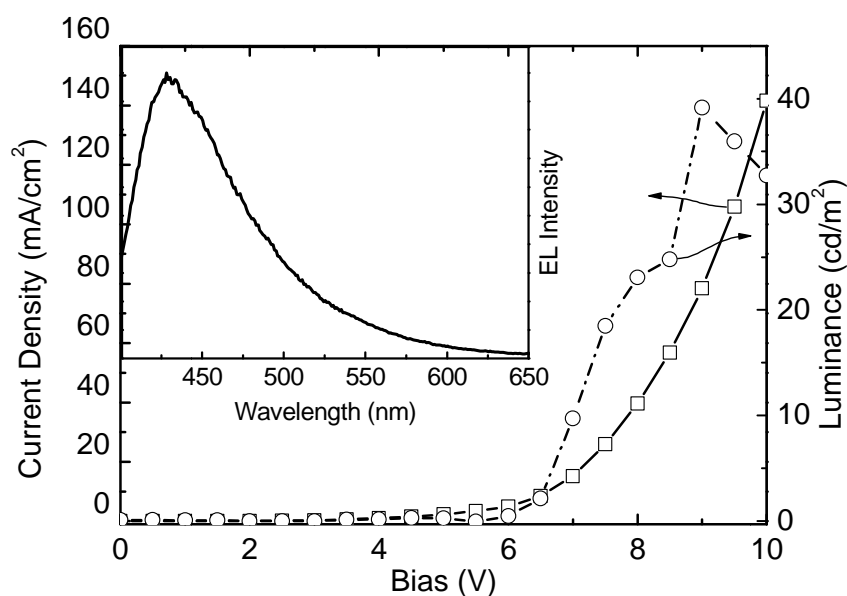
Figure 2-18: EL spectra (left) and I-V-L characteristics (right) of an ITO/PEDOT/**TPG2**:TPBi(1:1)/Ca/Al device.

Therefore the ETL/HBL should be applied by evaporation between the active layer and the top electrode to avoid recombination at the chemically unstable cathode interface. [64] Finally, **TPG2** were fabricated in the following configuration: ITO/PEDOT:PSS/**TPG2**/TPBI/CsF/Al. Figure 2-19 shows the *I-V* and *L-V* characteristics of **TPG2** based OLED with the ETL/HBL layer. The device emitted a deep-blue electroluminescence with a maximum brightness of 300 cd/m^2 at a bias voltage of 8 V and corresponding Commission Internationale de L'Eclairage (CIE) coordinates of (0.19, 0.18). The maximum of the EL spectrum located at 430 nm. Both the maximum and the shape of the EL spectrum are similar to the corresponding PL spectrum of a **TPG2** film. The excimer emission from chromophore aggregation and structure defect emission from oxidative degradation,[57, 66] which were always found for blue OLEDs, could not be observed in our dendritic system, indicating that the dendritic branches efficiently depress the intermolecular interaction. The device displayed an onset of electroluminescence at approximately 6 V and maximum efficiency of 0.4 cd/A.
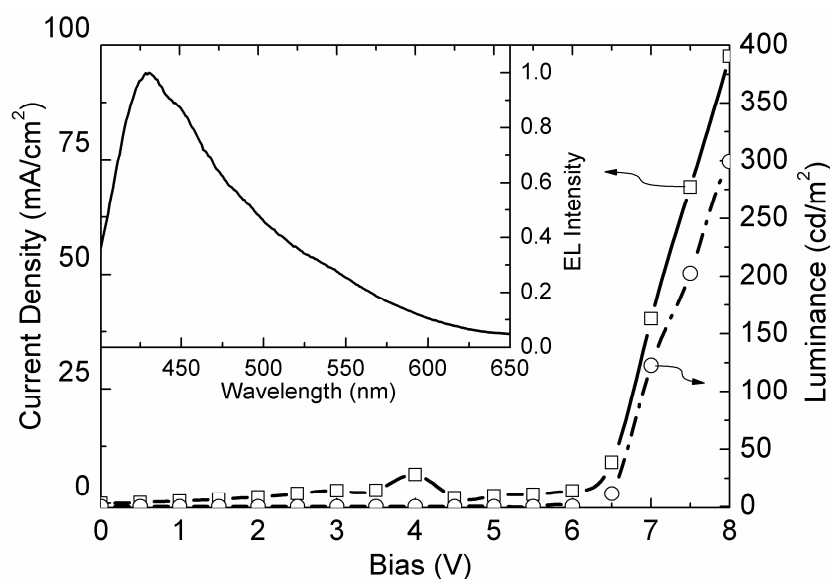
Figure 2-19: EL spectra (left) and I-V-L characteristics (right) of an ITO/PEDOT/**TPG2**/TPBi/CsF/Al device.

For comparison, the performance of the OLED based on dendrimer **TPG2'** was measured under identical conditions (Figure 2-20). The normalized EL spectrum resembled the thin

film PL spectrum very well and was located in a deeper blue region than **TPG2** with a maximum at 415 nm and corresponding CIE coordinates of (0.17, 0.10). At 10 V driving voltage, a maximum luminance of 400 cd/m² was found with an efficiency of 0.1 cd/A. Compared to **TPG2** this lower efficiency is mainly due to the relatively lower QY found from PL (Table 1). Another possibility may be that a remarkable part of the EL spectrum of **TPG2'** from the pentaphenyl shell is in the UV region and therefore does not contribute to the luminance value.
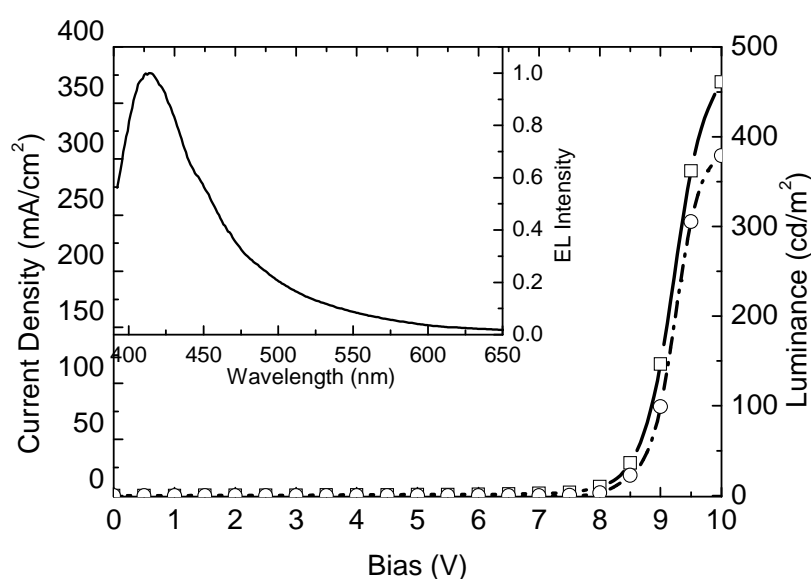
Figure 2-20: EL spectra (left) and I-V-L characteristics (right) of an ITO/PEDOT/**TPG2'**/TPBi/CsF/Al device.

Overall it became obvious that the performance of the presented devices can compete with the best reported fluorescence based blue emitting dendritic OLEDs with respect to device efficiency and brightness,[67] which also holds true for a comparison with fluorescent blue light emitting polymeric devices based on poly(*para*-phenylene) type polymers.[68] Utilizing transport moieties in the outer shell of the dendrimer and tuning of the emission color more from the UV to the blue region, both strategies successful implemented in OLED materials, will further allow for improvement of device performance in dendrimer based blue OLEDs.

From the point of view of synthesis, the divergent strategy shows high flexibility and provides a universal approach to adjusting the emission wavelength and increasing the quantum efficiency of these photoluminescence dendrimers. Theoretical considerations suggest that the addition of a highly PLQY blue emissive core such as pyrene, anthracene or fluorene to the aforementioned structure would result in a further significant improvement in luminance and efficiency. Moreover, the embedding of a longer wavelength emitting core, such as PDI, TDI or iridium complexes, as an acceptor opens a pathway to constrcut a light-harvesting system by using polytriphenylene dendrons as the donors. Therefore, the aim of this investigation is thus to assess the route of inserting an emissive core into the polytriphenylene dendrons, and its influences on the photophyical properties of the dendrimer as well as its OLED performances.

2.6 Blue fluorescent pyrene cored polytriphenylene dendrimers

To improve the efficiency of polytriphenylene dendrimer based blue light-emitting diodes, it is instructive to import other promising blue chromophores with high PLQYs into different positions of dendrimers. For example, starting from the fourfold ethynyl substituted blue chromophore 1,3,6,8-tetraethynyl-pyrene as the core, a series of polytriphenylene dendrimers based on pyrene core (**PYGx**) has been prepared in high yield.

2.6.1 Synthesis of pyrene cored polytriphenylene dendrimers

The synthesis of the 1,3,6,8-tetraethynylpyrene core (**2-24**) was according to a literature procedure[69] and depicted in Scheme 2-7. The bromination of pyrene resulted in the 1,3,6,8-tetrabromopyrene (**2-25**), which was recrystallized from nitrobenzene as a light brown solid in almost quantitative yield. The introduction of the ethynyl groups, required for the growth of the dendrimer, was firstly accomplished by four-fold

Sonogashira-Hagihara coupling reaction of **2-25** with trimethysilylethyne. While **2-25** is almost insoluble in common organic solvents, the trimethysilylethynyl groups in the product **2-26** provided a very good solubility, the pure 1,3,6,8-tetratrimethylsilylethynylpyrene was obtained by column chromatography as an orange solid. Subsequent cleavage of the trimethysilyl (TMS) protecting groups in **2-26** with TBAF in THF processed activated pyrene core **2-24** in quantitative yield. The solubility of **2-24** in common organic solvents was reduced because of the intermolecular stacking of the pyrene moieties. After repetitive precipitation and filtration, the 1,3,6,8-tetraethynylpyrene core was isolated and ready for the next dendrimer syntheses.
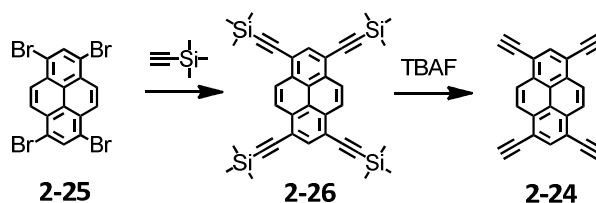
Scheme 2-7: Synthesis of 1,3,6,8-tetraethynylpyrene core (**2-24**).

The preparation of structurally defined polytriphenylene dendrimers with a pyrene core was realized by repetitive Diels-Alder cycloaddition and deprotection steps. The synthesis of the first- and second-generation dendrimer is depicted in Scheme 2-8. The first-generation pyrene cored polytriphenylene dendrimer **PYG1** was achieved from the Diels-Alder cycloaddition between 1 equivalents of 1,3,6,8-tetraethynylpyrene core **2-4** with 6 equivalents of phencyclone **2-18** in refluxing o-xylene in 91% yield. The first-generation dendrimer **PYG1** was as poorly soluble in common organic solvents as **TPG1**, thus the excess of **2-18** was removed by repetitive precipitation in methanol. The reaction of **2-24** with the AB$_2$ building unit 1,3-diphenyl-6,9-bis((triisopropylsilyl) ethynyl)-cyclopentaphenanthrenone (**2-9**) gave the first-generation dendrimer **2-29** in 91% yield, decorated with 8 triisopropylsily (TiPS) protected ethynyl groups. Quantitative desilylation of the TiPS protecting groups with TBAF yielded the first-generation dendrimer **2-30** in 88% yield with activated ethynyl groups for further dendrimer growth. The following Diels-Alder cycloaddition of dendrimer **2-28** with

termination unit **2-18** induced the unfunctionalized second-generation dendrimer **PYG2** in 84% yield, which is very good soluble in common organic solvents.
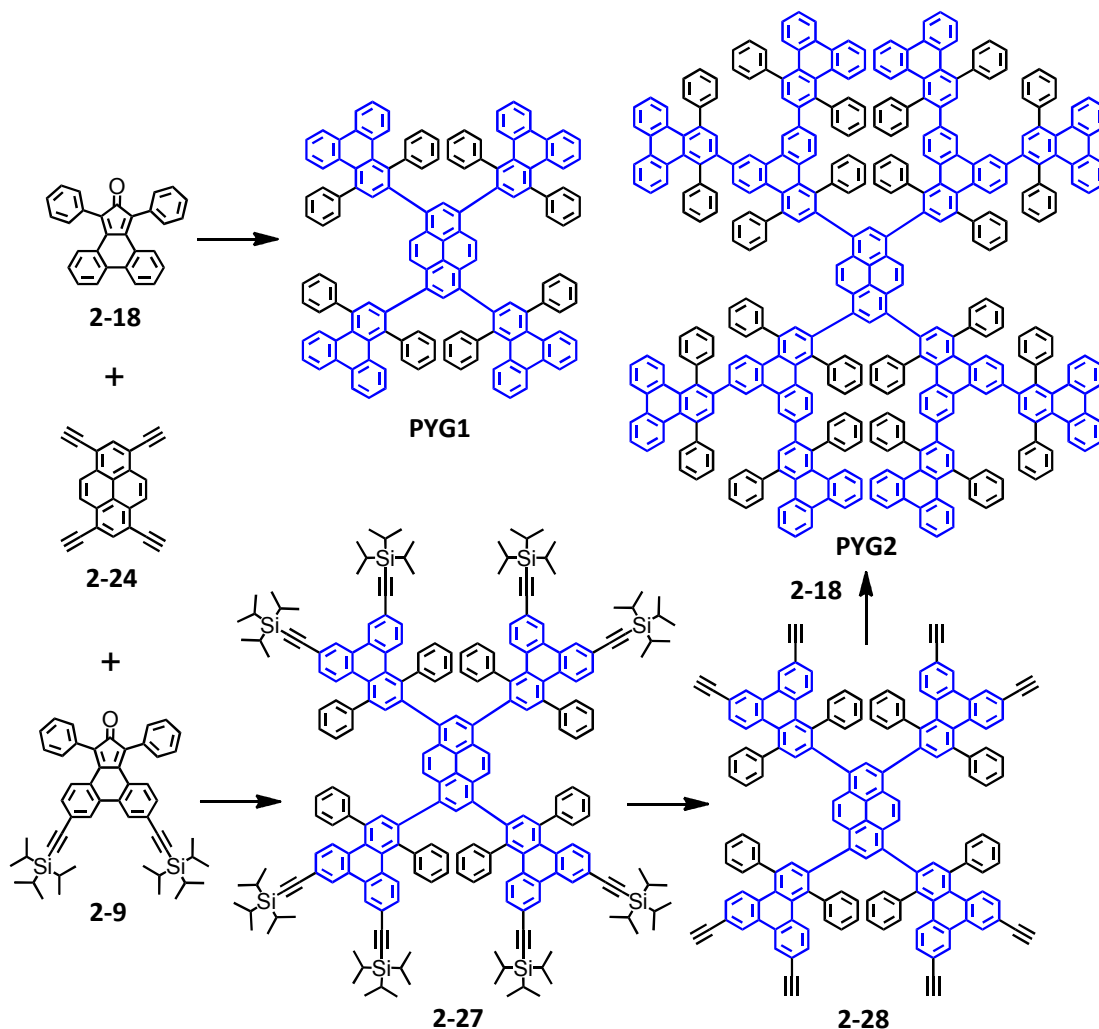
Scheme 2-8: Synthesis of first and second generation pyrene cored polytriphenylene dendrimers (**PYG1** and **PYG2**).

2.6.2 Characterization of pyrene cored polytriphenylene dendrimers

The MALDI-TOF mass spectra demonstrated a single intense signal corresponding to the calculated m/z ratio of all polytriphenylene dendrimers based on pyrene core, proving the monodispersity of the described dendrimers. Figure 2-21 shows the MALDI-TOF

mass spectra of first and second generation dendrimers **PYG1** and **PYG2** as typical examples.
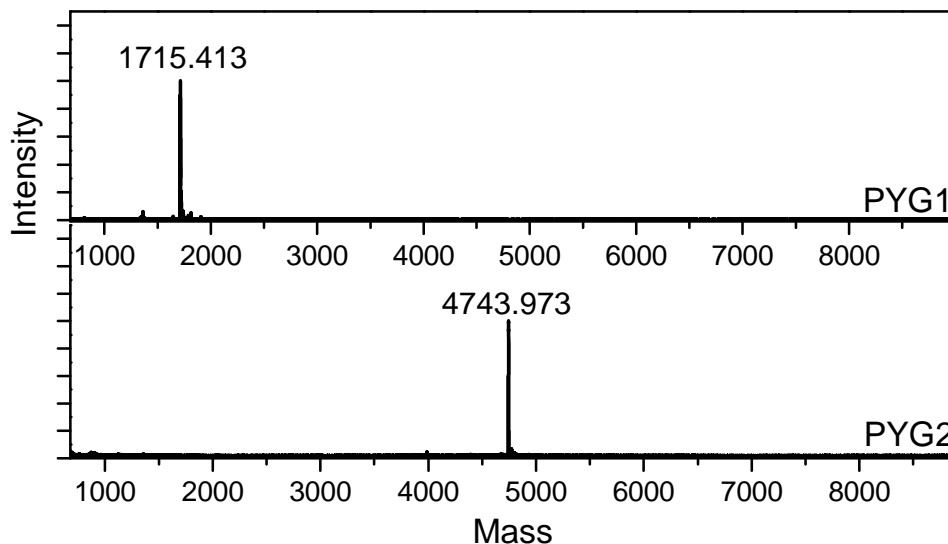
Figure 2-21: MALDI-TOF mass spectra of first and second generation pyrene cored polytriphenylene dendrimers **PYG1** and **PYG2**.

The spectra were measured using dithranol as matrix. For the first-generation dendrimer **PYG1** a molecular mass of 1715.413 g·mol^{-1} was detected, which is in good agreement with the calculated mass of 1715.645 g·mol^{-1}. It proved that although both the reagent 1,3,6,8-tetraethynylpyrene core (**2-26**) and product dendrimer **PYG1** were poor soluble in o-xylene, all four ethynyl bonds of **2-26** had been completely reacted during the Diels-Alder cycloaddition. The second-generation dendrimer **PYG2** also indicated a single signal at 4743.973 g·mol^{-1}, which is identical to the calculated mass of 4743.782 g·mol^{-1}.

2.6.3 Photophysical properties

In contrast to the **TPGx** dendrimers, which contain only one type of blue light-emitting chromophore - triphenylene, the **PYGx** dendrimers consist of two emissive moieties, the pyrene core and triphenylene dendrons. Therefore, a theoretically intramolecular energy transfer between triphenylene and pyrene should be active.[70] Moreover, the

pyrene core in **PYGx** could extend the effective conjugation among the whole dendritic system, inducing dissimilar photophysical properties in these two series of dendrimers. The normalized absorption and PL spectra of **TPG1**, **TPG2**, **PYG1** and **PYG2** in toluene solution are shown in Figure 2-22.
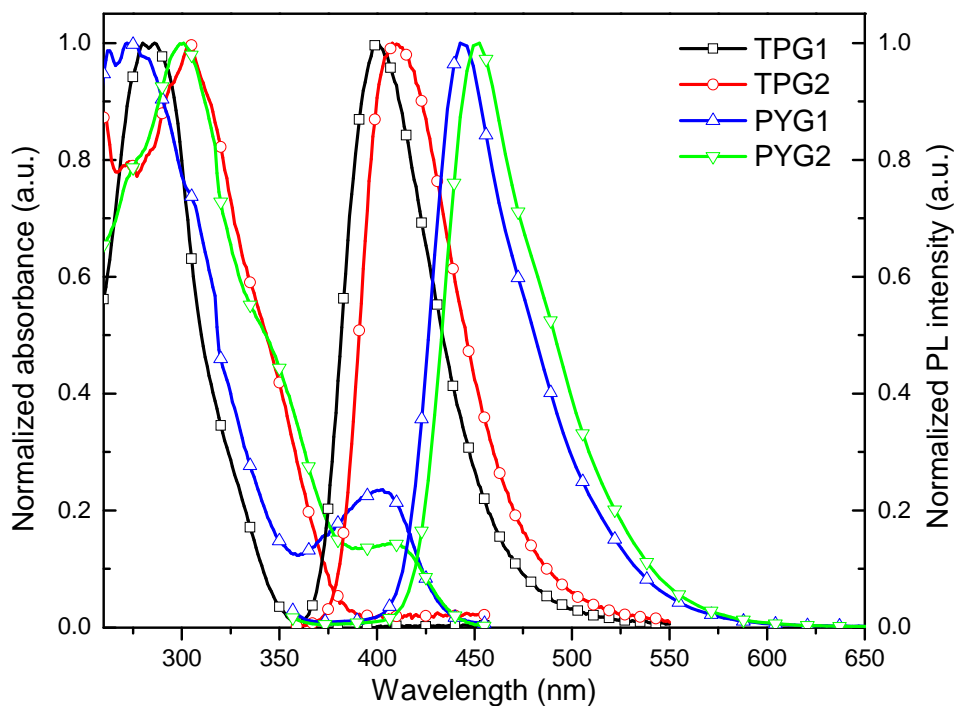
Figure 2-22: UV-Vis absorption and PL spectra of dendrimers **TPG1**, **TPG2**, **PYG1** and **PYG2** in toluene solution. The emission spectra are excited at 360 nm and normalized to the same optical density at the maximum emission intensity.

In the absorption spectra, the **TPG1** demonstrated only one significant peak around 280 nm due to the absorption of a single triphenylene unit, which was already proved by the identical absorption spectra between **TPG1** and **TTP** in Figure 2-22, as well as the **PYG1** displayed a similar main peak around 270 nm. In contrast, the second generation dendrimers **TPG2** and **PYG2** showed the main peaks around 300 nm, which were caused by some conjugation between neighboring triphenylene units in the second generation dendrons. Moreover, due to direct linking of triphenylene dendrons to the pyrene core, the dendrimers with pyrene core showed an additional peak in the longer wavelength region, such as the peak around 403 nm for **PYG1** and 409 nm for **PYG2**. From **PYG1** to

PYG2, the bathochromic shift of 6 nm could also be explained by some conjugation between neighboring triphenylene units.[71]

In the PL spectra, the second generation dendrimers **TPG2** and **PYG2** demonstrate slight bathochromic shifts (8 and 10 nm) of emission maximum compared to the first generation dendrimers **TPG1** and **PYG1**, from 400 nm and 443 nm to 408 nm and 453 nm, respectively. We ascribed these slight shifts to some conjugation of triphenylene units in dendrons, which were in accord with the phenomena in absorption spectra. In contrast, significant bathochromic shifts (43 nm and 45 nm) are shown from tetraphenylmethane cored polytriphenylene dendrimers (**TPGx**) to the pyrene cored dendrimers (**PYGx**). This phenomenon could be explained by Förster resonance energy transfer. The **PYGx** dendrimers were composed of two blue chromophores, the pyrene core and triphenylene dendrons. Considering a possible spectral overlap of the two constituents intramolecular energy transfer was likely to take place in such a configuration. In Figure 2-22, the absorption spectra of **PYGx** dendrimers consist of two componets: i) a main band below 370 nm was caused by the absorption of polytriphenylene dendrons, which could also be found in **TPGx** dendrimers; and ii) an additional shoulder at ca. 400 nm was assigned to the absorption of the pyrene core. Using the **PYGx** dendrimer absorption spectra in combination with the **TPGx** dendrimer PL spectra, in which the emission was only coming from the triphenylene dendrons, a visible spectral overlap can be detected between the absorption of the pyrene core and emission of the triphenylene dendrons. This indicates that an energy transfer occurs from triphenylene to pyrene. Therefore, **PYGx** dendrimers can be described as a single molecular light-harvesting system with the triphenylene units in the dendrons serving as donors and the pyrene core acting as an acceptor. In the PL spectra of **PYGx** dendrimers, the original emission bands of triphenylene dendrons (380 - 400 nm) disappeared and their excitation energies were completely transferred to the pyrene core, which emitted sky-blue light with maximum wavelength at 443 nm for **PYG1** and 453 nm for **PYG2**.

2.6.4 Comparison of PL and EL properties between TPG2 and PYG2

In the previous paragraphs, we already concluded that second generation dendrimer **TPG2** showed the most suitable molecular size for blue light-emitting materials compared to other generations. In this paragraph, we will mainly discuss the difference between **TPG2** and **PYG2** on several aspects, such as absorption, excitation, emission and device performance. Figure 2-23 shows the absorption and PL spectra of **TPG2** and **PYG2** in toluene solution and in spin-coated thin film.

The absorption spectra of both **TPG2** and **PYG2** in thin film showed the main peaks around 300 nm, which were identical to those in solution. The shoulder peak around 409 nm was also detected both in thin film and in solution of **PYG2**. The PL spectra showed significant difference between **TPG2** and **PYG2**. Dendrimer **TPG2** displayed a deeper blue emission with a maximum at 416 nm in solution and 428 nm in thin film, whereas dendrimer **PYG2** demonstrated a lighter blue emission with the peak at 454 nm in solution and 469 nm in solid state. A similar bathochromic shifts from in solution to solid state of both dendrimers indicated that the second generation dendrons had the same effect in the intermolecular aggregates among dendritic chromophores.

In the meantime, the photoluminescence quantum yield (PLQY) of **TPG2** was only 27% in solution, whereas the PLQY of **PYG2** was up to 40% under identical condition. Moreover, the PLQYs of both dendrimers in thin film with similar thickness were also investigated. The result showed that the PLQY of **PYG2** was nearly three times higher than that of **TPG2** in solid state. The raise of PLQYs in both solution and thin film demonstrated that the pyrene core could improve the whole dendrimer emitting efficiency, which was further confirmed by their OLED device performance tests.
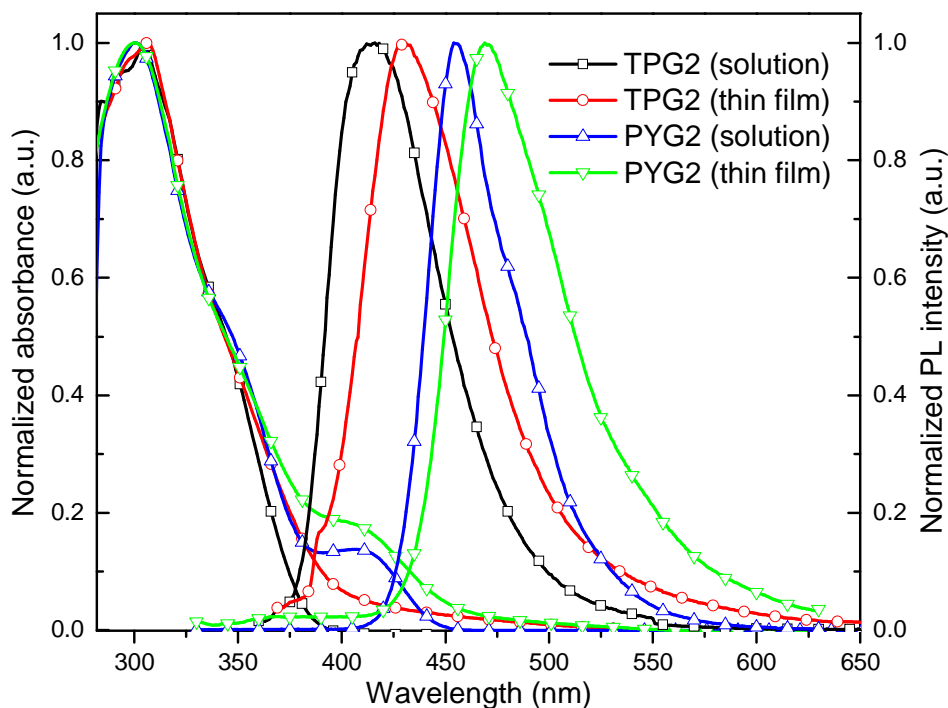
Figure 2-23: UV-Vis absorption and PL spectra of dendrimers **TPG2** and **PYG2** in both solution and thin film. The emission spectra are excited at 360 nm and normalized to the same optical density at the maximum emission intensity.

The OLEDs based on **PYG2** dendrimer were fabricated as the same configuration as the devices of **TPG2** dendrimer. Figure 2-24 shows the *I-V-L* characteristics of **PYG2** based OLED without the ETL/HBL. The maximum luminescence and current efficiency of **PYG2** device was increased up to 500 cd/m^2 and 0.12 cd/A, respectively, both were almost five times higher than those of **TPG2** device, indicating that the pyrene core could improve not only the emissive quantum yield, but also the charge injection and transportation properties of polytriphenylene dendrimers, which was further proved by the lower turn-on voltage of electroluminescence of **PYG2** device at 3.8 V. Besides that, the maximum of the EL spectrum was similar as the PL spectrum with a peak at 473 nm and corresponding CIE coordinates at (0.19, 0.30), which was located in sky-blue region.
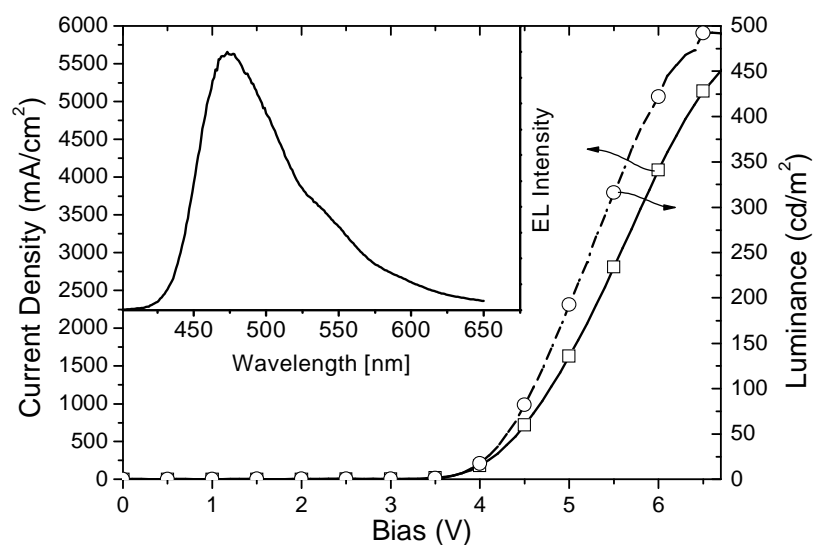
Figure 2-24: EL spectra (left) and I-V-L characteristics (right) of an ITO/PEDOT/**PYG2**/CsF/Al device.
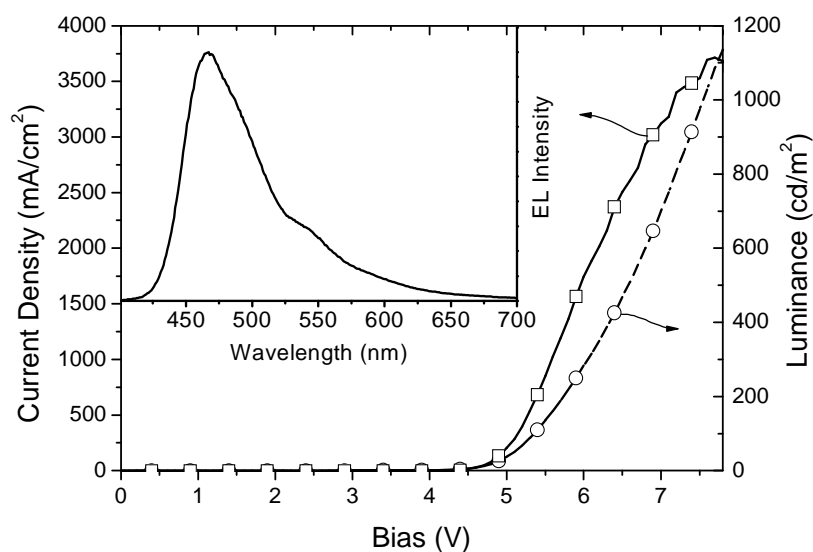
Figure 2-25: EL spectra (left) and I-V-L characteristics (right) of an ITO/PEDOT/**PYG2**/TPBI/CsF/Al device.

In order to achieve even higher efficiency, the TPBI with 10 nm thickness was introduced as an additional ETL/HBL. Figure 2-25 displays the *I-V-L* characteristics of OLED device with a configuration of ITO/PEDOT/**PYG2**/TPBI/CsF/Al. In comparison with the **TPG2** device performance, the **PYG2** device demonstrated a lower onset voltage of electroluminescence at 4.7 V and higher luminescence up to 1100 cd/m^2. The maximum

efficiency was also increased up to 0.57 cd/A at approximately 5.6 V. Although the maximum of the EL spectrum was red-shift to 466 nm with a very tiny red-tail at 530 nm, and the corresponding CIE coordinates moved to (0.20, 0.28), the EL color of **PYG2** based OLED was still located in sky-blue region.

In conclusion, the replacement of tetraphenylmethane by pyrene core could effectively enhance the photophysical properties and device performances. The pyrene core not only possessed its natural high PLQY and long fluorescence lifetime, but also acted as a connector between the conjugated polytriphenylene dendrons which were previously isolated by the central sp^3 carbon in the tetraphenylmethane core. Most importantly, the pyrene core could perform as an accepter to concentrate the energy from polytriphenylene dendrons. These single molecular light-harvesting dendrimers would suggest a potential application in the optical energy concentrator for blue laser light.

2.7 Summary

In this chapter, triphenylene emitters were introduced in the polytriphenylene dendrimers (**TPGx**) during the Diels-Alder cycloaddition reaction. This novel synthesis concept and unique procedure produced a series of blue fluorescent materials for OLEDs in high yield and without metal catalysts. Compared to small molecules, dendrimers with high molecular weights showed higher thermal and chemical stability and better solubility in common organic solvent thus providing light-emitting materials for solution processable OLEDs. Most importantly, the rigid and twisty triphenylene units, which were proved by the crystal structure of a first-generation dendrimer and the molecular modeling, could not only perform as chromophores, but also effectively prevent the inter- or intra-molecular fluorescence quenching.

These dendrimers exhibited stable and pure-blue emission in both PL and EL spectra. The increasing PLQYs with generation growth were according to the extending effective conjugation length of polytriphenylene dendrons and the suppressed aggregation of the fluorophores. Thermogravimetric analysis (TGA) measurement displayed that all

dendrimer exhibited degradation above 450 °C under N_2 atmosphere, which was much higher than for other blue light-emitting materials up to now. However, a remarkable feature is that only the devices based on second generation dendrimers **TPG2** and **TPG2'** demonstrated enough stable photonic and electronic properties during increasing voltage and extending time. Lower and higher generation dendrimers showed poor stability after annealing in air. The variable stabilities of different generations indicated that molecular sizes of dendrimers could significantly control their OLED performances. The investigation of relationship between molecular size and OLED performance will be presented in the subsequent chapters.

To improve the efficiency of polytriphenylene dendrimer based blue light-emitting diodes, it is instructive to import other promising blue chromophores with high PLQYs into different positions of dendrimers. For example, starting from the fourfold ethynyl substituted blue chromophore 1,3,6,8-tetraethynyl-pyrene as the core, a series of pyrene cored polytriphenylene dendrimers (**PYGx**) have been prepared in high yield. The UV and PL spectra of these **PYGx** dendrimers demonstrated an energy transfer from polytriphenylene dendrons to the pyrene core, resulting in the PLQY of **PYG2** were relatively three times higher than that of **TPG2** in both solution and solid state. Moreover, the OLED device performance of **PYG2** was also significantly higher than the efficiency of **TPG2** device. However, the emission color of the pyrene cored dendrimers (**PYGx**) had a slight red-shift to the blue-green region, due to the expanding conjugation between triphenylene dendrons and pyrene core. Therefore, the design of these multi-chromophoric dendrimers must be further developed.

On the other hand, according to the optimizing process of the OLED device configuration, an additional TPBI layer could not only effective transport electrons from CsF cathode to the emissive dendrimer layer, but also completely block holes entering it from the emissive layer because of the larger difference in the HOMO energy levels between TPGx (-5.1 eV) and TPBI (-6.2 eV). Therefore, the additional ETL/HBL layer in ITO/PEDOT:PSS/TPGx/TPBI/CsF/Al devices showed significantly higher EL efficiency and lower turn-on voltage in comparison with the ITO/PEDOT:PSS/TPGx/Ca/Al devices.

However, the large electron injection barrier in the LUMO energy levels from CsF (-4.1 eV) to TPBi (-2.7 eV) indicated that our polytriphenylene dendrimer based blue OLEDs still leave much space to improve. There are still many other factors effecting on the efficiency of these dendritic emissive materials, such as the size and electronic property of dendrons, which will be further discussed in the following chapters.

References

[1]   Wu, C. C., Sturm, J. C., Register, R. A., Thompson, M. E., *Appl. Phys. Lett.* **1996**, *69*, 3117.

[2]   a)Yang, Y., Pei, Q. B., *Appl. Phys. Lett.* **1996**, *68*, 2708; b)Tasch, S., Brandstatter, C., Meghdadi, F., Leising, G., Froyer, G., Athouel, L., *Adv. Mater.* **1997**, *9*, 33; c)Shen, Z. L., Burrows, P. E., Bulovic, V., Forrest, S. R., Thompson, M. E., *Science* **1997**, *276*, 2009.

[3]   a)Swanson, S. A., Wallraff, G. M., Chen, J. P., Zhang, W. J., Bozano, L. D., Carter, K. R., Salem, J. R., Villa, R., Scott, J. C., *Chem. Mater.* **2003**, *15*, 2305; b)Guha, S., Bojarczuk, N. A., *Appl. Phys. Lett.* **1998**, *73*, 1487; c)Niko, A., Tasch, S., Meghdadi, F., Brandstatter, C., Leising, G., *J. Appl. Phys.* **1997**, *82*, 4177.

[4]   Muller, C. D., Falcou, A., Reckefuss, N., Rojahn, M., Wiederhirn, V., Rudati, P., Frohne, H., Nuyken, O., Becker, H., Meerholz, K., *Nature* **2003**, *421*, 829.

[5]   Cho, H. N., Kim, D. Y., Kim, Y. C., Lee, J. Y., Kim, C. Y., *Adv. Mater.* **1997**, *9*, 326.

[6]   a)Cimrova, V., Schmidt, W., Rulkens, R., Schulze, M., Meyer, W., Neher, D., *Adv. Mater.* **1996**, *8*, 585; b)Schlotter, P., Schmidt, R., Schneider, J., *Appl. Phys. A-Mater.* **1997**, *64*, 417.

[7]   a)Scherf, U., List, E. J. W., *Adv. Mater.* **2002**, *14*, 477; b)Kraft, A., Grimsdale, A. C., Holmes, A. B., *Angew. Chem. Int. Ed.* **1998**, *37*, 402.

[8]   a)Burn, P. L., Holmes, A. B., Kraft, A., Bradley, D. D. C., Brown, A. R., Friend, R. H., *J. Chem. Soc., Chem. Commun.* **1992**, 32; b)Burroughes, J. H., Bradley, D. D. C., Brown, A. R., Marks, R. N., Mackay, K., Friend, R. H., Burns, P. L., Holmes, A. B., *Nature* **1990**, *347*, 539.

[9]   a)Ohmori, Y., Uchida, M., Muro, K., Yoshino, K., *Japanese Journal of Applied Physics Part 2-Letters* **1991**, *30*, L1941; b)Grem, G., Leditzky, G., Ullrich, B., Leising, G., *Adv. Mater.* **1992**, *4*, 36.

[10]   a)Pei, Q. B., Zuccarello, G., Ahlskog, M., Inganas, O., *Polymer* **1994**, *35*, 1347; b)Andersson, M. R., Berggren, M., Inganas, O., Gustafsson, G., Gustafssoncarlberg, J. C., Selse, D., Hjertberg, T., Wennerstrom, O., *Macromolecules* **1995**, *28*, 7525.

[11]   Gebler, D. D., Wang, Y. Z., Blatchford, J. W., Jessen, S. W., Lin, L. B., Gustafson, T. L., Wang, H. L., Swager, T. M., Macdiarmid, A. G., Epstein, A. J., *J. Appl. Phys.* **1995**, *78*, 4264.

[12]   a)Ranger, M., Rondeau, D., Leclerc, M., *Macromolecules* **1997**, *30*, 7686; b)Wong, K. T., Chien, Y. Y., Chen, R. T., Wang, C. F., Lin, Y. T., Chiang, H. H., Hsieh, P. Y., Wu, C. C., Chou, C. H., Su, Y. O., Lee, G. H., Peng, S. M., *J. Am. Chem. Soc.* **2002**, *124*, 11576.

[13]   a)Kim, Y. H., Jeong, H. C., Kim, S. H., Yang, K. Y., Kwon, S. K., *Adv. Funct. Mater.* **2005**, *15*, 1799; b)Shi, J. M., Tang, C. W., *Appl. Phys. Lett.* **2002**, *80*, 3201.

[14]   Tang, C., Liu, F., Xia, Y. J., Lin, J., Xie, L. H., Zhong, G. Y., Fan, Q. L., Huang, W., *Org. Electron.* **2006**, *7*, 155.

[15]   Freudenmann, R., Behnisch, B., Hanack, M., *J. Mater. Chem.* **2001**, *11*, 1618.

[16]   a)Mitschke, U., Bauerle, P., *J. Mater. Chem.* **2000**, *10*, 1471; b)Kim, D. Y., Cho, H. N., Kim, C. Y., *Prog. Polym. Sci.* **2000**, *25*, 1089.

[17]   a)Bliznyuk, V. N., Carter, S. A., Scott, J. C., Klarner, G., Miller, R. D., Miller, D. C., *Macromolecules* **1999**, *32*, 361; b)Weinfurtner, K. H., Fujikawa, H., Tokito, S., Taga, Y., *Appl. Phys. Lett.* **2000**, *76*, 2502; c)Fu, H. B., Yao, J. N., *J. Am. Chem. Soc.* **2001**, *123*, 1434.

[18]   a)Kreyenschmidt, M., Klaerner, G., Fuhrer, T., Ashenhurst, J., Karg, S., Chen, W. D., Lee, V. Y., Scott, J. C., Miller, R. D., *Macromolecules* **1998**, *31*, 1099; b)Shu, C. F., Dodda, R., Wu, F. I., Liu, M. S., Jen, A. K. Y., *Macromolecules* **2003**, *36*, 6698; c)Zeng, G., Yu, W. L., Chua, S. J., Huang, W., *Macromolecules* **2002**, *35*, 6907.

[19]   Setayesh, S., Grimsdale, A. C., Weil, T., Enkelmann, V., Mullen, K., Meghdadi, F., List, E. J. W., Leising, G., *J. Am. Chem. Soc.* **2001**, *123*, 946.

[20]   a)Halim, M., Pillow, J. N. G., Samuel, I. D. W., Burn, P. L., *Adv. Mater.* **1999**, *11*, 371; b)Freeman, A. W., Koene, S. C., Malenfant, P. R. L., Thompson, M. E., Frechet, J. M. J., *J. Am. Chem. Soc.* **2000**, *122*, 12385; c)Lupton, J. M., Samuel, I. D. W., Beavington, R., Burn, P. L., Bassler, H., *Adv. Mater.* **2001**, *13*, 258; d)Gorman, C. B., Smith, J. C., *Acc. Chem. Res.* **2001**, *34*, 60.

[21]   Zhao, L., Li, C., Zhang, Y., Zhu, X. H., Peng, J. B., Cao, Y., *Macromol. Rapid Commun.* **2006**, *27*, 914.

[22]   de Halleux, V., Calbert, J. P., Brocorens, P., Cornil, J., Declercq, J. P., Bredas, J. L., Geerts, Y., *Adv. Funct. Mater.* **2004**, *14*, 649.

[23]   Kwok, C. C., Wong, M. S., *Macromolecules* **2001**, *34*, 6821.

[24]   a)Meier, H., Lehmann, M., *Angew. Chem. Int. Ed.* **1998**, *37*, 643; b)Halim, M., Samuel, I. D. W., Pillow, J. N. G., Burn, P. L., *Synth. Met.* **1999**, *102*, 1113.

[25]   a)Xu, Z. F., Kahr, M., Walker, K. L., Wilkins, C. L., Moore, J. S., *J. Am. Chem. Soc.* **1994**, *116*, 4537; b)Ranasinghe, M. I., Hager, M. W., Gorman, C. B., Goodson, T., *J. Phys. Chem. B* **2004**, *108*, 8543.

[26]   a)Wang, J. L., Yan, J., Tang, Z. M., Xiao, Q., Ma, Y. G., Pei, J., *J. Am. Chem. Soc.* **2008**, *130*, 9952; b)Cao, X. Y., Zhang, W. B., Wang, J. L., Zhou, X. H., Lu, H., Pei, J., *J. Am. Chem. Soc.* **2003**, *125*, 12430.

[27]   Krebs, F. C., Nyberg, R. B., Jorgensen, M., *Chem. Mater.* **2004**, *16*, 1313.

[28]   Benning, S. A., Hassneider, T., Keuker-Baumann, S., Bock, H., Della Sala, F., Frauenheim, T., Kitzerow, H. S., *Liq. Cryst.* **2001**, *28*, 1105.

[29]   a)Freudenmann, R., Behnisch, B., Lange, F., Hanack, M., *Synth. Met.* **2000**, *111*, 441; b)Saleh, M., Park, Y. S., Baumgarten, M., Kim, J. J., Mullen, K., *Macromol. Rapid Commun.* **2009**, *30*, 1279.

[30]   Bagui, M., Melinger, J. S., Chakraborty, S., Keightley, J. A., Peng, Z. H., *Tetrahedron* **2009**, *65*, 1247.

[31]   Sasaki, T., Kanematsu, K., Iizuka, K., *J. Org. Chem.* **1976**, *41*, 1105.

[32]   a)Schuster, II, Craciun, L., Ho, D. M., Pascal, R. A., *Tetrahedron* **2002**, *58*, 8875; b)Yasuda, M., Harano, K., Kanematsu, K., *J. Org. Chem.* **1981**, *46*, 3836; c)Yasuda, M., Harano, K., Kanematsu, K., *J. Org. Chem.* **1980**, *45*, 659; d)Yoshitake, Y., Nakagawa, H., Eto, M., Harano, K., *Tetrahedron Lett.* **2000**, *41*, 4395; e)Eto, M., Setoguchi, K., Harada, A., Sugiyama, E., Harano, K., *Tetrahedron Lett.* **1998**, *39*, 9751; f)Bynum, K., Rothchild, R., *Spectrosc. Lett.* **1996**, *29*, 1621.

[33]   Pascal, R. A., Vanengen, D., Kahr, B., McMillan, W. D., *J. Org. Chem.* **1988**, *53*, 1687.

[34]   Morgenroth, F., Kubel, C., Mullen, K., *J. Mater. Chem.* **1997**, *7*, 1207.

[35]   Bhatt, M. V., *Tetrahedron* **1964**, *20*, 803.

[36]   Wiesler, U. M., Berresheim, A. J., Morgenroth, F., Lieser, G., Mullen, K., *Macromolecules* **2001**, *34*, 187.

[37]   Bauer, R. E., Enkelmann, V., Wiesler, U. M., Berresheim, A. J., Mullen, K., *Chem. Eur. J.* **2002**, *8*, 3858.

[38]   Caminati, G., Turro, N. J., Tomalia, D. A., *J. Am. Chem. Soc.* **1990**, *112*, 8515.

[39]   Hecht, S., Frechet, J. M. J., *Angew. Chem. Int. Ed.* **2001**, *40*, 74.

[40]   Halgren, T. A., *J. Comput. Chem.* **1996**, *17*, 490.

[41]   Boris, D., Rubinstein, M., *Macromolecules* **1996**, *29*, 7251.

[42]   a)Lupton, J. M., Samuel, I. D. W., Beavington, R., Frampton, M. J., Burn, P. L., Bassler, H., *Physical Review B* **2001**, *63*; b)Halim, M., Samuel, I. D. W., Pillow, J. N. G., Monkman, A. P., Burn, P. L., *Synth. Met.* **1999**, *102*, 1571.

[43]   a)Meier, H., Stalmach, U., Kolshorn, H., *Acta Polym.* **1997**, *48*, 379; b)Grimme, J., Kreyenschmidt, M., Uckert, F., Mullen, K., Scherf, U., *Adv. Mater.* **1995**, *7*, 292.

[44]   Wang, S. J., Oldham, W. J., Hudack, R. A., Bazan, G. C., *J. Am. Chem. Soc.* **2000**, *122*, 5695.

[45]   Elandaloussi, E. H., Frere, P., Richomme, P., Orduna, J., Garin, J., Roncali, J., *J. Am. Chem. Soc.* **1997**, *119*, 10774.

[46]   Marguet, S., Markovitsi, D., Millie, P., Sigal, H., Kumar, S., *J. Phys. Chem. B* **1998**, *102*, 4697.

[47]   Chu, L., Arzberger, M., Bohm, G., Abstreiter, G., *J. Appl. Phys.* **1999**, *85*, 2355.

[48]   a)Chojnacki, H., Laskowski, Z., Lewanowicz, A., Ruziewicz, Z., Wandas, R., *Chem. Phys. Lett.* **1986**, *124*, 478; b)Duzhko, V., Shi, H. F., Singer, K. D., Semyonov, A. N., Twieg, R. J., *Langmuir* **2006**, *22*, 7947.

[49]   Markovitsi, D., Germain, A., Millie, P., Lecuyer, P., Gallos, L. K., Argyrakis, P., Bengs, H., Ringsdorf, H., *J. Phys. Chem.* **1995**, *99*, 1005.

[50]   Fletcher, A. N., *Photochem. Photobiol.* **1969**, *9*, 439.

[51]   Marsitzky, D., Vestberg, R., Blainey, P., Tang, B. T., Hawker, C. J., Carter, K. R., *J. Am. Chem. Soc.* **2001**, *123*, 6965.

[52]   Pei, J., Wang, J. L., Cao, X. Y., Zhou, X. H., Zhang, W. B., *J. Am. Chem. Soc.* **2003**, *125*, 9944.

[53]   a)Segura, J. L., *Acta Polym.* **1998**, *49*, 319; b)Rothberg, L. J., Lovinger, A. J., *J. Mater. Res.* **1996**, *11*, 3174.

[54]   a)Kwon, T. W., Alam, M. M., Jenekhe, S. A., *Chem. Mater.* **2004**, *16*, 4657; b)Schenning, A., Peeters, E., Meijer, E. W., *J. Am. Chem. Soc.* **2000**, *122*, 4489.

[55]   Stuhr-Hansen, N., Christensen, J. B., Harrit, N., Bjornholm, T., *J. Org. Chem.* **2003**, *68*, 1275.

[56]   Saadeh, H., Goodson, T., Yu, L. P., *Macromolecules* **1997**, *30*, 4608.

[57]   a)List, E. J. W., Guentner, R., de Freitas, P. S., Scherf, U., *Adv. Mater.* **2002**, *14*, 374; b)Zojer, E., Pogantsch, A., Hennebicq, E., Beljonne, D., Bredas, J. L., de Freitas, P. S., Scherf, U., List, E. J. W., *J. Chem. Phys.* **2002**, *117*, 6794.

[58]   a)Berresheim, A. J., Muller, M., Mullen, K., *Chem. Rev.* **1999**, *99*, 1747; b)Muller, M., Kubel, C., Mullen, K., *Chem. Eur. J.* **1998**, *4*, 2099.

[59]   a)Gong, X. O., Iyer, P. K., Moses, D., Bazan, G. C., Heeger, A. J., Xiao, S. S., *Adv. Funct. Mater.* **2003**, *13*, 325; b)Scott, J. C., Kaufman, J. H., Brock, P. J., DiPietro, R., Salem, J., Goitia, J. A., *J. Appl. Phys.* **1996**, *79*, 2745.

[60]   a)Wu, C. C., Wu, C. I., Sturm, J. C., Kahn, A., *Appl. Phys. Lett.* **1997**, *70*, 1348; b)Kim, J. S., Granstrom, M., Friend, R. H., Johansson, N., Salaneck, W. R., Daik, R., Feast, W. J., Cacialli, F., *J. Appl. Phys.* **1998**, *84*, 6859.

[61]   Joswick, M. D., Campbell, I. H., Barashkov, N. N., Ferraris, J. P., *J. Appl. Phys.* **1996**, *80*, 2883.

[62]   a)Bernius, M. T., Inbasekaran, M., O'Brien, J., Wu, W. S., *Adv. Mater.* **2000**, *12*, 1737; b)Shirota, Y., Kuwabara, Y., Inada, H., Wakimoto, T., Nakada, H., Yonemoto, Y., Kawami, S., Imai, K., *Appl. Phys. Lett.* **1994**, *65*, 807; c)Kido, J., Iizumi, Y., *Appl. Phys. Lett.* **1998**, *73*, 2721.

[63]   a)Kulkarni, A. P., Tonzola, C. J., Babel, A., Jenekhe, S. A., *Chem. Mater.* **2004**, *16*, 4556; b)Adamovich, V. I., Cordero, S. R., Djurovich, P. I., Tamayo, A., Thompson, M. E., D'Andrade, B. W., Forrest, S. R., *Org. Electron.* **2003**, *4*, 77.

[64]   Gao, Z. Q., Lee, C. S., Bello, I., Lee, S. T., Chen, R. M., Luh, T. Y., Shi, J., Tang, C. W., *Appl. Phys. Lett.* **1999**, *74*, 865.

[65]   Hung, L. S., Tang, C. W., Mason, M. G., *Appl. Phys. Lett.* **1997**, *70*, 152.

[66]   a)Jenekhe, S. A., Osaheni, J. A., *Science* **1994**, *265*, 765; b)Mishra, A. K., Graf, M., Grasse, F., Jacob, J., List, E. J. W., Mullen, K., *Chem. Mater.* **2006**, *18*, 2879.

[67]   a)Pillow, J. N. G., Halim, M., Lupton, J. M., Burn, P. L., Samuel, I. D. W., *Macromolecules* **1999**, *32*, 5985; b)Fu, Y. Q., Li, Y., Li, J., Yan, S., Bo, Z. S., *Macromolecules* **2004**, *37*, 6395; c)Diez-Barra, E., Garcia-Martinez, J. C., Merino, S., del Rey, R., Rodriguez-Lopez, J., Sanchez-Verdu, P., Tejeda, J., *J. Org. Chem.* **2001**, *66*, 5664; d)Lupton, J. M., Hemingway, L. R., Samuel, I. D. W., Burn, P. L., *J. Mater. Chem.* **2000**, *10*, 867.

[68]   Jacob, J., Sax, S., Gaal, M., List, E. J. W., Grimsdale, A. C., Mullen, K., *Macromolecules* **2005**, *38*, 9933.

[69]   Bernhardt, S., Kastler, M., Enkelmann, V., Baumgarten, M., Mullen, K., *Chem. Eur. J.* **2006**, *12*, 6117.

[70]   Gronheid, R., Hofkens, J., Kohn, F., Weil, T., Reuther, E., Mullen, K., De Schryver, F. C., *J. Am. Chem. Soc.* **2002**, *124*, 2418.

[71]   Padmanaban, G., Ramakrishnan, S., *J. Am. Chem. Soc.* **2000**, *122*, 2244.

Chapter 3

A divergent synthesis of very large fac-tris[2-phenylpyridyl] iridium(III) cored polyphenylene dendrimers: molecular size effect on the performance of green phosphorescent materials

In this chapter, a new divergent protocol to design very large dendritic iridium(III) (Ir(III)) complexes for green phosphorescent organic light-emitting diodes (PhOLEDs) will be presented. A series of high generation Ir(III) dendrimers up to fourth generation which is, up to now, the largest Ir(III) dendrimer with a molecular diameter of 8 nm, were achieved in high yields. Their phosphorescent emission and PhOLED efficiency were studied. Most important, the relationship between molecular sizes of dendrimers and their device performances was also investigated.

3.1 Phosphorescent materials and their applications in OLEDs

For an organic molecule in its ground state, all electrons are paired in orbitals. In the excited state two electrons are orbitally unpaired.[1] Consequently, the ground state of an organic molecule is the singlet state, while its excited states may either be singlet or triplet states, depending on the relative orientation of the electron spin momenta. Singlet and triplet excited sates that are derived from the same electron orbital configuration have a difference in energy.[2] The triplet excited state represents a lower energy than the singlet excited sate as a result of less electron-electron repulsion.[3] The Jablonski state energy diagram of an organic molecule is shown in Figure 3-1. When organic molecules are excited by exterior energy, both singlet and triplet excited states are created. Based on straightforward spin statistics, assuming equal formation cross sections for both types of excited states, the ratio between singlet and triplet would be

1:3, meaning that 75% of all excited states that are formed upon the recombination of injected charge carriers are of the triplet variety.[4]
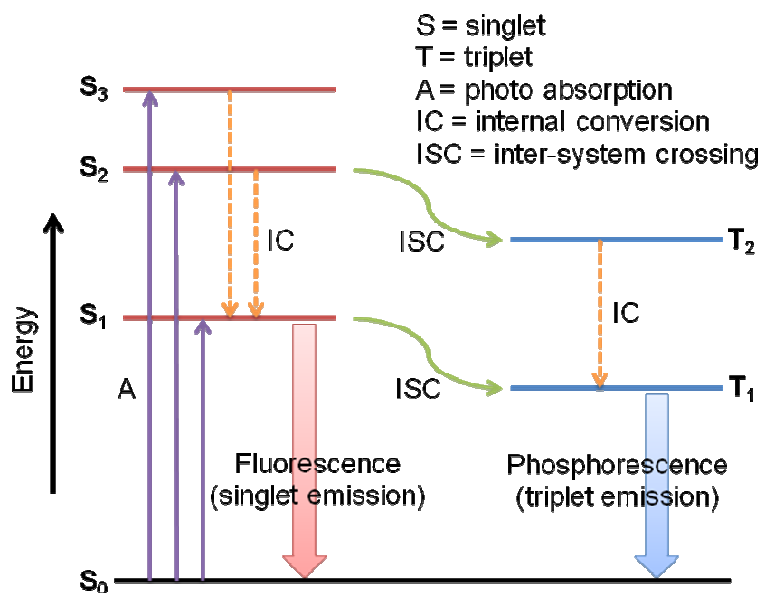

Figure 3-1: Jablonski state energy diagram

However, the interaction between an electron's spin and orbital magnetic moments, which is called spin-orbit coupling, essentially mixes singlet and triplet states, which allows inter-system crossing to a certain extent. The strength of this spin-orbit coupling depends on the nuclear charge, and the stronger the spin-orbit coupling the inter-system crossing will be more allowed.[5] In organic molecules, the spin-orbit coupling strength is weak, which means that organic molecules mainly emit light from the singlet states, since the excited triplet states are nonradiatively deactivated at ambient temperature.[6] The creation of nonradiative triplet excited states poses a fundamental limit on the efficiency of an OLED. Fortunately, this limitation can be relieved through the use of compounds that contain heavy atoms. As mentioned before, on a heavy atom, spin-orbit coupling is relatively strong which makes a transition between triplet and singlet levels more favorable.[7]

Unfortunately, the efficiency of pure layers of most phosphorescent emitters is very low because of severe self-quenching.[8] Therefore, the commonly used concept is to blend a

small molecular phosphorescent emitter as guest into a proper matrix as host.[9] However, in a physically blended system, whether evaporated or solution processed,[10] there is always the issue of how evenly the guest is distributed in the host. The dendritic architectures can overcome this weakness and combine the host-guest composition at a molecular level to control the ratio between host and guest.[11] With a rigid scaffold, dimensionally stable and well-defined dendritic host can be accurately located as a matrix around a phosphorescent core. Intermolecular interactions can also be controlled very efficiently at the molecular level by use of dendrimers. The phosphorescent core in the centre of the macromolecule can determine the light-emitting properties. In the meantime, dendrons are generally attached to the core and act as a spacer that controls the interactions between phosphorescent cores in the solid state by increasing the distance between them. Both parts of the dendrimer can be adjusted to provide tuning of properties, and molecule construction gives remarkable scope for molecular engineering.[12]

3.2 Iridium(III) dendrimers, a self-host phosphorescent system

In recent decades, the photophysics of cyclometalated Ir(III) complexes has been the subject of extensive studies.[13] These complexes have attracted much attention because of their long lived excited states, high luminescence quantum yields, high chemical stability, and most importantly charge neutralization,[14] which made the Ir(III) complexes possible to be performed by common purification techniques, such as column chromatography. Since King et al. firstly synthesized triply coordinated neutral *fac*-**Ir(ppy)₃** [*fac* = facial, Ir(ppy)₃ = tris(2-phenylpyridinato-C^2,N) Ir(III)] (**3-1**, Scheme 3-1) and investigated its photophysical and photochemical properties in 1985,[15] many researcher groups showed that Ir(III) complexes were promising for various applications such as biological labeling agents[16] and phosphorescent sensors.[17] Facile generation of triplet states then enables encouraging applications as sensitizers for charge-transfer reactions in DNA,[18] photo-catalysts for CO_2 reduction[19] and singlet oxygen

sensitizers.[20] Above all, the most important projected use of the Ir(III) complexes is electrophosphorescence including light-emitting electrochemical cells (LECs)[21] and phosphorescent organic light-emitting devices (PhOLEDs). [13, 22] This is due to the above mentioned characteristics of Ir(III) complexes, which enable both nearly 100% internal device quantum efficiency[23] and versatile color tuning.[24] Such promising features prompted the development of a number of novel phosphorescent Ir(III) complex cored dendrimers with polyphenylene[25] (**3-2**) or polycarbazole[26] (**3-3**) dendrons (Scheme 3-1).
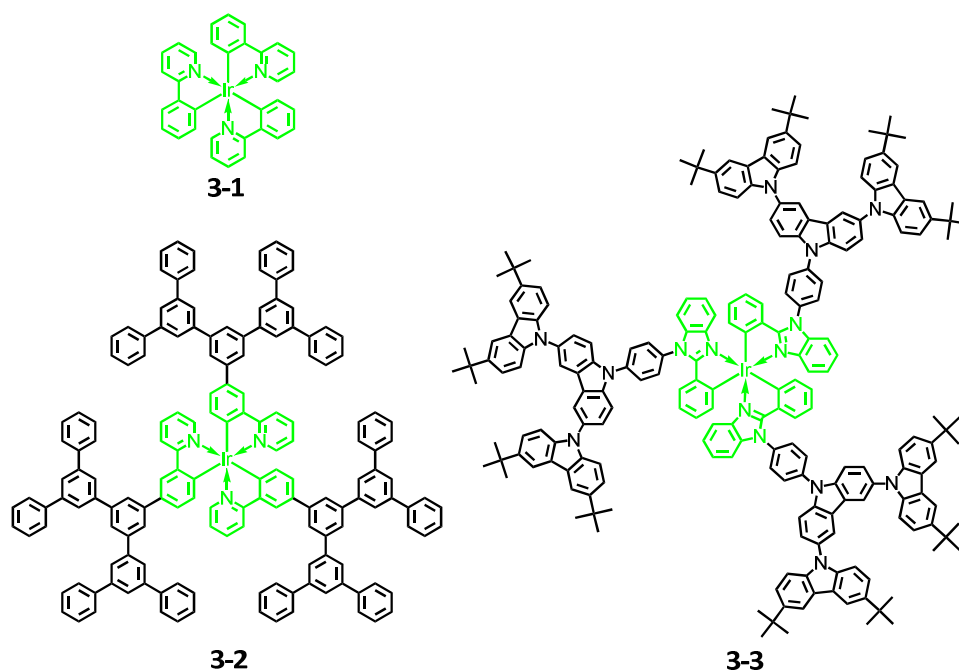
Scheme 3-1: Structures of the *fac*-Ir(ppy)₃ complex (**3-1**), Ir(III) cored polyphenylene dendrimer (**3-2**), and Ir(III) cored polycarbazole dendrimer (**3-3**).

These Ir(III) dendrimers demonstrated good solubility in common solvents, such as dichloromethane (DCM), tetrahydrofuran (THF) and toluene, and thus high solution processibility in PhOLED devices.[25-27] From the molecular design point of view, the combination of polyphenylene or polycarbazole dendrons with a Ir(III) core could form a molecule composed of a Ir(III) phosphorescent emitter as a guest molecule coupled with rigid dendrons as the host materials.[11, 28] This self-host system provided a new strategy

for designing highly efficient, solution-processable phosphorescent materials for non-doped PhOLED devices.[11, 28] However, most previous reported Ir(III) dendrimers demonstrated unsatisfying electro-luminescence (EL) properties because of their low generations. The development of such higher-generation Ir(III) dendrimers represented a synthetic challenge due to the stability and solubility of Ir(III) complexes. The coordination between Ir(III) and the 2-phenylpyridine ligands could be destroyed by most metal-based catalysts such as nickel and copper. Stability was only preserved in palladium-catalyzed reactions such as *Suzuki-* and *Stille*-coupling,[29] resulting in a lack of efficient synthetic routes towards higher generation dendrons. Therefore, most previous Ir(III) dendrimers have been synthesized via a convergent strategy: This route involves the preparation of the polyphenylene or polycarbazole dendronized ligands and subsequent complexation with Ir(III) salts in glycerol to give Ir(III) dendrimers. To the best of our knowledge, the third generation dendronized ligand so far reported was the largest ligand complexed with Ir(III).[30] However, the low yield was in the range of 10 - 35%. The fourth generation Ir(III) dendrimers have never been reported, since their larger dendronized ligands possess limited solubility in glycerol, resulting in incomplete complexation.

Hence, we herein developed a novel divergent strategy that rapidly led to first, second, third and even fourth generation polyphenylene dendrimers with Ir(ppy)₃ cores (**GIrG1**, **GIrG2**, **GIrG3** and **GIrG4**, Scheme 3-3) in high yield (> 80%). Up to now, dendrimer **GIrG4** is the largest Ir(III) dendrimer with a radius of up to 4 nm.

GIrG1

GIrG2

GIrG3

GIrG4
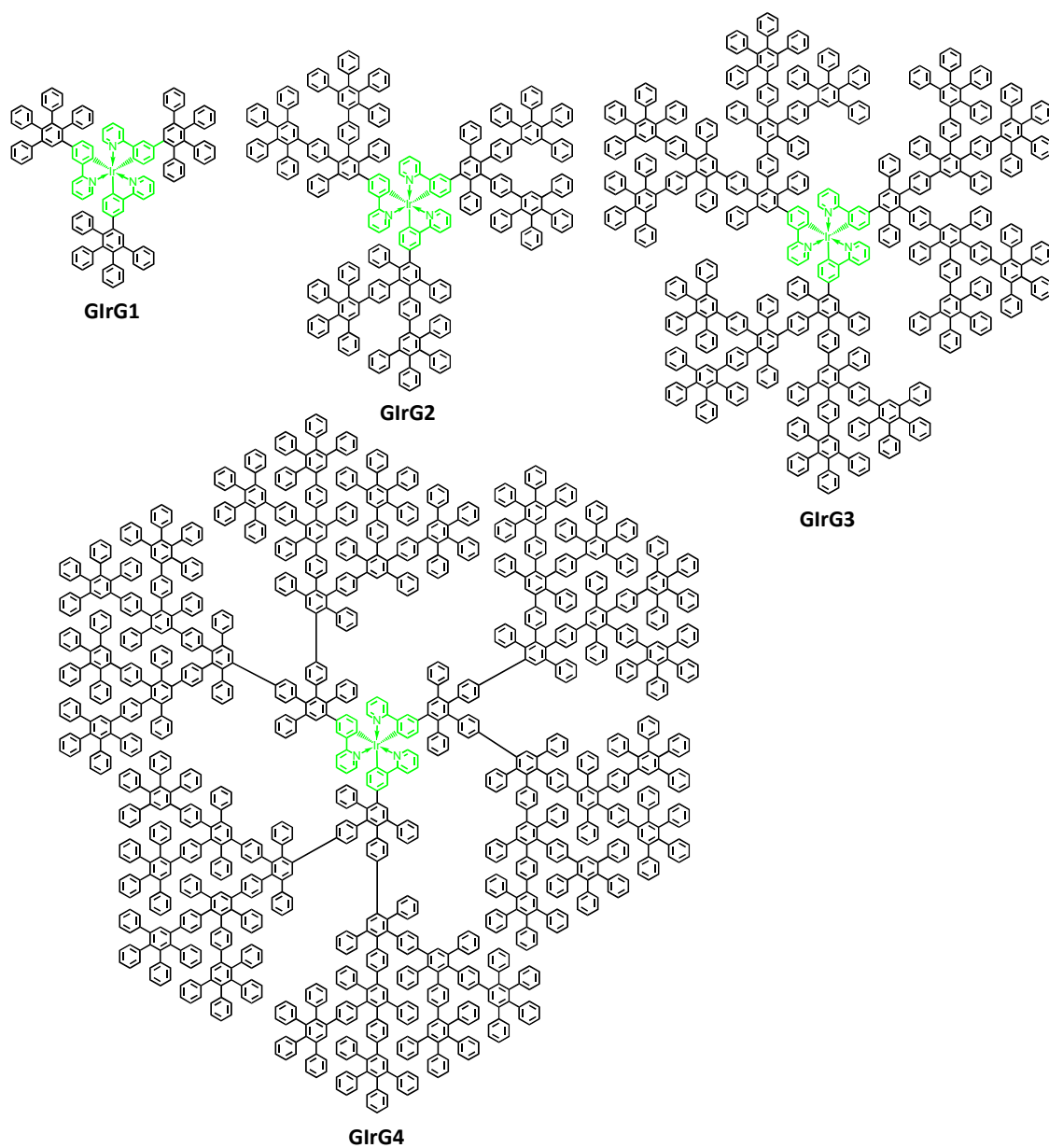
Scheme 3-3: Structures of first to fourth generation Ir(ppy)₃ cored polyphenylene dendrimers (**GIrG1**, **GIrG2**, **GIrG3** and **GIrG4**).

3.3 Green Phosphorescent Ir(ppy)₃ cored polyphenylene dendrimers

Regarding the straightforward strategies for the preparation of dendrimers, not only phosphorescent Ir(III) cores with high stability had to be considered in the divergent

synthetic route but it should also include selective coupling reactions with a high yield. Herein, the simplest *fac*-tris(2-phenylpyridinato)Ir(III) core with a high phosphorescent quantum yield and a non-catalytic [4+2] *Diels-Alder* cycloaddition were selected for constructing very large polyphenylene dendrimers.

3.3.1 Synthesis of the Ir(ppy)₃ derivative core

The most important compound for dendrimer synthesis is the Ir(III) complex core with three ethynyl groups, *i.e.*, *fac*-tris[2-(3-ethynylphenyl)pyridyl]Ir(III) **3-4**, which was synthesized from the following procedure (Scheme 3-4). The first step involved the iodination of *fac*-tris(2-phenylpyridyl)Ir(III) (**Ir(ppy)₃**) with iodine and iodobenzene diacetate in dichloromethane to obtain *fac*-tris[2-(3-iodophenyl)pyridyl]Ir(III) **3-5** in quantitative yield.[31] In the next step, the complex **3-5** was reacted with trimethyl((tributylstannyl)ethynyl)silane in THF by using dichloro-bis(triphenylphosphine)palladium(II) as the catalyst under *Stille*-coupling conditions. It was found that using THF as the solvent resulted in higher yields (60%) of *fac*-tris[2-(3-((trimethylsilyl)ethynyl)phenyl)pyridyl]Ir(III) **3-6** compared to the use of toluene as solvent (32%). Deprotection of **3-6** was achieved by treatment with tetrabutylammonium fluoride in THF at room temperature and Ir(III) core **3-4** was isolated in 88 % yield.
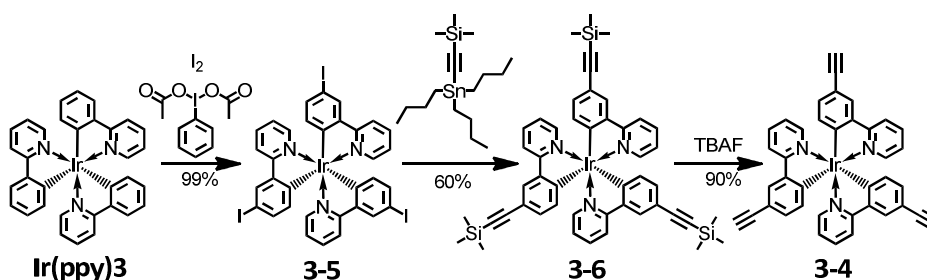
Scheme 3-4: Synthesis of Ir(ppy)₃ derivative core (**3-4**).

3.3.2 Characterization of the Ir(ppy)$_3$ derivative core

Figure 3-4 shows that the FD-mass spectrum of *fac*-tris[2-(3-iodophenyl)pyridyl]Ir(III) **3-5** displays a single signal at a mass of 1032.8 g·mol^{-1}, perfectly agreeing with the calculated molecular weight of 1032.9 g·mol^{-1}. No signals at lower mass are observed, proving the complete iodination of the three-fold iodide groups which is a prerequisite for the subsequent defined *Stille*-coupling. Furthermore, the complete three-fold *Stille*-coupling product **3-6** demonstrates a single mass signal at 943.8 g·mol^{-1}, according with its calculated mass of 943.3 g·mol^{-1}.
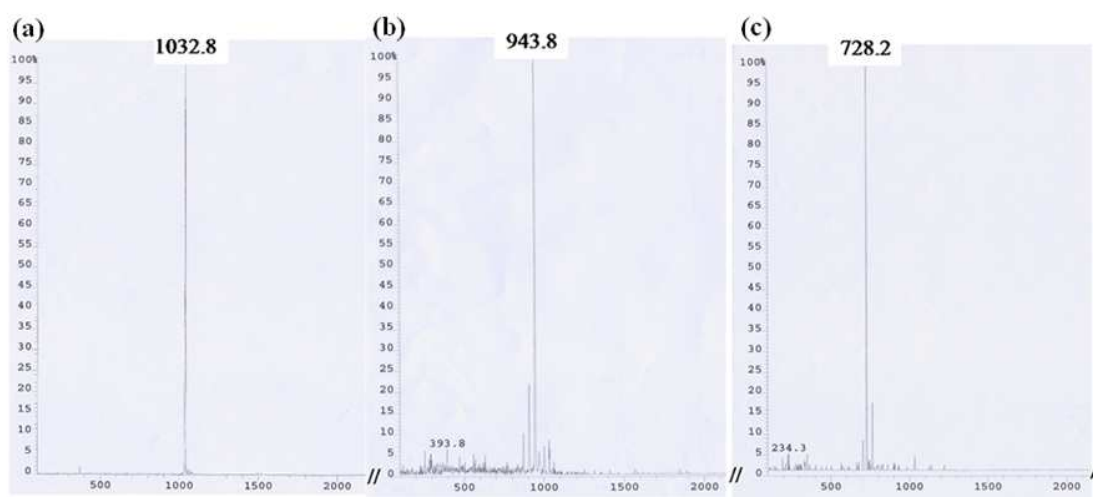
Figure 3-4: FD-mass spectra of **3-5** (a), **3-6** (b), and **3-4** (c).

Finally, The most important Ir(III) core **3-4** also indicates a single distinct mass signal at 728.2 g·mol^{-1}, matching to its calculated molecular weight of 727.2 g·mol^{-1}. The full characterization of **3-4** by ^{1}H-NMR spectrum in Figure 3-5 shows well-defined signals according with respective protons. The four aromatic peaks between 7.90 and 7.50 ppm can be attributed to the four pyridyl protons (H$_a$-H$_d$), whereas the other three aromatic peaks from 7.01 to 6.70 ppm are assigned to the three phenyl protons (H$_e$-H$_g$). Moreover, the ethynyl proton H$_h$ exhibits a singlet at 3.04 ppm. The signal intensity ratios between aromatic protons and ethynyl proton all corresponded to their expected values.
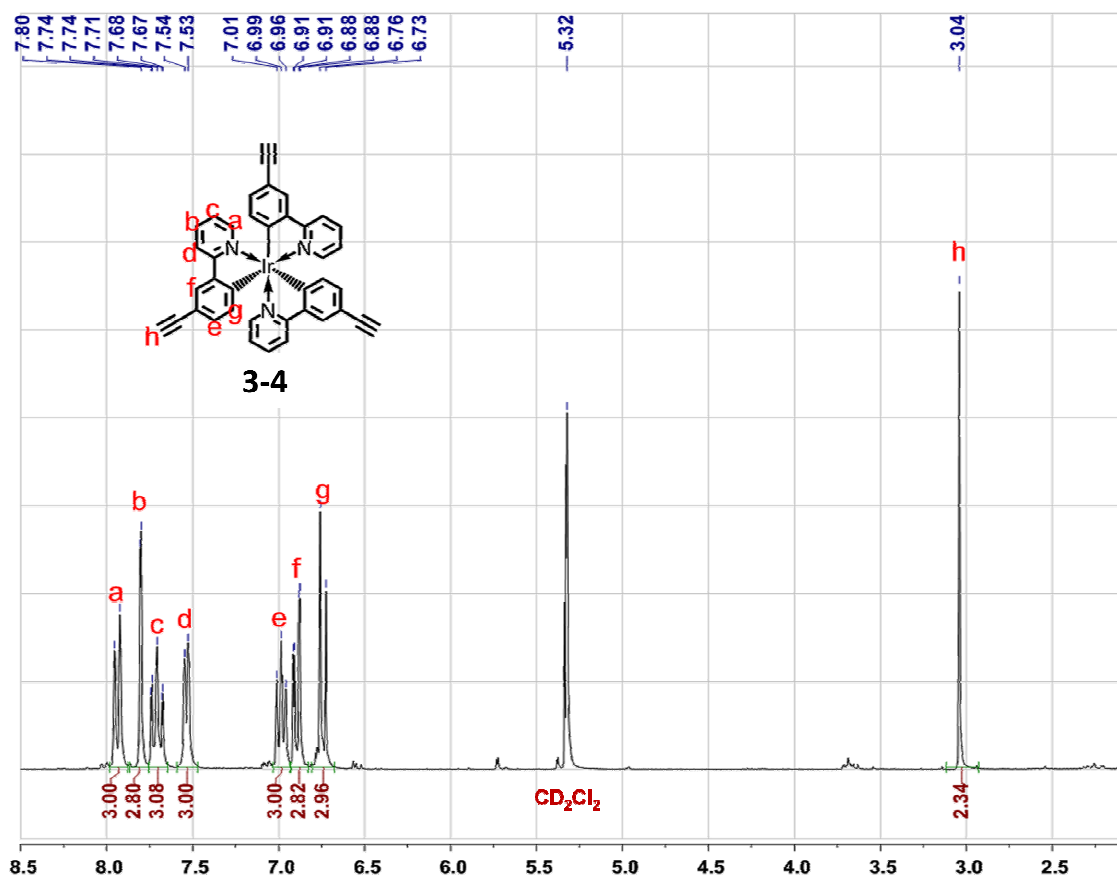
**Figure 3-5:** ^{1}H-NMR spectrum of Ir(ppy)₃ derivative core **3-10.**

3.3.1 Synthesis of Ir(ppy)₃ cored polyphenylene dendrimers

The first-generation dendrimer **GIrG1** (Scheme 3-5), with three polyphenylene dendronized ligands, was synthesized by refluxing an *o*-xylene solution of the Ir(III) core **3-4** and commercially available tetraphenylcyclopentadienone (**3-7**) in a microwave reactor for 2 h. After GPC column separation, the first-generation dendrimer **GIrG1** was precipitated in methanol as a yellow powder in 92% yield.
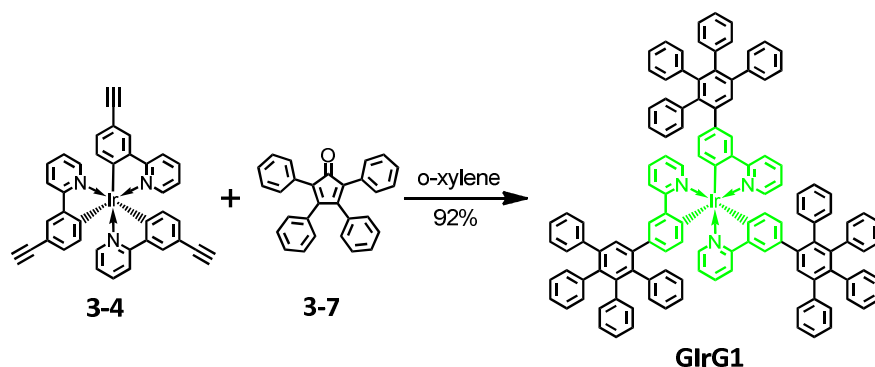
Scheme 3-5: Synthesis of the first generation Ir(ppy)₃ cored polyphenylene dendrimer (**GIrG1**).

The synthesis of the higher-generation Ir(III) dendrimers was carried out following a divergent synthetic protocol (Scheme 3-6). By employing a [4+2] *Diels–Alder* cycloaddition procedure of the triisopropylsilyl (TiPS) protected ethynyl-substituted cyclopentadienone branching unit **3-8** to the ethynyl-substituted core **3-4**, the first-generation dendrimer **3-9** (Scheme 4) with TiPS-ethynyl groups was formed in 86% yield. After the cleavage of the TiPS groups in **3-9** with tetra-*n*-butylammonium fluoride (TBAF), dendrimer **3-10** was achieved with "free" ethynyl groups in 87%. The resulting activated ethynyl groups were further treated with "end-capping" building block **3-7** to achieve the second-generation dendrimer **GIrG2** (84%), or with "adaptable" building block **3-8**. Then this cycle of cycloaddition, deprotection and end-capping was repeated to third and fourth generation dendrimers (**GIrG3** and **GIrG4**) with high yields (> 80%) for all steps. These detailed reaction condition and full characterization of each compound will present in the experiment part.
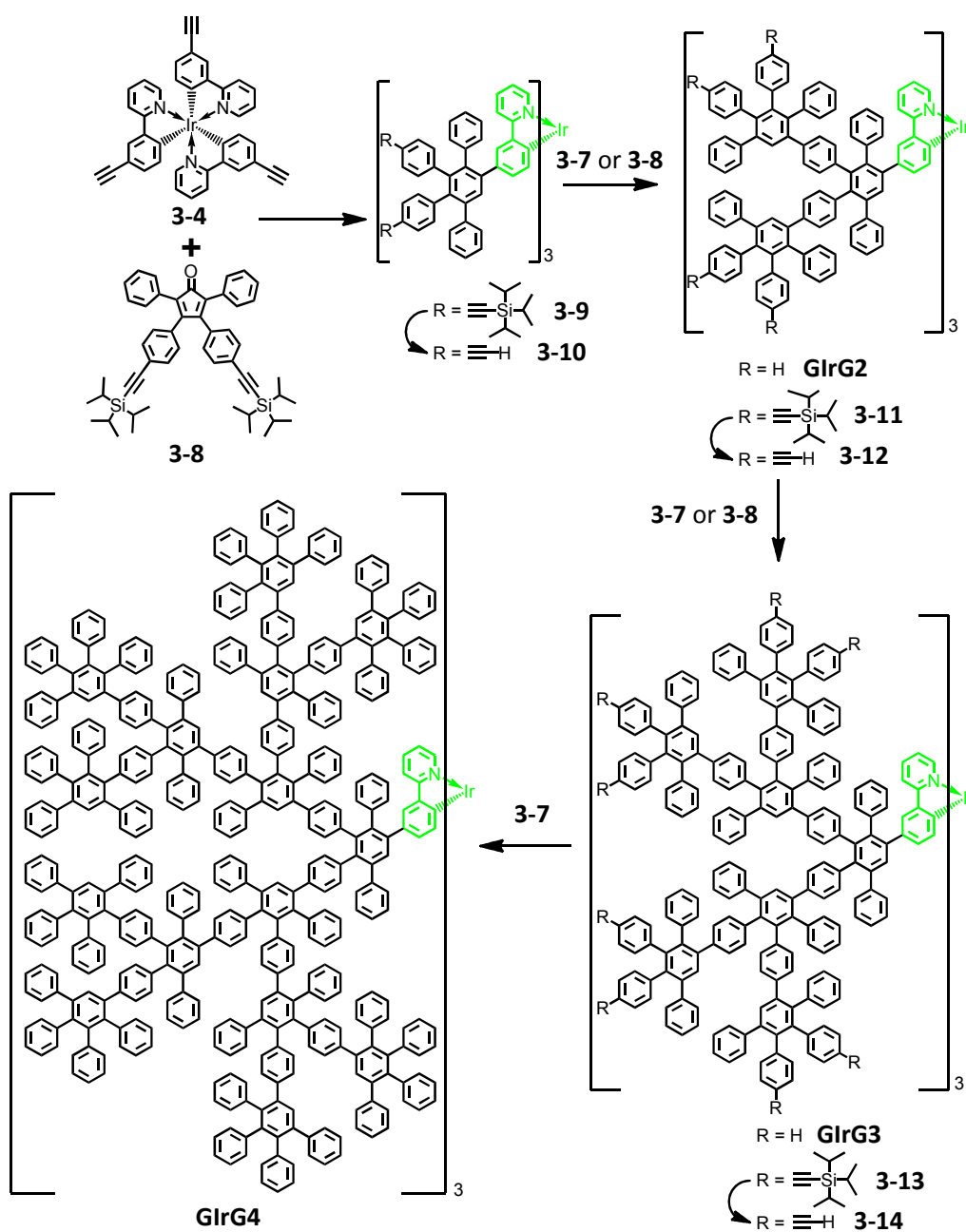
Scheme 3-6: Synthesis of second to fourth generation Ir(ppy)₃ cored polyphenylene dendrimers (**GIrG2**, **GIrG3** and **GIrG4**).

3.3.4 Characterization of Ir(ppy)$_3$ cored polyphenylene

The structures of dendrimers **GIrG1**, **GIrG2**, **GIrG3** and **GIrG4** were elucidated by NMR spectroscopy and MALDI-TOF mass spectrometry. The MALDI-TOF mass spectra (Figure 3-6) demonstrate a main intense signal corresponding to the calculated mass of the four dendrimers with three dendronized ligands (IrDL$_3$), and an additional signal belonging to fragments with only two dendronized ligands (IrDL$_2$).[32]
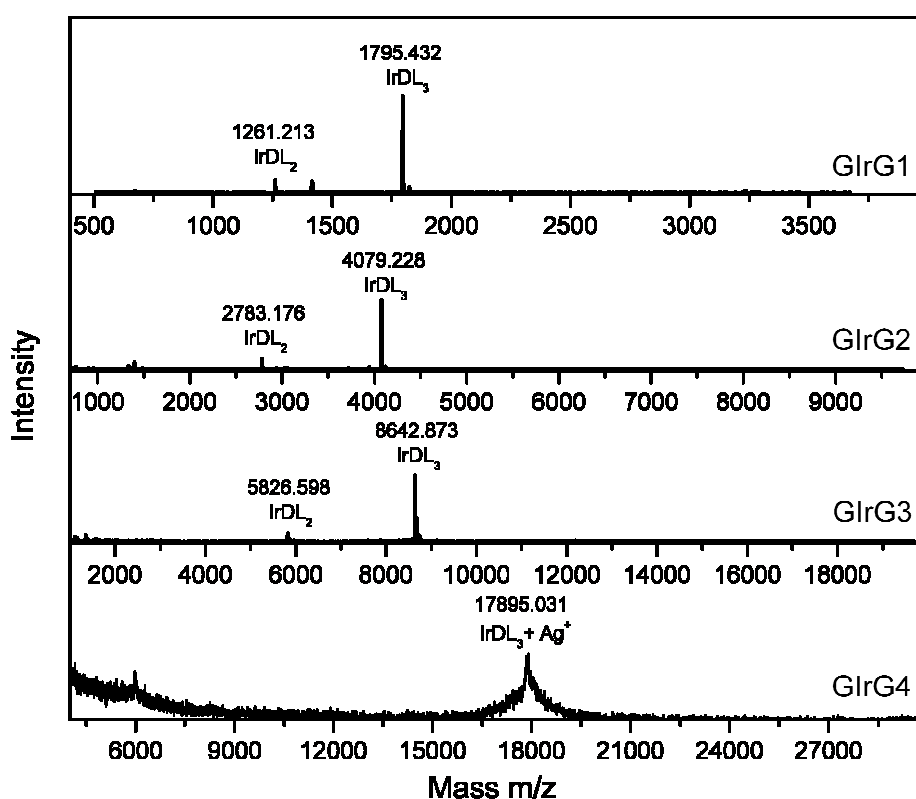
Figure 3-6: MALDI-TOF mass spectra of Ir(ppy)$_3$ cored polyphenylene dendrimers (**GIrGx**).

For the first-generation dendrimers **GIrG1**, the high resolution MALDI-TOF mass spectrum shows a single signal at 1795.432 g·mol^{-1}, perfectly agreeing with the calculated molecular weight of 1795.629 g·mol^{-1}, and an additional single signal at 1261.213 g·mol^{-1}, according with the calculated value of the fragment with two dendronized ligands of 1261.407 g·mol^{-1}. For second- dendrimer **GIrG2**, the MALDI-TOF

mass spectrum display two single intense signals at 4079.228 and 2783.176 g·mol^{-1}, as well as the mass spectrum of **GIrG3**, which reveals two single intense signals at 8642.873 and 5826.598 g·mol^{-1}, both being identical to the calculated m/z ratios of molecule (IrDL$_3$) and fragment (IrDL$_2$). The largest dendrimer **GIrG4** demonstrates a peak at 17895.031 g·mol^{-1}, which is attributed to the molecule attached with a silver ion. The experimental and calculated masses of **GIrG1**-**GIrG4** dendrimers and their fragments are listed in Table 3-3.

Table 3-3: Experimental molecular weights (M$_e$), calculated molecular weights (M$_c$), molecular diameters (D) of four generations of dendrimers (**GIrG1**, **GIrG2**, **GIrG3** and **GIrG4**).

	M_e (Ir(DL)$_3$) [gmol^{-1}] [a]	M_e (Ir(DL)$_2$) [gmol^{-1}] [a]	M_c (Ir(DL)$_3$) [gmol^{-1}] [b]	M_c (Ir(DL)$_2$) [gmol^{-1}] [b]	D [Å] [c]
GIrG1	1795.432	1261.213	1795.629	1261.407	30
GIrG2	4079.228	2783.176	4079.579	2783.472	50
GIrG3	8642.873	5826.598	8643.463	5827.310	60
GIrG4	10895.031*	-	17884.240*	-	80

[a] Measured by MALDI-TOF mass spectrometry using dithranol as matrix, * means Ag$^+$ cationization agent was added. [b] Calculated by ChemBioOffice 2008. [c] Calculated by PC Spartan 06 from MMFF simulation method.

The well-defined MALDI-TOF mass spectra can prove that all four generations of dendrimers are structurally perfect and extremely pure. Moreover, all generation dendrimers reveals good solubilities in common organic solvent thus allowing their full characterization by NMR spectroscopy. Characterization by ^{1}H NMR spectroscopy shows well-separated and clearly assignable signals for the aromatic protons as well as for the ethynyl or TiPS protons. Figure 3-7 demonstrates the ^{1}H NMR of **3-10** as an example.
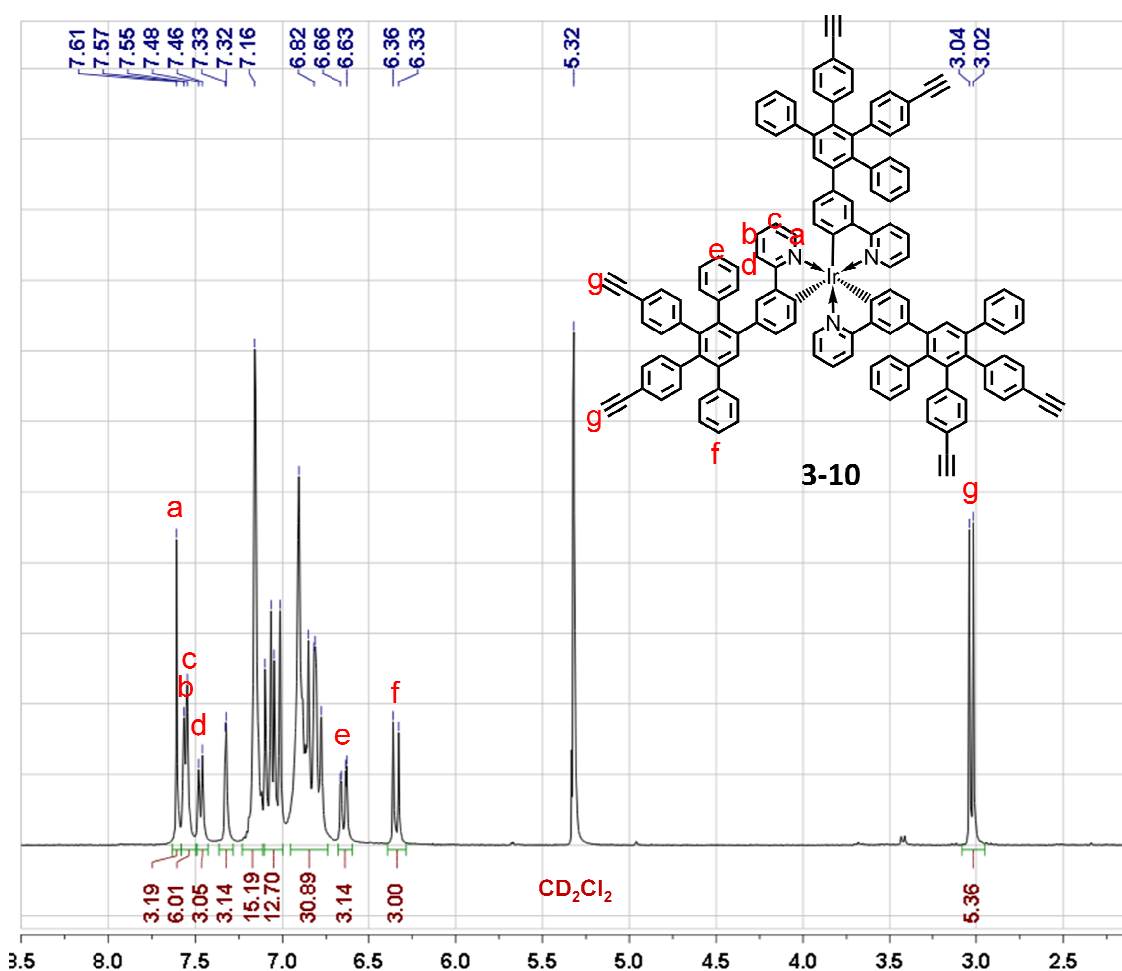
Figure 3-7: ^{1}H-NMR spectrum of Ir(ppy)₃ cored dendrimer **3-10.**

At high field (δ = 7.61 - 7.46 ppm), resonances of the aromatic protons H_a - H_d of the pyridine unit could be observed. The protons of the polyphenylene dendrons showed up between δ = 7.33 ppm and 6.33 ppm, among which the protons on the *para*-position of phenyl groups in dendrons (H_e and H_f) appeared two doublets in relatively low field at 6.64 and 6.34. In the aliphatic region, the protons of the ethynyl groups in the periphery (H_g) appeared as two singlets at δ = 3.04 ppm and δ = 3.02 ppm, respectively. The slightly different chemical shifts were due to the asymmetric twisting of the covalent bonds between polyphenylene dendrons and ligands. The integrations of all characteristic signals completely accorded with their theoretical ratios.

From both MALDI-TOF mass spectrometry and NMR spectroscopy, all dendrimers are well-defined for physical characteristics and PhOLED device processes which will be discussed in the following paragraphs.

3.4 Visualization and simulation of Ir(ppy)₃ cored polyphenylene dendrimers

In order to demonstrate that the goal of this work has been reached, namely to generate very large dendrimers based on Ir(III) complex cores, which can be regarded as models to investigate the relationship between molecular sizes of Ir(III) dendrimers and their photophysical properties, the three-dimensional structures of the species from **GIrG1** to **GIrG4** were simulated, employing PC Spartan 06 from the molecular modeling force field (MMFF) method.

For all four generations of dendrimers, the structures of the Ir(III) complex core and polyphenylene dendrons were optimized separately. Each generation bore three equivalent dendrons in the respective dendrimer. For any generation dendrimer, a combination of one single dendron with the Ir(III) core was minimized, to which the next dendron was subsequently attached for the following optimization. This was repeated until three dendrons had completed the whole structure of the dendrimer. The simulated structures of these dendrimers are presented in Figure 3-8, and their molecular diameters are listed in Table 3-3. In the following paragraphs the relationship between these calculated molecular sizes of different generation dendrimers and their photophysical properties as well as device performances were investigated.
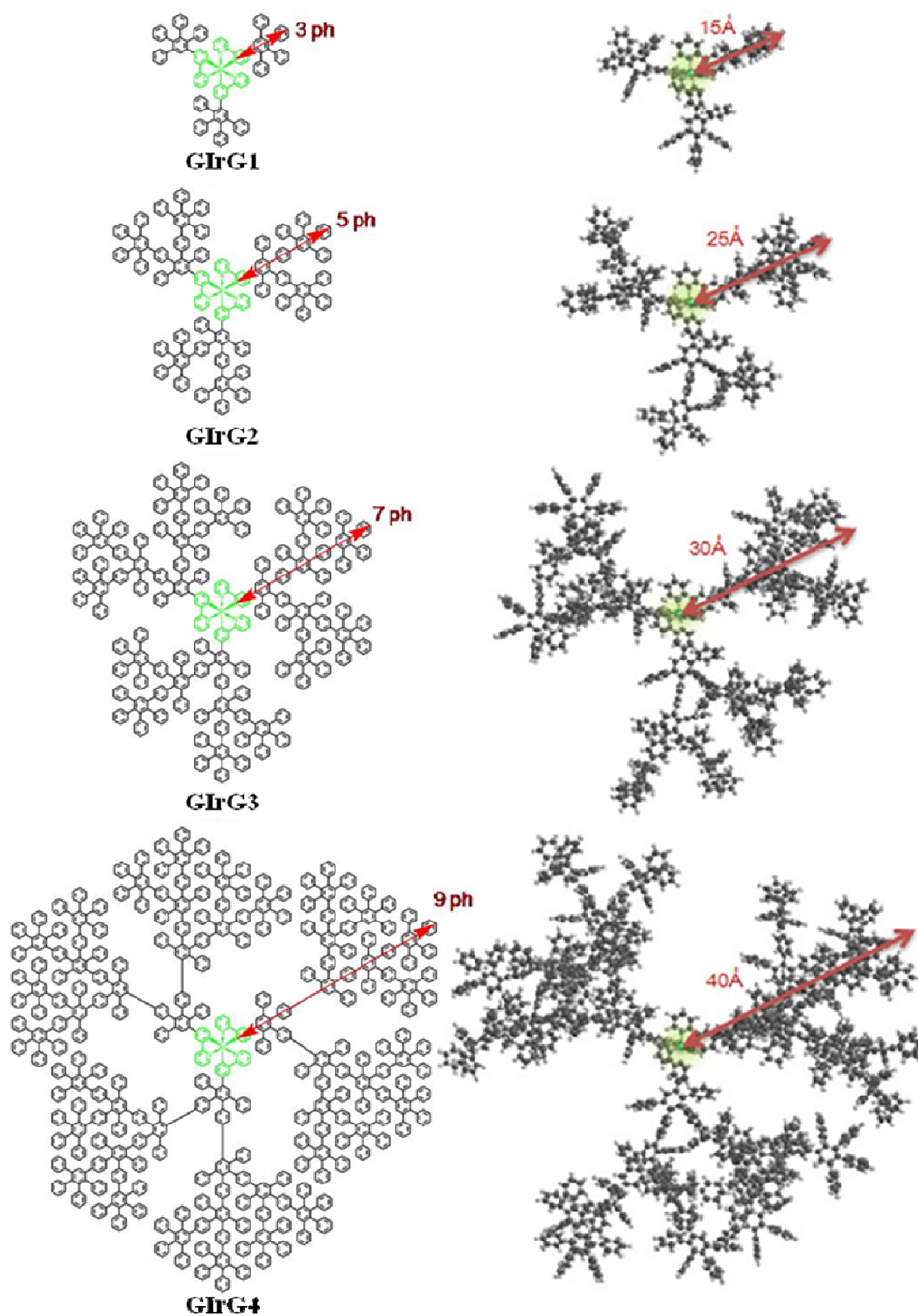
Figure 3-8: Three-dimensional structures of dendrimers **GIrG1**, **GIrG2**, **GIrG3** and **GIrG4**, obtained by molecular simulation using MMFF method.

3.4 Physical properties of Ir(ppy)₃ cored polyphenylene dendrimers

In this chapter, the influence of the surrounding polyphenylene dendronized shell upon the photo-physical properties of the *fac*-tris(2-phenylpyridyl)Ir(III) cores is investigated using UV-Vis spectroscopy in solution as well as in the solid state. Furthermore, photoluminescence spectroscopy and quantum yield in solution and in thin film are applied for the optical characterization of these phosphorescent dendrimers. Finally, the electrochemical properties and energy levels of these dendrimers are developed by cyclic voltammetry measurement.

3.4.1 UV-vis absorption and photoluminescence spectroscopic measurements

The UV-Vis absorption spectra (Figure 3-9) of Ir(III) dendrimers **GIrG1**, **GIrG2**, **GIrG3** and **GIrG4** were measured in dichloromethane solutions at 298 K (Table 3-4). In general, the absorption spectra of lower generation dendrimers **GIrG1** and **GIrG2** could be divided into two components. The short wavelength regions below 300 nm were predominantly attributed to the intra-ligand π-π* transition of the polyphenylene dendrons,[33] while the longer wavelength absorptions at around 350 – 450 nm were primarily due to the metal-to-ligand charge transfer (MLCT) state of the Ir(III) core.[34] For instance, the singlet and triplet MLCT bands for **GIrG1** fall at 414 nm ([1]MLCT) and 460 nm ([3]MLCT),[35] respectively (Figure 3-9 and Table 3-4). However, for higher generation dendrimers **GIrG3** and **GIrG4**, the MLCT shoulders could not be clearly detected due to the intense absorption of their larger dendritic ligands.[36]
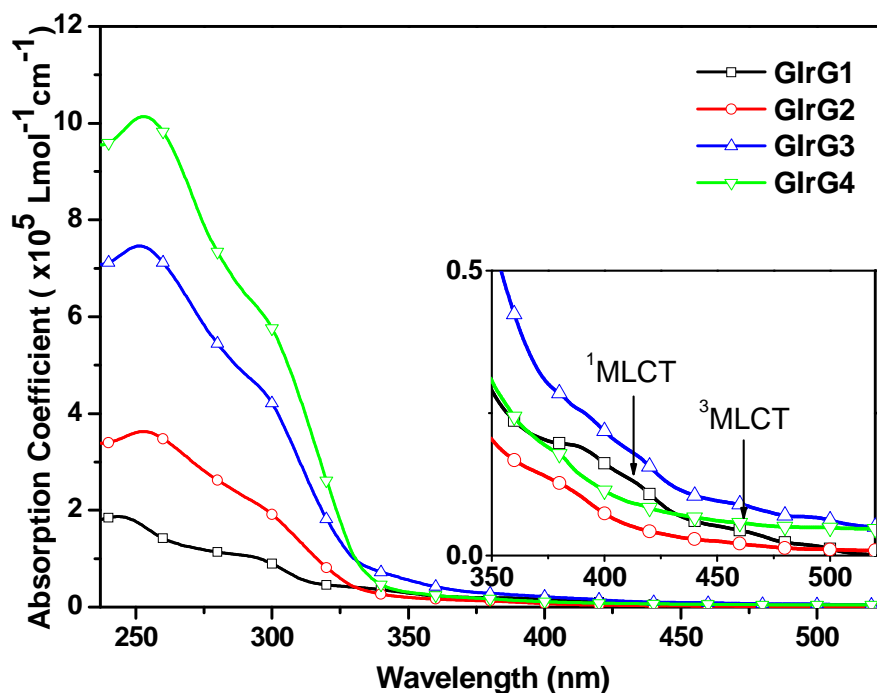
Figure 3-9: UV-Vis absorption spectra of **GIrGx** dendrimers in DCM solutions with a concentration of 10^{-6} M.

The photoluminescence (PL) spectra of dendrimers **GIrG1**, **GIrG2**, **GIrG3** and **GIrG4** in dichloromethane solutions and in solid films are shown in Figure 3a and 3b. Similar to **Ir(ppy)₃**,[15] all dendrimers exhibited only one green emission peak at 516 nm. In contrast, in the solid state, the PL maximum of dendrimer **G1** showed a bathochromic shift of 11 nm compared to the dichloromethane solution, indicating that the first generation polyphenylene dendrons were not sufficient to prevent intermolecular interaction.[37] However, with the dendrimer generation increasing from the second to the fourth, the aggregation induced bathochromic shift was reduced from 9 nm to 0 nm. This suggested that intermolecular interactions of the emissive cores could be effectively avoided by larger dendrons in higher generation dendrimers.[28]
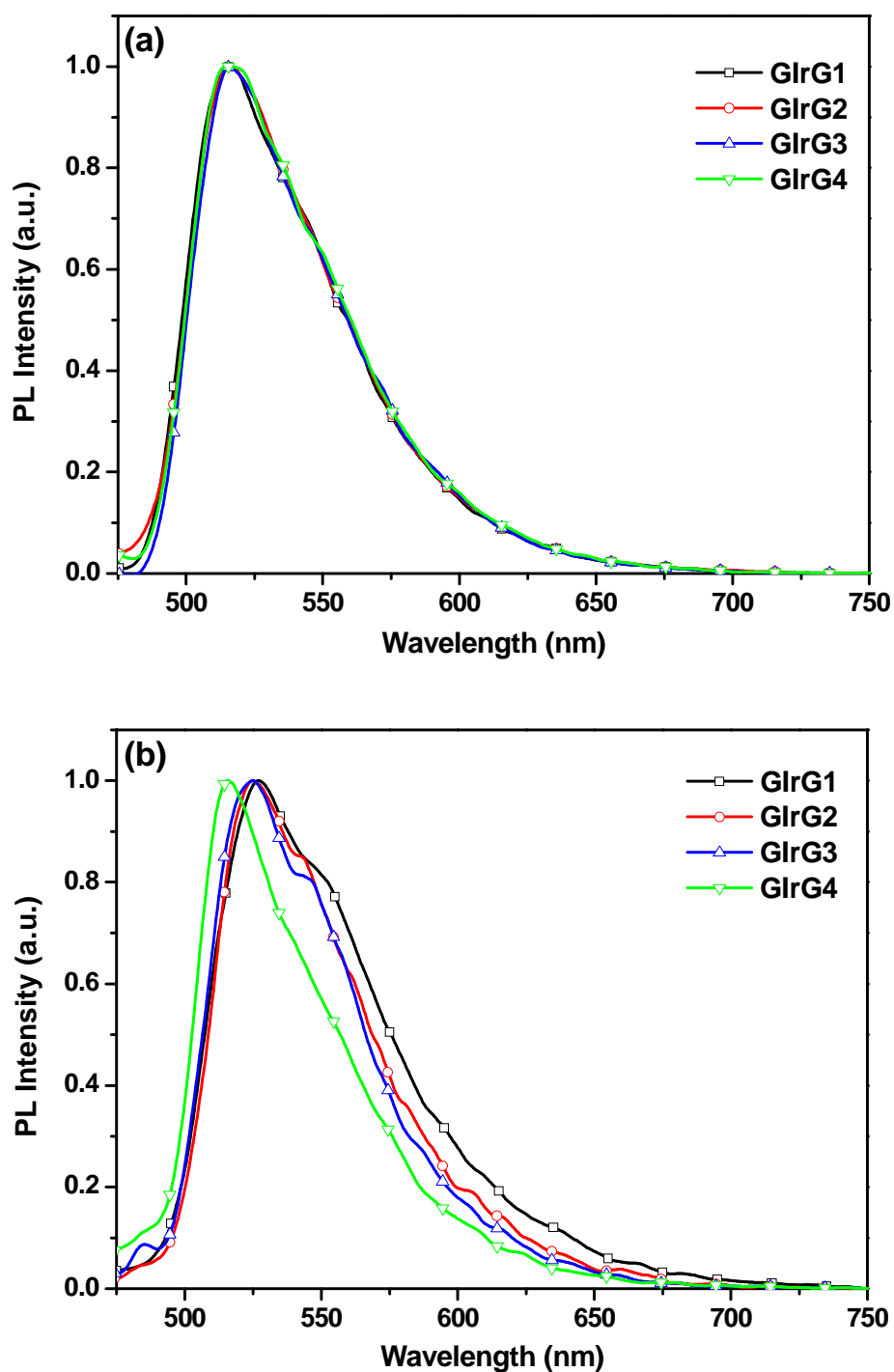
Figure 3-10: Photoluminescence (PL) spectra of **GIrGx** dendrimers (a) in DCM solutions with a concentration of 10^{-5} M (λ_{ex} = 380 nm) and (b) in thin films (λ_{ex} = 410 nm).

3.4.2 Photoluminescence quantum yield

We further probed the photophysical properties of the dendrimers by measuring their PL quantum yields (PLQYs) in solutions and in solid films (Table 3-4) with **Ir(ppy)₃** (40%) as the reference.[15]

Table 3-4: Absorption (λ_{abs}) and emission (λ_{em}) maxima, and photoluminescence quantum yield (Φ_P) of **GIrGx** dendrimers in solution and thin film.

|	λ_{abs} [nm] (log ξ)[a]	λ_{em} [nm][b]	Φ_P (%)[c]	λ_{em} [nm][d]	Φ_P (%)[d]
GIrG1	244 (5.3), 294 (5.0), 336 (4.6), 390 (4.3), 414 (4.1), 460 (4.0)	516	39	527	8
GIrG2	253 (5.6), 298 (5.3), 384 (4.1)	516	49	525	22
GIrG3	253 (5.9), 298 (5.6)	516	53	525	30
GIrG4	253 (6.0), 298 (5.8)	516	56	516	36

[a] Measured in DCM at 298 K with a concentration of 10^{-6} M. [b] Measured in DCM at 298 K with a concentration of 10^{-5} M and excitation wavelength of 380 nm. [c] Measured in N_2-saturated toluene at 298 K with Ir(ppy)₃ as the reference and the excitation wavelength of 390 nm. [d] The data of neat films measured at 298 K, which were prepared by drop-coating on quartz substrates. PL spectra were measured with the excitation wavelength of 410 nm.

In N_2-saturated toluene solutions, dendrimer **GIrG1** possessed nearly the same relative PLQY (39%) as Ir(ppy)₃, the relative PLQYs of higher generation dendrimers increased along with their growing generations, from 49% for **GIrG2**, 53% for **GIrG3** to 56% for **GIrG4**, respectively, because of their better chromophore separation. The film PLQYs were measured with an integrating sphere under an excitation wavelength of 409 nm.[38] The film of the largest dendrimer **GIrG4** exhibited an absolute Φ_P of 36%, which was 4 times higher than that of **GIrG1** (8%), indicating a significantly reduced quenching between Ir(III) cores.[8] Moreover, the absolute Φ_P of **GIrG4** in film was nearly the same as the relative Φ_P of **GIrG1** in solution, which suggested that the fourth-generation

dendrons were almost completely able to suppress the self-quenching between Ir(III) cores when going from solution to film.[28]

3.4.3 Electrochemical properties

To understand at which potential charges would be injected into the dendrimers in PhOLEDs, cyclic voltammetry (CV) measurements were performed to study the electrochemical properties of all dendrimers. The oxidation cyclic voltammograms of three dendrimers (**GIrG1**, **GIrG2**, and **GIrG3**) are shown in Figure 3-11 (the oxidation of **GIrG4** was too weak to be recognized).[39]
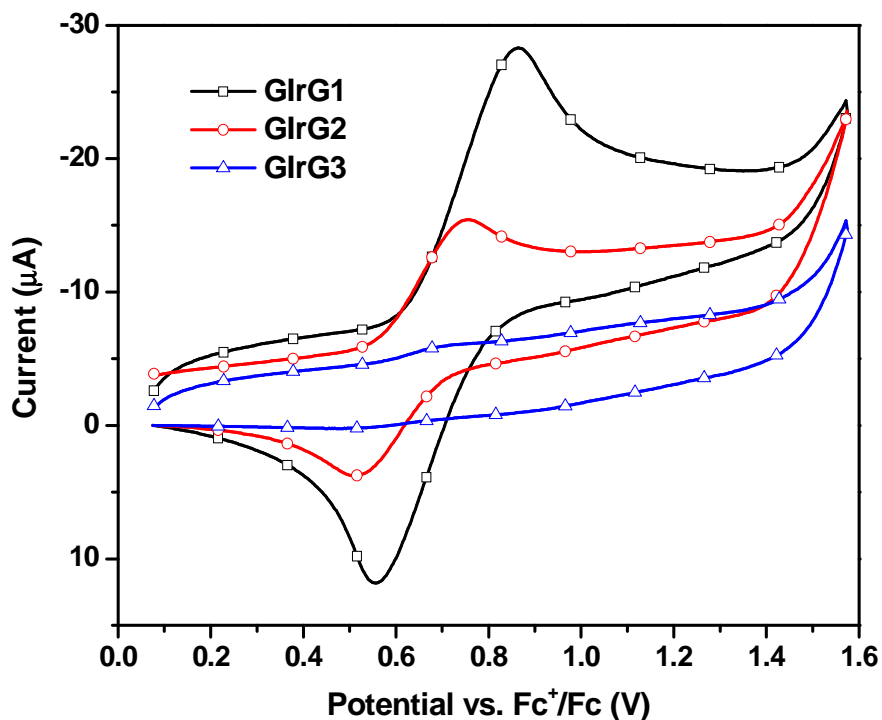
Figure 3-11: Cyclic voltammetry of **GIrGx** dendrimers in DCM solution. All the oxidation potentials are quoted against the ferricenium/ferrocene couple.

All three dendrimers demonstrated reversible oxidation potentials at ca. 0.63 V vs. an Ag/Ag⁺ electrode, which were assigned to the oxidation of iridium metal cationic site (Ir(III)→Ir(IV)).[40] According to the onset potential of the oxidation process (0.63 V), the highest occupied molecular orbitals (HOMOs) of dendrimers **GIrG1**, **GIrG2**, and **GIrG3**

were estimated to be around −5.0 eV according to the formula $E_{HOMO} = -(E^{ox} + 4.34)$.[41] The energy levels of lowest unoccupied molecular orbital (E_{LUMO}) of the three dendrimers were calculated to be around −2.6 eV by subtraction of the optical band gap (2.4 eV, taken from the onset of absorption at 516 nm, Figure 3-9) from the E_{HOMO}.[42]

3.5 Green PhOLEDs based on Ir(ppy)$_3$ cored polyphenylene dendrimers

Both in vacuum-deposited small molecular and solution-processable polymeric PhOLEDs, doping Ir(III) complexes into a host materials was necessary to improve their device performances.[9] However, the triplet energy level of the doping host has to be finely tuned to avoid back energy transfer from the emissive guest molecules to the host molecules.[43] Moreover, the phase separation that occurs in doped systems inevitably impedes improved device performance.

Recently, several types of phosphorescent dendrimers have been successfully used in the fabrication of non-doped PhOLEDs by means of a host-free system.[25-27] These non-doped dendrimer based devices were desirable, especially for low-cost, large-area displays and lighting sources, due to their simple device configurations. Some of these non-doped PhOLEDs achieved comparable efficiency to that of doped PhOLEDs based on small molecules. Therefore, we firstly fabricated the non-doped PhOLEDs based on the Ir(ppy)$_3$ cored polyphenylene dendrimers and investigated their performances.

3.5.1 Non-doped green phosphorescent OLEDs

The Ir(ppy)$_3$ cored polyphenylene dendrimer based OLED devices were processed and characterized by our corporate partners, Dr Junqiao Ding and Prof. Lixiang Wang at Chinese Academy of Sciences.

All the devices were prepared used indium tin oxide (ITO) as the anode and LiF/Al as the cathode. The non-doped PhOLEDs fabricated in a standard sandwich geometry using the following structure: ITO/PEDOT:PSS/**GIrGx**/TPBI/LiF/Al, leading to the energy diagram

depicted in (Figure 3-12). As we already discussed in the previous chapter, an additional TPBI layer has been used as the ETL/HBL in the **GIrGx** based phosphorescent device.
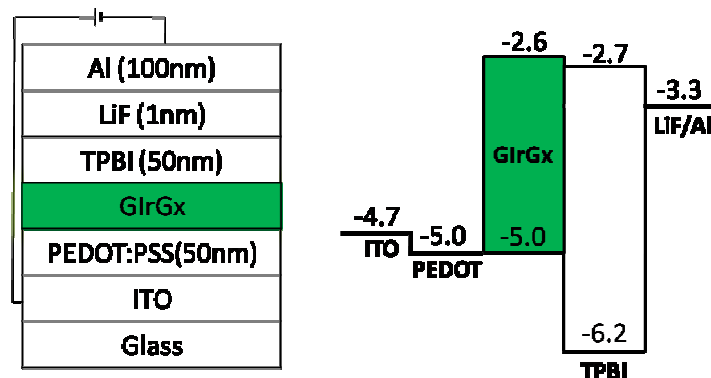
Figure 3-12: Schematic diagram of non-doped **GIrGx** dendrimer based electroluminescence (EL) device configurations (left), and energy levels of EL devices (right).

All Ir(ppy)$_3$ cored polyphenylene dendrimer (**GIrGx**) devices showed pure green phosphorescence with Commission International de L'Eclairege (CIE 1931) coordinates of (0.33, 0.60), (0.31, 0.63), (0.30, 0.63) and (0.29, 0.58), respectively (Figure 3-13).[44]
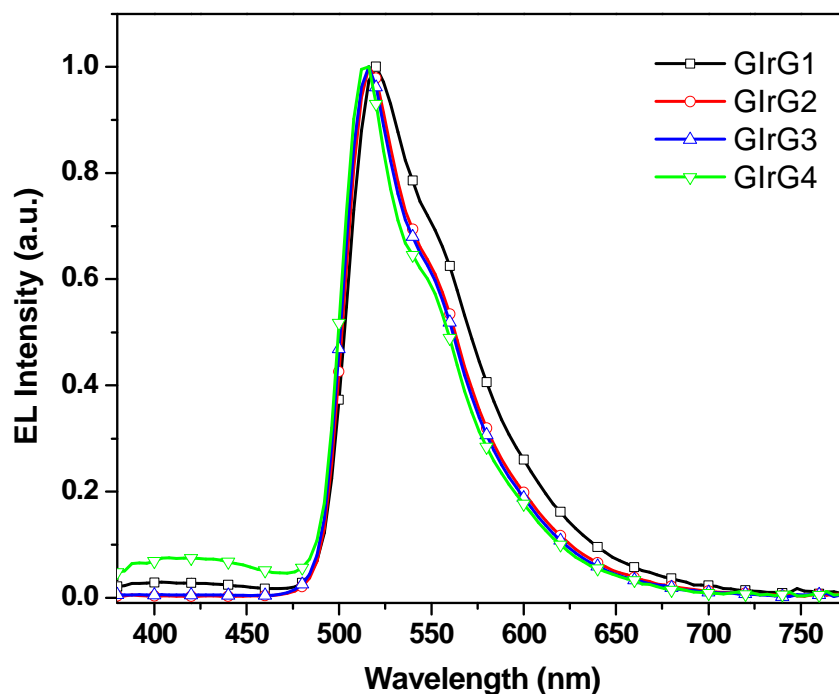

Figure 3-13: EL spectra of **GIrGx** dendrimer based devices at driving voltage of 8 V.

The EL spectra of all dendrimers were independent of the applied voltage varying from 6 to 16 V, which were attributed to their rigid polyphenylene frameworks. The longer maximum wavelength and larger red tail in EL emission of the **GIrG1** than those of other higher generation dendrimers might be due to the excimer emission,[45] which illustrated that the first generation polyphenylene dendrons have not prevented the interactions of the emissive cores. This was not surprising since the higher generation dendrimers (**GIrG2** to **GIrG4**) exhibited EL maxima identical to their solution PL counterparts. According to a previous paper,[46] the polyphenylene dendrons emitted a strong fluorescence in solution with a maximum in emission at ca. 365 nm, this would obviously overlap with the absorption bands from the MLCT states of the Ir(ppy)₃ complex.[34] Considering this spectral overlap between the emission of polyphenylene dendrons and absorption of Ir(III) core, an intramolecular energy transfer should take place from dendrons to the core. Therefore, in both PL and EL spectra of **GIrG1** to **GIrG3** dendrimers, these emissions in the UV region were undetectable. This clearly proved that the excitiation energies of polyphenylene dendrons were completely transfered to the Ir(III) core. Finally, these dendrimes emitted green phosphorescences with maximum emissions at 520 nm for **GIrG1**, and 516 nm for **GIrG2** and **GIrG3**. Moreover, dendrimer **GIrG4** possessed a similar maximum emission at 516 nm, but with an additional peak at around 380 - 450 nm. This shoulder bands were estimated to the emission of the polyphenylene dendrons, indicating that the very large size of dendrons in **GIrG4** induced an incomplete energy transfer from the peripheral polyphenylene to the Ir(III) core.

The device I-V-L characteristics of all **GIrGx** dendrimer based devices were displayed in Figure 3-14 and tabulated in Table 3-5. These performance values of our **GIrGx** dendrimer based non-doped devices were comparable to those of vacuum-deposited small molecular phosphorescent emitters and significantly higher than those of **TPGx** and **PYGx** dendrimers. Besides the influence of color tuning, the main reason for this was the high quantum efficiency of phosphorescent Ir(III) complexes. One point needs our attention: the luminescences of all **GIrGx** dendrimer devices at identical voltage, 14

V for example, decreased along with dendrimer generation growth, from 1900 cd/m^2 of **GIrG1** to 270 cd/m^2 of **GIrG4**. Moreover, the open-circuit voltages (defined as the bias at a current density of 0.01 mA/cm^2) slightly increased with the increasing generation, from 4.2 V of **GIrG1** to 5.9 V of **GIrG4**. We ascribed these phenomena to the increasing size of polyphenylene dendrons, which would reduce the charge mobility from periphery to the emissive core.[47]
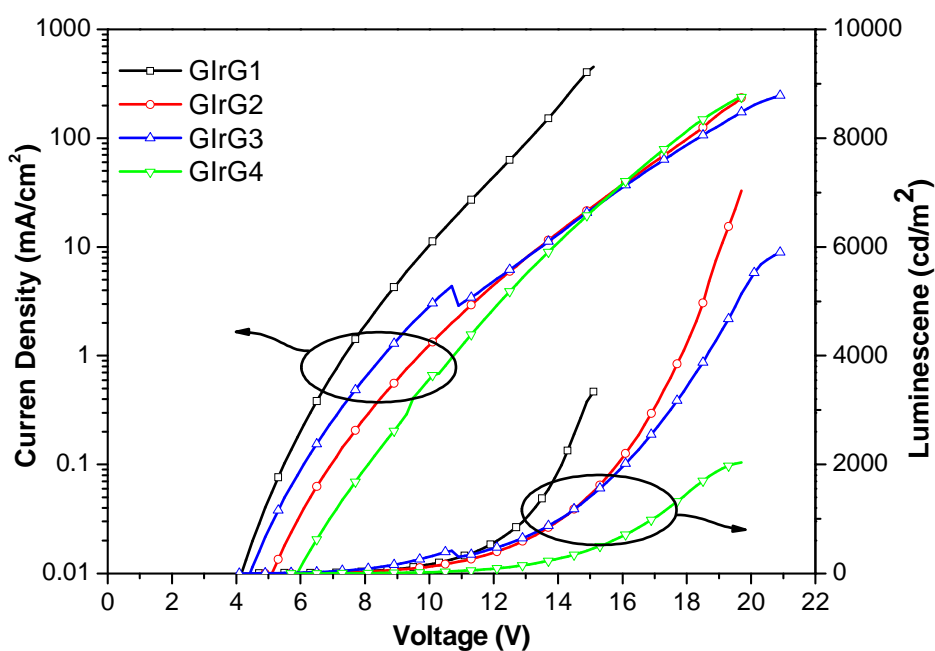

Figure 3-14: I-V-L characteristics of non-doped **GIrGx** dendrimer based devices.

The reduction of mobility increases the waiting time of the charge carriers on the transport sites which in turn increases the probability of recombination. Like in the case of bilayer OLEDs, the recombination occurs at the interface between the electron transporting and hole transporting material,[48] or the case of hole conducting hosts doped with electron transporting guest molecules.[49] In both cases the device efficiency is increased dramatically and independently of the cathode workfunction. The fact that the dispersion became stronger with higher generation dendrons was indicative of an increase in the waiting time of majority charge carriers. The increase in efficiency with generation suggested that the adverse effect of increased spacing of hopping sites has a greater effect on the majority than on the minority charge carriers. The minority charge carriers appear to be trapped on the chromophores,[50] and a reduction in effective

majority carrier mobility leads to a significant rise in device efficiency. We conclude that in this case the effect of the generation on transport is merely to increase the chromophores spacing.

Figure 3-15 shows a maximum luminous efficiency of 4.6, 14.4, 21.9 and 12.2 cd/A, and a maximum extern quantum yield (EQE) of 1.3, 4.0, 6.1 and 3.8 % for **GIrG1**, **GIrG2**, **GIrG3** and **GIrG4**, respectively. Herein, non-doped devices based on dendrimer**s GIrG2** and **GIrG3** showed better performances than other lower and/or higher generation dendrimers (**GIrG1** and **GIrG4**). Even at a current density of 10 mA/cm^2, the luminous efficiency still remained as high as 7.5 cd/A (770 cd/m^2) for **GIrG2** and 8.1 cd/A (810 cd/m^2) for **GIrG3**. These non-doped device performance values were significantly higher than that of previously reported doped devices (2.9%, 9.3 cd/A), which were made from the blend of the first-generation polyphenylene Ir(III) dendrimer with 4-bis-(carbazol-9-yl)biphenyl (CBP).[51]
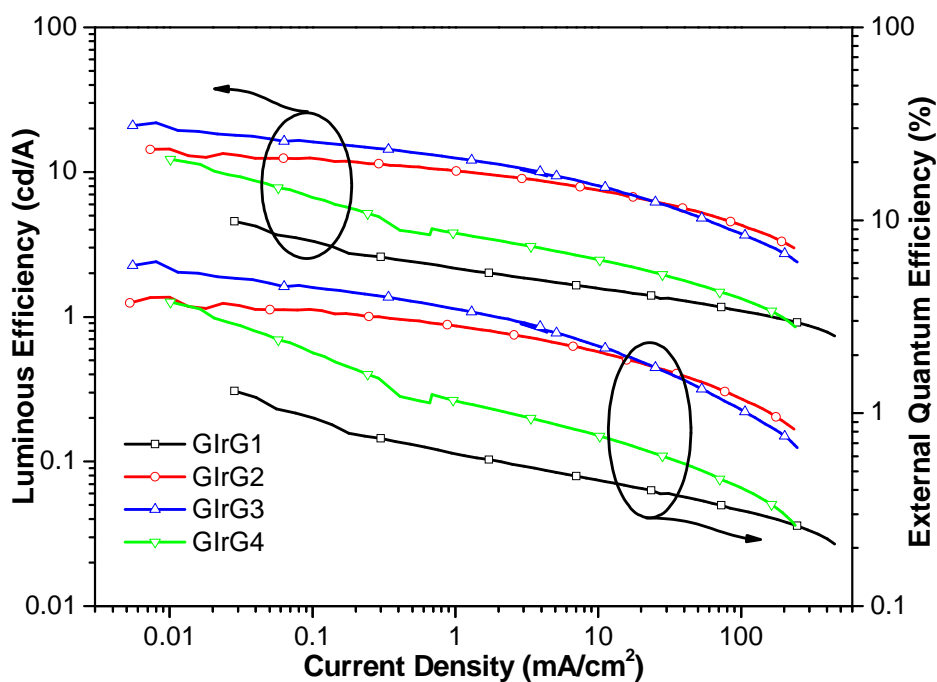

Figure 3-15: Luminous efficiency and external quantum yield versus current density diagram of non-doped **GIrGx** dendrimer based devices.

The difference in trends between luminous efficiency (EQE) and current density (luminescence) indicated that the high generation polyphenylene dendrons could not only effectively prevent the triplet-triplet annihilations among phosphorescent Ir(III) cores, but also reduce the charge transportation from dendrimer periphery to the emissive core. Therefore, if we doped the **GIrGx** dendrimers with charge-transporting materials, the device performance could be further improved.[52]

3.5.2 TCTA doped green phosphorescent OLEDs

In order to further improve the device performance, the **GIrGx** dendrimer based devices doped with 4,4',4''-tri(carbozol-9-yl)-triphenylamine (TCTA) were fabricated by using the following structure: ITO/PEDOT:PSS/**GIrGx**:TCTA/TPBI/LiF/Al, leading to the energy diagram depicted in (Figure 3-16).
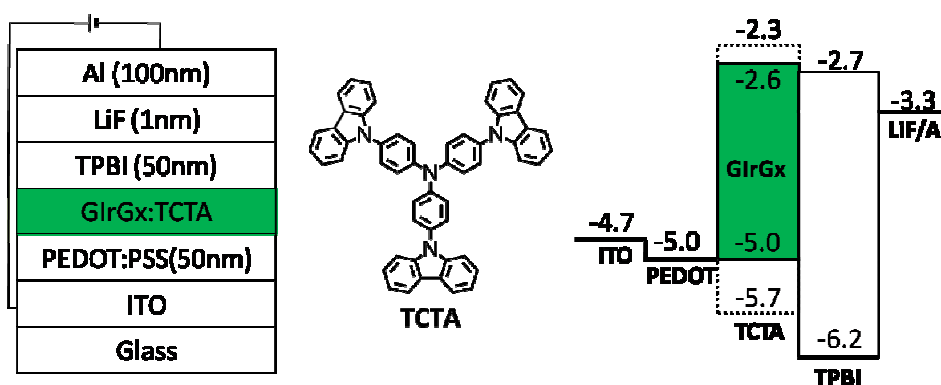

Figure 3-16: Schematic diagram of doped **GIrGx** dendrimer based electroluminescence (EL) device configurations (left), structure of 4,4',4''-tri(carbozol-9-yl)-triphenylamine (TCTA) (middle), and energy levels of EL devices (right).

The TCTA molecule contains three carbazole units around a central triphenylamine, which is considered to impart great hole-transport character.[53] TCTA was used as the host because of its long triplet lifetime, when compared to **GIrGx**, and the fact that it can transfer this energy to the Ir(III) core for emission. The synergy of energy levels is one of the important factors that gives rise to efficient Ir(III) phosphorescent devices.[54] For TCTA we found that the HOMO energy was at 5.7 eV, which is 0.7 eV lower than that

of the dendrimer, as well as the LUMO level of TCTA was at 2.3 eV, which is 0.3 eV higher than in the dendrimer. Therefore, both holes and electrons would be trapped on the dendrimer in the blend, resulting in a very high electron-hole recombination probability in the emissive layer adjacent to the hetero-junction.[55]

The **GIrGx**:TCTA layer was firstly prepared in blending solution with different ratios and then deposited by spin-coating. The devices were completed by evaporation of TPBI and the cathode materials. The **GIrGx**:TCTA layer was approximately 40 nm thick and the thickness of the TPBI layer was determined to be 50 nm. It is important to note that TCTA itself cannot be spin-coated from solution to form good quality thin film. We have found that, providing the concentration of the **GIrGx** in TCTA was greater than 10 wt.-%, the blend formed reasonably uniform thin films. When the **GIrGx** concentration was below this level the TCTA host was prone to crystallization in the as-formed films and the device shorted. This illustrates the power of the dendritic architecture for enhancing the processing properties of materials.

The best performances of TCTA doped devices were obtained with concentrations of the **GIrGx** in TCTA at 30 wt.-% for all generations, and their I-V-L characteristics was shown in Figure 3-17.
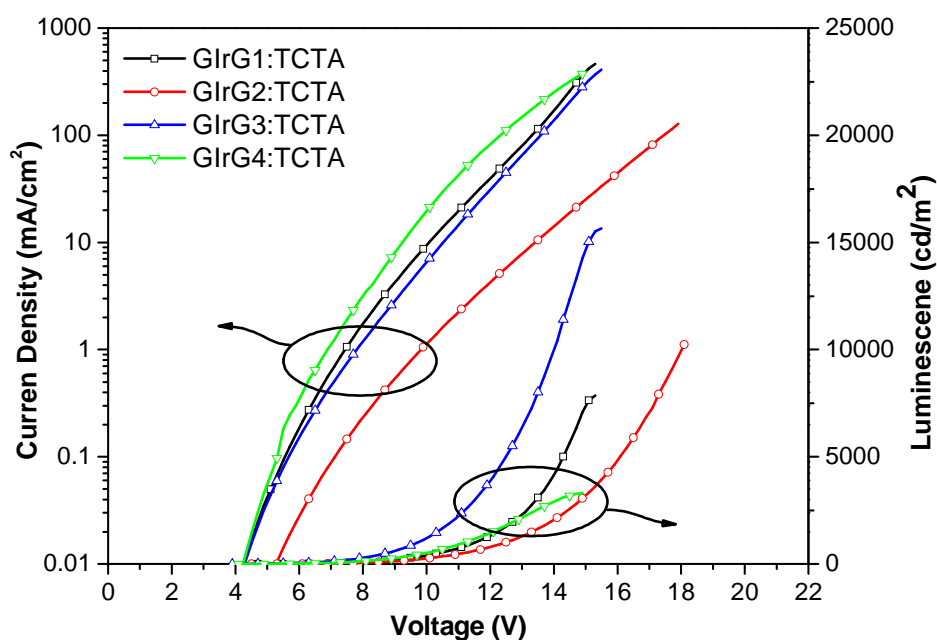
Figure 3-17: I-V-L characteristics of TCTA doped **GIrGx** dendrimer based devices.

All doped devices had lower open-circuit voltage and higher luminescence under an identical voltage than non-doped devices. These results pointed out the contribution of TCTA host in the mobility of at least one charge carrier to the polyphenylene dendrons. Moreover, non-doped and doped devices of **GIrG1** and **GIrG2** possessed almost identical I-V-L curves, but the doped systems of **GIrG3** and **GIrG4** had higher current densities than their non-doped systems. These phenomena proved that the TCTA molecules could be bound into the dendritic frameworks of higher generation dendrimers to transport holes from periphery to the Ir(III) core.[56] The performances of doped devices were comparable to that of dendrimers previously reported.[25-27] However, the divergent synthesis approach will lead to further improvements in the molecular design.

As shown in Figures 3-18, similar to the results of non-doped devices, the TCTA doped **GIrG2** or **GIrG3** device possessed much higher EQE and luminous efficiency than **GIrG1** or **GIrG4** doped devices. The maximum EQE and brightness of doped devices were up to 10.3%, 37.0 cd/A for **GIrG2** and 10.2%, 36.5 cd/m^2 for **GIrG3**, respectively, which was more than 5 times higher than that of the doped **GIrG1** device.
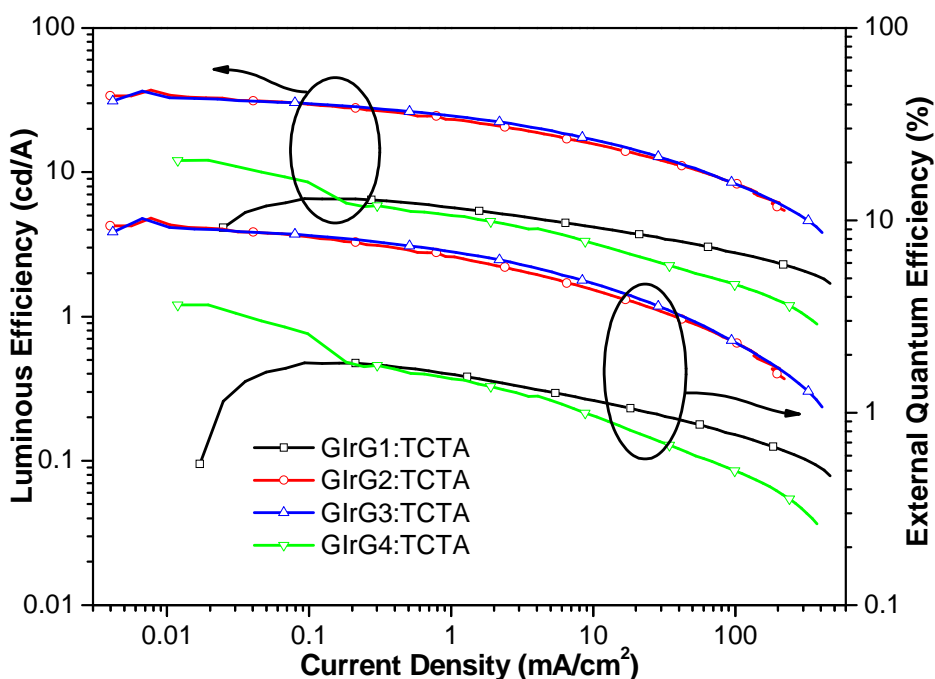
Figure 3-18: Luminous efficiency and external quantum yield versus current density diagram of TCTA doped **GIrGx** dendrimer based devices.

These significant improvements indicated that the powerful hole-transporting character of TCTA could increase the charge injection to the emissive Ir(III) core, and thus significantly optimize the device performance. However, the EQEs and luminous efficiencies of non-doped **GIrG2** (4.0%, 14.4 cd/A) and **GIrG3** (6.1%, 21.9 cd/A) devices were still much higher than those of doped **GIrG1** (1.8%, 6.5 cd/A) device with TCTA. This could be attributed to the dendritic architecture controlling the intermolecular interactions of the Ir(III) cores of the dendrimers.

Nevertheless, the performances of both non-doped and doped devices of the largest Ir(III) dendrimer **GIrG4** were suddenly reduced because of its overlarge molecular size ($R_4 \approx 40$ Å) from the outer dendrimer periphery to the Ir(III) core, which was above the value of ca. 30 Å for the Förster resonance energy transfer (FRET) from dendrimer periphery to the Ir(III).[57] As it was shown earlier for other core derivatives and extended polyphenylene dendrimers, the twisted polyphenylene spacers interrupt the π-conjugation and reduce the charge carrier-mobility with the number of units increasing.[47a] Therefore, the charge injection to the core is hampered. Partial charges prefer to delocalize on the outer phenylene units and after considerable equilibration time the charges can enter the core. This is the reason why dendrimer **G4** demonstrated the highest PLQY but lower device performance.

3.6 Summary

In conclusion, we developed a novel divergent strategy to synthesize high generation Ir(III) cored polyphenylene dendrimers up to **GIrG4**, which is the largest Ir(III) dendrimer up to now and have never been synthesized by previous methods. Nevertheless, the novel divergent procedure can simplify the color tuning of Ir(III) dendrimers not only by using different homoleptic cyclometalated ligands,[33, 58] but also by importing multi-color chromophores into the core, dendrons and shell-groups in dendrimers.[59] Besides many of the desired properties achieved at appropriate molecular size, the efficiency of simple device architectures can easily balance the effort required for their synthesis.

In this chapter, our four different generations of Ir(III) dendrimers offer a unique opportunity to develop the relationship between the Ir(III) dendrimer sizes and their PhOLEDs performances. The modular molecular architecture gives tremendous scope for tuning a wide range of properties in addition to color, such as intermolecular interactions, charge mobility, and exciton diffusion. The most important issue is that our investigation of the device performances on differently sized dendrimers indicate that the effective charge injection distance into the Ir(III) core is around 30 Å. The suitable molecular size can not only prevent intermolecular triplet-triplet annihilation thus increasing the PLQY, but also provide an effective charge carrier-mobility from the periphery of the dendrimer to the Ir(III) core.

Moreover, for the OLEDs based on the Ir(III) cored polyphenylene dendrimers, challenges remain that device configuration must be optimized to achieve higher performance. Apart from the fact that a separate TPBI layer was fabricated in all of these green PhOLED devices as the ETL/HBL layer, which had been discussed in the previous chapter and could significantly improve the electron properties and emissive efficiencies of devices, the emissive dendrimer layer was further doped with TCTA as the host material. The device performances showed that the TCTA was a promising hole-transporting material and could effectively improve the electron properties, such as the current density and turn-on voltage, as well as the emissive efficiencies, such as luminous efficiency and EQE. These results prompted us to design a self-host dendritic system as the emissive materials to simplify the configuration and increase the performance of OLED devices. These self-host phosphorescent dendrimers should carry the Ir(III) complex emitter as the guest in the center in combination with hole-transporting units, e.g. triphenylamine, as the host in the periphery. Therefore, in the next chapter, a new series of self-host dendrimers with a modified Ir(III) core and peripheral multi-triphenylamine units will be presented.

References

[1]   a)Bardeen, J., Cooper, L. N., Schrieffer, J. R., *Physical Review* **1957**, *108*, 1175; b)Gunnarsson, O., Lundqvist, B. I., *Physical Review B* **1976**, *13*, 4274.

[2]   a)Perry, J. W., Mansour, K., Lee, I. Y. S., Wu, X. L., Bedworth, P. V., Chen, C. T., Ng, D., Marder, S. R., Miles, P., Wada, T., Tian, M., Sasabe, H., *Science* **1996**, *273*, 1533; b)Baldo, M. A., O'Brien, D. F., You, Y., Shoustikov, A., Sibley, S., Thompson, M. E., Forrest, S. R., *Nature* **1998**, *395*, 151.

[3]   a)Salem, L., *J. Am. Chem. Soc.* **1968**, *90*, 543; b)Foresman, J. B., Headgordon, M., Pople, J. A., Frisch, M. J., *J. Phys. Chem.* **1992**, *96*, 135.

[4]   McClure, D. S., *J. Chem. Phys.* **1949**, *17*, 905.

[5]   a)Christodouleas, N., McGlynn, S. P., *J. Chem. Phys.* **1964**, *40*, 166; b)McGlynn, S. P., Daigre, J., Smith, F. J., *J. Chem. Phys.* **1963**, *39*, 675.

[6]   a)Elsayed, M. A., *J. Chem. Phys.* **1963**, *38*, 2834; b)Henry, B. R., Siebrand, W., *J. Chem. Phys.* **1971**, *54*, 1072.

[7]   a)McGlynn, S. P., Sunseri, R., Christod.N, *J. Chem. Phys.* **1962**, *37*, 1818; b)Gouterma.M, Schwarz, F. P., Smith, P. D., Dolphin, D., *J. Chem. Phys.* **1973**, *59*, 676; c)Greene, C. H., Aymar, M., *Phys. Rev. A* **1991**, *44*, 1773.

[8]   a)Dexter, D. L., Schulman, J. H., *J. Chem. Phys.* **1954**, *22*, 1063; b)Xie, H. Z., Liu, M. W., Wang, O. Y., Zhang, X. H., Lee, C. S., Hung, L. S., Lee, S. T., Teng, P. F., Kwong, H. L., Zheng, H., Che, C. M., *Adv. Mater.* **2001**, *13*, 1245; c)Kawamura, Y., Brooks, J., Brown, J. J., Sasabe, H., Adachi, C., *Phys. Rev. Lett.* **2006**, *96*; d)Kalinowski, J., Stampor, W., Mezyk, J., Cocchi, M., Virgili, D., Fattori, V., Di Marco, P., *Physical Review B* **2002**, *66*; e)Reineke, S., Walzer, K., Leo, K., *Physical Review B* **2007**, *75*; f)Wu, F. I., Shih, P. I., Tseng, Y. H., Chen, G. Y., Chien, C. H., Shu, C. F., Tung, Y. L., Chi, Y., Jen, A. K. Y., *J. Phys. Chem. B* **2005**, *109*, 14000.

[9]   a)Adachi, C., Baldo, M. A., Forrest, S. R., Thompson, M. E., *Appl. Phys. Lett.* **2000**, *77*, 904; b)Ikai, M., Tokito, S., Sakamoto, Y., Suzuki, T., Taga, Y., *Appl. Phys. Lett.* **2001**, *79*, 156; c)He, G. F., Pfeiffer, M., Leo, K., Hofmann, M., Birnstock, J., Pudzich, R., Salbeck, J., *Appl. Phys. Lett.* **2004**, *85*, 3911; d)Jiang, C. Y., Yang, W., Peng, J. B., Xiao, S., Cao, Y., *Adv. Mater.* **2004**, *16*, 537; e)Chen, F. C., Yang, Y., Thompson, M. E., Kido, J., *Appl. Phys. Lett.*

2002, *80*, 2308; f)Brunner, K., van Dijken, A., Borner, H., Bastiaansen, J., Kiggen, N. M. M., Langeveld, B. M. W., *J. Am. Chem. Soc.* **2004**, *126*, 6035.

[10]   a)Gong, X., Ostrowski, J. C., Moses, D., Bazan, G. C., Heeger, A. J., *Adv. Funct. Mater.* **2003**, *13*, 439; b)Vaeth, K. M., Tang, C. W., *J. Appl. Phys.* **2002**, *92*, 3447; c)Negres, R. A., Gong, X., Ostrowski, J. C., Bazan, G. C., Moses, D., Heeger, A. J., *Physical Review B* **2003**, *68*.

[11]   a)Lupton, J. M., Samuel, I. D. W., Frampton, M. J., Beavington, R., Burn, P. L., *Adv. Funct. Mater.* **2001**, *11*, 287; b)Anthopoulos, T. D., Markham, J. P. J., Namdas, E. B., Samuel, I. D. W., Lo, S. C., Burn, P. L., *Appl. Phys. Lett.* **2003**, *82*, 4824; c)Ding, J. Q., Wang, B., Yue, Z. Y., Yao, B., Xie, Z. Y., Cheng, Y. X., Wang, L. X., Jing, X. B., Wang, F. S., *Angew. Chem. Int. Ed.* **2009**, *48*, 6664.

[12]   a)Lupton, J. M., Samuel, I. D. W., Burn, P. L., Mukamel, S., *J. Phys. Chem. B* **2002**, *106*, 7647; b)Tsuzuki, T., Shirasawa, N., Suzuki, T., Tokito, S., *Adv. Mater.* **2003**, *15*, 1455; c)Namdas, E. B., Anthopoulos, T. D., Samuel, I. D. W., Frampton, M. J., Lo, S. C., Burn, P. L., *Appl. Phys. Lett.* **2005**, *86*.

[13]   a)Anthopoulos, T. D., Frampton, M. J., Namdas, E. B., Burn, P. L., Samuel, I. D. W., *Adv. Mater.* **2004**, *16*, 557; b)Lo, S. C., Male, N. A. H., Markham, J. P. J., Magennis, S. W., Burn, P. L., Salata, O. V., Samuel, I. D. W., *Adv. Mater.* **2002**, *14*, 975; c)Adachi, C., Baldo, M. A., Forrest, S. R., Lamansky, S., Thompson, M. E., Kwong, R. C., *Appl. Phys. Lett.* **2001**, *78*, 1622; d)Baldo, M. A., Lamansky, S., Burrows, P. E., Thompson, M. E., Forrest, S. R., *Appl. Phys. Lett.* **1999**, *75*, 4; e)Nazeeruddin, M. K., Humphry-Baker, R., Berner, D., Rivier, S., Zuppiroli, L., Graetzel, M., *J. Am. Chem. Soc.* **2003**, *125*, 8790.

[14]   a)Wilkinson, A. J., Goeta, A. E., Foster, C. E., Williams, J. A. G., *Inorg. Chem.* **2004**, *43*, 6513; b)Hay, P. J., *J. Phys. Chem. A* **2002**, *106*, 1634; c)Laskar, I. R., Chen, T. M., *Chem. Mater.* **2004**, *16*, 111.

[15]   King, K. A., Spellane, P. J., Watts, R. J., *J. Am. Chem. Soc.* **1985**, *107*, 1431.

[16]   a)Lo, K. K. W., Chung, C. K., Lee, T. K. M., Lui, L. H., Tsang, K. H. K., Zhu, N. Y., *Inorg. Chem.* **2003**, *42*, 6886; b)Lo, K. K. W., Ng, D. C. M., Chung, C. K., *Organometallics* **2001**, *20*, 4999; c)Hsieh, J. M., Ho, M. L., Wu, P. W., Chou, P. T., Tsai, T. T., Chi, Y., *Chem. Commun.* **2006**, 615.

[17]   a)Goodall, W., Williams, J. A. G., *Journal of the Chemical Society-Dalton Transactions* **2000**, 2893; b)DiMarco, G., Lanza, M., Pieruccini, M., Campagna, S., *Adv. Mater.* **1996**, *8*, 576; c)Licini, M., Williams, J. A. G., *Chem. Commun.* **1999**, 1943.

[18]   a)Shao, F. W., Elias, B., Lu, W., Barton, J. K., *Inorg. Chem.* **2007**, *46*, 10187; b)Shao, F. W., Barton, J. K., *J. Am. Chem. Soc.* **2007**, *129*, 14733; c)Elias, B., Shao, F. W., Barton, J. K., *J. Am. Chem. Soc.* **2008**, *130*, 1152.

[19]   a)Kainz, S., Brinkmann, A., Leitner, W., Pfaltz, A., *J. Am. Chem. Soc.* **1999**, *121*, 6421; b)Hanna, T. A., Baranger, A. M., Bergman, R. G., *J. Am. Chem. Soc.* **1995**, *117*, 11363; c)Herskovitz, T., *J. Am. Chem. Soc.* **1977**, *99*, 2391.

[20]   a)DeRosa, M. C., Hodgson, D. J., Enright, G. D., Dawson, B., Evans, C. E. B., Crutchley, R. J., *J. Am. Chem. Soc.* **2004**, *126*, 7619; b)Gao, R. M., Ho, D. G., Hernandez, B., Selke, M., Murphy, D., Djurovich, P. I., Thompson, M. E., *J. Am. Chem. Soc.* **2002**, *124*, 14828; c)Di Marco, G., Lanza, M., Mamo, A., Stefio, I., Di Pietro, C., Romeo, G., Campagna, S., *Anal. Chem.* **1998**, *70*, 5019; d)Amao, Y., Ishikawa, Y., Okura, I., *Anal. Chim. Acta* **2001**, *445*, 177.

[21]   a)Nazeeruddin, M. K., Wegh, R. T., Zhou, Z., Klein, C., Wang, Q., De Angelis, F., Fantacci, S., Gratzel, M., *Inorg. Chem.* **2006**, *45*, 9245; b)Rodriguez-Redondo, J. L., Costa, R. D., Orti, E., Sastre-Santos, A., Bolink, H. J., Fernandez-Lazaro, F., *Dalton Trans* **2009**, 9787; c)He, L., Qiao, J., Duan, L., Dong, G. F., Zhang, D. Q., Wang, L. D., Qiu, Y., *Adv. Funct. Mater.* **2009**, *19*, 2950; d)Costa, R. D., Orti, E., Bolink, H. J., Graber, S., Schaffner, S., Neuburger, M., Housecroft, C. E., Constable, E. C., *Adv. Funct. Mater.* **2009**, *19*, 3456.

[22]   a)Tokito, S., Iijima, T., Tsuzuki, T., Sato, F., *Appl. Phys. Lett.* **2003**, *83*, 2459; b)Duan, J. P., Sun, P. P., Cheng, C. H., *Adv. Mater.* **2003**, *15*, 224; c)Grushin, V. V., Herron, N., LeCloux, D. D., Marshall, W. J., Petrov, V. A., Wang, Y., *Chem. Commun.* **2001**, 1494; d)Lee, C. L., Lee, K. B., Kim, J. J., *Appl. Phys. Lett.* **2000**, *77*, 2280.

[23]   Adachi, C., Baldo, M. A., Thompson, M. E., Forrest, S. R., *J. Appl. Phys.* **2001**, *90*, 5048.

[24]   a)Kwon, T. H., Cho, H. S., Kim, M. K., Kim, J. W., Kim, J. J., Lee, K. H., Park, S. J., Shin, I. S., Kim, H., Shin, D. M., Chung, Y. K., Hong, J. I., *Organometallics* **2005**, *24*, 1578; b)Hwang, F. M., Chen, H. Y., Chen, P. S., Liu, C. S., Chi, Y., Shu, C. F., Wu, F. L., Chou, P. T., Peng, S. M., Lee, G. H., *Inorg. Chem.* **2005**, *44*, 1344; c)Coppo, P., Plummer, E. A., De Cola, L., *Chem. Commun.* **2004**, 1774; d)Adamovich, V., Brooks, J., Tamayo, A., Alexander, A. M.,

Djurovich, P. I., D'Andrade, B. W., Adachi, C., Forrest, S. R., Thompson, M. E., *New J. Chem.* **2002**, *26*, 1171; e)You, Y. M., Park, S. Y., *J. Am. Chem. Soc.* **2005**, *127*, 12438.

[25]   Markham, J. P. J., Lo, S. C., Magennis, S. W., Burn, P. L., Samuel, I. D. W., *Appl. Phys. Lett.* **2002**, *80*, 2645.

[26]   Ding, J. Q., Gao, J., Cheng, Y. X., Xie, Z. Y., Wang, L. X., Ma, D. G., Jing, X. B., Wang, F. S., *Adv. Funct. Mater.* **2006**, *16*, 575.

[27]   a)Lo, S. C., Namdas, E. B., Burn, P. L., Samuel, I. D. W., *Macromolecules* **2003**, *36*, 9721; b)Wong, W. Y., Ho, C. L., Gao, Z. Q., Mi, B. X., Chen, C. H., Cheah, K. W., Lin, Z. Y., *Angew. Chem. Int. Ed.* **2006**, *45*, 7800; c)Lo, S. C., Namdas, E. B., Shipley, C. P., Markham, J. P. J., Anthopolous, T. D., Burn, P. L., Samuel, I. D. W., *Org. Electron.* **2006**, *7*, 85.

[28]   Lo, S. C., Anthopoulos, T. D., Namdas, E. B., Burn, P. L., Samuel, I. D. W., *Adv. Mater.* **2005**, *17*, 1945.

[29]   a)Evans, N. R., Devi, L. S., Mak, C. S. K., Watkins, S. E., Pascu, S. I., Kohler, A., Friend, R. H., Williams, C. K., Holmes, A. B., *J. Am. Chem. Soc.* **2006**, *128*, 6647; b)Zhen, H. Y., Jiang, C. Y., Yang, W., Jiang, J. X., Huang, F., Cao, Y., *Chem. Eur. J.* **2005**, *11*, 5007; c)Jiang, J. X., Jiang, C. Y., Yang, W., Zhen, H. G., Huang, F., Cao, Y., *Macromolecules* **2005**, *38*, 4072; d)Tian, N., Thiessen, A., Schiewek, R., Schmitz, O. J., Hertel, D., Meerholz, K., Holder, E., *J. Org. Chem.* **2009**, *74*, 2718.

[30]   a)Knights, K. A., Stevenson, S. G., Shipley, C. P., Lo, S. C., Olsen, S., Harding, R. E., Gambino, S., Burn, P. L., Samuel, I. D. W., *J. Mater. Chem.* **2008**, *18*, 2121; b)Ding, J. Q., Lu, J. H., Cheng, Y. X., Xie, Z. Y., Wang, L. X., Jing, X. B., Wang, F. S., *Adv. Funct. Mater.* **2008**, *18*, 2754.

[31]   Stoessel, P., Spreitzer, H., Becker, H., in *Ger. Offen.*, DE10116962, **2002**.

[32]   Haberecht, M. C., Schnorr, J. M., Andreitchenko, E. V., Christopher, C. G., Wagner, M., Mullen, K., *Angew. Chem. Int. Ed.* **2008**, *47*, 1662.

[33]   Tsuboyama, A., Iwawaki, H., Furugori, M., Mukaide, T., Kamatani, J., Igawa, S., Moriyama, T., Miura, S., Takiguchi, T., Okada, S., Hoshino, M., Ueno, K., *J. Am. Chem. Soc.* **2003**, *125*, 12971.

[34]   Lamansky, S., Djurovich, P., Murphy, D., Abdel-Razzaq, F., Lee, H. E., Adachi, C., Burrows, P. E., Forrest, S. R., Thompson, M. E., *J. Am. Chem. Soc.* **2001**, *123*, 4304.

[35]   Lamansky, S., Djurovich, P., Murphy, D., Abdel-Razzaq, F., Kwong, R., Tsyba, I., Bortz, M., Mui, B., Bau, R., Thompson, M. E., *Inorg. Chem.* **2001**, *40*, 1704.

[36]   Li, X. H., Chen, Z., Zhao, Q., Shen, L., Li, F. Y., Yi, T., Cao, Y., Huang, C. H., *Inorg. Chem.* **2007**, *46*, 5518.

[37]   Namdas, E. B., Ruseckas, A., Samuel, I. D. W., Lo, S. C., Burn, P. L., *J. Phys. Chem. B* **2004**, *108*, 1570.

[38]   deMello, J. C., Wittmann, H. F., Friend, R. H., *Adv. Mater.* **1997**, *9*, 230.

[39]   Cameron, C. S., Gorman, C. B., *Adv. Funct. Mater.* **2002**, *12*, 17.

[40]   Tamayo, A. B., Alleyne, B. D., Djurovich, P. I., Lamansky, S., Tsyba, I., Ho, N. N., Bau, R., Thompson, M. E., *J. Am. Chem. Soc.* **2003**, *125*, 7377.

[41]   Bard, A. J., Abruna, H. D., Chidsey, C. E., Faulkner, L. R., Feldberg, S. W., Itaya, K., Majda, M., Melroy, O., Murray, R. W., Porter, M. D., Soriaga, M. P., White, H. S., *J. Phys. Chem.* **1993**, *97*, 7147.

[42]   Miller, D. A. B., Chemla, D. S., Damen, T. C., Gossard, A. C., Wiegmann, W., Wood, T. H., Burrus, C. A., *Physical Review B* **1985**, *32*, 1043.

[43]   Sudhakar, M., Djurovich, P. I., Hogen-Esch, T. E., Thompson, M. E., *J. Am. Chem. Soc.* **2003**, *125*, 7796.

[44]   Smith, T., Guild, J., *Transactions of the Optical Society|Transactions of the Optical Society* **1931**, 10.1088/1475.

[45]   Jenekhe, S. A., Osaheni, J. A., *Science* **1994**, *265*, 765.

[46]   Liu, D. J., De Feyter, S., Cotlet, M., Stefan, A., Wiesler, U. M., Herrmann, A., Grebel-Koehler, D., Qu, J. Q., Mullen, K., De Schryver, F. C., *Macromolecules* **2003**, *36*, 5918.

[47]   a)Lupton, J. M., Samuel, I. D. W., Beavington, R., Frampton, M. J., Burn, P. L., Bassler, H., *Physical Review B* **2001**, *63*; b)Lupton, J. M., Samuel, I. D. W., Beavington, R., Burn, P. L., Bassler, H., *Adv. Mater.* **2001**, *13*, 258.

[48]   Brown, A. R., Bradley, D. D. C., Burroughes, J. H., Friend, R. H., Greenham, N. C., Burn, P. L., Holmes, A. B., Kraft, A., *Appl. Phys. Lett.* **1992**, *61*, 2793.

[49]   Cao, Y., Yu, G., Heeger, A. J., *Adv. Mater.* **1998**, *10*, 917.

[50]   Blom, P. W. M., deJong, M. J. M., Vleggaar, J. J. M., *Appl. Phys. Lett.* **1996**, *68*, 3308.

[51]   Cumpstey, N., Bera, R. N., Burn, P. L., Samuel, I. D. W., *Macromolecules* **2005**, *38*, 9564.

[52]   a)Hughes, G., Bryce, M. R., *J. Mater. Chem.* **2005**, *15*, 94; b)Adamovich, V. I., Cordero, S. R., Djurovich, P. I., Tamayo, A., Thompson, M. E., D'Andrade, B. W., Forrest, S. R., *Org. Electron.* **2003**, *4*, 77.

[53]   Kuwabara, Y., Ogawa, H., Inada, H., Noma, N., Shirota, Y., *Adv. Mater.* **1994**, *6*, 677.

[54]   Qin, D. S., Tao, Y., *Appl. Phys. Lett.* **2005**, *86*.

[55]   Yersin, H., *Transition Metal and Rare Earth Compounds Iii* **2004**, *241*, 1.

[56]   a)Tsuzuki, T., Shirasawa, N., Suzuki, T., Tokito, S., *Japanese Journal of Applied Physics Part 1-Regular Papers Short Notes & Review Papers* **2005**, *44*, 4151; b)Markham, J. P. J., Samuel, I. D. W., Lo, S. C., Burn, P. L., Weiter, M., Bassler, H., *J. Appl. Phys.* **2004**, *95*, 438.

[57]   Gong, X., Robinson, M. R., Ostrowski, J. C., Moses, D., Bazan, G. C., Heeger, A. J., *Adv. Mater.* **2002**, *14*, 581.

[58]   Okada, S., Okinaka, K., Iwawaki, H., Furugori, M., Hashimoto, M., Mukaide, T., Kamatani, J., Igawa, S., Tsuboyama, A., Takiguchi, T., Ueno, K., *Dalton Transactions* **2005**, 1583.

[59]   Gui-Jiang, Z., Wai-Yeung, W., Bing, Y., Zhiyuan, X., Lixiang, W., *J. Mater. Chem.* **2008**, 1799.

Chapter 4

fac-Tris(2-benzo[b]thiophenylpyridyl) iridium(III) cored polyphenylene dendrimers with peripheral triphenylamines: surface functionalization of red phosphorescent materials

In this chapter, the surface functionalization of red phosphorescent polyphenylene dendrimers based on Ir(III) complex cores will be presented. A series of high generation red phosphorescent Ir(III) dendrimers with triphenylamine end-groups in the periphery were synthesized. The triphenylamine units are excellent hole-transporting materials, which improve the ability in capturing and carrying holes from the dendrimer surface into the Ir(III) core, resulting in a highly efficient non-doped red phosphorescent materials, suitable to low-cost solution processing technologies.

4.1 From green to red – color tuning of Ir(III) complexes

Since the first synthesis of red-phosphorescent metal complexes for use in highly efficient PhOLEDs, the scope and diversity of studies on metal-organic phosphorescent emitters in color tuning have continued to expand at an exponential rate.[1] To fabricate highly efficient red-emissive PhOLEDs, it is necessary to search for red-emissive metal complexes with high luminescence quantum yields. However, while great success has been achieved in green-light phosphorescent emitters, the design and synthesis of efficient red emitters is intrinsically more difficult, since the luminescence quantum yields tend to decrease along with a bathochromic shift in the emission peak wavelength according to the energy gap law.[2]

As we mentioned in the chapter 3, the PhOLED devices based on dendronized metal complexes have been mainly used due to their advantages such as solution processibility, preventable intermolecular triplet-triplet annihilation and controllable

122

host-guest ratio.[3] In this regard, however, only a limited number of examples of red phosphorescent dendrimers have been developed, and their solution-processed PhOLEDs show relatively low external quantum efficiency (EQE).[4] Despite this situation, the apparently poorer performance of the red PhOLEDs fabricated by spin-coating than that of their vacuum-deposited counterparts suggests the need for more efforts in developing highly amorphous Ir(III) complexes with new dendritic frameworks.[5] Generally, a large hole-injection barrier for organic materials often limits the device efficiency.[6] Since most of the hole-transporting materials reported are derived from aromatic amines,[7] the incorporation of arylamine units into the dendritic wedges should improve the charge injection and the morphological stability of the red Ir(III) phosphors.[8]

Based on the divergent polyphenylene Ir(III) dendrimer synthesis protocol,[9] in order to achieve highly efficient red phosphorescent dendrimers, two important components should be imported into the dendritic macromolecules: i) a red triplet emissive Ir(III) core with multi-ethynyl functional groups for the growth of dendrimers, and ii) functionalized end-groups containing hole-transport units, which increase the possibility of charges injecting into the periphery of dendrimers. Therefore, we adopt the priori group introduction method and firstly synthesized the tri-ethynyl red phosphorescent Ir(III) cores and diphenylcyclopentadiene with two triphenylamine moieties as the end-caps.[10] Afterwards, different generations of red phosphorescent polyphenylene dendrimers with Ir(III) core and triphenylamine groups in the periphery are achieved via divergent synthesis method. Compared to previously reported red phosphorescent Ir(III) dendrimers with polyphenylene (**4-1**),[11] polytriphenylamine (**4-2**)[8a] and polycarbazole[8b] (**4-3**) dendrons, which were synthesized via convergent method and limited to low generation (Scheme 4-1), our divergently synthesized high generations of dendrimers can provide a significantly enhanced steric shielding which results in an even more pronounced site-isolation of the emissive cores.[12] Moreover, the peripheral multi-triphenylamine functional end-groups can induce excellent hole-injection and transportation from the surface of dendrimers into the core.[8]

4-1

4-2

4-3
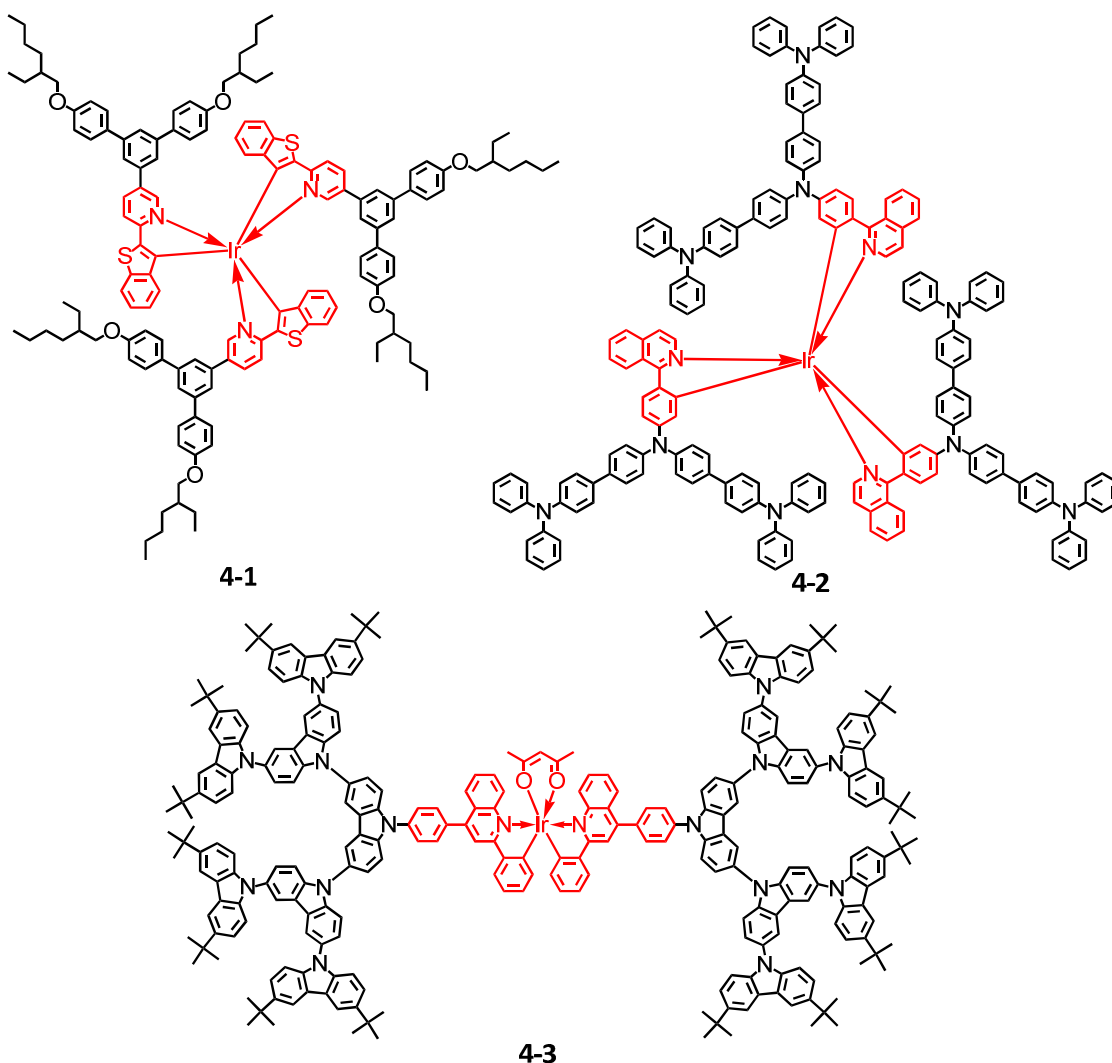
Scheme 4-1: Structures of red phosphorescent Ir(III) dendrimers with polyphenylene (**4-1**), polytriphenylamine (**4-2**) and polycarbazole (**4-3**) dendrons.

4.2 Red phosphorescent Ir(btp)₃ cored polyphenylene dendrimers

Molecules having intermolecular donor-acceptor (DA) systems exhibited bathochromic shifts of both absorption and emission spectra.[13] Originally, 2-phenylpyridine itself had a DA character resulting from the interaction between an electron-rich phenyl group and an electron-deficient pyridine group.[14] Replacement of a more electron-rich group, 2- benzo[b]thiophene with phenyl was considered to enhance the DA character of the

ligand.[15] Thus, we designed *fac*-tris(2-benzo[b]thiophenylpyridyl) iridium(III) (**Ir(btp)₃**) as the core for red phosphorescent dendrimers.

4.2.1 Synthesis of Ir(btp)₃ derivative core

First of all, the synthesis of *fac*-tris(2-benzo[b]thiophenylpyridyl) iridium(III) (Ir(btp)₃) derivate with three ethynyl units as the red phosphorescent core was our primary work. It was a great challenge since the standard halogenation of the unsubstituted Ir(btp)₃ has shown to be unsuccessful. An alternative way is by importing the halide groups in the ligand prior to the complexation. Therefore, the red emissive Ir(btp)₃ core **4-4** was prepared using an efficient synthetic strategy shown in Scheme 4-2.
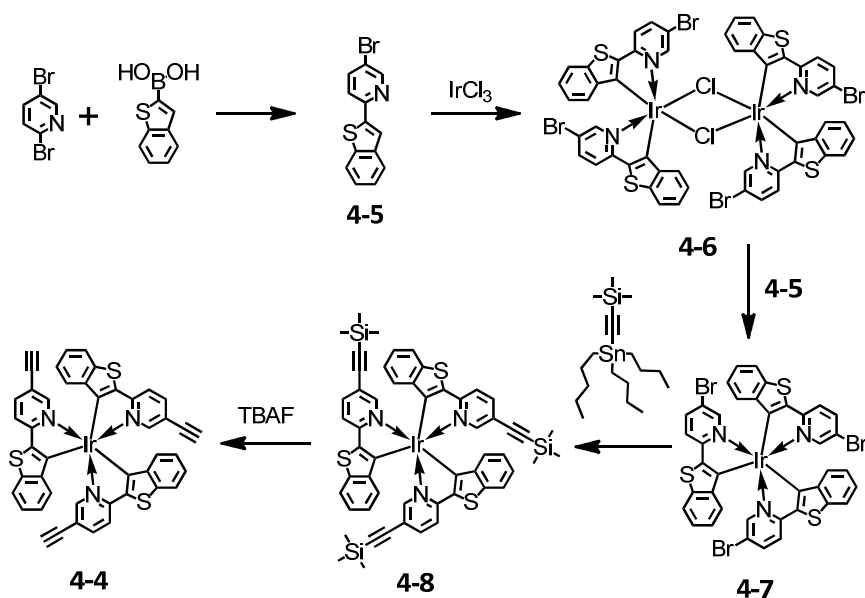
Scheme 4-2: Synthesis of the red phosphorescent Ir(btp)₃ core **4-4.**

The syntheses started from a previously reported asymmetric *Suzuki* coupling reaction between one equivalent of 2,5-dibromopyridine and one equivalent of 2-benzo[b]thiophenylboronic acid with tetrakis(triphenylphosphine)palladium(0) as the catalyst in a mixture of *2*-methoxyethanol and 2M Na₂CO₃ in 2:1 volume ratio,[16] obtaining the 2-(2'-benzo[*b*]thienyl)-5-bromopyridine (**4-5**) as the ligand in a yield of 82%. The ligand **4-5** firstly complexed with iridium trichloride, achieving the di-chloride

bridge complex **4-6**. The intermediate **4-6** subsequently reacted directly with added ligand **4-5** resulting in the red emissive *fac*-tris(2-benzo[b]thiophenyl)-5-bromopyridyl iridium(III) **4-7** in a total yield of 38% from iridium trichloride. The *fac*-tris(2-benzo[b]thiophenyl)-5-trimethylsilylethynylpyridyl iridium(III) **4-8** could be derived from three-fold Stille coupling of **4-7** and trimethyl((tributylstannyl)ethynyl)silane in a yield of 52%. The deprotection of compound **4-8** with TBAF in THF solution resulted in *fac*-tris(2-benzo[b]thiophenyl)-5-ethynylpyridyl iridium(III) **4-4**, the core for divergent synthesis of polyphenylene dendrimers, in a yield of 88%.

4.2.2 Synthesis and characterization of Ir(btp)$_3$ cored polyphenylene dendrimers

For the improvement of the charge injection and transportation from the periphery of dendrimers into the core thus optimize the dendrimer based device performances, triphenylamine was chosen as the functional end-groups on the dendrimer surface due to three reasons: i) triphenylamine was a promising hole-transporting material; ii) triphenylamine could improve the solubility of dendrimers; and iii) triphenylamine is stable under Diels-Alder reaction condition.[17] Therefore, the 3,4-bis(4-triphenylamino)-2,5-diphenylcyclopentadienone (**4-9**) was synthesized in order to import the multi-triphenylamine end-groups on dendrimer surface via Diels-Alder cycloaddition reaction (Scheme 4-3). The building unit **4-9** was obtained from Buchwald-Hartwig amination between diphenylamine and 3,4-bis(4-bromophenyl)-2,5-diphenylcyclopentadienone (**4-10**) in toluene by using tris(dibenzylideneacetone)dipalladium(0) as the catalyst.[17] The first-generation dendrimer **RIrG1** with six peripheral triphenylamines, was synthesized by refluxing an *o*-xylene solution of the Ir(btp)$_3$ core **4-4** and end-capping unit **4-10** in a microwave reactor for 2 h. After the purification by GPC column, the first-generation dendrimer **RIrG1** was precipitated in methanol as a red powder in 81% yield.
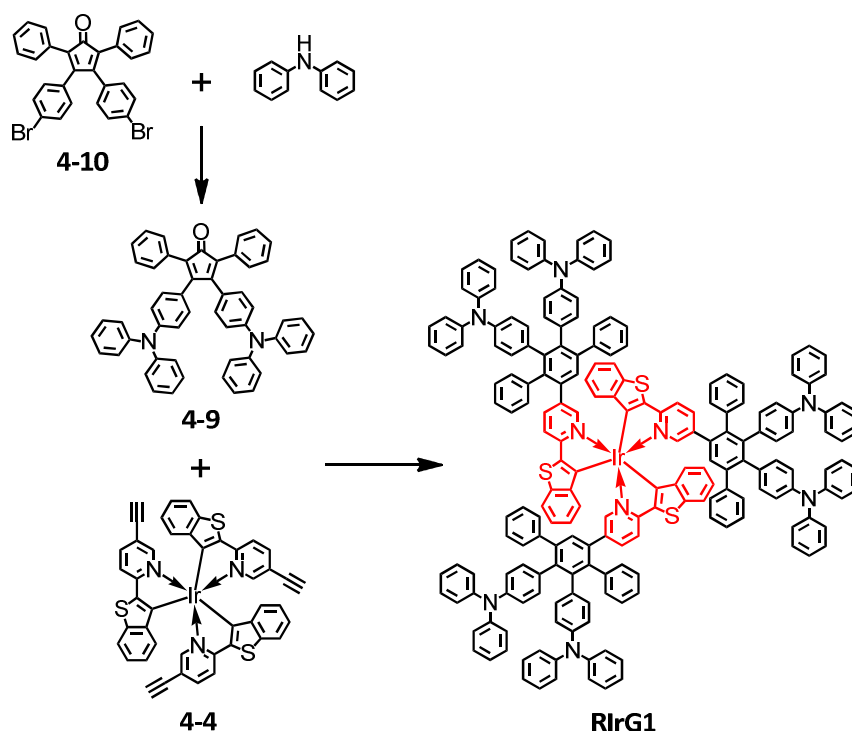
Scheme 4-3: Synthesis of first generation Ir(btp)₃ cored polyphenylene dendrimer (**RIrG1**).

The higher-generation Ir(btp)₃ cored polyphenylene dendrimers was synthesized via a stepwise divergent strategy (Scheme 4-4).[9] Firstly, the first-generation Ir(btp)₃ dendrimers with six triisopropylsilylethynyl units (**4-11**) were obtained in 84% yield by employing a [4+2] *Diels–Alder* cycloaddition procedure of the AB₂ branching unit **4-12** and the Ir(btp)₃ core **4-4** in refluxing *o*-xylene under microwave for 2 h. The TiPS groups in **4-11** were completely removed by TBAF in THF to achieve first-generation Ir(btp)₃ dendrimers with six peripheral ethynyl groups (**4-13**) in 85% yield. The activated dienophile units in **4-13** could be either reacted with end-capping unit **4-9** to get second-generation Ir(btp)₃ dendrimer **RIrG2** with 12 peripheral triphenylamine groups in 78% yield or with AB₂ building block **4-12** to obtain dendrimer **4-14** with 12 TiPS-ethynyl units in 80% yield. The dendrimer **4-14** was continuously treated with TBAF, resulting in second-generation dendrimer **4-15** with 12 ethynyl groups in 75% yield. Finally, the dendrimer **4-15** was reacted with end-capping unit **4-9**, obtaining the third-generation Ir(btp)₃ dendrimers **RIrG3** with 24 peripheral triphenylamine groups in 70% yield.
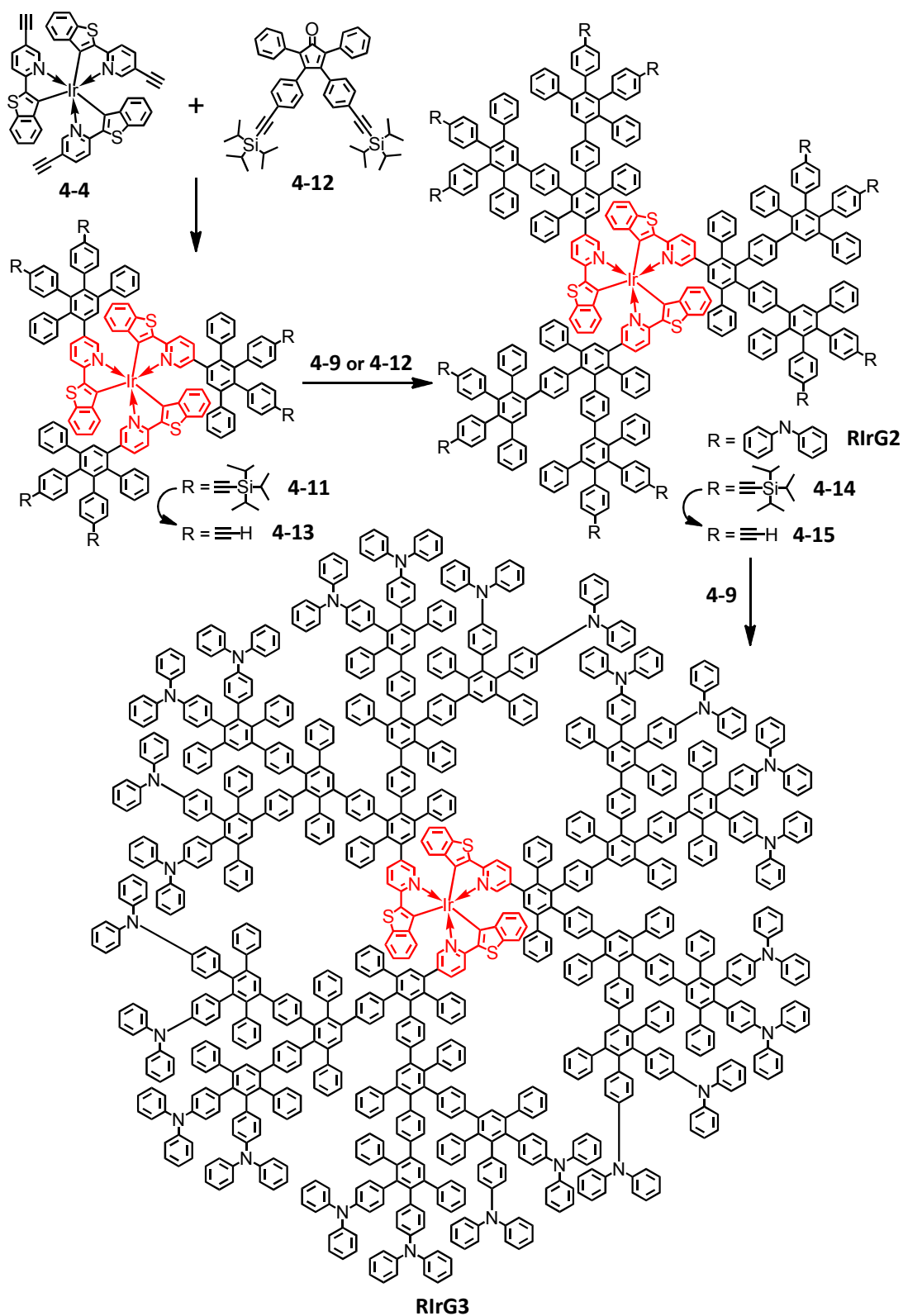
Scheme 4-4: Synthesis of second and third generation Ir(btp)₃ cored polyphenylene dendrimer (**RIrG2** and **RIrG3**).

Since the third-generation dendrimer was proven to possess the most suitable molecular size with the best device performance in the previous chapter, the even higher generation dendrimers were not synthesized. The monodispersity of all polyphenylene dendrimers based on Ir(btp)₃ core was characterized and proven by the MALDI-TOF mass spectrometry. Figure 4-1 depicts the MALDI-TOF mass spectrum of first to third generation dendrimers with Ir(btp)₃ core and triphenylamine end-groups (**RIrG1**-**RIrG3**).
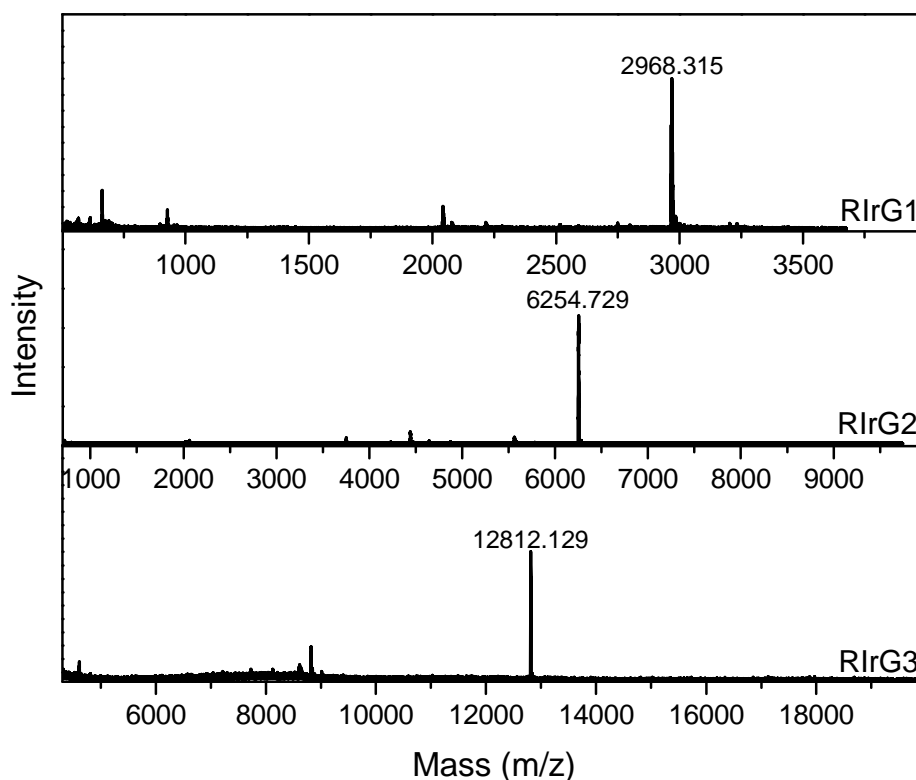
Figure 4-1: MALDI-TOF mass spectra of Ir(btp)₃ cored polyphenylene dendrimers (**RIrGx**).

The first generation dendrimer **RIrG1** shows a monodisperse peak at 2968.315 g·mol⁻¹, which can be assigned to the calculated molecular weight of 2967.993 g·mol⁻¹; and the second generation dendrimer **RIrG2** appears as a single signal at 6254.729 g·mol⁻¹, well corresponding with the calculated mass of 6253.380 g·mol⁻¹; as well as the third generation dendrimer **RIrG3** displays a major peak at 11812.129 g·mol⁻¹, which is attributed to the calculated molecular weight of 12816.127 g·mol⁻¹. All three dendrimers demonstrate no signals with lower or higher molecular mass thereby proving the

quantitative yields and defect-free Diels-Alder cycloaddition reactions during their stepwise syntheses.

4.3 Physical properties of Ir(btp)₃ cored polyphenylene dendrimers

In this chapter, the influences of the surrounding polyphenylene dendrons and triphenylamine peripheries upon the photophysical properties of the *fac*-tris(2-benzo[b]thiophenylpyridyl)Ir(III) cores are investigated using UV-Vis absorption and photoluminescence spectroscopy in solution as well as in solid state. Furthermore, the quantum yields in solution are applied for the optical characterization of these phosphorescent dendrimers. Finally, the electrochemical properties and energy levels of these dendrimers are developed by cyclic voltammetry measurement.

4.3.1 UV-Vis absorption spectroscopic measurement

The UV-Vis absorption spectra of three generations of Ir(btp)₃ dendrimers **RIrG1**, **RIrG2** and **RIrG3** with peripheral triphenylamines were measured both in DCM solutions with a concentration of 10^{-6} M and in thin films at 298 K (Figure 4-2). All three dendrimers showed identical absorption bands (Table 4-1). The absorption bands of all three dendrimers in solution showed two major types: i) the absorption band below 400 nm, which was attributed to spin-allowed ligand-centered (LC) transitions; and ii) the weak absorption shoulders in the visible region, which were assigned to the metal-to-ligand charge transfer (MLCT) state of the Ir(III) complexes. [11, 18] Herein, all three dendrimers demonstrated similar singlet MLCT bands around 423-424 nm and triplet MLCT at 484 nm (Figure 4-2 and Table 4-1). After the normalization, the former bands below 280 nm, which were consistent with the polyphenylene dendrons, were enhanced with the increasing number of phenylene units due to the dendrimer generation growth. Thereby, the intensity of MLCT bands reduced along with the growing generation number, since the ratios between Ir(III) complex core and polyphenylene dendrons are decreasing. In

the solid state, all dendrimers showed similar absorption bands as in solutions, indicating that the interactions among Ir(III) complex cores could be effectively isolated by the polyphenylene dendrons and triphenylamine peripheral units in solid state.[19]
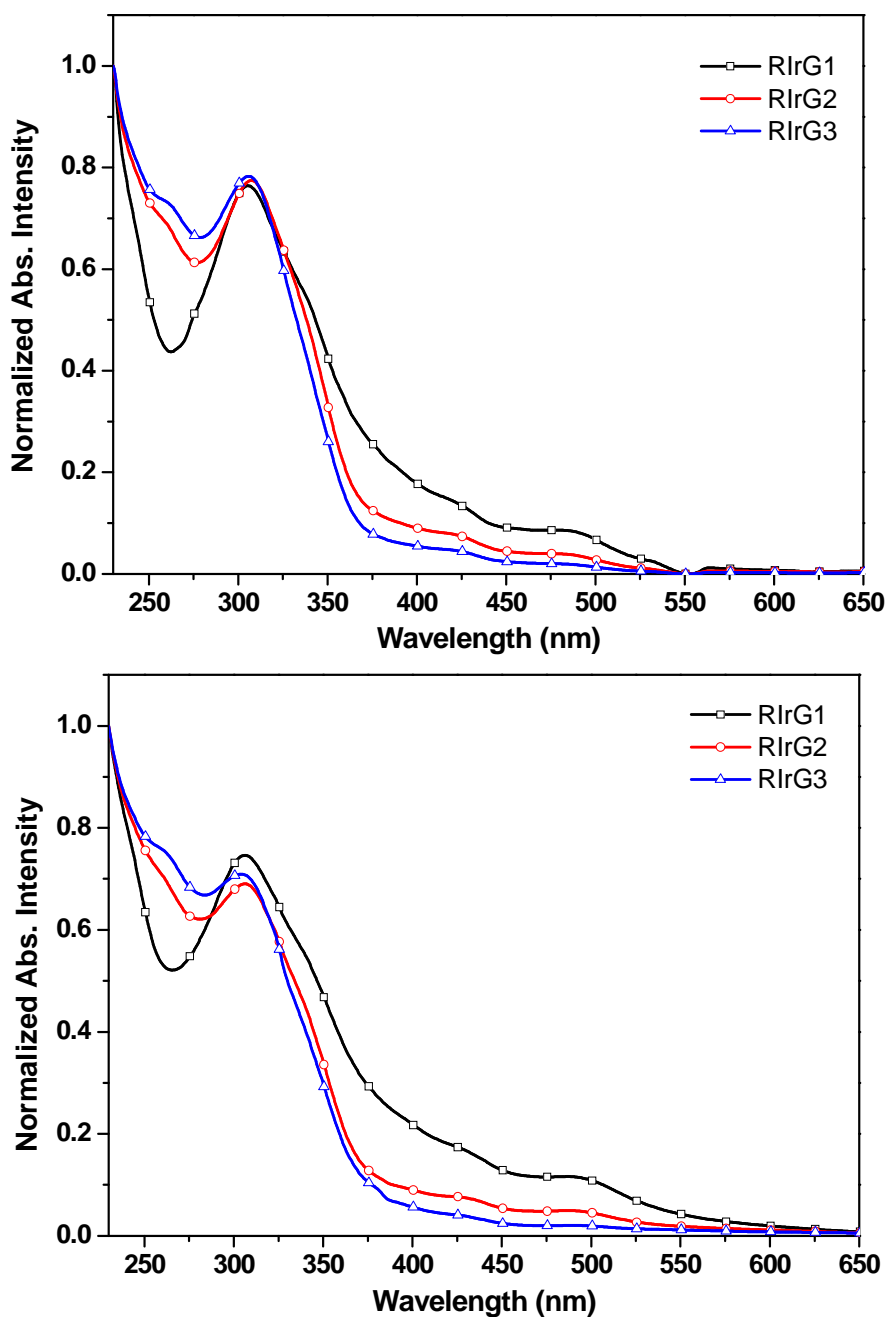
Figure 4-2: UV-Vis absorption spectra of Ir(btp)₃ cored dendrimers (**RIrG1**, **RIrG2**, and **RIrG3**) in DCM solutions (top) and thin film (bottom).

Table 4-1: Absorption (λ_{abs}) and emission (λ_{em}) maxima, and solution relative photoluminescence quantum yield (Φ_P) of Ir(btp)$_3$ cored dendrimers (**RIrG1**, **RIrG2**, and **RIrG3**).

	λ_{abs} [nm] (log ξ) [a]	λ_{em} [nm] [b]	λ_{abs} [nm] [c]	λ_{em} [nm] [c]	Φ_P (%) [d]
	solution		thin film		
RIrG1	230 (5.3), 305 (5.2), 424 (4.5), 484 (4.3)	621, 670	230, 306, 424, 487	624, 675	6
RIrG2	230 (5.7), 305 (5.6), 423 (4.5), 484 (4.2)	621, 670	230, 306, 424, 487	624, 675	7
RIrG3	230 (6.0), 305 (5.9), 424 (4.6), 484 (4.2)	621, 670	230, 304, 423, 489	624, 675	9

[a] Measured in DCM at 298 K with a concentration of 10^{-6} M. [b] Measured in toluene at 298 K with a concentration of 10^{-4} M and excitation wavelength of 470 nm. [c] The data of neat films measured at 298 K, which were prepared by drop-coating on quartz substrates. PL spectra were measured with the excitation wavelength of 409 nm. [d] Measured in N$_2$-saturated toluene at 298 K with Ir(ppy)$_3$ as the reference and the excitation wavelength of 470 nm.

4.3.2 Photoluminescence spectroscopic measurement

In toluene solution, all the dendrimers exhibit bright red photoluminescence with a similar quantum yield (0.06-0.09). The normalized PL spectra of dendrimers in toluene solutions with a concentration of 10^{-4} M and in thin films are presented in Figure 4-3. All three Ir(btp)$_3$ dendrimers possess similar emission bands at 621 nm and additional shoulders at 670 nm (Table 4-1), which are independent of dendrimer generation (Table 4-1), indicating that extension of the twisted framework of the polyphenylene dendrons can efficiently separate the chromophores and has almost no influence on the optical properties of the Ir(btp)$_3$ complex.[20] From solution to thin film, the PL spectra of the dendrimers had a small bathochromic shift of 3 nm for all three dendrimers, which further confirmed that the interactions among chromophoric cores had been well controlled by the dendrons and peripherys in the solid state.[19]
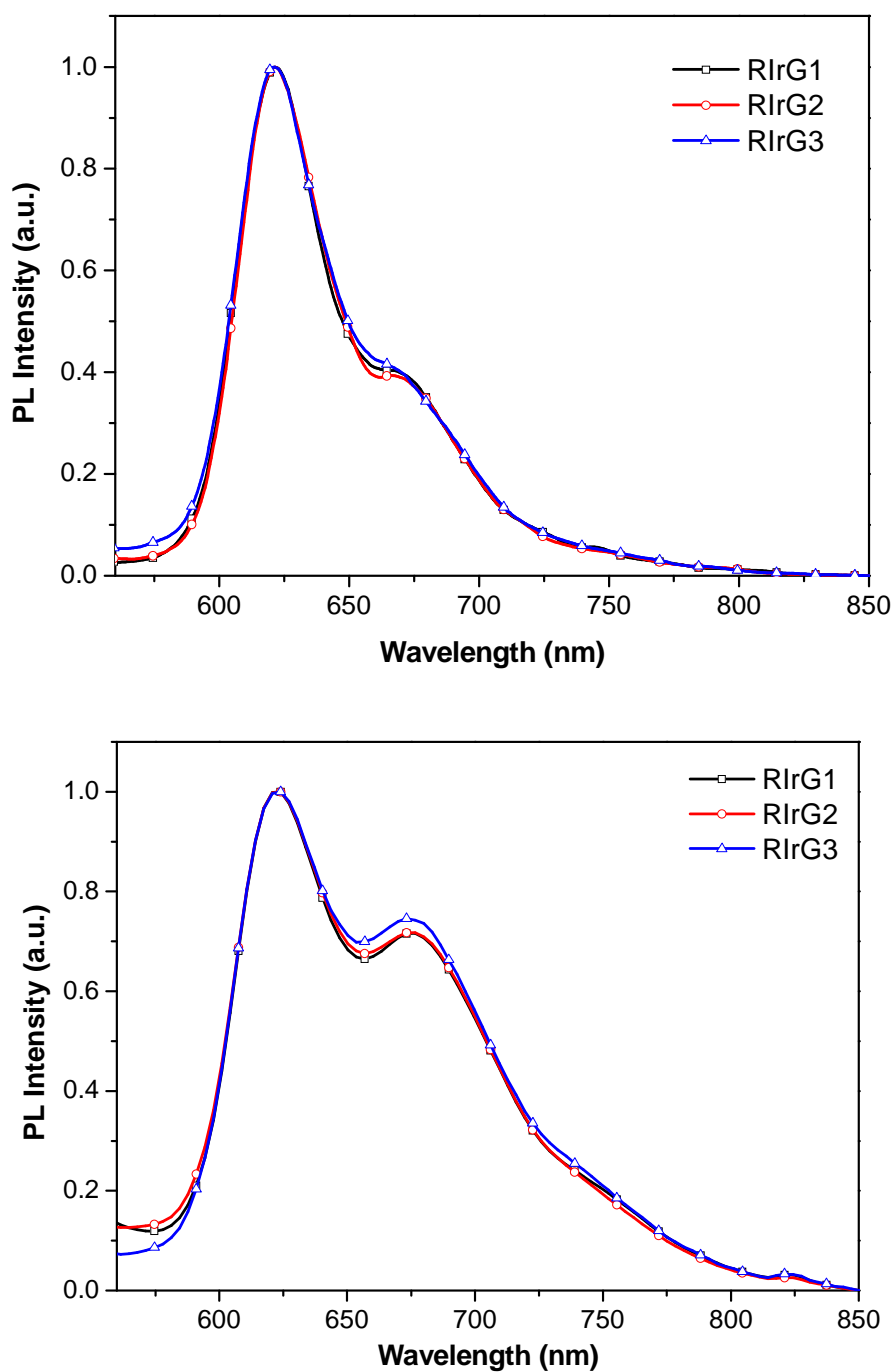
Figure 4-3: UV-Vis absorption spectra of Ir(btp)₃ cored dendrimers (**RIrG1**, **RIrG2**, and **RIrG3**) in toluene solutions (top) and thin film (bottom).

4.3.3 Electrochemical properties

The cyclic voltammetry (CV) measurements show that all Ir(btp)₃ cored dendrimers (**RIrG1**, **RIrG2**, and **RIrG3**) possess two oxidation waves in dichloromethane (Figure 4-4). The HOMO and LUMO energy levels were calculated from CV data together with absorption spectra (Table 4-2).
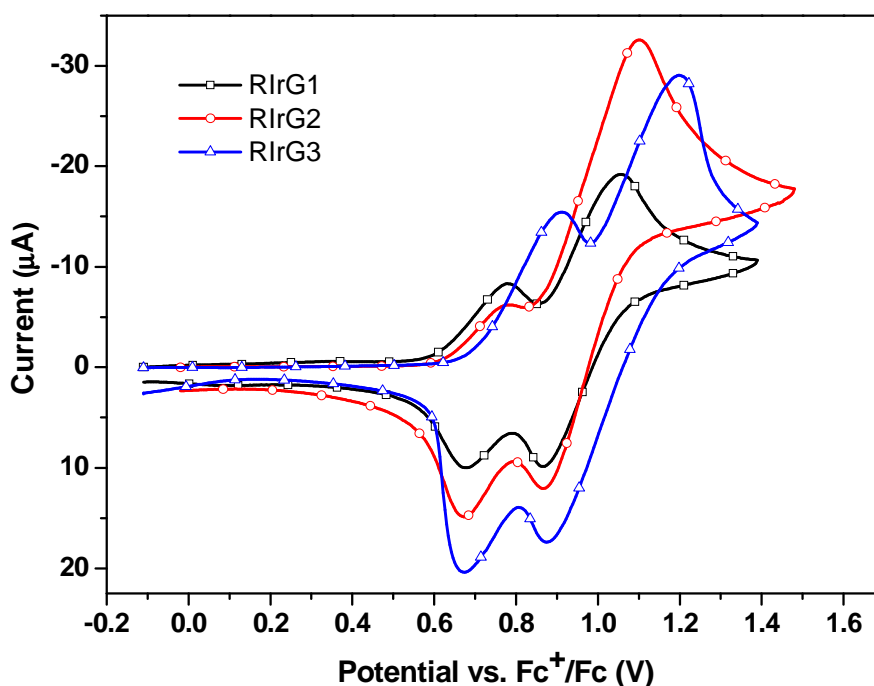
Figure 4-4: Cyclic voltammetry of dendrimers **RIrG1**, **RIrG2**, and **RIrG3**. All the oxidation potentials are quoted against the ferricenium/ferrocene couple.

The first oxidation potentials were at ca. 0.61 V of **RIrG1**, 0.64 V of **RIrG2** and 0.70 V of **RIrG3** vs. an Ag/Ag⁺ electrode, that corresponded to the oxidation of the Ir(III) complex core.[21] According to the onset potentials of the oxidation process, the HOMOs of dendrimers **RIrG1**, **RIrG2**, and **RIrG3** were estimated to be around −4.95 eV, −4.98 eV and −5.04 eV, respectively, according to the formula $E_{HOMO} = -(E^{ox} + 4.34)$.[22] On the other hand, the energy band gaps (E_{opt}) could be estimated at 2.00 eV for **RIrG1**, 1.99 eV for **RIrG2** and 1.98 eV for **RIrG3** from the onset of the maximum absorption edge.[23] Therefore, the LUMOs of dendrimers **RIrG1**, **RIrG2**, and **RIrG3** were calculated to be

around −2.95 eV, −2.99 eV and −3.06 eV, respectively. Furthermore, the second oxidation waves at higher potential could be ascribed to the oxidation of triphenylamine units at the periphery of the dendrimers.[24] This indicated that the polyphenylene dendrons could also participate in the electrochemical process and charge transport of the dendrimers in addition to controlling intermolecular interactions. The introduction of polyphenylene dendrons could directly transport energies from the outer triphenylamine units to the inner Ir(III) complex core.[17, 25]

Table 4-2: Electrochemical properties of Ir(btp)₃ dendrimers (**RIrG1**, **RIrG2**, and **RIrG3**).

	E^{ox} [V][a]	E_{opt} [eV] [b]	HOMO [eV] [c]	LUMO [eV] [d]
RIrG1	0.61, 0.87	2.00	−4.95	−2.95
RIrG2	0.64, 0.87	1.99	−4.98	−2.99
RIrG3	0.70, 0.99	1.98	−5.04	−3.06

[a] All the values are referred to Fc/Fc⁺. [b] Estimated from the onset of the absorption edge. [c] HOMO = − (E^{ox} + 4.34). [d] LUMO = E_{opt} + HOMO.

4.4 Red PhOLEDs based on Ir(btp)₃ cored polyphenylene dendrimers

The Ir(btp)₃ cored polyphenylene dendrimer based OLED devices were processed and characterized by our corporate partners, Dr Junqiao Ding and Prof. Lixiang Wang at the Chinese Academy of Sciences.

All the Ir(btp)₃ cored polyphenylene dendrimers (**RIrG1**, **RIrG2** and **RIrG3**) can form high quality films by spin coating, either alone or blend with other small molecular host materials. As shown in Figure 4-5, red PhOLED were fabricated with the configuration of ITO/PEDOT:PSS (50 nm)/TCCz:**RIrGx** (x%) (50 nm)/BCP (20 nm)/Alq (30 nm)/LiF (1 nm)/Al (100 nm). In these device, 2,9-dimethyl-4,7-diphenyl-1,10-phenanthroline (BCP)[26] and tris(8-hydroxyquino) aluminum (Alq)[27] were used as the hole block material and the electron transport material, respectively. In the emissive layer, dendrimers were mixed with N-(4-[9,3';6',9'']tercarbazol-9'-yl)phenylcarbazole (TCCz),[27] which was used as the hole transporting host material for balancing charges. The electrons and holes would be

expected to recombine in the dendrimers layer due to its appropriate energy levels (Figure 4-5).
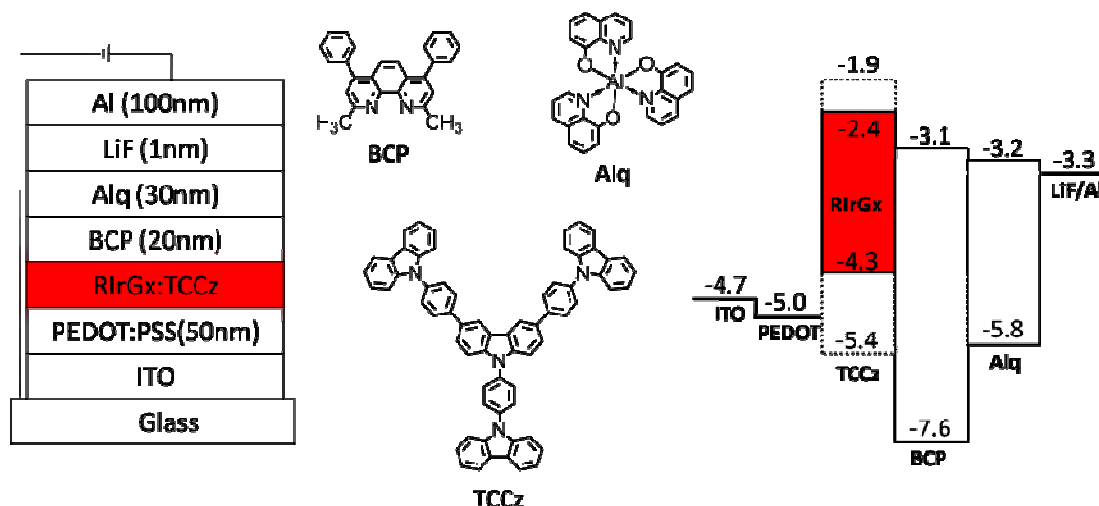
Figure 4-5: Schematic diagram of doped **RIrGx** dendrimer based electroluminescence (EL) device configurations (left), structure of 2,9-dimethyl-4,7-diphenyl-1,10-phenanthroline (BCP), tris(8-hydroxyquino) aluminum (Alq), and N-(4-[9,3';6',9'']tercarbazol-9'-yl)phenylcarbazole (TCCz) (middle), and energy levels of EL devices (right).
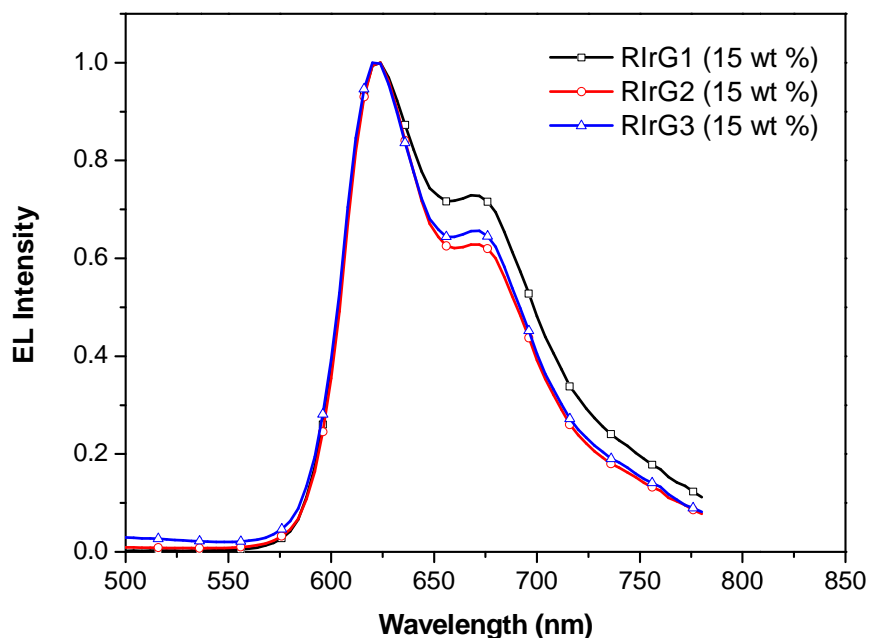
Figure 4-6: EL spectra of **RIrGx** dendrimer based devices at driving voltage of 8 V.

136

As shown in the EL spectra (Figure 4-6), all of the doped devices with different ratio of dendrimers in TCCz (5-20%) emitted pure red light, e.g. the EL spectra of all three doped dendrimer devices demonstrated similar maximum peaks at 624 nm and the shoulder bands around 670 nm, with CIE coordinates of (0.68, 0.32), (0.66, 0.32), and (0.63, 0.32) for **RIrG1**, **RIrG2** and **RIrG3**, respectively. These coordinates are very close to the National Television System Committee (NTSC) standard for red subpixels (0.67, 0.33) of cathode ray tube (CRT) displays,[28] and are found to be independent of current density. The EL spectra of the dendrimers matched well with their PL counterparts, which indicated that all EL emissions are from the triplet excited states of the Ir(III) complexes.
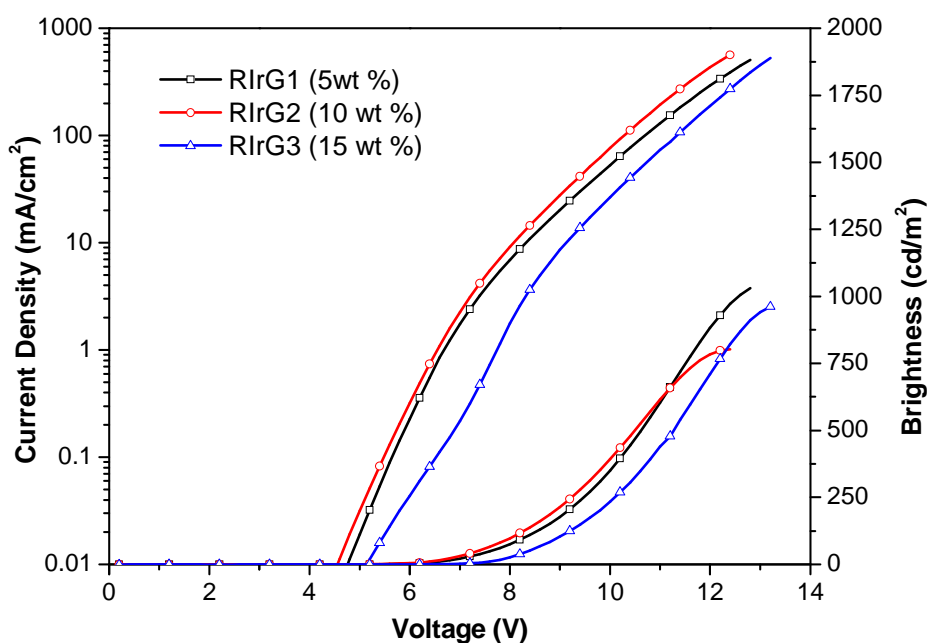
Figure 4-7: I-V-L characteristics of TCTA doped **RIrGx** dendrimer based devices.

Figure 4-7 shows the current density-voltage-luminescence characteristics of devices based on 15 wt % dendrimers doped in TCCz. It should be noticed that the current density of devices based on **RIrG1** and **RIrG2** was higher than that of the device based on **RIrG3** at the same driving voltage. This phenomenon could be attributed to the problem of charge carrier-mobility reduction with increasing dendrimer generations.[29] As shown in Table 4-3, the EQEs of the devices were stable at 1.7% from **RIrG1** to **RIrG3**, indicating that the intermolecular interactions between the emissive cores were

reduced in the same level upon different sizes of dendrons,[30] which matched the above mentioned PL conclusion. However, the device performance of these Ir(btp)$_3$ core dendrimers were relatively lower than other reported dendrimers based on *fac*-tris(1-phenylisoquinoline)Ir(III) (Ir(piq)$_3$) and *fac*-tris(1-phenylquinoline)Ir(III) (Ir(pq)$_3$) cores.[8]

In the next paragraph, we will further discuss the reason and try to design a new series of red phosphorescent dendrimers with even higher efficiencies.

4.5 Theoretical study on the lowest excited state of iridium(III) complexes

In order to achieve higher OLED device performance, in the other word, to increase the emission quantum yield (ɸ) of the red phosphorescent dendrimers, which was only 0.06 - 0.09 for the Ir(btp)$_3$ core dendrimers (Table 4-1), Firstly, we should understand the nature of the emission quantum yield.

The emission quantum yield (ɸ) from an emissive excited state to a ground state is generally expressed as

$$\phi = k_r/(k_r + k_{nr}) \qquad (1)$$

where k_r and k_{nr} are the radiative and nonradiative rate constant, respectively.[31]

In order to qualitatively understand the nature of the phosphorescent excited state of cyclometalated Ir(III) complexes, the results of the HOMO/LUMO calculation on Ir(ppy)$_3$ are shown in Figure 4-8.[32] The HOMO distributes over the phenyl ring and the iridium atom, while the LUMO is localized at the pyridine ring. Supposing that an emissive lowest excited state is formed via the HOMO→LUMO electronic transition, the excited state should be mixing of MLCT and LC π-π* excited states.[33]
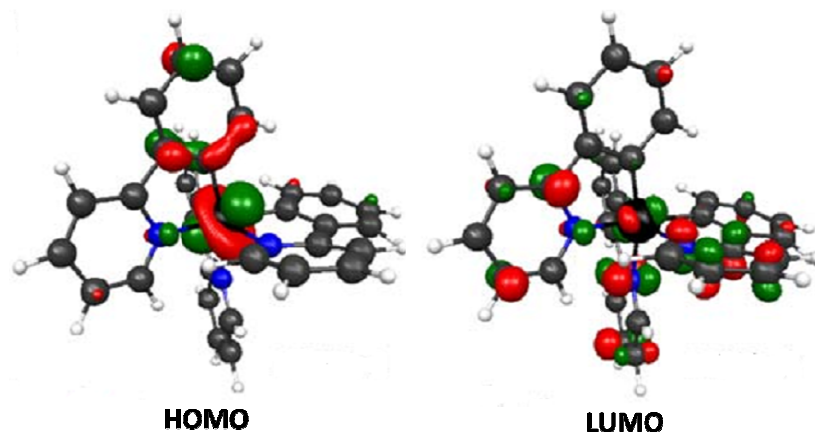
Figure 4-8: The simulated molecular orbitals of **Ir(ppy)₃** (optimized with MMFF method).

The lowest triplet excited state, ϕ_T, responsible for phosphorescence, of the cyclometalated iridium complexes is principally expressed as

$$\phi_T = a\phi(MLCT)_T + b\phi(LC)_T \qquad (2)$$

where a and b are the normalized coefficients as well as $\phi(MLCT)_T$ and $\phi(LC)_T$ are the wavefunctions of the MLCT and the ligand-centered triplet excited state, respectively.[34] Equation (2) implies that the phosphorescent excited state, ϕ_T, of the iridium complexes is an admixture of $\phi(MLCT)_T$ and $\phi(LC)_T$. The triplet excited state is attributed to the predominantly ^{3}MLCT excited state when $a>b$ and the predominantly $^3\pi\text{-}\pi^*$ excited state when $a<b$. In general, the k_r values of emission from the ^{3}MLCT-based excited state are two or three orders of magnitude larger than those from the $^3\pi\text{-}\pi^*$ excited state.[34-35] Therefore, as the result from the equation (1), Ir(III) complexes with the predominantly ^{3}MLCT excited state possess higher phosphorescence quantum yield than the counterpart. Unfortunately, according to the previous paper,[36] Ir(btp)₃ has been ascribed to the predominantly $^3\pi\text{-}\pi^*$ excited state, leading to a phosphorescence quantum yield of only to 0.12. In contrast, the large k_r of Ir(ppy)₃ induces high phosphorescence quantum yield up to 0.4. Thus, we should focus our attention on designing Ir(III) complexes that provide red emission from the ^{3}MLCT excited state, since their quantum efficiencies were much higher than those of their counterparts emitted from the $^3\pi\text{-}\pi^*$ excited state.[34-35]

4.6 Red phosphorescent Ir(piq)₃ cored polyphenylene dendrimers

As pointed out above for the cyclometalated iridium complexes having the emissive [3]MLCT excited state, the HOMO level of the complex should not change unless the coordination structure significantly varies. The [3]MLCT energy is expected to effectively decrease when a complex has a ligand with lower LUMO level.[37] Since the isoquionoline ring, more electron-accepting moiety than pyridine ring, is introduced to the ligands. Accordingly, we designed the of *fac*-tris(1-phenylisoquinoline)Ir(III) (**Ir(piq)₃**) as the dendrimer core.

The synthesis of *fac*-tris(1-phenylisoquinolinato) iridium(III) (**Ir(piq)₃**) cored polyphenylene dendrimer (**4-16**) is shown in Scheme 4-5. The synthesis began from the *Suzuki* coupling reaction of appropriate 1-chloroisoquinoline and phenylboronic acid with tetrakis(triphenylphosphine)palladium(0) as the catalyst in a mixture of *2-methoxyethanol* and 2M Na₂CO₃ in 2:1 volume ratio, resulting in the ligand 1-phenylisoquinoline (**4-17**) with a yield of 90 %. The subsequent complexation of **4-5** with iridium acetylacetonate in glycerin gave the red phosphorescent iridium complex **Ir(piq)₃** in 47% yield. Similar to the halogenation of **Ir(ppy)₃**, the bromination of **Ir(piq)₃** with 4.5 equivalents of N-bromosuccinimide in dichloromethane at room temperature, achieving *fac*-tris(1-(3-bromidephenyl)isoquinolinato) iridium(III) (**4-18**) in 84 % yield. The following three-fold *Stille*-coupling between 1 equivalent of 4-6 and 4.5 equivalents of trimethyl((tributylstannyl)ethynyl)silane   in   THF   by   using   dichloro-bis(triphenylphosphine)palladium(II) as the catalyst resulted in *fac*-tris(1-(3-trimethyl silylethynylphenyl)isoquinolinato) **4-19** with an acceptable yield of 57%. After treatment with tetrabutylammonium fluoride in THF at 0 °C, the trimethylsilyl groups in **4-19** were all cleaved, providing the *fac*-tris(1-(3-ethynylphenyl)isoquinolinato) iridium(III) (**4-20**) in 84% yield. Finally, Diels-Alder cycloaddition of the Ir(III) core 4-4 with 2,5-diphenyl-3,4-bis(4-triisopropylsilyethynylphenyl)cyclopentadienone 4-X afforded the first generation dendrimer **4-16** in 78% yield.
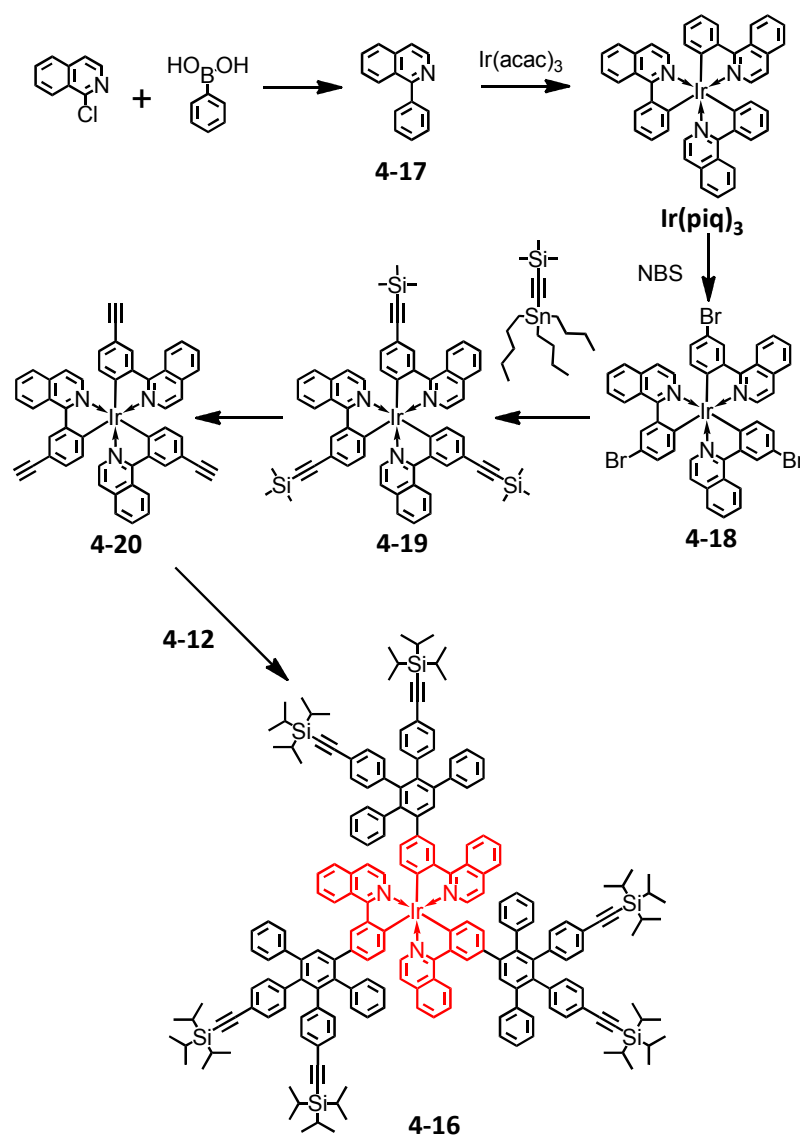
Scheme 4-5: Synthesis of Ir(piq)₃ cored polyphenylene dendrimer **4-16.**
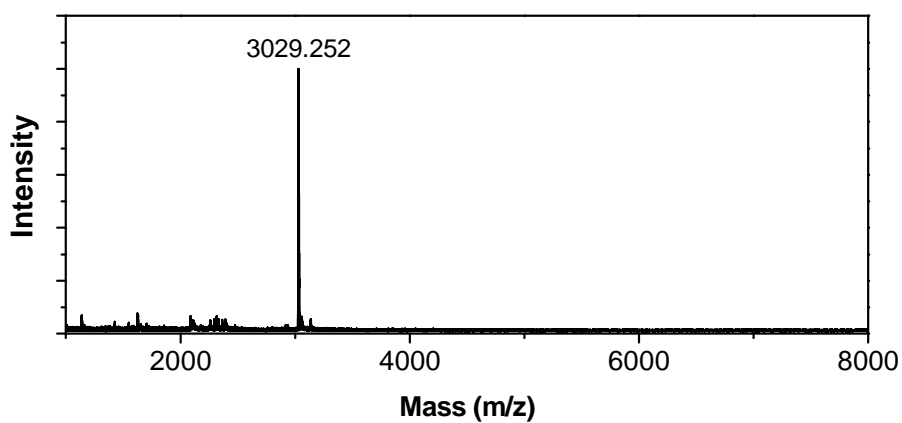

Figure 4-9: MALDI-TOF mass spectra of dendrimer **4-16**.

The well-defined MADLI-TOF mass spectrum showed a monodisperse molecular weight and proved structural perfection and purity of the Ir(piq)₃ cored dendrimer **4-16** (Figure 4-9).

4.7 Comparison of photophysical properties between different Ir(III) cores

For comparison, we measured the UV-Vis absorption and PL spectra of first generation dendrimers based on Ir(ppy)₃, Ir(btp)₃ and Ir(piq)₃ cores, (**3-9**, **4-11** and **4-16** in Scheme 4-3), respectively.

3-9   **4-11**   **4-16**
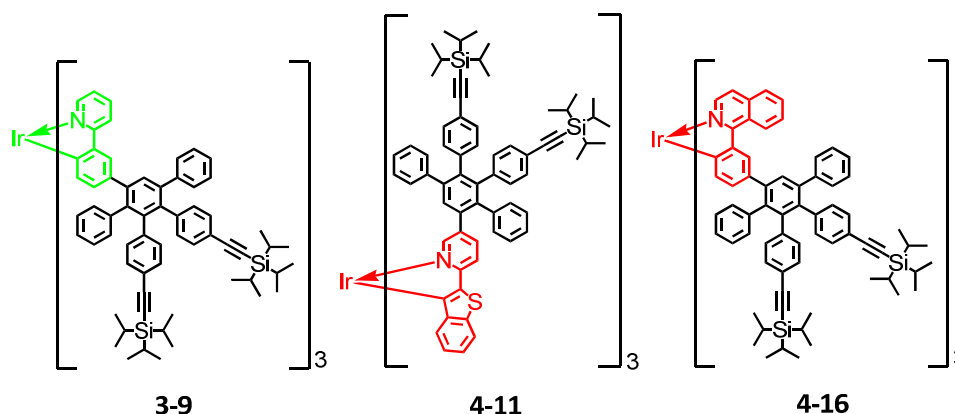
Scheme 4-3: Structures of Ir(ppy)₃ cored dendrimer **3-9**, Ir(btp)₃ cored dendrimer **4-11**, and Ir(piq)₃ core dendrimer **4-16**.

Figure 4-10 shows the absorption spectra of **3-9**, **4-11** and **4-16** in DCM solution with a concentration of 10^{-6} M. The absorption bands of both **4-11** and **4-16** demonstrate sigificantly bathochromic shifts compared to that of **3-9**. In the short wavelength range, as we discussed above, the absorption bands below 360 nm and 400 nm of **3-9** and **4-11**, respectively, are predominantly attributed to the spin-allowed ligand centered (LC) transitions.[38] The absorption wavelength below 400 nm of **4-16** can also be ascribed to the π-π* transition of the polyphenylene dendrons.[39] In contrast, the long wavelength range is more important for the Ir(III) complexes, since this range is primarily caused by MLCT state which can significantly influence their photophysical properties.[34-35] Relative to dendrimer **3-9**, which demonstrates the ¹MLCT and ³MLCT characteristic

peaks at 412 nm and 462 nm, both dendrimer **4-11** and **4-16** show bathochromic shifts in ^{1}MLCT and ^{3}MLCT bands, but to a different degree (Table 4-3). The bathochromic shift is caused by the size of π-conjugation spacer and/or the strength of intermolecular donor-acceptor interaction in the ligands.[40] Therefore, we can deduce that the influence of isoquionoline electron-accepting character of in **4-16** is stronger than that of benzothiophene electron-donating character in **4-11**.
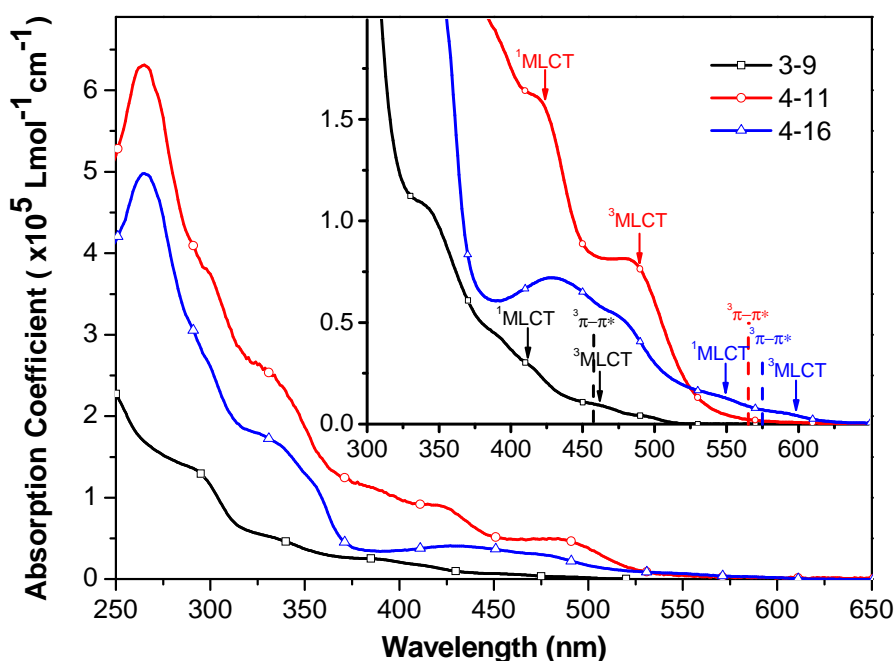
Figure 4-10: Absorption spectra of dendrimers **3-9**, **4-11** and **4-16**.

To the best of our knowledge, the ^{3}π-π* transition for phenylpyridine gives rise to an absorption at 460 nm,[41] which puts it at a sufficiently high energy such that the ^{3}MLCT becomes the lowest energy excited state. Due to the extended planarity of the ligands in the cores of **4-11** and **4-16**, both absorption bands of their ligand-center ^{3}π-π* level show significantly bathochromic shifts to ca. 565 nm for benzo[b]thienylpyridine[42] and ca. 575 nm for phenylisoquinoline,[43] respectively. However, due to their different ^{3}MLCT levels, the lowest energy excited state is predominantly based on LC ^{3}π-π* transition for **4-11**, but ^{3}MLCT for **4-16**, respectively. Therefore, dendrimer **3-9** and **4-16** exhibits very small Stokes shifts of 20 - 30 nm between the maximum absorption and emission bands, while dendrimer **4-11** give a larger shift of 56 nm.[44]

Table 4-3: Absorption (λ_{abs}) and emission (λ_{em}) maxima, ligand-center $^3\pi$-π^* level (**LC $^3\pi$-π^***), relative photoluminescence intensity (I_p) and photoluminescence quantum yield (Φ_P) of dendrimers **3-9**, **4-11** and **4-16** in solution.

	λ_{abs} [nm] (log ξ) [a]	LC $^3\pi$-π^* [nm]	λ_{em} [nm] [b]	PL I_p (%) [c]	Φ_P (%) [c]
3-9	294 (5.0), 336 (4.6), 388 (4.3), 412[i] (4.1), 462[ii] (4.0), 496 (3.6)	460	516	100	39
4-11	265 (6.7), 305 (6.6), 329 (6.1), 386 (5.7), 423[i] (5.5), 484[ii] (5.2)	565	621, 673	37	6
4-16	265 (6.5), 294 (6.1), 333 (5.2), 354 (5.1), 430 (4.9), 483 (4.8), 550[i] (4.3), 600[ii] (3.8)	575	630	97	21

[a] Measured in DCM at 298 K with a concentration of 10^{-6} M, i = ^{1}MLCT and ii = ^{3}MLCT. [b] Measured in DCM at 298 K with a concentration of 10^{-5} M by using excitation wavelength of 380 nm for **3-9** and 470 nm for **4-11** and **4-16**. [c] Calculated from the integration of PL bands, based on the normalization of the emission maximum intensity of **3-9**. [d] Measured in N_2-saturated toluene at 298 K with Ir(ppy)₃ as the reference and the excitation wavelength of 390 nm.

Moreover, different lowest energy excited states indicate that two types of Ir(III) dendrimers have dissimilar line shapes of PL spectra. As shown in Figure 4-11, the PL spectra are measured at a similar concentration of 10^{-5} M in DCM for all dendrimers. The emission spectra of **3-9** and **4-16** are similar to each other, supporting that their phosphorescence can be assigned to the emission from the predominantly ^{3}MLCT excited state.[44] Since vibronic fine structure is absent for the Ir(ppy)₃ and Ir(piq)₃ complexes but clearly observed for the Ir(btp)₃ complex, emission bands from MLCT states are generally broad and featureless, while $^3\pi$-π^* states typically give highly structured emission, which is located at ca. 673 nm in dendrimer **4-11**.[34] After the normalization by the maximum intensity of **3-9**, the two red phosphorescent dendrimers display unequal emission intensities of ca. 37% and 97% for **4-11** and **4-16**, respectively, compared to that of **3-9**, pointing out that the emission quantum yield of Ir(piq)₃ cored

dendrimer **4-16** should be almost three times higher than that of Ir(btp)$_3$ cored **4-11**, which is further proved by their relative PLQYs (Table 4-3).
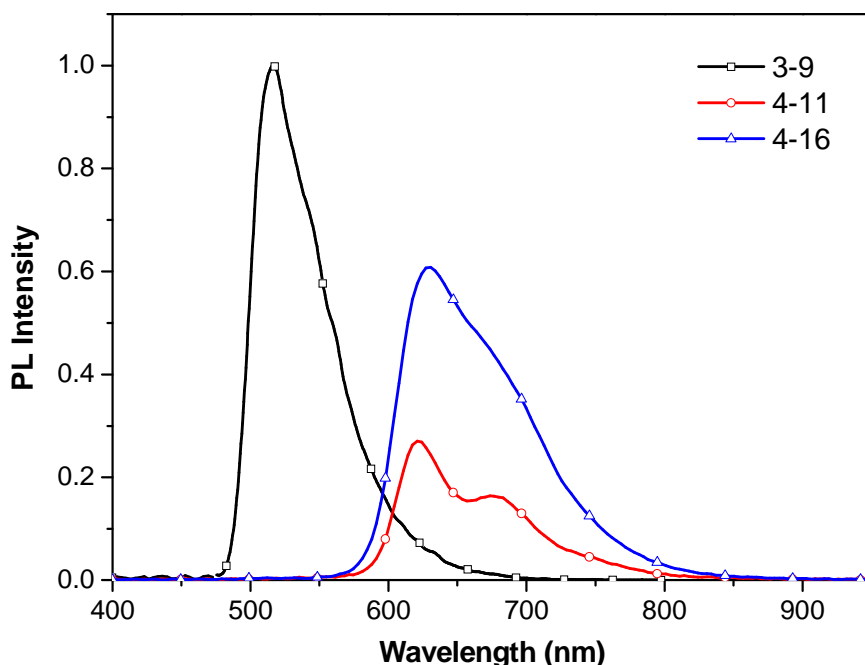

Figure 4-11: PL spectra of dendrimers **3-9**, **4-11** and **4-16**.

As the above results, in comparison with Ir(btp)$_3$ cored dendrimers (**RIrG1**, **RIrG2** and **RIrG3**), the new Ir(piq)$_3$ cored dendrimer can produce pure red emission spectra with longer λ_{max} and higher quantum yield due to its dominantly ^{3}MLCT excited states. Therefore, we can conclude that this new series of Ir(piq)$_3$ cored dendrimers will be more promising candidates than Ir(btp)$_3$ cored dendrimers for high performance red phosphorescent OLEDs.

4.8 Summary

In this chapter, a series of red phosphorescent dendrimers with *fac*-tris(2-benzo[b]thiophenylpyridyl) iridium(III) (Ir(btp)$_3$) core and multi-triphenylamine end-groups were successfully prepared via a divergent route by Diels-Alder cycloaddition reactions. These dendrimers represent monodisperse molecular weights and larger

molecular sizes compared to previous by reported red light-emitting dendrimers. All dendrimers showed good solubility in organic solvent thus allowing easy solution processibility in device fabrication. Steady state UV-Vis and PL spectroscopy have been proven the efficient isolation of emitting cores from each other and the environment by the surrounding polyphenylene dendrons and triphenylamine out-shells. The cyclic voltammetry measurement has been applied to determine the influence of electronic properties of the encapsulated Ir(III) complex core.

Electroluminescent properties and device performance displayed that these Ir(btp)₃ cored dendrimers emitted pure red light with CIE coordinates almost identical to the NTSC standard for red subpixels. All red phosphorescent dendrimers (**RIrGx**) showed excellent current intensity up to 500 mA/cm², even better than the values of green emissive dendrimers (**GIrGx**), indicating that the peripheral hole-transporting multi-triphenylamine units can improve the charge injection ability at the dendrimer surface. However, the luminescence of **RIrGx** based devices was much lower than that of **GIrGx** devices, due to the low PLQYs of Ir(btp)₃ cores. Therefore, in order to achieve high performance red phosphorescent OLEDs, we designed a new series of Ir(piq)₃ cored dendrimers, which possessed more than three times higher in PLQYs. According to the previous papers and our theoretical study, these phenomena could be explained by their different lowest excited energy levels. In contrast to the fact that the lowest excited energy level was located on the $^3\pi$-π^* transition of benzothienylpyridine ligand in the Ir(btp)₃ cored dendrimer (**4-11**), the phenylisoquinoline ligand in Ir(piq)₃ cored dendrimer (**4-16**) could effectively reduce the ^{3}MLCT excited state to the lowest excited energy level and thus improve the quantum efficiency.

In conclusion, the iridium complex cored dendrimers for high performance red phosphorescent OLEDs should be designed and synthesized based on the following two concepts.

i)   The electron transporting units such as triphenylamine, carbazole or phenylene can improve the charge injection ability at the dendrimer surface, thus increasing the

current density and decreasing the on-set voltage. Nevertheless, the peripheral triphenylamine units efficiently extend the size of the dendrons, which can not only improve the solubility of dendrimer, but also well isolate the chromophores in solid states.

ii)   For the iridium complexes having the emissive ^{3}MLCT excited state, the HOMO level of the complex should not change unless the coordination structure significantly varies, therefore the benzothiophene units have to be avoided. On the other hand, the ^{3}MLCT energy is expected to effectively decrease when a complex has a ligand with lower LUMO level. Thus the strong electron-accepting isoquinoline moiety was depicted as the ligand to Ir(III) core and decorated with polyphenylene dendrons.

References

[1]   a)Balzani, V., Juris, A., Venturi, M., Campagna, S., Serroni, S., *Chem. Rev.* **1996**, *96*, 759; b)Baldo, M. A., O'Brien, D. F., You, Y., Shoustikov, A., Sibley, S., Thompson, M. E., Forrest, S. R., *Nature* **1998**, *395*, 151; c)Welter, S., Brunner, K., Hofstraat, J. W., De Cola, L., *Nature* **2003**, *421*, 54; d)You, Y. M., Park, S. Y., *J. Am. Chem. Soc.* **2005**, *127*, 12438; e)Kwon, T. H., Cho, H. S., Kim, M. K., Kim, J. W., Kim, J. J., Lee, K. H., Park, S. J., Shin, I. S., Kim, H., Shin, D. M., Chung, Y. K., Hong, J. I., *Organometallics* **2005**, *24*, 1578; f)Hwang, F. M., Chen, H. Y., Chen, P. S., Liu, C. S., Chi, Y., Shu, C. F., Wu, F. L., Chou, P. T., Peng, S. M., Lee, G. H., *Inorg. Chem.* **2005**, *44*, 1344; g)Tsuzuki, T., Shirasawa, N., Suzuki, T., Tokito, S., *Adv. Mater.* **2003**, *15*, 1455; h)D'Andrade, B. W., Thompson, M. E., Forrest, S. R., *Adv. Mater.* **2002**, *14*, 147; i)Bulovic, V., Deshpande, R., Thompson, M. E., Forrest, S. R., *Chem. Phys. Lett.* **1999**, *308*, 317.

[2]   a)Siebrand, W., *J. Chem. Phys.* **1967**, *46*, 440; b)Neve, F., Crispini, A., Campagna, S., Serroni, S., *Inorg. Chem.* **1999**, *38*, 2250; c)Yersin, H., *Transition Metal and Rare Earth Compounds Iii* **2004**, *241*, 1.

[3]   a)Lo, S. C., Burn, P. L., *Chem. Rev.* **2007**, *107*, 1097; b)Burn, P. L., Lo, S. C., Samuel, I. D. W., *Adv. Mater.* **2007**, *19*, 1675; c)Ding, J. Q., Gao, J., Cheng, Y. X., Xie, Z. Y., Wang, L. X., Ma, D. G., Jing, X. B., Wang, F. S., *Adv. Funct. Mater.* **2006**, *16*, 575; d)Markham, J. P. J., Lo, S. C., Magennis, S. W., Burn, P. L., Samuel, I. D. W., *Appl. Phys. Lett.* **2002**, *80*, 2645; e)Lo, S. C., Male, N. A. H., Markham, J. P. J., Magennis, S. W., Burn, P. L., Salata, O. V., Samuel, I. D. W., *Adv. Mater.* **2002**, *14*, 975; f)Lo, S. C., Namdas, E. B., Burn, P. L., Samuel, I. D. W., *Macromolecules* **2003**, *36*, 9721; g)Lupton, J. M., Samuel, I. D. W., Frampton, M. J., Beavington, R., Burn, P. L., *Adv. Funct. Mater.* **2001**, *11*, 287.

[4]   a)Ho, C. L., Wong, W. Y., Gao, Z. Q., Chen, C. H., Cheah, K. W., Yao, B., Xie, Z. Y., Wang, Q., Ma, D. G., Wang, L. A., Yu, X. M., Kwok, H. S., Lin, Z. Y., *Adv. Funct. Mater.* **2008**, *18*, 319; b)Anthopoulos, T. D., Frampton, M. J., Namdas, E. B., Burn, P. L., Samuel, I. D. W., *Adv. Mater.* **2004**, *16*, 557.

[5]   a)Jiang, C. Y., Yang, W., Peng, J. B., Xiao, S., Cao, Y., *Adv. Mater.* **2004**, *16*, 537; b)Duan, J. P., Sun, P. P., Cheng, C. H., *Adv. Mater.* **2003**, *15*, 224; c)Chen, X. W., Liao, J. L., Liang, Y. M., Ahmed, M. O., Tseng, H. E., Chen, S. A., *J. Am. Chem. Soc.* **2003**, *125*, 636.

[6]   a)Zhang, K., Chen, Z., Yang, C. L., Gong, S. L., Qin, J. G., Cao, Y., *Macromol. Rapid Commun.* **2006**, *27*, 1926; b)Meerheim, R., Walzer, K., Pfeiffer, M., Leo, K., *Appl. Phys. Lett.* **2006**, *89*; c)Kwong, R. C., Weaver, M. S., Lu, M. H. M., Tung, Y. J., Chwang, A. B., Zhou, T. X., Hack, M., Brown, J. J., *Org. Electron.* **2003**, *4*, 155.

[7]   a)Lin, B. C., Cheng, C. P., Lao, Z. P. M., *J. Phys. Chem. A* **2003**, *107*, 5241; b)Zhou, X., Pfeiffer, M., Blochwitz, J., Werner, A., Nollau, A., Fritz, T., Leo, K., *Appl. Phys. Lett.* **2001**, *78*, 410; c)Sakanoue, K., Motoda, M., Sugimoto, M., Sakaki, S., *J. Phys. Chem. A* **1999**, *103*, 5551; d)He, Y., Gong, S., Hattori, R., Kanicki, J., *Appl. Phys. Lett.* **1999**, *74*, 2265; e)Bellmann, E., Shaheen, S. E., Grubbs, R. H., Marder, S. R., Kippelen, B., Peyghambarian, N., *Chem. Mater.* **1999**, *11*, 399; f)Tamoto, N., Adachi, C., Nagai, K., *Chem. Mater.* **1997**, *9*, 1077.

[8]   a)Zhou, G. J., Wong, W. Y., Yao, B., Xie, Z. Y., Wang, L. X., *Angew. Chem. Int. Ed.* **2007**, *46*, 1149; b)Ding, J. Q., Lu, J. H., Cheng, Y. X., Xie, Z. Y., Wang, L. X., Jing, X. B., Wang, F. S., *Adv. Funct. Mater.* **2008**, *18*, 2754.

[9]   Qin, T. S., Ding, J. Q., Wang, L. X., Baumgarten, M., Zhou, G., Mullen, K., *J. Am. Chem. Soc.* **2009**, *131*, 14329.

[10]   a)Bauer, R. E., Grimsdale, A. C., Mullen, K., *Functional Molecular Nanostructures* **2005**, *245*, 253; b)Wiesler, U. M., Weil, T., Mullen, K., *Dendrimers Iii: Design, Dimension, Function* **2001**, *212*, 1.

[11]   Frampton, M. J., Namdas, E. B., Lo, S. C., Burn, P. L., Samuel, I. D. W., *J. Mater. Chem.* **2004**, *14*, 2881.

[12]   Lo, S. C., Anthopoulos, T. D., Namdas, E. B., Burn, P. L., Samuel, I. D. W., *Adv. Mater.* **2005**, *17*, 1945.

[13]   a)van Mullekom, H. A. M., Vekemans, J., Meijer, E. W., *Chem. Eur. J.* **1998**, *4*, 1235; b)BlanchardDesce, M., Alain, V., Bedworth, P. V., Marder, S. R., Fort, A., Runser, C., Barzoukas, M., Lebus, S., Wortmann, R., *Chem. Eur. J.* **1997**, *3*, 1091.

[14]   Bradamante, S., Facchetti, A., Pagani, G. A., *J. Phys. Org. Chem.* **1997**, *10*, 514.

[15]   Adachi, C., Baldo, M. A., Forrest, S. R., Lamansky, S., Thompson, M. E., Kwong, R. C., *Appl. Phys. Lett.* **2001**, *78*, 1622.

[16]   Sandee, A. J., Williams, C. K., Evans, N. R., Davies, J. E., Boothby, C. E., Kohler, A., Friend, R. H., Holmes, A. B., *J. Am. Chem. Soc.* **2004**, *126*, 7041.

[17]   Qu, J. Q., Pschirer, N. G., Liu, D. J., Stefan, A., De Schryver, F. C., Mullen, K., *Chem. Eur. J.* **2004**, *10*, 528.

[18]   Li, X. H., Chen, Z., Zhao, Q., Shen, L., Li, F. Y., Yi, T., Cao, Y., Huang, C. H., *Inorg. Chem.* **2007**, *46*, 5518.

[19]   Liang, B., Wang, L., Xu, Y., Shi, H., Cao, Y., *Adv. Funct. Mater.* **2007**, *17*, 3580.

[20]   Jung, K. M., Kim, K. H., Jin, J. I., Cho, M. J., Choi, D. H., *Journal of Polymer Science Part a-Polymer Chemistry* **2008**, *46*, 7517.

[21]   Xu, M. L., Wang, G. Y., Zhou, R., An, Z. W., Zhou, Q., Li, W., *Inorg. Chim. Acta* **2007**, *360*, 3149.

[22]   Bard, A. J., Abruna, H. D., Chidsey, C. E., Faulkner, L. R., Feldberg, S. W., Itaya, K., Majda, M., Melroy, O., Murray, R. W., Porter, M. D., Soriaga, M. P., White, H. S., *J. Phys. Chem.* **1993**, *97*, 7147.

[23]   Miller, D. A. B., Chemla, D. S., Damen, T. C., Gossard, A. C., Wiegmann, W., Wood, T. H., Burrus, C. A., *Physical Review B* **1985**, *32*, 1043.

[24]   Roquet, S., Cravino, A., Leriche, P., Aleveque, O., Frere, P., Roncali, J., *J. Am. Chem. Soc.* **2006**, *128*, 3459.

[25]   a)Thomas, K. R. J., Huang, T. H., Lin, J. T., Pu, S. C., Cheng, Y. M., Hsieh, C. C., Tai, C. P., *Chem. Eur. J.* **2008**, *14*, 11231; b)Qu, J. Q., Zhang, J. Y., Grimsdale, A. C., Mullen, K., Jaiser, F., Yang, X. H., Neher, D., *Macromolecules* **2004**, *37*, 8297.

[26]   O'Brien, D. F., Baldo, M. A., Thompson, M. E., Forrest, S. R., *Appl. Phys. Lett.* **1999**, *74*, 442.

[27]   Jordan, R. H., Rothberg, L. J., Dodabalapur, A., Slusher, R. E., *Appl. Phys. Lett.* **1996**, *69*, 1997.

[28]   Bowie, R. M., Tyson, B. F., *Sylvania Technologist|Sylvania Technologist* **1952**, 10.

[29]   Lupton, J. M., Samuel, I. D. W., Beavington, R., Frampton, M. J., Burn, P. L., Bassler, H., *Physical Review B* **2001**, *63*.

[30]   Lupton, J. M., Schouwink, P., Keivanidis, P. E., Grimsdale, A. C., Mullen, K., *Adv. Funct. Mater.* **2003**, *13*, 154.

[31]   Olshansky, R., Su, C. B., Manning, J., Powazinik, W., *IEEE J. Quantum Electron.* **1984**, *20*, 838.

[32]   Frisch, M. J., Pople, J. A., Binkley, J. S., *J. Chem. Phys.* **1984**, *80*, 3265.

[33]   Demas, J. N., Crosby, G. A., *J. Am. Chem. Soc.* **1971**, *93*, 2841.

[34]   Tsuboyama, A., Iwawaki, H., Furugori, M., Mukaide, T., Kamatani, J., Igawa, S., Moriyama, T., Miura, S., Takiguchi, T., Okada, S., Hoshino, M., Ueno, K., *J. Am. Chem. Soc.* **2003**, *125*, 12971.

[35]   Okada, S., Okinaka, K., Iwawaki, H., Furugori, M., Hashimoto, M., Mukaide, T., Kamatani, J., Igawa, S., Tsuboyama, A., Takiguchi, T., Ueno, K., *Dalton Transactions* **2005**, 1583.

[36]   Colombo, M. G., Brunold, T. C., Riedener, T., Gudel, H. U., Fortsch, M., Burgi, H. B., *Inorg. Chem.* **1994**, *33*, 545.

[37]   Dedeian, K., Djurovich, P. I., Garces, F. O., Carlson, G., Watts, R. J., *Inorg. Chem.* **1991**, *30*, 1685.

[38]   Lamansky, S., Djurovich, P., Murphy, D., Abdel-Razzaq, F., Kwong, R., Tsyba, I., Bortz, M., Mui, B., Bau, R., Thompson, M. E., *Inorg. Chem.* **2001**, *40*, 1704.

[39]   a)Namdas, E. B., Anthopoulos, T. D., Samuel, I. D. W., Frampton, M. J., Lo, S. C., Burn, P. L., *Appl. Phys. Lett.* **2005**, *86*; b)Herrmann, A., Weil, T., Sinigersky, V., Wiesler, U. M., Vosch, T., Hofkens, J., De Schryver, F. C., Mullen, K., *Chem. Eur. J.* **2001**, *7*, 4844.

[40]   Tamayo, A. B., Garon, S., Sajoto, T., Djurovich, P. I., Tsyba, I. M., Bau, R., Thompson, M. E., *Inorg. Chem.* **2005**, *44*, 8723.

[41]   Sarkar, A., Chakravorti, S., *J. Lumin.* **1995**, *65*, 163.

[42]   You, Y., An, C. G., Kim, J. J., Park, S. Y., *J. Org. Chem.* **2007**, *72*, 6241.

[43]   a)Fang, K. H., Wu, L. L., Huang, Y. T., Yang, C. H., Sun, I. W., *Inorg. Chim. Acta* **2006**, *359*, 441; b)Li, C. L., Su, Y. J., Tao, Y. T., Chou, P. T., Chien, C. H., Cheng, C. C., Liu, R. S., *Adv. Funct. Mater.* **2005**, *15*, 387.

[44]   Lamansky, S., Djurovich, P., Murphy, D., Abdel-Razzaq, F., Lee, H. E., Adachi, C., Burrows, P. E., Forrest, S. R., Thompson, M. E., *J. Am. Chem. Soc.* **2001**, *123*, 4304.

Chapter 5

Conclusion and outlook

As introduced earlier in the motivation, the main goals of this thesis were the design, synthesis, characterization of novel functional polyphenylene dendrimers for blue, green, and red light emitting diodes. These light-emitting polyphenylene dendrimers are a distinct class of macromolecules that are comprised of molecular components. They can be formed reproducibly with monodispersity, high levels of purity and three-dimensional shape-persistent architecture.

The first chapter presented a novel synthetic strategy of the blue light-emitting polytriphenylene dendrimers, based on non-catalytic Diels-Alder reaction. The blue fluorescent chromophores – triphenylene units were forming synchronously from the [4+2] cycloaddition between phencyclone moieties and ethynyl groups during the dendrimer generation growth. According to the single crystal X-ray crystallography, the crystal packing diagram of dendrimers showed that the triphenylene units are almost perpendicular to each other, which completely broke the π-π stacking often observed in most triphenylene derivatives. It could be concluded that for all generation dendrimers, the highly twisted repeating units and stiff dendritic structure could effectively prevent the self quenching among chromophores, which always reduced the performance of OLED devices based on small molecules and linear polymers. The suppressed aggregation of the chromophores resulted in highly photoluminescence quantum yield with a defined pure blue emission spectrum. The optical and chemical stabilities were further investigated by using thermal degradation and thermogravimetric analysis, which revealed that polytriphenylene dendrimers (**TPGx**) were promising candidates for blue OLEDs, and thus their devices were later prepared. During the device fabrication, various configurations and different generation dendrimers were attempted and tested. Thereamong, the second generation polytriphenylene dendrimers demonstrated an acceptable device performance, such as the color purity, optical stability, long time

stability and low onset voltage, due to its appropriate dendrimer size. However, the luminescence efficiency was relatively low and could be potentially modified. In order to achieve even higher device efficiency, the core of polytriphenylene dendrimers was further functionalized from tetraphenylmethane to pyrene, an excellent blue emitter with high quantum yield and long life time. These pyrene cored dendrimers (**PYGx**) exhibited nearly three times higher photoluminescence quantum yield as well as almost four times luminescence intensity than the original contrast (**TPGx**), since the pyrene core not only possessed high PLQY, but also acted as a connector between conjugated triphenylene units. Most importantly, the **PYGx** dendrimers could be described as a single molecular light-harvesting system with the polytriphenylene units in dendrons acting as donors and the pyrene core serving as an energy acceptor. Therefore, combining multi-chromophoric scaffolds and a highly efficient chromophoric core in a shape-persistent dendritic architecture yielded spherical nanoparticles with improved electro-optical properties. These properties are rendering this novel type of polytriphenylene dendrimers as promising candidates on the field of semiconductors.

The electroluminescence properties of the light-emitting dendrimers demonstrated that the efficiency of emissive core and number of generation could extremely influence the processibility, stability and even performance of these dendritic OLEDs. Thus the iridium complex phosphors were introduced as the core into the dendrimer, since they theoretically had three times higher quantum efficiency than fluorescent emitters. On account of a divergent synthetic strategy, the Ir(ppy)$_3$ cored dendrimers (**GIrGx**) were firstly successfully obtained up to the 4th generation, which is the largest iridium complex till now. This new synthesis concept could overcome the disadvantage of traditional convergent synthesis which often limited dendrimers in low generations. Afterward, these monodisperse phosphoresent dendrimers from 1st to 4th generation provided a unique opportunity in researching the effect of molecular sizes on the device performance. The photoluminescence spectra resolved out that all dendrimers emitted pure green light. More importantly, the bathochromic shift in emission from solution to thin film was completely prevented in the 4th generation dendrimer, indicating that the

large dendron size can effectively isolated the phosphorescent core from each other and the environment in the solid state. It was further proved by that the phosphorescence quantum yield still increased up to the 4th generation. However, the full OLED device characterization showed that the 3rd generation dendrimer with a radius of ca 3 nm was regarded as the optimum molecular size for high electroluminescence efficiency, since its appreciate dendron size would not limit the good charge transfer from periphery to emissive core, but still efficiently protect against the triplet-triplet annihilation. The quantum efficiency and electronic performance of green phosphorescent OLED devices based on our 3rd generation $Ir(ppy)_3$ cored polyphenylene dendrimer have already entered the top-level in the dendritic phosphorescent emitter field. Going one step further, we noticed the efficiency of non-doped device based on 3rd generation dendrimer demonstrated were almost three times higher than that of doped device from 1st generation dendrimer. It revealed that the polyphenylene dendron was a potential host material for the iridium guest core. This self host-guest system, which could extremely simplify the device structure of phosphorescent OLEDs, would be further optimized by the surface functionalization to combine charge transporting units in the periphery of dendrimer.

The last chapter demonstrated the synthesis of solution processable red iridium cored polyphenylene dendrimers (**RIrGx**) with hole-transporting multi-triphenylamine units at the surface and their application in electrophosphorescent devices. The current densities of OLED devices based on peripheral multifunctionalized polyphenylene dendrimer (**RIrGx**) were even higher than the original polyphenylene dendrimers (**GIrGx**), since triphenylamine units could availably improved the hole-transproting property and charge injection ability from matrix to dendrimer surface. However, the luminescence and quantum efficiency of the red emissive devices based on $Ir(btp)_3$ core dendrimer were significantly lower than those of the green devices. We ascribed it to the low phosphorescent quantum efficiency of the $Ir(btp)_3$ complex core, whose lowest excited transition state was dominantly on the ligand-centered $^3\pi$-π^* level. In order to obtain high performance red phosphorescent materials, we designed and synthesized a new

154

series of Ir(piq)$_3$ cored dendrimers, whose lowest excited transition state was dominantly on the ^{3}MLCT level and thus photoluminescence quantum yield was increased nearly four times. Based on the results described here, it could be envisaged that ligands controls strongly affect phosphorescence quantum efficiency.

In this thesis, highly efficient blue, green and red light-emitting dendrimers have been developed and used in OLEDs. In additional to the above mentioned advantages of dendrimer based OLEDs, the modular molecular architecture and various functionalized units at different locations in polyphenylene dendrimers open up a tremendous scope for tuning a wide range of properties in addition to color, such as intermolecular interactions, charge mobility, quantum yield, and exciton diffusion. Research into dendrimer containing OLEDs combines fundamental aspects of organic semiconductor physics, novel and highly sophisticated organic synthetic chemistry and elaborate device technology. Dendrimers provide a model example of the methodology of scientific research. Starting out from mere curiosity, they have developed into a key technology and now constitute one of the most efficient electrical light sources known. This is surely an impressive feat, considering the sheer volume of input generated into organic and metallorganic chemistry by the systematic research into dendrimers. Dendrimer OLED technology is now actively being researched in an industrial environment and forms an integral part of the materials strategy of Cambridge Display Technology. There remains, however, plenty to do. Thus far, reports on the operational stability of dendrimer OLEDs have been few, but there is no reason to doubt that this will be successful. It has yet to be demonstrated that the technology can compete with existing material classes in terms of operational lifetime requirements.

As Matthews, Shipway and Stoddart put it in their review "Dendrimers – Branching out from curiosities into new technologies" a mere decade ago: "There must somewhere be a dendrimer 'El Dorado' waiting to be discovered".[1] Although it indeed looks like the key to this magic chest has now been turned, the rapid development of dendrimer technology holds promise for even more sophisticated applications in the future. The intrinsically modular conception of dendrimers, together with the increasingly exploited

power of molecular self-assembly, allow the prediction that dendrimer technology will further the construction of ever more sophisticated electronically active supramolecular units for future generations of molecular electronics.

For the future, the remaining challenges in developing light-emitting dendrimers are to realize: i) multi-color functionalities and their controls, ii) high efficiency deep blue phosphorescence, and iii) supramolecular structures.

The first aim will be realized by combining the divergent synthetic protocols of Ir(piq)$_3$ core and surface functionalization of Ir(ppy)$_3$ building units which will result in a new type of multi-color-phosphorous dendrimers (**5-1**) (Scheme 5-1), containing a Ir(piq)$_3$ core as an acceptor and multiple Ir(ppy)$_3$ peripheral units as donors.

5-1
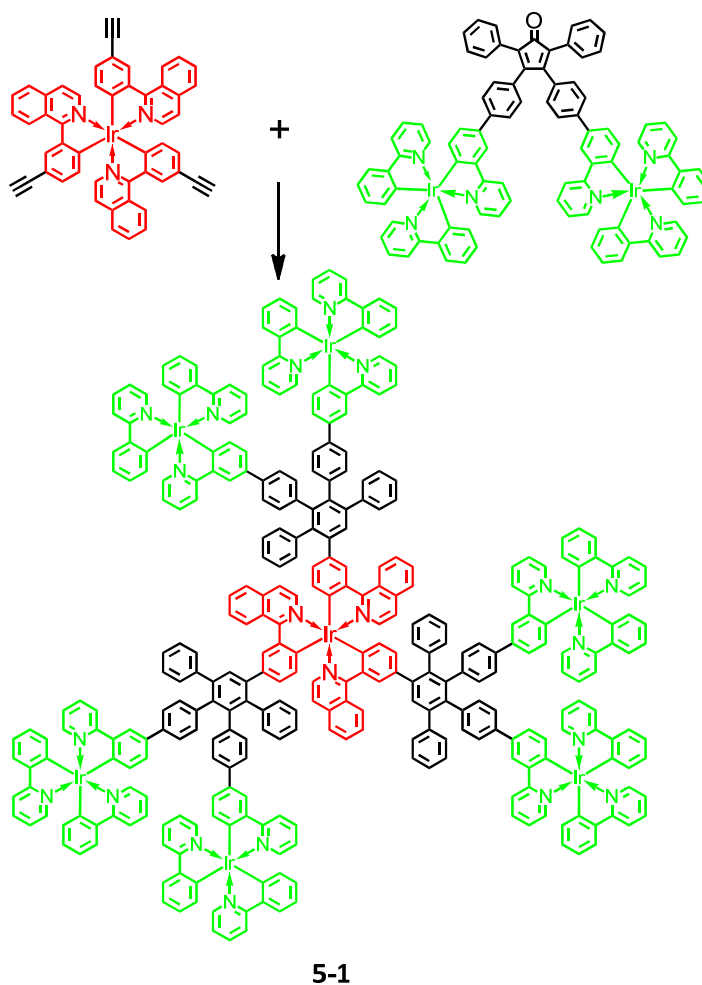
Scheme 5-1: Structure of multi-color-phosphorous Ir(III) dendrimer **5-1**.

This dendrimer holding two types of iridium complexes will be highly interesting from the points of view of triplet energy transfer process and multi-chromophoric excited phosphorescence.

The second aim, deep blue phosphorescent iridium complex cored dendrimers, inevitably require modulation in the ligand structures.[2] Thus, reliable principles for ligand control and their effect on phosphorescence quantum efficiency would be greatly helpful for the molecular design. By adding the electron-accepting fluorine atoms to the phenyl ring *in* ligand, it is possible to decrease the HOMO level and shift the emission from green to blue. Furthermore, this fluoride phenylpyridyl iridium complex should emit high quantum efficiency, since its ^{3}MLCT energy level is expected to be the lowest excited transition state. Therefore, a blue phosphorescent iridium core (**5-2**, Scheme 5-2) and its dendrimers (**5-3**) will be later synthesized.
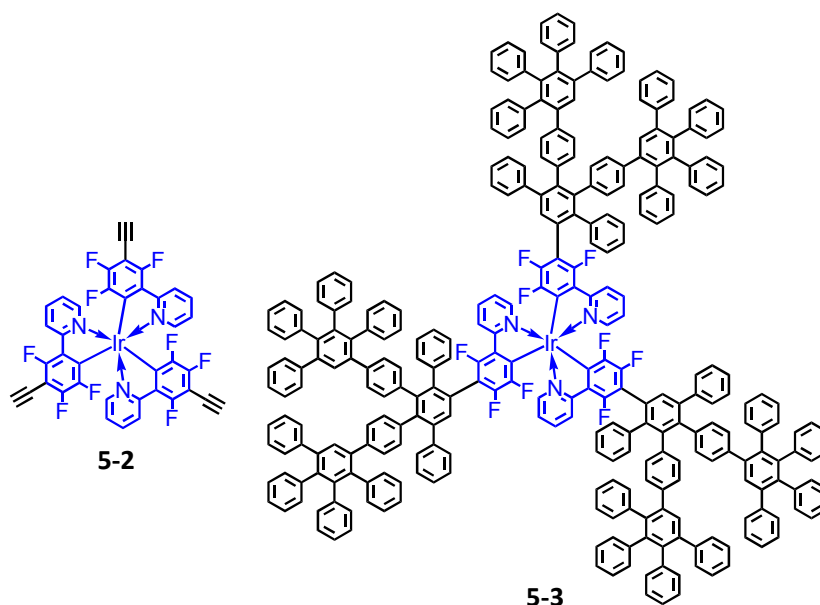
Scheme 5-2: Structure of blue phosphorescent Ir(III) core **5-2** and polyphenylene dendrimer **5-3**.

References

[1]   Matthews, O. A., Shipway, A. N., Stoddart, J. F., *Prog. Polym. Sci.* **1998**, *23*, 1.

[2]   a)Yang, C. H., Cheng, Y. M., Chi, Y., Hsu, C. J., Fang, F. C., Wong, K. T., Chou, P. T., Chang, C. H., Tsai, M. H., Wu, C. C., *Angew. Chem. Int. Ed.* **2007**, *46*, 2418; b)Chang, C. F., Cheng, Y. M., Chi, Y., Chiu, Y. C., Lin, C. C., Lee, G. H., Chou, P. T., Chen, C. C., Chang, C. H., Wu, C. C., *Angew. Chem. Int. Ed.* **2008**, *47*, 4542.

Chapter 6

Experimental section

6.1 Reagents and analysis instruments

Materials:

All starting materials, solvents and catalysts for chemical reactions were purchased from Aldrich, Acros, Fluka, ABCR, TIC, etc. and used as received without purification.

Chromatography:

Preparative column chromatography was performed on silica gel from Merck with particle size of 0.063-0.200 mm (Geduran Si 60). For analytical thin layer chromatography (TLC) silica gel coated substrates 60 F254 from Merck were used. Compounds were detected by fluorescence quenching at 254 nm and self-fluorescence at 366 nm. Gel permeation chromatography (GPC) was performed on Bio-Beads S-X1 beads with 200-400 mesh from Bio-Rad Laboratories Inc using DCM or toluene as eluent.

NMR Spectroscopy:

^{1}H NMR and ^{13}C NMR spectra were recorded in CD_2Cl_2, $C_2D_2Cl_4$, THF-d_8, DMF-d_7 or DMSO-d_6 on a Bruker DPX 250, Bruker AMX 300, Bruker DRX 500 or Bruker DRX 700 spectrometer with use of the solvent proton or carbon signal as an internal standard.

Mass spectrometry:

Field desorption mass spectra (FDMS) were performed with a VG Instruments ZAB 2-SE-FDP using 8 kV accelerating voltage.

MALDI-TOF mass spectra were measured on a Bruker Reflex II using a 337 nm nitrogen laser, calibrated against poly(ethylene glycol) (3,000 g/mol). Samples for MALDI-TOF MS were prepared by mixing the analyte with the matrix (dithranol) in THF in a ratio of 1:250. Cationization was performed by mixing the matrix with potassium trifluoroacetate (K^+) or silver trifluoroacetate (Ag^+). The mass instrument is not dedicated to isotopic measurements, and the deviations of relative intensities of peak, from those calculated, can be more than 10%.

UV-vis spectroscopy:

UV-vis absorbance spectra were measured by Perkin-Elmer Lambda 35 UV-vis spectrometer.

Photoluminescence spectroscopy:

Photoluminescence (PL) spectra were recorded on a Perkin-Elmer LS 50B spectrofluorometer.

Cyclic voltammetry:

The cyclic voltammetry (CV) measurements were conducted at a scan rate of 50 mVs^{-1} at room temperature under argon protection in deoxygenated 0.1 mmol/L DCM solutions with 0.1 mol/L tetrabutylammonium hexafluorophosphate (n-Bu$_4$NPF$_6$) as the supporting electrolyte. A platinum electrode was used as the working electrode and an Ag/Ag$^+$ electrode as the reference electrode.

Thermal analysis:

Thermogravimetric analysis (TGA) was measured on Mettler TG 50.

Single crystal analysis:

The X-ray crystallography of single crystals was measured on a Stoe IPDS II area detector diffractometer on the ANKA-SCD beamline at the ANKA synchrotron source by Dr. Christopher Anson at the Forschungszentrum Karlsruhe, by using Si-monochromated

radiation of wavelength 0.79999 Å. The crystal was cooled to 150 K, and a hemisphere of data was measured to a resolution of 0.88 Å. Crystals of TPG1 grown from $C_2H_2Cl_4$/hexane mixtures formed very thin white needles that were very weakly diffracting, particularly at higher angles even using synchrotron radiation. However, the data are more than adequate to demonstrate the overall conformation of the molecule. The H atoms were refined with fixed isotropic temperature factors in the riding mode.

Device fabrication:

Polytriphenylene dendrimer based OLED devices were fabricated by Horst Scheiber and Wolfgang Wiedemair at Graz University of Technology and built in a sandwich geometry (glass/ITO/PEDOT:PSS/dendrimer/TPBi/CsF/Al). The ITO covered glass substrates for the OLEDs were thoroughly cleaned in a variety of organic solvents and exposed to an oxygen plasma dry cleaning step. PEDOT:PSS (Baytron P from Bayer Inc.) layers were spin-coated under ambient conditions and dried according to specifications by Bayer Inc. in argon atmosphere and vacuum. The emissive dendrimer films were spin-cast from a 10 g/l toluene solution and dried at 80 °C for 2 hours in high vacuum conditions. Afterwards, a 10 nm layer of 4,4',4''-Tris(N-3-methylphenyl-N-phenyl-amino)triphenylamine (TPBi; LT-E302 from Rubipy Scientific Inc.) as hole blocking/electron transport layer was evaporated onto the emissive film at a pressure of 4×10^{-6} mbar. Finally, a thin layer (1 nm) of CsF and aluminum electrodes (100 nm) were evaporated on top of the device via physical vapor deposition at a base pressure of below 2×10^{-6} mbar.

Ir(III) complex cored polyphenylene dendrimer based PhOLED devices were fabricated by Dr. Junqiao Ding at Chinese Academy of Sciences and built in a sandwich geometry (glass/ITO/PEDOT:PSS/dendrimer/TPBi/LiF/Al). Firstly, a 50-nm-thick poly(ethylenedioxythiophene): poly(styrene sulfonic acid) (PEDOT : PSS, purchased from H. C. Starck) film was deposited on the pre-cleaned ITO-glass substrates (20 Ω/square) and then cured at 120 °C in air for 30 min.. Then the film of dendrimers was spin-coated with chlorobenzene as the solvent, and annealed at 90 °C for 30 min. Successively, TPBi,

LiF and Al were evaporated at a base pressure less than 10^{-6} Torr (1 Torr = 133.32 Pa) through a shadow mask with an array of 14 mm^2 openings.

Electroluminescence spectroscopy:

The electroluminescence (EL) spectra of polytriphenylene dendrimers were recorded using an ORIEL Multispec spectrometer with an attached ANDOR DB401-UV CCD camera. The current/luminance/voltage (ILV) characteristics were recorded in a customized setup using a Keithley 236 source measure unit for recording the current / voltage characteristics while recording the luminance using a calibrated photodiode attached to an integrating Ulbrich sphere.

The EL spectra and Commission Internationale de L'Eclairage (CIE) coordinates were measured using a PR650 spectra colorimeter. The (ILV) characteristics of devices were measured using a Keithley 2400/2000 source meter and a calibrated silicon photodiode. All the experiments and measurements were carried out at room temperature under ambient conditions.

6.2 General synthetic procedures

Diels-Alder cycloaddition:

A mixture of the ethynyl derivative and tetraphenylcyclopentadiene derivative was refluxed in o-xylene under an argon atmosphere. When tetraphenylcyclopentadienone was used as the endcapping reagent, the cooled reaction mixture was poured into pentane to remove the excess of reagent. The precipitated product was filtered and the filter washed with pentane until the filtrate became colorless. All crude products were purified by column chromatography or GPC column. Reactions were monitored by MALDI-TOF mass spectrometry to ensure their completeness.

Deprotection of TiPS groups:

The tri-iso-propylsilylethynyl derivative was dissolved in dry THF and one equivalent of TBAF (dissolved in THF) per tri-iso-propylsilylethynyl group was added under argon atmosphere. The end of the reaction (~ 5-15 min) was determined by TLC (silica gel). The reaction was quenched with H_2O, and extracted with H_2O and DCM. The organic phase was separated and dried over $MgSO_4$. Having removed the solvent under reduced pressure, the crude product was purified by column chromatography on silica gel.

6.3 Syntheses of the blue fluorescent dendrimers (Chapter 2)

3,6-Dibromo-9,10-dimethoxyphenanthrene (2-12):
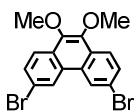
3,6-Dibromo-9,10-phenanthrenedione **2-10** (4.25 g, 11.6 mmol), Bu$_4$NBr (1.48 g, 4.6 mmol), $Na_2S_2O_4$ (8.20 g, 47.0 mmol), THF (100 mL) and H_2O (100 mL) were combined in a 500 mL round bottom flask and shaken for 5 min, after which dimethyl sulfate (7.5 mL, 79.5 mmol) was added, followed by aqueous sodium hydroxide (20 mL, 14.0 M). The mixture was stirred for 3 min, during which, 50 g of ice was added. Afterwards, the mixture was additionally stirred for 15 minutes. The aqueous layer was separated and extracted with ethyl acetate (EtOAc) (3 × 750 mL). The combined organic layers were washed with water (3 x 100 mL), NH_4OH solution (2 × 500 mL) and brine (1 × 500 mL). The organic layer was dried with $MgSO_4$, filtered and the solvents were removed under vacuum, resulting in a fluffy yellow solid. Washing the product with methanol (MeOH) gave a white solid. Additional impurities were removed by flashing the product through silica with a 1:1 mixture of hexanes and dichloromethane, affording 4.27 g (10.8 mmol) pure product as white crystal in 92% yield.

^{1}H NMR (250 MHz, CD_2Cl_2) δ 8.69 (d, 2H, J = 1.8 Hz, aromatic CH), 8.10 (d, 2H, J = 8.8 Hz, aromatic CH), 7.72 (dd, 2H, J1 = 8.8 Hz, J2 = 1.8 Hz, aromatic CH), 4.06 (s, 6H, OCH_3);

^{13}C NMR (62.5 MHz, CD$_2$Cl$_2$) δ 144.2, 130.9, 129.2, 128.8, 125.8, 124.5, 120.7, 61.3;

FD-MS: Calcd. for C$_{16}$H$_{12}$Br$_2$O$_2$: 396.1, found: 398.1.

Elemental analysis: Calcd. C 48.52%, H 3.05%, found: C 48.35%, H 2.79%

9,10-Dimethoxy-3,6-bis((triisopropylsilyl)ethynyl)phenanthrene (2-13):
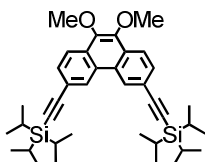
Compound **2-12** (3.4 g, 8.6 mmol), Pd(PPh$_3$)$_2$Cl$_2$ (0.68 g, 0.96 mmol), CuI (0.38g, 2.0mmol) and PPh$_3$ (0.52 g, 2.0 mmol) were dissolved in 100 mL of toluene/triethylamine solution and degassed by three freeze/pump/thaw cycles. The solution was heated to reflux under argon, 5 mL (33.8 mmol) triisopropylsilylacetylene was quickly added by a syringe to obtain a brown solution. The solution was kept stirring at 80 °C for 16 h. The solution was filtered and the solvent was removed by vacuum. After redissolution in DCM, the solution was washed with NH$_4$Cl, 1M HCl, and NaHCO$_3$. The organic phase was evaporated and purified by column chromatography (silica gel, PE:DCM = 4:1), affording 4.32 g (7.22 mmol) pure product as light yellow oil in 84% yield.

^{1}H NMR (250 MHz, CD$_2$Cl$_2$) δ 8.73 (s, 2H, aromatic CH), 8.14 (s, 2H, J = 8.5 Hz, aromatic CH), 7.68 (d, 2H, J1 = 8.4 Hz, aromatic CH), 4.07 (s, 6H, OCH_3), 1.19 (s, 42H, TiPS CH_2 and CH_3).

^{13}C NMR (62.5 MHz, CD$_2$Cl$_2$) δ 144.9, 130.7, 129.5, 128.0, 126.8, 122.6, 121.4, 107.8, 92.0, 61.3, 18.9, 11.8.

FD-MS: Calcd. for C$_{38}$H$_{54}$O$_2$Si$_2$: 598.4, found: 598.5.

Elemental analysis: Calcd. C 76.19%, H 9.09%, found: C 75.94%, H 8.97%

3,6-Bis((triisopropylsilyl)ethynyl) -9,10-phenanthrenedione (2-14):
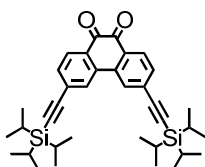
Compound **2-13** (2.80 g, 4.6 mmol) was dissolved in acetonitrile (20 mL) and DCM (20 mL) under argon protection. Afterwards, the mixture was added with stirring ammonium cerium (IV) nitrate (6.20 g, 11.4 mmol) in water (60 mL) over 15 min. The reaction was diluted with 100 mL H_2O and extracted with 3 × 100 mL DCM, and the organic phase was concentrated and purified by column chromatography (silica gel, PE:DCM = 1:1), affording 2.24 g (3.94 mmol) pure product as orange powder in 84% yield.

^{1}H NMR (250 MHz, CD_2Cl_2) δ 8.12 (d, 2H, $J1$ = 1.9 Hz, aromatic C*H*), 8.10(s, 2H, aromatic C*H*), 7.56 (d, 2H, $J1$ = 8.1 Hz, aromatic C*H*), 1.18 (s, 36H, silyl CH_3), 1.17 (s, 6H, CH_2).

^{13}C NMR (62.5 MHz, CD_2Cl_2) δ 197.9, 144.9, 130.7, 129.5, 128.0, 126.8, 122.6, 121.4, 107.8, 92.0, 18.9, 11.8.

FD-MS: Calcd. for $C_{36}H_{48}O_2Si_2$: 568.3, found: 568.8.

Elemental analysis: Calcd. C 76.00%, H 8.50%, found: C 75.74%, 8.53%.

1,3-Diphenyl-6,9-bis((triisopropylsilyl)ethynyl)-cyclopentaphenanthrenone (2-9):
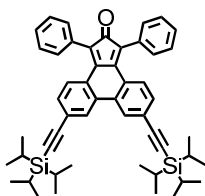
Compound **2-14** (1.36 g, 2.4 mmol) and 1,3-diphenyl-2-propanone (0.75 g, 3.6 mmol) were dissolved in anhydrate MeOH (50 mL) under argon atmosphere, 0.14 g KOH methanolic solution was added dropwise, and the mixture was heated up to 80 °C for 5 min. The brown mixture was rapidly frozen to 0 °C and 1.9 mL HCl (1.25 M in MeOH) was added with stirring to neutralize the pH to 5. The green precipitated was filtered, washed with cold MeOH and purified by colunm chromatography (silica gel, PE:DCM = 2:1), affording 1.08 g (1.45 mmol) pure product as dark green powder in 61% yield.

^{1}H NMR (250 MHz, CD_2Cl_2) δ 7.92 (s, 2H, aromatic *CH*), 7.48 (s, 2H, aromatic *CH*), 7.43 (dd, 4H, $J1$ = 9.7 Hz, $J2$ = 2.2 Hz, aromatic C*H*), 7.40 (s, 2H, aromatic *CH*), 7.34 (dd, 4H, $J1$

= 9.4 Hz, *J*2 = 1.6 Hz, aromatic C*H*), 7.03 (dd, 2H, *J*1 = 9.6 Hz, *J*2 = 1.3 Hz, aromatic C*H*), 1.14 (s, 42H, silyl *CH₃* and *CH₂*).

^{13}C NMR (62.5 MHz, CD$_2$Cl$_2$) δ 197.8, 147.4, 137.8, 136.2, 134.4, 133.0, 132.6, 132.1, 130.2, 129.0, 128.7, 128.6, 128.2, 127.1, 126.7, 124.2, 123.8, 106.8, 94.9, 93.9, 18.8, 11.7.

FD-MS: Calcd. for C$_{51}$H$_{58}$OSi$_2$: 742.4, found: 743.7.

1st Generation polytriphenylene dendrimer (TPG1):
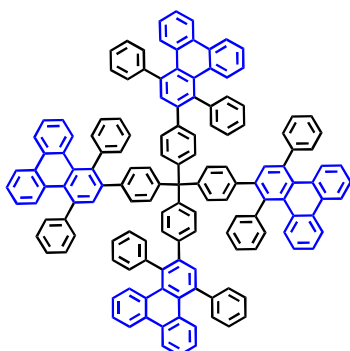
Tetrakis(4-ethynylphenyl)methane **2-17** (0.060 g, 0.144 mmol) and **2-18** (0.440 g, 1.152 mmol,) were put under Argon, dissolved in *o*-xylene (2 mL) in a microwave tube and stirred at 170 °C for 4 h. After cooling to RT, the reaction mixture was precipitated in MeOH, then washed with DCM till green color disappeared, affording 0.255 g (0.140 mmol) pure product as light yellow powder in 97% yield.

^{1}H NMR (700 MHz, $C_2D_2Cl_4$) δ 8.35 (t, 8H, , *J* = 7.1 Hz, aromatic *H*1), 7.69 (s, 4H, aromatic *H*2), 7.64 (d, 4H, *J* = 8.5 Hz, aromatic *H*3), 7.50 (t, 12H, , *J* = 8.8 Hz, aromatic *H*4), 7.40 – 7.32 (n.r., 20H), 7.12 (d, 4H, *J* = 7.3 Hz, aromatic *H*5), 7.08 (t, 4H, *J* = 14.8 Hz, aromatic *H*6), 7.04 (d, 12H, *J* = 7.4 Hz, aromatic *H*7), 6.96 (t, 4H, *J* = 7.7 Hz, aromatic *H*8), 6.89 (d, 8H, *J* = 8.2 Hz, aromatic *H*9), 6.81 (d, 8H, *J* = 8.2 Hz, aromatic *H*10).

^{13}C NMR (125 MHz, $C_2D_2Cl_4$) δ 145.0, 144.8, 144.7, 142.5, 142.4, 142.4, 140.6, 140.3, 140.1, 140.0, 139.9, 138.6, 137.4, 137.0, 132.8, 132.5, 132.4, 132.2, 132.0, 131.92, 131.7, 131.5, 131.1, 131.1, 130.8, 130.5, 130.4, 130.2, 130.0, 129.5, 129.4, 129.3, 129.2, 129.1, 128.8, 128.7, 128.7, 127.7, 127.6, 127.5, 127.4, 127.3, 127.0, 126.9, 126.7, 125.9, 125.5, 124.8, 123.5.

MALDI-TOF (Ag$^+$): Calcd. for $C_{145}H_{92}$: 1832.7, found: 1941.1 ([M+Ag]$^+$).

Elemental analysis: Calcd. C 94.94%, H 5.06%, found: 93.48%, H 5.06%

1st Generation TiPS protected ethynyl polytriphenylene dendrimer (2-19):
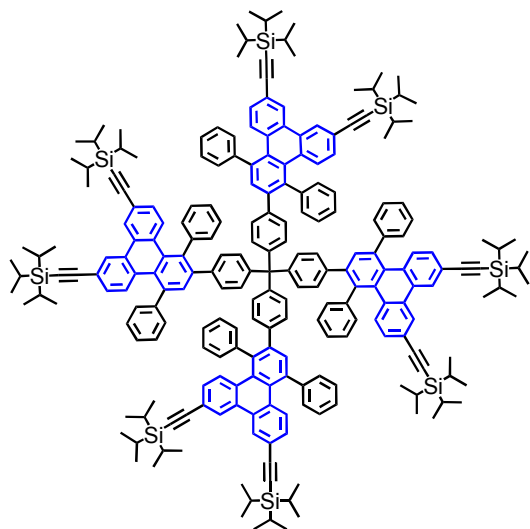
The core **2-17** (0.042 g, 0.100 mmol) and building unit **2-9** (0.350 g, 0.472 mmol,) were put under Argon, dissolved in *o*-xylene (2 mL) in a microwave tube and stirred at 170 °C for 4 h. After cooling to RT, the reaction mixture was evaporated *in vacuo*. The residue was further purified by column chromatography (silica gel, PE:DCM = 6:1), affording 0.266 g (0.081 mmol) pure product as light yellow powder in 81% yield.

^{1}H NMR (500 MHz, CD$_2$Cl$_2$) δ 8.55 (d, 8H, , *J* = 2.3 Hz, aromatic *H*1), 7.78 (s, 4H, aromatic *H*2), 7.64 (d, 4H, *J* = 8.7 Hz, aromatic *H*3), 7.52 (t, 12H, , *J* = 8.4 Hz, aromatic *H*4), 7.43 (dd, 12H, *J*1 = 3.2 Hz, *J*2 = 10.6 Hz, aromatic *H*5), 7.21 − 7.15 (n.r., 16H), 7.08 (d, 12H, *J* = 6.9 Hz, aromatic *H*6), 6.98 (d, 8H, *J* = 8.5 Hz, aromatic *H*7), 6.87 (d, 8H, *J* = 8.5 Hz, aromatic *H*8), 1.14 (s, 168H; T*i*PS).

^{13}C NMR (125 MHz, CD$_2$Cl$_2$) δ 149.0, 148.7, 146.9, 146.4, 145.1, 145.0, 144.4, 144.3, 144.1, 143.4, 143.0, 141.8, 141.7, 137.7, 136.8, 136.7, 136.5, 136.3, 135.9, 135.7, 135.6, 135.3, 135.1, 134.7, 134.6, 134.4, 134.0, 133.9, 133.8, 133.8, 133.6, 133.5, 133.4, 133.2, 133.2, 132.3, 132.1, 132.0, 131.9, 131.5, 129.2, 126.4, 126.2, 111.9, 111.8, 96.6, 96.5, 23.3, 16.2.

MALDI-TOF (Ag$^+$): Calcd. for C$_{233}$H$_{252}$Si$_8$: 3273.8, found: 3384.1 ([M+Ag]$^+$).

1st Generation ethynyl polytriphenylene dendrimer (2-20):
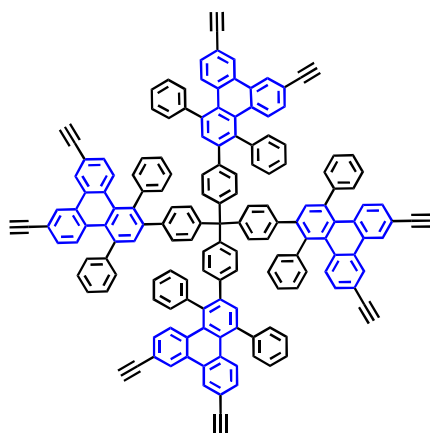
To a solution of **2-19** (0.063 g, 0.019 mmol) in THF (3 mL) was added dropwise a solution of TBAF (0.065 g, 0.250 mmol) in THF (2 mL). The reaction was stirred at RT for 1 h and precipitate in MeOH. The product was dissolved again in THF and repeatedly precipitated in MeOH three times, affording 0.034 g (0.016 mmol) pure product as light yellow powder in 90% yield.

^{1}H NMR (250 MHz, $C_2D_2Cl_4$) δ 8.57 (s, 8H, aromatic *H*1), 7.80 (s, 4H, aromatic *H*2), 7.64 (d, 4H, *J* = 8.7 Hz, aromatic *H*3), 7.57 – 7.44 (n.r., 24H), 7.26 – 7.09 (n.r., 28H), 6.96 (d, 8H, *J* = 8.3 Hz, aromatic *H*9), 6.87 (d, 8H, *J* = 8.3 Hz, aromatic *H*10), 3.22 (d, 8H, *J* = 8.8 Hz, C≡C*H*).

^{13}C NMR (75 MHz, $C_2D_2Cl_4$) δ 144.3, 143.4, 141.3, 140.8, 138.7, 138.2, 137.0, 132.4, 131.7, 131.3, 131.1, 130.5, 130.4, 130.1, 129.9, 129.5, 129.4, 129.2, 128.9, 128.7, 128.5, 128.4, 128.3, 127.5, 127.1, 127.0, 126.8, 119.9, 119.6, 83.7, 83.6, 29.6.

MALDI-TOF (Ag$^+$): Calcd. for $C_{161}H_{92}$: 2024.7, found: 2028.4.

2nd Generation polytriphenylene dendrimer (TPG2):
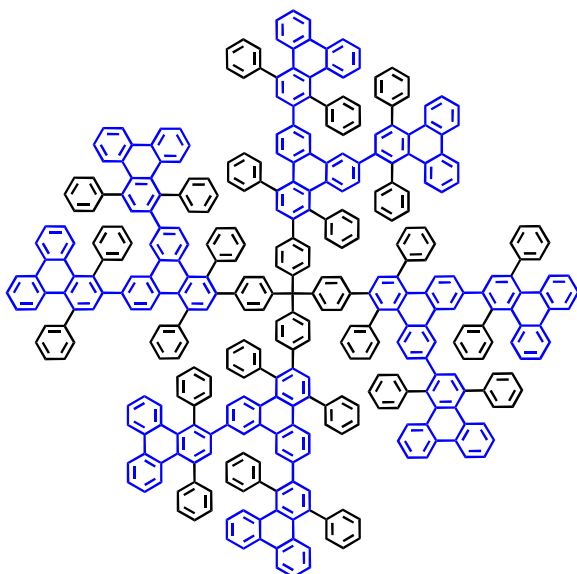
Dendrimer **2-20** (0.040 g, 0.020 mmol) and end-capping unit **2-18** (0.122 g, 0.320 mmol) were dissolved in *o*-xylene (2 mL) in a microwave tube under Argon and stirred at 170 °C for 8 h. After cooling to RT, the reaction mixture was precipitated in MeOH, then further purified by a column chromatography (PE:DCM = 1:1), affording 0.090 g (0.019 mmol) pure product as light yellow powder in 94% yield.

^{1}H NMR (700 MHz, CD$_2$Cl$_2$) δ 8.40 (d, 16H, , *J* = 7.8 Hz, aromatic *H*1), 8.06 (s, 8H, aromatic *H*2), 7.73 (s, 4H, aromatic *H*3), 7.67 (ss, 16H, aromatic *H*4), 7.52 − 7.31 (n.r., 84H), 7.16 (d, 16H, *J* = 7.2 Hz, aromatic *H*5), 7.10 − 6.94 (n.r., 76H), 6.87 (d, 8H, *J* = 8.2 Hz, aromatic *H*6), 6.61 (d, 4H, *J* = 8.5 Hz, aromatic *H*7), 6.55 (d, 4H, *J* = 8.7 Hz, aromatic *H*8).

^{13}C NMR (125 MHz, CD$_2$Cl$_2$) δ 145.0, 144.8, 144.7, 142.5, 142.4, 142.4, 140.6, 140.3, 140.1, 140.0, 139.9, 138.6, 137.4, 137.0, 132.8, 132.5, 132.4, 132.2, 132.0, 131.9, 131.7, 131.5, 131.2, 131.1, 130.8, 130.5, 130.4, 130.2, 130.0, 129.5, 129.4, 129.3, 129.2, 129.1, 128.8, 128.7, 128.7, 127.7, 127.6, 127.5, 127.4, 127.3, 127.0, 126.9, 126.7, 125.9, 125.5, 124.8, 123.5.

MALDI-TOF (Ag$^+$): Calcd. for C$_{385}$H$_{236}$: 4857.9, found: 4966.8 ([M+Ag]$^+$).

2nd Generation TiPS protected ethynyl polytriphenylene dendrimer (2-21):
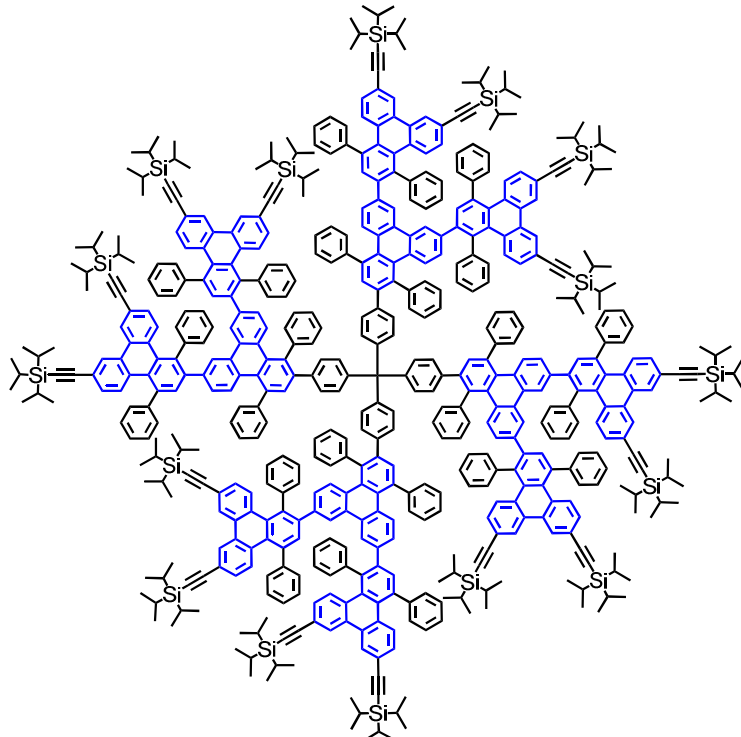
Dendrimer **2-20** (0.034 g, 0.017 mmol) and building unit **2-9** (0.280 g, 0.377 mmol,) were dissolved in *o*-xylene (2 mL) in a microwave tube under Argon and stirred at 170 °C for 8 h. After cooling to RT, the reaction mixture was precipitated in MeOH, then further purified by a column chromatography (PE:DCM = 3:1), affording 0.113 g (0.015 mmol) pure product as light yellow powder in 88% yield.

^{1}H NMR (700 MHz, CD_2Cl_2) δ 8.51 (s, 16H, aromatic *H*1), 8.05 (s, 8H, aromatic *H*2), 7.71 (t, 16H, *J* = 8.1 Hz, aromatic *H*3), 7.59 (dd, 12H, *J*1 = 4.1 Hz, *J*2 = 8.6 Hz, aromatic *H*4), 7.52 – 7.31 (n.r., 72H), 7.16 – 6.98 (n.r., 80H), 6.86 (d, 8H, *J* = 8.2 Hz, aromatic *H*5), 6.60 (d, 4H, *J* = 8.7 Hz, aromatic *H*6), 6.54 (d, 4H, *J* = 8.7 Hz, aromatic *H*7), 1.15 (s, 336H; T*i*PS).

^{13}C NMR (62.5 MHz, CD_2Cl_2) δ 149.0, 148.7, 146.8, 146.4, 145.1, 145.0, 144.8, 144.7, 142.5, 142.4, 142.4, 140.6, 140.3, 140.1, 140.0, 139.9, 138.6, 137.4, 137.0, 132.8, 132.5, 132.4, 132.2, 132.0, 131.9, 131.7, 131.5, 131.2, 131.1, 130.8, 130.5, 130.4, 130.2, 130.0, 129.5, 129.4, 129.3, 129.2, 129.1, 128.8, 128.7, 128.7, 127.7, 127.6, 127.5, 127.4, 127.3, 127.0, 126.9, 126.7, 125.9, 125.5, 124.8, 123.5, 111.9, 111.8, 96.6, 96.5, 23.2, 16.4;

MALDI-TOF (Ag$^+$): Calcd. for $C_{561}H_{556}Si_{16}$: 7740.0, found: 7850.3 ([M+Ag]$^+$).

2nd Generation ethynyl polytriphenylene dendrimer (2-22):
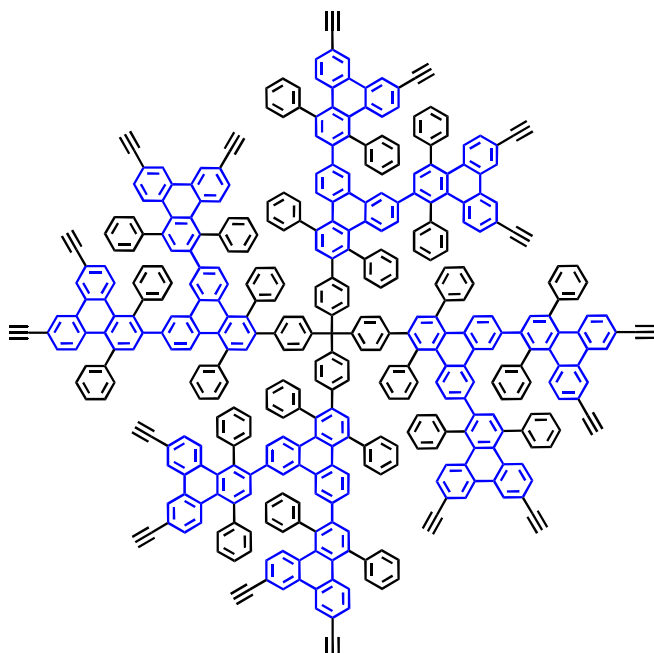
To a solution of **2-21** (0.110 g, 0.014 mmol) in THF (3 mL) was added dropwise a solution of TBAF (0.150 g, 0.575 mmol) in THF (2 mL). The reaction was stirred at RT overnight and poured into 50 mL DCM and 50 mL H_2O. The organic phase was concentrated and purified by a column chromatography (PE:DCM=2:3), affording light yellow powder. Yield: 0.070 g, 0.013 mmol, 94%.

^{1}H NMR (250 MHz, CD_2Cl_2) δ 8.53 (s, 16H, aromatic H1), 8.06 (s, 8H, aromatic H2), 7.70 (d, 12H, J = 4.1 Hz, aromatic H3), 7.59 (d, 8H, J = 8.6 Hz, aromatic H4), 7.52 − 7.29 (n.r., 76H), 7.16 − 6.96 (n.r., 84H), 6.84 (d, 8H, J = 8.0 Hz, aromatic H5), 6.55 (dd, 8H, J1 = 8.8 Hz, J2 = 16.8 Hz, aromatic H6), 3.22 (d, 16H, J = 4.7 Hz, C≡CH).

^{13}C NMR (62.5 MHz, CD_2Cl_2) δ 148.2, 146.8, 146.3, 145.0, 144.3, 143.4, 143.0, 141.3, 140.9, 138.7, 137.8, 137.0, 136.7, 136.5, 135.9, 135.7, 135.6, 135.3, 135.1, 134.7, 134.6, 134.4, 134.0, 133.9, 133.8, 132.7, 132.6, 131.5, 131.4, 131.2, 130.2, 130.0.3, 132.1, 132.0, 131.9, 131.5, 129.9, 129.5, 129.4, 129.2, 128.9, 128.7, 128.5, 128.4, 128.3, 127.5, 127.1, 127.0, 126.8, 119.9, 119.6, 84.1, 83.8, 31.8.

3rd Generation polytriphenylene dendrimer (TPG3):
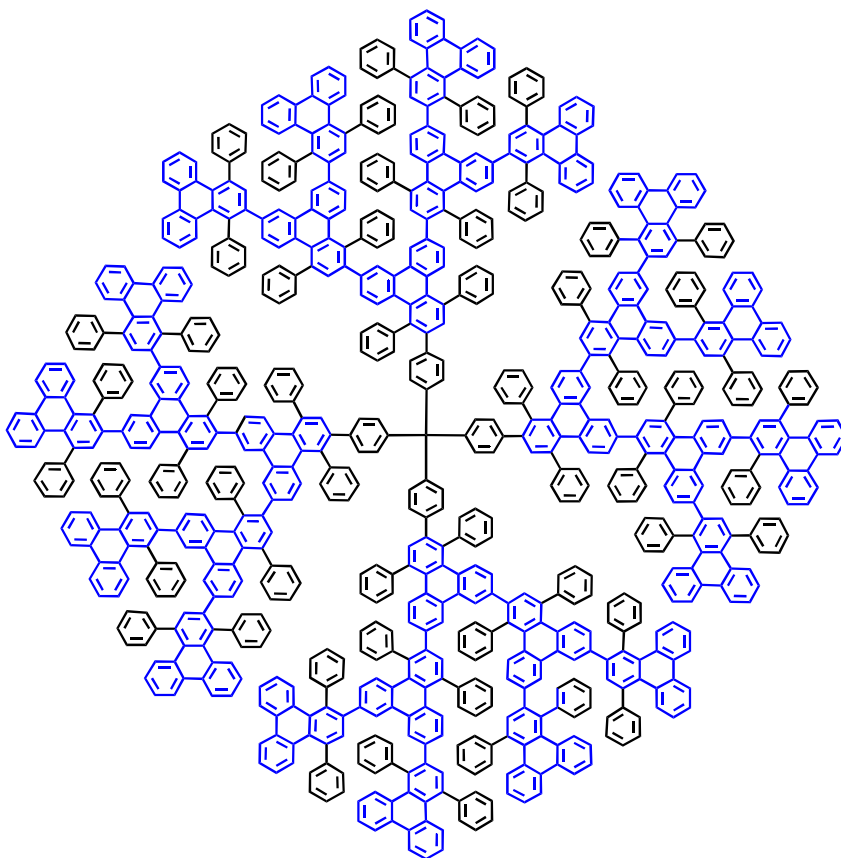
Dendrimer **2-22** (0.053 g, 0.010 mmol) and end-capping unit **2-7** (0.250 g, 0.654 mmol,) were dissolved in *o*-xylene (3 mL) in a microwave tube under Argon and stirred at 170 °C for 8 h. After cooling to RT, the reaction mixture was precipitated in MeOH, then further purified by a GPC column using DCM as the eluent, affording light yellow powder. Yield: 0.098 g, 0.019 mmol, 90%.

^{1}H NMR (700 MHz, CD$_2$Cl$_2$) δ 8.41 – 8.34 (n.r., 32H), 8.02 (ss, 24H, aromatic *H*1), 7.74 (s, 4H, aromatic *H*2), 7.69 – 7.65 (n.r., 36H), 7.52 – 6.88 (n.r., 404H), 6.67 – 6.58 (n.r., 16H), 6.49 (dd, 8H, *J*1 = 8.7 Hz, *J*2 = 17.0 Hz, aromatic *H*3);

^{13}C NMR (75 MHz, CD$_2$Cl$_2$) δ 144.7, 144.6, 142.4, 142.3, 142.1, 140.5, 140.2, 140.0, 139.9, 138.5, 137.0, 136.9, 132.9, 132.8, 132.3, 132.1, 131.9, 131.8, 131.6, 131.5, 131.4, 131.2, 131.1, 131.04, 130.8, 130.8, 130.7, 130.6, 130.6, 130.5, 130.4, 130.3, 130.1, 129.9, 129.6, 129.4, 129.2, 129.1, 129.0, 128.9, 128.7, 128.6, 128.5, 128.3, 128.3, 128.2, 128.1, 128.0,

127.9, 127.9, 127.9, 127.8, 127.5, 127.4, 127.4, 127.3, 127.2, 127.1, 126.9, 126.9, 126.8, 126.7, 126.7, 126.6, 126.5, 126.5, 125.8, 125.6, 125.5, 124.7, 124.6, 123.6, 123.5;

MALDI-TOF (Ag$^+$): Calcd. for C$_{865}$H$_{524}$: 10908.1, found: 11009.8 ([M+Ag]$^+$).

1st Generation polytriphenylene dendrimer based on pyrene core (PYG1):
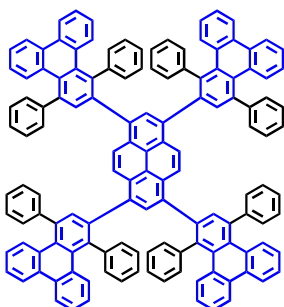
1,3,6,8-Tetraethynylpyrene **2-24 (**0.060 g, 0.201 mmol) and phencyclone **2-18** (0.460 g, 1.204 mmol) were dissolved in *o*-xylene (2 mL) in a microwave tube under Argon and stirred at 170 °C for 4 h. After cooling to RT, the reaction mixture was precipitated in MeOH, then washed with DCM till green color disappeared, affording 0.310 g (0.181 mmol) pure product as yellow powder in 91% yield.

^{1}H NMR (300 MHz, CD$_2$Cl$_2$) δ 8.89 (t, 2H, *J* = 8.3 Hz), 8.82 (d, 2H, *J* = 8.5 Hz), 8.44 (d, 4H, *J* = 8.0 Hz), 7.85 - 6.61 (m, 70H), 6.49 (m, 2H), 6.31 (m, 2H).

^{13}C NMR (75 MHz, CD$_2$Cl$_2$) δ 138.55, 131.79, 131.74, 131.50, 131.30, 130.08, 129.32, 129.17, 128.88, 128.69, 128.54, 128.47, 128.29, 128.25, 128.13, 127.81, 127.47, 127.33, 127.29, 127.20, 127.10, 127.04, 126.92, 126.84, 126.69, 126.38, 126.05, 125.87, 125.74, 125.35, 125.06, 124.19, 124.02, 123.67.

MALDI-TOF: Calcd. for C$_{136}$H$_{82}$: 1714.6, found: 1715.4.

1st Generation TiPS protected ethynyl polytriphenylene dendrimer based on pyrene core (2-27):
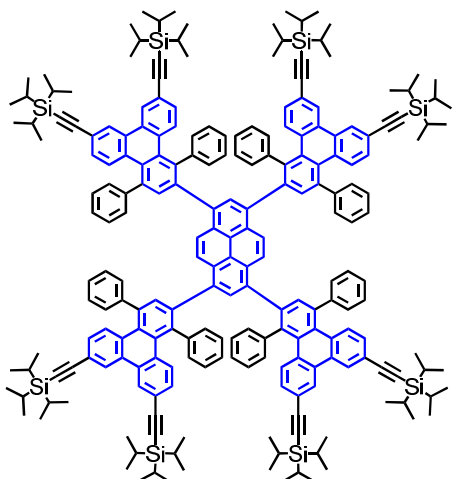
1,3,6,8-Tetraethynylpyrene **2-24 (**0.060 g, 0.201 mmol) and building unit **2-9** (0.715 g, 0.963 mmol) were dissolved in *o*-xylene (2 mL) in a microwave tube under Argon and stirred at 170 °C for 2 h. After cooling to RT, the reaction mixture was precipitated in MeOH, and then further purified by a GPC column chromatography using toluene as eluent, affording 0.577 g (0.182 mmol) pure product as light yellow powder in 91% yield.

^{1}H NMR (300 MHz, CD_2Cl_2) δ 8.51 (s, 8H), 7.77 − 6.50 (m, 66H), 1.14 (s, 24H), 1.12 (s, 144H).

^{13}C NMR (75 MHz, CD_2Cl_2) δ 174.13, 148.70, 144.21, 138.51, 131.20, 130.81, 130.63, 130.26, 129.99, 129.45, 129.08, 127.00, 124.08, 122.06, 121.79, 119.12, 107.47, 105.69, 92.11, 80.50, 30.06, 18.81, 11.74.

MALDI-TOF: Calcd. for $C_{224}H_{242}Si_8$: 3155.7, found: 3157.0.

1st Generation ethynyl polytriphenylene dendrimer based on pyrene core (2-28):
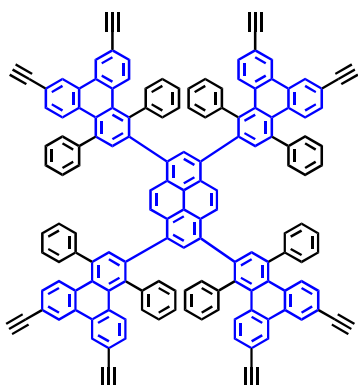
To a solution of **2-27 (**0.473 g, 0.150 mmol) in THF (5 mL) was added dropwise a solution of TBAF (0.468 g, 1.8 mmol) in THF (5 mL). The reaction was stirred at RT for 1 h and precipitate in MeOH. The product was dissolved again in THF and repeatedly precipitated in MeOH three times, affording 0.252 g (0.132 mmol) pure product as light yellow powder in 88% yield.

^{1}H NMR (300 MHz, CD$_2$Cl$_2$) δ 8.55 (s, 8H), 7.82 – 6.48 (m, 66H), 3.20 (s, 8H).

^{13}C NMR (75 MHz, CD$_2$Cl$_2$) δ 148.07, 133.73, 131.74, 131.50, 131.30, 130.08, 129.47, 129.27, 128.73, 128.59, 128.51, 128.44, 128.25, 128.21, 128.18, 127.69, 127.35, 127.31, 127.19, 127.11, 127.04, 126.92, 126.84, 126.33, 126.05, 125.87, 102.99, 86.46, 84.31, 30.05.

MALDI-TOF: Calcd. for C$_{152}$H$_{82}$: 1906.6, found: 1907.4.

2nd Generation polytriphenylene dendrimer based on pyrene core (PYG2)
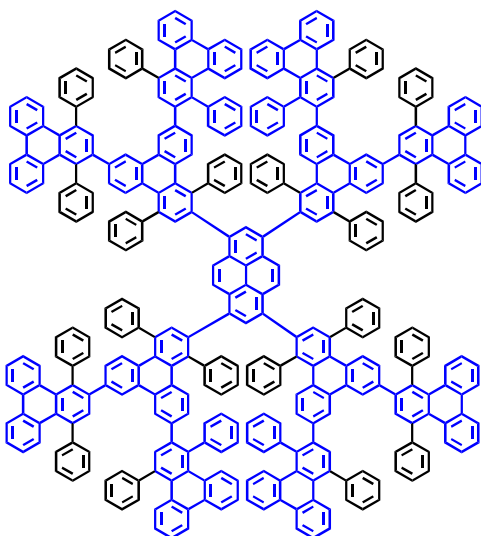
Dendrimer **2-28 (**0.095 g, 0.050 mmol) and end-capping unit **2-7** (0.230 g, 0.6 mmol) were dissolved in *o*-xylene (2 mL) in a microwave tube under Argon and stirred at 170 °C for 8 h. After cooling to RT, the reaction mixture was precipitated in MeOH, then further purified by a GPC column chromatography using toluene as eluent, affording 0.200 g (0.042 mmol) pure product as light yellow powder in 84% yield.

^{1}H NMR (300 MHz, CD$_2$Cl$_2$) δ 8.43 (s, 8H), 8.40 (t, 8H, *J* = 4.2 Hz), 7.74- 6.81 (m, 194H), 6.59 (m, 8H).

^{13}C NMR (75 MHz, CD$_2$Cl$_2$) δ 144.81, 142.42, 140.28, 140.06, 139.93, 139.40, 138.62, 138.35, 136.98, 132.88, 132.47, 132.21, 131.99, 131.71, 131.45, 131.09, 130.48, 129.99, 129.44, 128.81, 128.66, 127.60, 127.27, 127.01, 126.75, 125.87, 125.55, 124.75, 123.54.

MALDI-TOF: Calcd. for C$_{376}$H$_{226}$: 4739.8, found: 4744.0.

6.4 Syntheses of the Green Phosphorescent dendrimers (Chapter 3)

fac-**Tris[2-(3-iodophenyl)pyridyl]Ir(III) (3-5):**
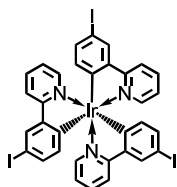
5.08g (20 mmol) iodine and 3.22 g (10 mmol) iodobenzene diacetate were added to a solution of 1.32 g (2 mmol) Ir(ppy)$_3$ in 500 mL dichloromethane. The mixture was stirred at room temperature under argon for 36 h. The solvent was concentrated to 50 mL and mixed with 500 mL ethanol. The yellow precipitate was collected by filtration and washed with water and ethanol. After it was dried, 2.05 g product was recrystallized in hexane as yellow crystal in a quantitively yield.

^{1}H NMR (250 MHz, DMSO-d6) δ 8.22 (d, *J* = 8.4 Hz, 3H), 8.06 (d, *J* = 2.0 Hz, 3H), 7.83 (m, 3H), 7.45 (d, *J* = 5.4 Hz, 3H), 7.40 (m, 3H), 7.02 (dd, *J* = 2.0, 8.0 Hz, 3H), 6.41 (d, *J* = 8.0 Hz, 3H).
FDMS (*m/z*): Calcd. for C$_{33}$H$_{21}$I$_3$IrN$_3$: 1032.5, found: 1032.7.
Elemental analysis: Calcd. C 38.39%, H 2.05%, N 4.07%, found: C 38.24%, H 2.31%, N 4.26%.

fac-**Tris[2-(3-((trimethylsilyl)ethynyl)phenyl)pyridyl]Ir(III) (3-6):**
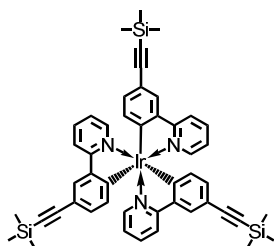
A mixture of 2.00 g (1.93 mmol) complex **3-5** and 4.50 g (11.60 mmol) (tributylstannyl)trimethylsilane were dissolved in 150 mL anhydrate THF in the presence

of 120 mg (0.17 mmol) Pd(PPh$_3$)$_2$Cl$_2$ and refluxed for 24 h at 85 °C. After cooling to room temperature, the reaction mixture was extracted with toluene followed by washing with aqueous solution of potassium fluoride to remove extra stannane. The organic phase was dried over MgSO$_4$, and then purified by column chromatography using toluene as the eluent, affording 1.09 g pure compound as a yellow powder in 60% yield.

^{1}H NMR (250 MHz, CD$_2$Cl$_2$) δ 7.94 (d, J = 8.2 Hz, 3H), 7.76 (d, J = 1.6 Hz, 3H), 7.73 − 7.64 (m, 3H), 7.52 (d, J = 4.7 Hz, 3H), 6.97 (t, J = 5.9 Hz, 3H), 6.83 (dd, J = 1.7, 7.8 Hz, 3H), 6.70 (d, J = 7.8 Hz, 3H), 0.22 (s, 27H).

MALDI-TOF (m/z): Calcd. for C$_{48}$H$_{48}$IrN$_3$Si$_3$: 943.4, found: 943.3.

fac-Tris[2-(3-ethynyl)phenyl)pyridyl]Ir(III) (3-4):
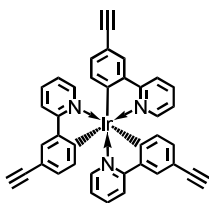
To a solution of 1.00 g (1.06 mmol) complex **3-6** in THF (25 mL) was added dropwise a solution of TBAF (1.25 g, 4.77 mmol) in THF (15 mL). The reaction was stirred at 0 °C for 1 h and precipitate in 100 mL MeOH. The solid was dissolved in DCM and purified by column chromatography using DCM as eluent, affording 700 mg pure product as yellow powder in 90% yield.

^{1}H NMR (250 MHz, CD$_2$Cl$_2$) δ 7.93 (d, J = 8.2 Hz, 3H), 7.74 (d, J = 1.6 Hz, 3H), 7.72 − 7.63 (m, 3H), 7.52 (d, J = 4.8 Hz, 3H), 6.96 (t, J = 5.8 Hz, 3H), 6.82 (dd, J = 1.8, 7.8 Hz, 3H), 6.70 (d, J = 7.6 Hz, 3H), 3.00 (d, J = 11.0 Hz, 3H);

FDMS (m/z): Calcd. for C$_{39}$H$_{24}$IrN$_3$: 727.2, found: 727.0.

1st Generation Ir(ppy)₃ cored polyphenylene dendrimer (GIrG1):
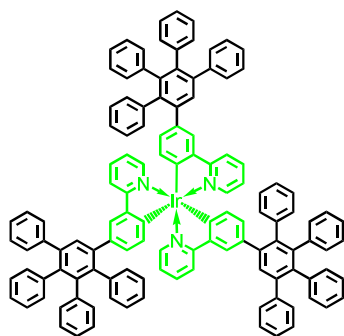
100 mg (0.137 mmol) Ir(ppy)$_3$ core **3-4** and 237 mg (0.617 mmol) tetraphenylcyclopentadienone **3-7** were dissolved in *o*-xylene (5 mL) in a microwave tube. The argon bubbled mixture was stirred at 170 °C in microwave reactor for 4 h. After cooling to RT, the reaction mixture was precipitated in MeOH, further purified by a GPC column using toluene as the eluent, affording 225 mg pure product as yellow powder in 92% yield.

^{1}H NMR (500 MHz, CD$_2$Cl$_2$) δ 7.59 (s, 3H), 7.56 (s, 3H), 7.55 (d, *J* = 1.5 Hz, 3H), 7.48 (d, *J* = 5.4 Hz, 3H), 7.34 (d, *J* = 1.8 Hz, 3H), 7.18 – 7.11 (m, 15H), 6.95 – 6.85 (m, 48H), 6.67 (dd, *J* = 1.8, 7.8 Hz, 3H), 6.36 (d, *J* = 7.8 Hz, 3H);

^{13}C NMR (125 MHz, CD$_2$Cl$_2$) δ 166.74, 159.24, 147.40, 143.74, 142.41, 142.37, 141.95, 141.22, 141.02, 140.90, 140.83, 139.72, 138.87, 136.48, 136.20, 133.44, 132.12, 132.01, 131.93, 131.59, 131.36, 130.39, 127.87, 127.19, 127.02, 126.92, 126.88, 126.48, 126.35, 125.84, 125.60, 122.38, 119.13;

MALDI-TOF (*m/z*): Calcd. for C$_{123}$H$_{84}$IrN$_3$: 1795.6, found: 1795.4.

1st Generation TiPS protected ethynyl Ir(ppy)₃ cored polyphenylene dendrimer (3-9)
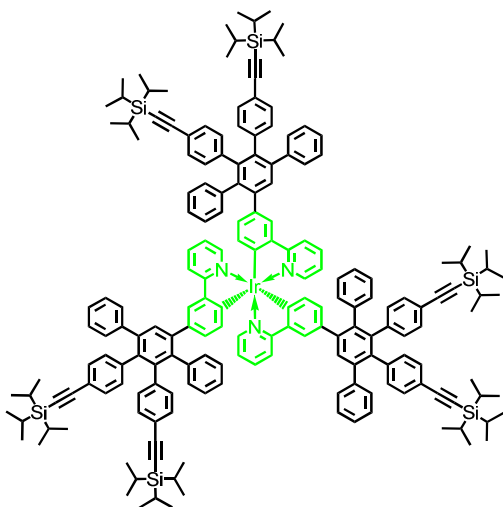
200mg Ir(ppy)$_3$ core **3-4** (0.274 mmol) and 918 mg building unit **3-8** (1.223 mmol) were dissolved in *o*-xylene (2 mL) in a microwave tube under Argon and stirred at 170 °C for 2 h. After cooling to RT, the reaction mixture was precipitated in MeOH, and then further purified by a GPC column chromatography using toluene as eluent, affording 678 mg (0.235 mmol) pure product as yellow powder in 86% yield.

^{1}H NMR (500 MHz, C$_2$D$_2$Cl$_4$) δ 7.64 (s, 3H), 7.61 (d, *J* = 8.1, 3H), 7.54 (t, *J* = 7.7 Hz, 3H), 7.46 (d, *J* = 4.9 Hz, 3H), 7.37 (s, 3H), 7.21 (dd, *J* = 6.3, 18.1 Hz, 18H), 7.12 (d, *J* = 8.1 Hz, 6H), 7.07 (d, *J* = 8.1 Hz, 6H), 6.91 (s, 15H), 6.88 – 6.78 (m, 15H), 6.64 (d, *J* = 7.3, 3H), 6.49 (s, 3H), 1.19, (s, 18H), 1.18 (s, 108H);

^{13}C NMR (125 MHz, C$_2$D$_2$Cl$_4$) δ 166.88, 158.96, 146.66, 143.01, 142.25, 141.78, 140.90, 140.53, 140.48, 140.09, 139.25, 137.45, 136.12, 135.29, 132.47, 131.51, 131.30, 131.16, 130.85, 130.42, 130.17, 129.83, 127.36, 126.87, 126.56, 126.00, 125.54, 125.28, 121.11, 120.65, 120.42, 118.43, 107.82, 107.73, 89.98, 89.80, 18.44, 11.66, 11.44;

MALDI-TOF (*m/z*): Calcd. for C$_{189}$H$_{207}$IrN$_3$Si$_6$: 2881.5, found: 2880.8.

1st Generation ethynyl Ir(ppy)₃ cored polyphenylene dendrimer (3-10)
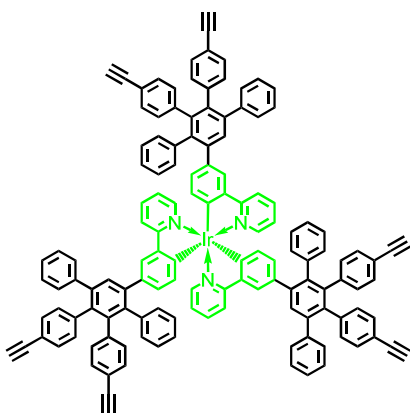
To a solution of 600 mg (0.208 mmol) dendrimer **3-9** in THF (25 mL) was added dropwise a solution of 489 mg TBAF (1.872 mmol) in THF (15 mL). The mixture was stirred at 0 °C for 1 h, then most solvent was distilled and the residue was precipitated in 100 mL MeOH. The solid was dissolved in DCM solution and purified by column chromatography using DCM as eluent, affording 350 mg (0.181 mmol) pure product as yellow powder in 87% yield.

^{1}H NMR (500 MHz, C$_2$D$_2$Cl$_4$) δ 7.61 (s, 3H), 7.57 (s, 3H), 7.55 (s, 3H), 7.47 (d, J = 7.9 Hz, 3H), 7.32 (s, 3H), 7.16 (s, 18H), 7.13 (d, J = 8.1 Hz, 6H), 7.08 (d, J = 8.2 Hz, 6H), 6.94 – 6.83 (m, 30H), 6.64 (d, J = 7.5 Hz, 3H), 6.34 (d, J = 7.5 Hz, 3H), 3.01 (d, J = 11.8 Hz, 6H);

^{13}C NMR (125 MHz, C$_2$D$_2$Cl$_4$) δ 166.83, 159.04, 146.67, 143.05, 142.31, 141.60, 141.48, 141.05, 140.51, 140.33, 139.98, 139.21, 137.24, 136.13, 135.32, 132.34, 131.47, 131.41, 131.11, 130.85, 130.62, 130.36, 129.79, 127.39, 126.59, 126.08, 125.56, 125.35, 121.14, 119.13, 118.87, 118.43, 76.66, 76.49;

MALDI-TOF (*m/z*): Calcd. for C$_{135}$H$_{87}$IrN$_3$: 1940.3, found: 1940.5

2nd Generation Ir(ppy)₃ cored polyphenylene dendrimer (GIrG2):
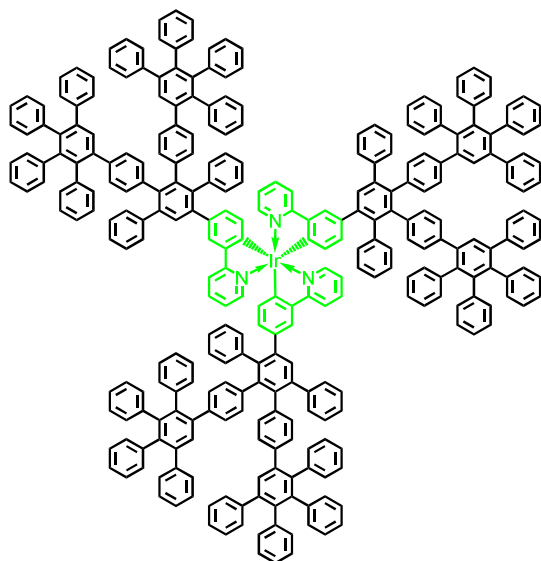
100 mg (0.051 mmol) dendrimer **3-10** and 141 mg (0.367 mmol) end-capping unit **3-7** were dissolved in *o*-xylene (5 mL) in a microwave tube. The argon bubbled mixture was stirred at 170 °C in microwave reactor for 6 h. After cooling to RT, the reaction mixture was precipitated in MeOH, further purified by a GPC column using toluene as the eluent, affording 174 mg (0.043 mmol) pure product as yellow powder in 84% yield.

^{1}H NMR (500 MHz, CD_2Cl_2) δ 7.55 (s, 3H), 7.54 (s, 6H), 7.47 (d, *J* = 5.5 Hz, 3H), 7.43 (s, 3H), 7.39 (s, 3H), 7.29 (s, 3H), 7.17 – 7.15 (m, 39H), 7.09 – 7.06 (m, 6H), 6.96 - 6.70 (m, 114H), 6.68 (d, *J* = 8.0 Hz, 6H), 6.60 (dd, *J* = 1.0, 7.7 Hz, 3H), 6.56 (d, *J* = 6.2 Hz, 6H), 6.52 (d, *J* = 6.1 Hz, 6H), 6.34 (d, *J* = 7.9 Hz, 3H);

^{13}C NMR (125 MHz, CD_2Cl_2) δ 142.29, 142.07, 141.07, 140.84, 140.65, 140.45, 139.53, 139.46, 131.92, 131.49, 130.31, 127.88, 127.20, 127.14, 126.85, 126.56, 125.92, 125.62; MALDI-TOF (*m/z*): Calcd. for $C_{303}H_{204}IrN_3$: 4079.1, found: 4079.2.

2nd Generation TiPS protected ethynyl Ir(ppy)₃ cored polyphenylene dendrimer (3-11)
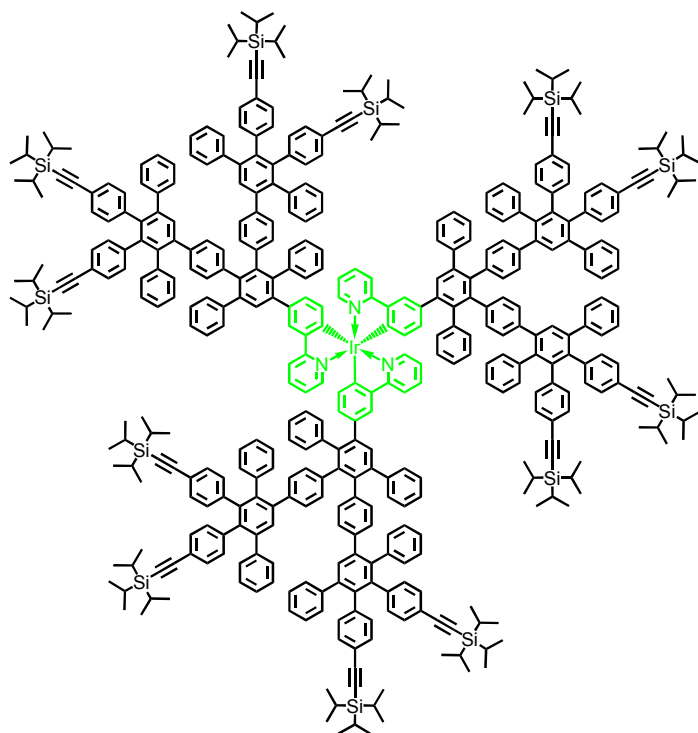
150 mg dendrimer **3-10** (0.077 mmol) and 413 mg building unit **3-8** (0.554 mmol) were dissolved in *o*-xylene (5 mL) in a microwave tube under Argon and stirred at 170 °C for 6 h. After cooling to RT, the reaction mixture was precipitated in MeOH, and then further purified by a GPC column chromatography using toluene as eluent, affording 423 mg (0.235 mmol) pure product as yellow powder in 88% yield.

^{1}H NMR (500 MHz, C$_2$D$_2$Cl$_4$) δ 7.56 (s, 3H), 7.53 (s, 3H), 7.48 (s, 3H), 7.43 (d, *J* = 3.3 Hz, 9H), 7.33 (s, 6H), 7.18 (d, *J* = 13.6 Hz, 42H), 7.10 (d, *J* = 7.7 Hz, 15H), 7.05 (d, *J* = 7.2 Hz, 15H), 6.94 (s, 21H), 6.89 − 6.68 (m, 63H), 6.64 (d, *J* = 7.4 Hz, 9H), 6.59 (s, 6H), 1.17 (s, 252H);

^{13}C NMR (125 MHz, C$_2$D$_2$Cl$_4$) δ 141.52, 140.82, 140.55, 140.08, 139.57, 139.03, 138.21, 131.33, 131.15, 130.97, 130.44, 130.16, 129.70, 128.31, 128.13, 127.43, 126.73, 126.16, 125.49, 120.81, 120.53, 107.59, 89.97, 18.43, 11.42;

MALDI-TOF (*m/z*): Calcd. for C$_{435}$H$_{447}$IrN$_3$Si$_{12}$: 6243.4, found: 6243.1.

**2nd Generation ethynyl Ir(ppy)₃ cored polyphenylene dendrimer (3-12)**
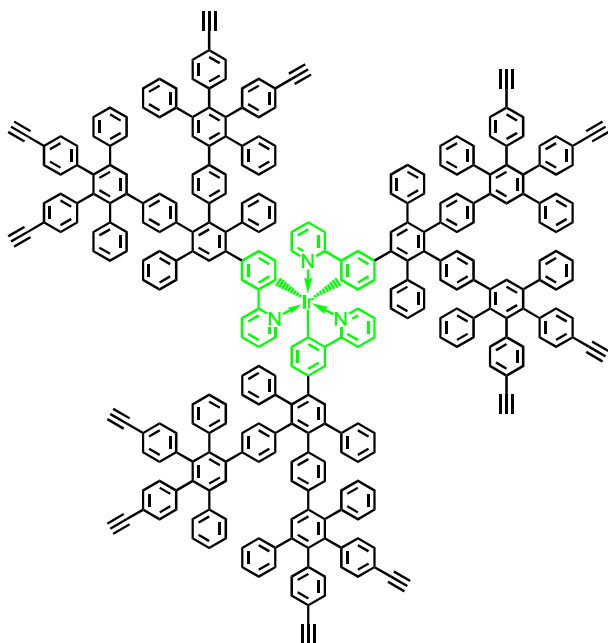
To a solution of 400 mg (0.064 mmol) dendrimer **3-11** in THF (25 mL) was added dropwise a solution of 300 mg TBAF (1.152 mmol) in THF (15 mL). The mixture was stirred at 0 °C for 1 h, then most solvent was distilled and the residue was precipitated in 100 mL MeOH. The solid was dissolved in DCM solution and purified by a short column chromatography using DCM as eluent, affording 245 mg (0.056 mmol) pure product as yellow powder in 87% yield.

^{1}H NMR (500 MHz, C$_2$D$_2$Cl$_4$) δ δ 7.58 (s, 6H), 7.53 (d, J = 7.6 Hz, 3H), 7.49 (s, 3H), 7.44 (s, 6H), 7.33 (s, 6H), 7.19 – 7.11 (m, 60H), 7.09 – 7.02 (m, 15H), 6.94 (d, J = 2.0 Hz, 21H), 6.89 – 6.69 (m, 63H), 6.65 (d, J = 7.7 Hz, 6H), 6.61 (d, J = 7.4 Hz, 6H), 3.01 (d, J = 10.3 Hz, 12H);

^{13}C NMR (125 MHz, C$_2$D$_2$Cl$_4$) δ 141.35, 141.13, 140.91, 140.61, 140.40, 139.42, 139.09, 138.05, 131.26, 130.98, 130.64, 130.36, 129.93, 129.67, 128.30, 128.02, 127.45, 127.16, 126.76, 126.37, 126.23, 125.61, 119.30, 119.00, 84.17, 76.61;

MALDI-TOF (m/z): Calcd. for C$_{327}$H$_{207}$IrN$_3$: 4367.4, found 4367.4.

3rd Generation Ir(ppy)₃ cored polyphenylene dendrimer (GIrG3):
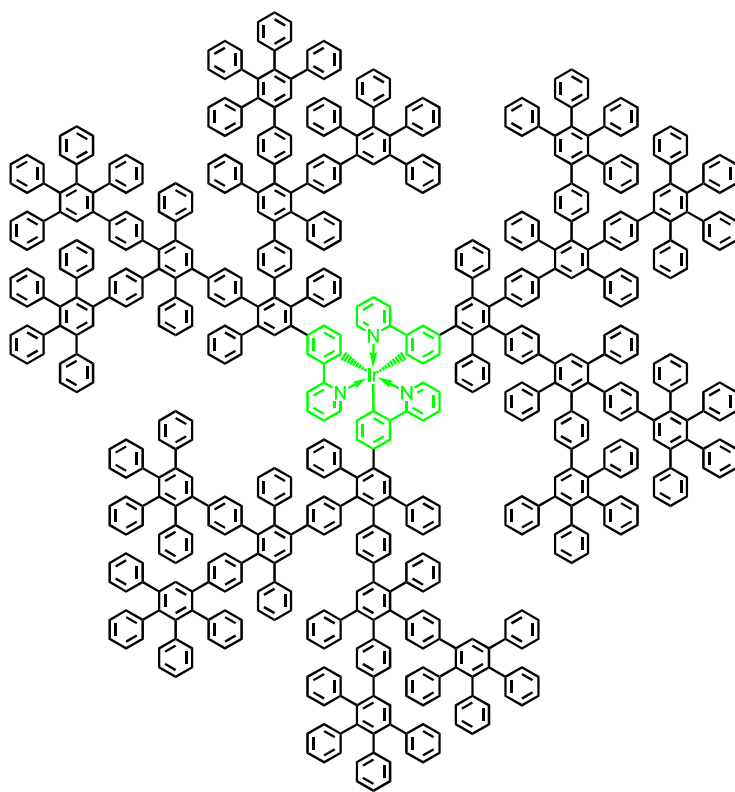
100 mg (0.023 mmol) dendrimer **3-12** and 160 mg (0.414 mmol) end-capping unit **3-7** were dissolved in *o*-xylene (5 mL) in a microwave tube. The argon bubbled mixture was stirred at 170 °C in microwave reactor for 12 h. After cooling to RT, the reaction mixture was precipitated in MeOH, further purified by a GPC column using toluene as the eluent, affording 165 mg (0.019 mmol) pure product as yellow powder in 83% yield.

^{1}H NMR (500 MHz, CD$_2$Cl$_2$) δ 7.53 (s, 9H), 7.47 (d, 3H, *J* = 4.6 Hz), 7.41 (d, *J* = 2.2 Hz, 6H), 7.37 (s, 9H), 7.33 (s, 3H), 7.27 (s, 6H), 7.21 – 6.99 (m, 108H), 6.97 – 6.57 (m, 264H), 6,56 – 6.41 (m, 33H), 6.33 (d, *J* = 7.5 Hz, 3H);

^{13}C NMR (125 MHz, CD$_2$Cl$_2$) δ 142.27, 142.08, 141.08, 141.01, 140.62, 140.42, 139.55, 139.44, 131.90, 131.41, 130.30, 128.93, 128.65, 127.89, 127.15, 126.86, 126.58, 125.93, 125.62;

MALDI-TOF (*m/z*): Calcd. for C$_{663}$H$_{444}$IrN$_3$: 8642.5, found: 8642.9.

3rd Generation TiPS protected ethynyl Ir(ppy)₃ cored polyphenylene dendrimer (3-13)
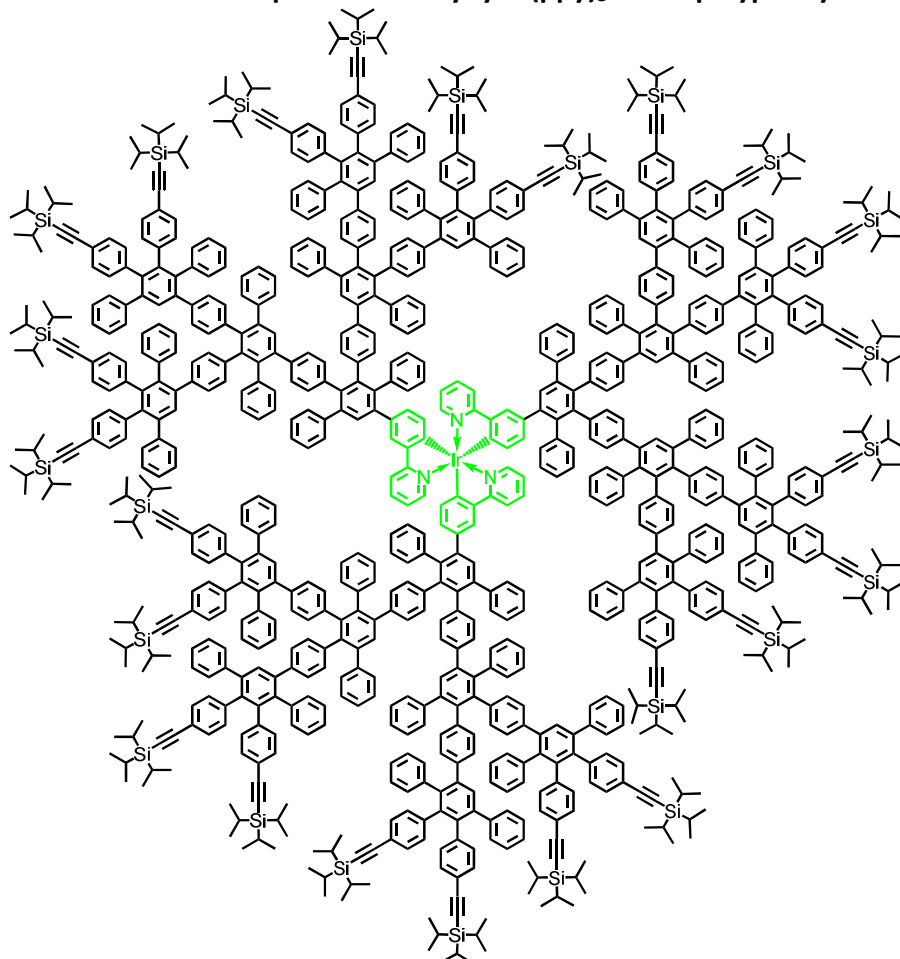
100 mg dendrimer **3-12** (0.023 mmol) and 308 mg building unit **3-8** (0.414 mmol) were dissolved in *o*-xylene (5 mL) in a microwave tube under Argon and stirred at 170 °C for 12 h. After cooling to RT, the reaction mixture was precipitated in MeOH, and then further purified by a GPC column chromatography using toluene as eluent, affording 255 mg (0.020 mmol) pure product as yellow powder in 86% yield.

^{1}H NMR (500 MHz, C₂D₂Cl₄) δ 7.46 (s, 6H), 7.42 (s, 6H), 7.36 (s, 6H), 7.31 − 6.40 (m, 405H), 1.17 (s, 504H);

^{13}C NMR (125 MHz, C₂D₂Cl₄) δ 145.39, 141.49, 140.83, 140.51, 140.08, 139.54, 139.06, 138.39, 131.30, 131.15, 130.82, 130.44, 130.16, 129.68, 127.73, 127.44, 126.73, 126.17, 125.40, 125.26, 120.82, 120.55, 107.66, 90.01, 18.43, 11.42.

MALDI-TOF (*m/z*): Calcd. for C₉₂₇H₉₂₇IrN₃Si₂₄: 12961.6, found: 12964.4.

3rd Generation ethynyl Ir(ppy)$_3$ cored polyphenylene dendrimer (3-14)
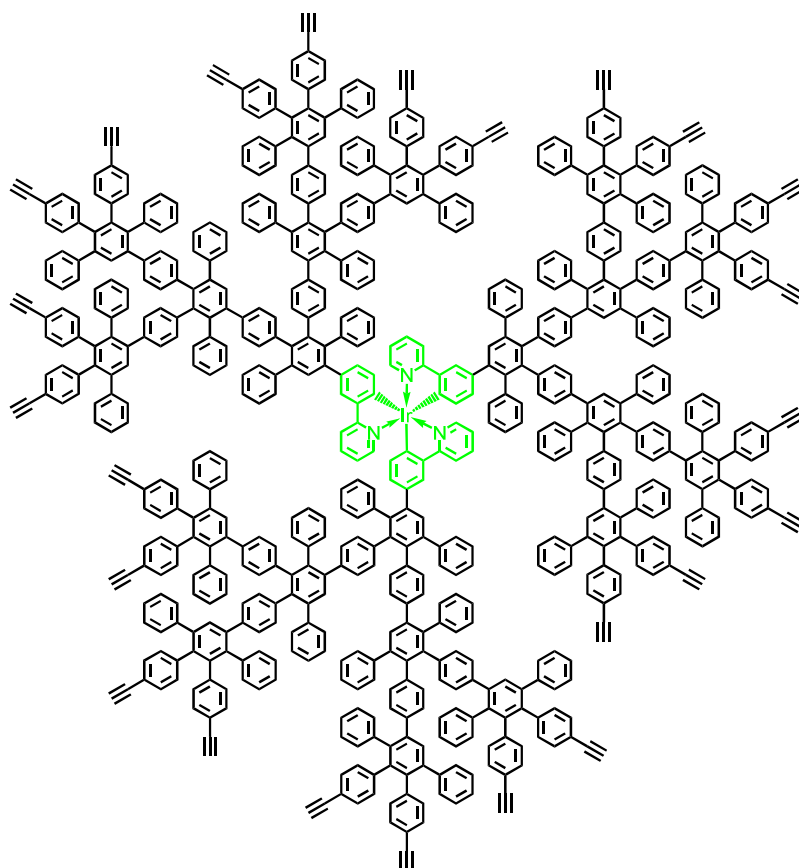
To a solution of 200 mg (0.015 mmol) dendrimer **3-13** in THF (25 mL) was added dropwise a solution of 145 mg TBAF (0.555 mmol) in THF (15 mL). The mixture was stirred at 0 °C for 1 h, then most solvent was distilled and the residue was precipitated in 100 mL MeOH. The solid was dissolved in DCM solution and purified by a short column chromatography using DCM as eluent, affording 123 mg (0.013 mmol) pure product as yellow powder in 89% yield.

^{1}H NMR (500 MHz, C$_2$D$_2$Cl$_4$) δ 7.48 (s, 6H), 7.43 (s, 6H), 7.38 (s, 6H), 7.31 − 6.40 (m, 405H), 3.00 (d, J = 10.3 Hz, 24H);

^{13}C NMR (125 MHz, C$_2$D$_2$Cl$_4$) δ 141.39, 141.17, 140.43, 140.11, 140.03, 139.47, 139.21, 138.99, 131.47, 131.25, 130.93, 130.64, 130.26, 130.01, 129.55, 127.53, 127.34, 126.62, 126.04, 125.31, 125.16, 120.73, 120.57, 107.66, 84.01, 76.23;

MALDI-TOF (*m/z*): Calcd. for C$_{711}$H$_{447}$IrN$_3$: 9214.4, found: 9214.7.

4th Generation Ir(ppy)₃ cored polyphenylene dendrimer (GIrG4):
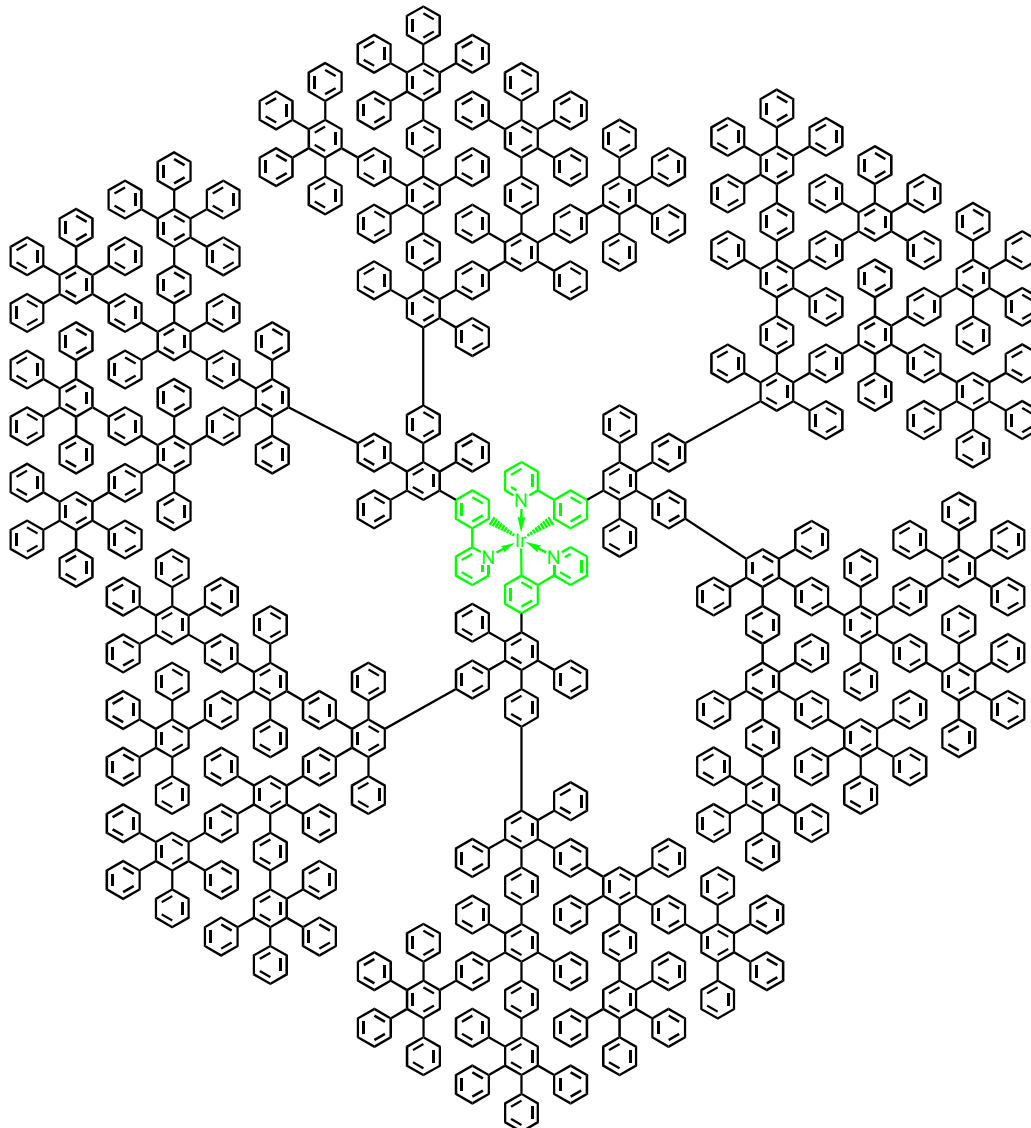
65 mg (0.007 mmol) dendrimer **3-14** and 100 mg (0.252 mmol) end-capping unit **3-7** were dissolved in *o*-xylene (4 mL) in a microwave tube. The argon bubbled mixture was stirred at 170 °C in microwave reactor for 24 h. After cooling to RT, the reaction mixture was precipitated in MeOH, further purified by a GPC column using toluene as the eluent, affording 100 mg (0.0057 mmol) pure product as yellow powder in 81% yield.

^{1}H NMR (500 MHz, CD$_2$Cl$_2$) δ 7.53 (s, 6H), 7.41 (s, 9H), 7.37 (s, 6H), 7.36 (s, 6H), 7.31 (s, 6H), 7.27 (s, 6H), 7.27 – 6.20 (m, 891H);

^{13}C NMR (125 MHz, CD$_2$Cl$_2$) δ 131.50, 129.90, 128.05, 127.49, 126.76, 125.67;

MALDI-TOF (*m/z*): Calcd. for C$_{663}$H$_{444}$IrN$_3$: 17776.4, found: 17787.0 (M+Ag^{+}).

6.5 Syntheses of red phosphorescent dendrimers (Chapter 4)

2-(2'-Benzo[*b*]thienyl)-5-bromopyridine (4-5):
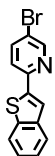
3.8 g (21.3 mmol) 2-Benzo[b]thiophenylboronic acid and 5.0 g (21.3 mmol) 2,5-dibromopyridine were dissolved in 50 mL 2-methoxyethanol and mixed with 25 mL (2M) aqueous sodium carbonate solution. 700 mg (0.61 mmol) Tetrakis(triphenylphosphane) palladium was added to the mixture under argon atmosphere. The mixture was stirred at 80 °C overnight. After cooling to room temperature, the reaction mixture was poured into water and extracted with ethyl acetate. The organic layer was washed with brine several times, and the solvent was then evaporated. The product thus obtained was purified by silica gel column chromatography (hexane/ ethyl acetate, 9:1), affording 7.26 g (25.2 mmol) pure product as white solid in 82 % yield.

^{1}H NMR (250 MHz, CD$_2$Cl$_2$): δ 8.70 (d, J = 2.3, 1H), 7.99 – 7.83 (m, 4H), 7.77 (dd, J = 7.8 Hz, 0.7 Hz, 1H), 7.49 – 7.35 (m, 2H);

^{13}C NMR (CD$_2$Cl$_2$, 75 MHz): δ 119.5, 120.8, 121.9, 122.8,124.4, 124.8, 125.5, 139.3, 140.5, 140.9, 143.7, 150.9, 151.3;

FD-MS (*m/z*): Calcd. for C$_{13}$H$_8$BrNS: 290.2, found: 290.9.

Elemental analysis: Calcd. C 53.81%, H 2.78%, N 4.83%, S 11.05%, found: C 53.15 %,H 2.46%,N 4.85%, S 10.66%.

Diiridium(III) di-μ-chlorotetrakis(2-(2'-benzo[*b*]thienyl)-5-bromopyridinato) (4-6):
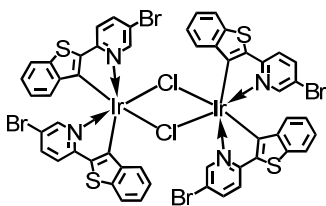
3.0 g (10.3 mmol) **4-5** and 1.5 g (5.0 mmol) iridium(III) trichloride were dissolved in a 2-ethoxyethanol (30 mL) and water (10 mL). The solution was heated to 111 ºC for 18 h. The suspension was filtered and the precipitate washed with ethanol (100 mL). The red-orange product (was insoluble in most organic solvents preventing chromatography and showing sparing solubility in DCM, sufficient for FD mass spectrometry. The product was directly used for the next reaction without further purification.

FD-MS (m/z): Calcd. for $C_{52}H_{28}Br_4Cl_2Ir_2N_4S_4$: 1611.7, found: 1611.6 [M]$^+$, 805 [M/2]$^+$.

fac-Tris[2-(2'-benzo[*b*]thienyl)-5-bromopyridyl]Ir(III) (4-7)
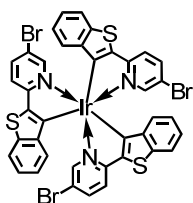
To a glycerol solution (20 mL) containing 3.0 g (10.3 mmol) **4-5** and *i*-chloride-Ir(III) dimer **4-6** was delivered potassium carbonate (7.0 g, 50 mmol). Prior to raising the temperature, the reaction mixture was thoroughly degassed via repetitive vacuum-freeze-thaw technique. Then, refluxing at 200 °C was performed for 24 h. After being cooled down to room temperature, the reaction mixture was poured into water. The red precipitate was further washed with water (100 mL), methanol (50 mL), and then ether (50 mL). A dark orange colored powder was obtained after silica gel column purification with DCM eluent. Finally, recrystallization in toluene gave the red phosphorescent product (2.0 g, 1.9 mmol) in a total yield of 38% from iridium trichloride.

^{1}H NMR (250 MHz, CD$_2$Cl$_2$): δ 8.25 (td, J = 6.6, 8.6 Hz, 1H), 7.86 (d, J = 3.7 Hz, 1H), 7.50 – 7.25 (m, 16H), 7.09 – 6.77 (m, 3H);

^{13}C NMR (75 MHz, CD$_2$Cl$_2$): δ 147.9, 144.4, 126.7, 126.0, 125.8, 125.4, 124.4, 124.3, 123.9, 123.3, 122.6, 120.0, 118.7.

FD-MS (m/z): Calcd. for $C_{39}H_{21}Br_3IrN_3S_3$: 1059.7, found: 1062.6.

Elemental analysis: Calcd. C 44.20%, H 2.00%, N 3.97%, S 9.08%, found: C: 44.35, H 1.98%, N 4.18%, S 8.80%.

fac-Tris[2-(2'-benzo[_b_]thienyl)-5-trimethylsilylethynylpyridyl]Ir(III) (4-8):
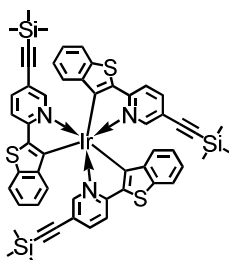
A mixture of 1.50 g (1.42 mmol) complex **4-7** and 3.43 g (8.52 mmol) (tributylstannyl)trimethylsilane were dissolved in 120 mL anhydrate THF in the presence of 125 mg (0.09 mmol) Pd(PPh₃)₂Cl₂ and refluxed for 24 h at 85 °C. After cooling to room temperature, the reaction mixture was extracted with toluene followed by washing with aqueous solution of potassium fluoride to remove extra stannane. The organic phase was dried over MgSO₄, and then purified by column chromatography using toluene as the eluent, affording 820 mg (0.74 mmol) pure compound as a red powder in 52% yield.

^{1}H NMR (250 MHz, CD₂Cl₂) δ 7.96 (s, 1H), 7.89 – 7.31 (m, 10H), 7.25 – 7.00 (m, 3H), 6.97 – 6.41 (m, 5H), 6.35 – 6.10 (m, 2H), 0.19 (s, 27H);

FD-MS (_m/z_): Calcd. for C₅₄H₄₈IrN₃S₃Si₃: 1111.2, found: 1111.0.

fac-Tris[2-(2'-benzo[_b_]thienyl)-5-ethynylpyridyl]Ir(III) (4-4):
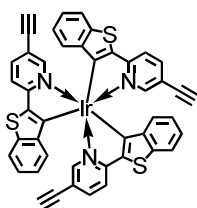
To a solution of 800 mg (0.72 mmol) complex **4-8** in THF (25 mL) was added dropwise a solution of TBAF (1.13 g, 4.32 mmol) in THF (15 mL). The reaction was stirred at 0 °C for 1 h and precipitate in 100 mL methanol. The solid was dissolved in DCM and purified by column chromatography using DCM as eluent, affording 565 mg (0.63 mmol) pure product as red powder in 88% yield.

^{1}H NMR (250 MHz, CD$_2$Cl$_2$) δ 7.99 (d, J = 4.1 Hz, 1H), 8.74 – 7.31 (m, 10H), 7.19 – 7.12 (m, 3H), 6.95 – 6.63 (m, 4H), 6.49 – 6.44 (m, 1H), 6.25 (d, J = 7.6 Hz, 2H), 3.15 (d, J = 2.4 Hz, 2H), 3.08 (d, J = 1.2 Hz, 1H)

FD-MS (*m/z*): Calcd. for C$_{45}$H$_{24}$IrN$_3$S$_3$: 895.1, found: 897.0.

3,4-Bis(4-triphenylamino)-2,5-diphenylcyclopentadienone (4-9):
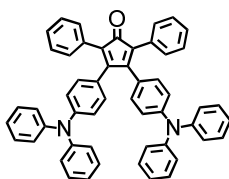
Dibromocyclopentadienone **4-10** (4.4 g, 8.0 mmol), diphenylamine (3.6 g, 16.0 mmol), [Pd$_2$(dba)$_3$] (150 mg), and tBuONa (2.3 g, 24.0 mmol) were added to a 100 mL Schlenk flask in a glove box. Toluene (60 mL) was poured into the flask to dissolve the mixture, and tri-tert-butylphosphane toluene solution (2.4 mL, 20 mg/mL, prepared from pure tri-tertbutylphosphane and distilled toluene in the glove box) was added by injection. The mixture was stirred at room temperature for 1 h under argon. Then the solution was filtered under suction, and the filtrate extracted with water (500 mL). The organic phase was dried under vacuum to give a dark crude product, and then purified by column chromography (DCM), afford 5.2 g (8.0 mmol) pure product as black solid in 99% yield.

^{1}H NMR (250 MHz, CD$_2$Cl$_2$): δ 7.18 (m, 18H), 7.00 (m, 12H), 6.74 (m, 8H);

^{13}C NMR (75 MHz, CD$_2$Cl$_2$): δ 200.5, 154.6, 148.4, 147.5, 131.9, 131.0, 130.5, 129.7, 128.2, 127.5, 126.7, 125.3, 124.9, 123.9, 121.5;

FD-MS (*m/z*): Calcd. for C$_{53}$H$_{38}$N$_2$O: 718.3, found: 718.2.

## 1st Generation Ir(btp)₃ cored polyphenylene dendrimer (RIrG1):
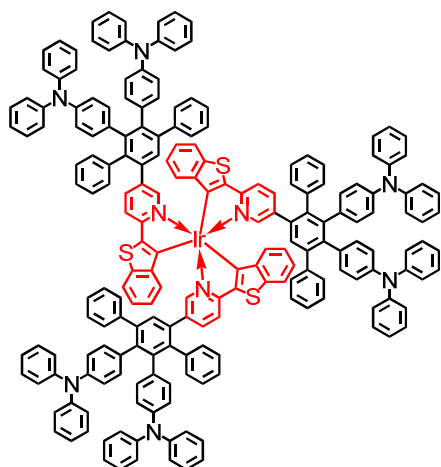
100 mg (0.112 mmol) Ir(btp)$_3$ core **4-4** and 362 mg (0.504 mmol) ditriphenylaminocyclopentadienone **4-9** were dissolved in *o*-xylene (5 mL) in a microwave tube. The argon bubbled mixture was stirred at 170 °C in microwave reactor for 4 h. After cooling to RT, the reaction mixture was precipitated in MeOH, further purified by a GPC column using toluene as the eluent, affording 268 mg (0.091 mmol) pure product as red powder in 81% yield.

^{1}H NMR (500 MHz, CD$_2$Cl$_2$) δ 7.42 – 7.35 (m, 3H), 7.28 – 7.04 (m, 45H), 7.00 – 6.81 (m, 48H), 6.79 – 6.54 (m, 33 H), 6.51 – 6.21 (m, 9H);

^{13}C NMR (125 MHz, CD$_2$Cl$_2$) δ 148.11, 148.06, 145.88, 145.58, 145.50, 144.63, 142.98, 142.76, 142.62, 141.76, 141.58, 141.41, 140.61, 139.53, 137.23, 135.72, 135.54, 134.97, 134.03, 132.74, 132.51, 131.42, 130.37, 130.30, 130.27, 129.49, 129.47, 129.41, 128.03, 127.98, 127.92, 127.81, 127.48, 126.89, 126.69, 125.33, 124.10, 124.05, 123.85, 123.49, 123.42, 122.77, 122.62, 108.80, 93.21;

MALDI-TOF (*m/z*): Calcd. for C$_{201}$H$_{138}$IrN$_9$S$_3$: 2967.7, found: 2968.3.

1st Generation TiPS protected ethynyl Ir(btp)$_3$ cored polyphenylene dendrimer (4-11)
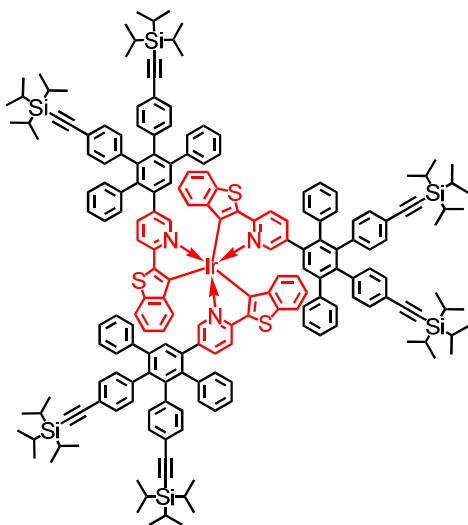
200 mg (0.224 mmol) Ir(btp)$_3$ core **4-4** and 750 mg (1.008 mmol) building unit **4-12** were dissolved in *o*-xylene (2 mL) in a microwave tube under Argon and stirred at 170 °C for 2 h. After cooling to RT, the reaction mixture was precipitated in MeOH, and then further purified by a GPC column chromatography using toluene as eluent, affording 572 mg (0.188 mmol) pure product as red powder in 84% yield.

^{1}H NMR (700 MHz, CD$_2$Cl$_2$) δ 8.04 - 6.25 (m, 78H), 1.09 - 1.07 (m, 126H);

^{13}C NMR (175 MHz, CD$_2$Cl$_2$) δ 148.69, 148.69, 141.70, 141.70, 141.47, 141.47, 141.22, 141.22, 140.62, 140.62, 140.43, 140.43, 140.22, 140.22, 139.53, 139.53, 139.22, 139.22, 138.67, 138.67, 137.99, 137.99, 136.56, 136.56, 135.76, 135.76, 131.97, 131.97, 131.66, 131.66, 131.57, 131.57, 131.51, 131.51, 131.38, 131.38, 131.11, 131.11, 130.91, 130.91, 130.79, 130.79, 130.17, 130.17, 130.13, 130.13, 130.07, 130.07, 128.25, 128.25, 128.17, 128.17, 128.07, 128.07, 127.61, 127.61, 127.11, 127.11, 126.98, 126.98, 121.41, 121.41, 121.32, 121.32, 121.07, 121.07, 107.18, 107.18, 91.10, 91.10, 91.05, 91.05, 18.77, 18.76, 18.45, 14.26, 11.85, 11.69, 11.68, 11.52, 11.42;

MALDI-TOF (*m/z*): Calcd. for C$_{195}$H$_{204}$IrN$_3$S$_3$Si$_6$: 3046.7, found: 3046.1.

1st Generation ethynyl Ir(btp)₃ cored polyphenylene dendrimer (4-13)
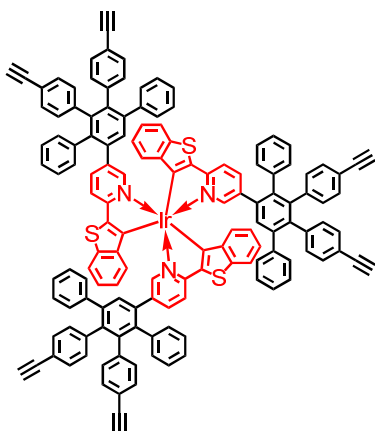
To a solution of 500 mg (0.164 mmol) dendrimer **4-11** in THF (25 mL) was added dropwise a solution of 385 mg TBAF (1.476 mmol) in THF (15 mL). The mixture was stirred at 0 °C for 1 h, then most solvent was distilled and the residue was precipitated in 100 mL MeOH. The solid was dissolved in DCM solution and purified by column chromatography using DCM as eluent, affording 290 mg (0.140 mmol) pure product as red powder in 85% yield.

^{1}H NMR (500 MHz, CD$_2$Cl$_2$) δ 8.06 (s, 1H), 7.82 (d, *J* = 8.0 Hz, 1H), 7.78 − 7.71 (m, 2H), 7.68 (s, 1H), 7.65 (d, *J* = 8.0 Hz, 1H), 7.58 (d, *J* = 8.0 Hz, 1H), 7.44 (s, 1H), 7.35 (s, 1H), 7.31 (s, 1H), 7.29 - 6.21 (m, 69H), 3.36 − 3.30 (m, 6H).

^{13}C NMR (125 MHz, CD$_2$Cl$_2$) δ 175.80, 172.31, 164.48, 163.02, 161.94, 161.06, 155.18, 154.11, 151.69, 150.36, 149.55, 148.69, 148.56, 148.22, 147.85, 144.67, 144.21, 143.05, 142.85, 142.71, 141.72, 141.64, 141.58, 141.52, 141.48, 141.22, 141.08, 141.04, 141.01, 140.92, 140.88, 140.74, 140.68, 140.62, 139.72, 139.58, 139.49, 139.38, 139.32, 139.29, 139.15, 139.11, 138.86, 138.74, 138.71, 138.41, 138.00, 137.18, 136.83, 136.60, 136.23, 135.80, 134.82, 134.50, 133.79, 133.68, 132.58, 132.38, 131.95, 131.84, 131.74, 131.65, 131.59, 131.42, 131.32, 131.11, 131.05, 130.96, 130.86, 130.74, 130.18, 130.08, 128.48, 128.26, 128.21, 128.17, 128.07, 127.94, 127.79, 127.63, 127.12, 127.03, 126.72, 126.55, 126.06, 125.49, 125.40, 125.24, 123.92, 123.88, 123.81, 123.71, 123.30, 123.00, 122.54, 122.30, 120.10, 120.02, 119.95, 119.91, 119.77, 119.65, 118.31, 118.09, 117.56, 117.46, 117.02, 116.80, 83.70, 77.58, 77.48, 77.35;

MALDI-TOF (*m/z*): Calcd. for C$_{141}$H$_{84}$IrN$_3$S$_3$: 2108.6, found: 2108.7.

2nd Generation Ir(btp)₃ cored polyphenylene dendrimer (RIrG2):
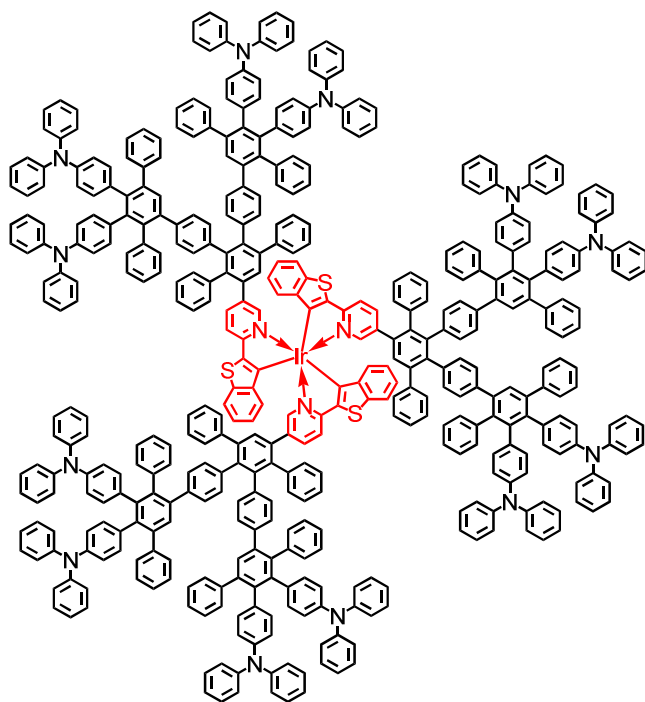
100 mg (0.047 mmol) dendrimer **4-13** and 316 mg (0.423 mmol) end-capping unit **4-9** were dissolved in *o*-xylene (5 mL) in a microwave tube. The argon bubbled mixture was stirred at 170 °C in microwave reactor for 6 h. After cooling to RT, the reaction mixture was precipitated in MeOH, further purified by a GPC column using toluene as the eluent, affording 230 mg (0.037 mmol) pure product as red powder in 78% yield.

^{1}H NMR (500 MHz, CD$_2$Cl$_2$) δ 7.57 – 6.17 (m, 312H, aromatic);

^{13}C NMR (125 MHz, CD$_2$Cl$_2$) δ 148.16, 145.76, 145.41, 142.16, 141.04, 140.48, 139.48, 136.22, 135.59, 132.93, 131.95, 131.24, 130.41, 129.47, 129.40, 128.96, 127.93, 127.24, 126.68, 125.91, 124.01, 123.78, 123.62, 122.71, 122.55;

MALDI-TOF (*m/z*): Calcd. for C$_{453}$H$_{312}$IrN$_{15}$S$_3$: 6253.8, found: 6254.7.

2nd Generation TiPS protected ethynyl Ir(btp)₃ cored polyphenylene dendrimer (4-14)
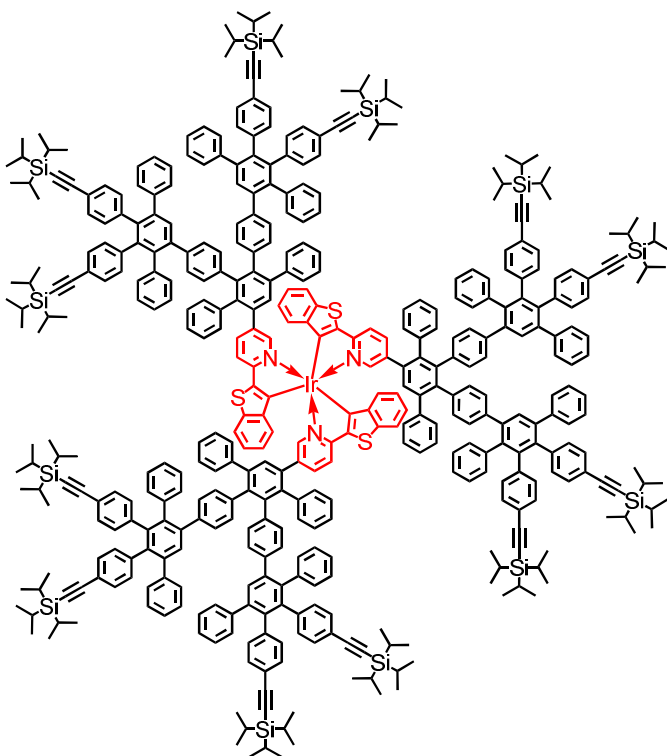
150 mg (0.071 mmol) dendrimer **4-13** and 477 mg (0.640 mmol) building unit **4-12** were dissolved in *o*-xylene (5 mL) in a microwave tube under Argon and stirred at 170 °C for 6 h. After cooling to RT, the reaction mixture was precipitated in MeOH, and then further purified by a GPC column chromatography using toluene as eluent, affording 360 mg (0.057 mmol) pure product as red powder in 80% yield.

^{1}H NMR (700 MHz, CD$_2$Cl$_2$) δ 8.01 - 6.21(m, 192H), 1.09 (s, 252H);

^{13}C NMR (175 MHz, CD$_2$Cl$_2$) δ 160.53, 141.87, 141.22, 141.13, 140.00, 139.64, 139.51, 138.69, 131.80, 131.34, 131.03, 130.77, 130.20, 128.09, 127.37, 126.84, 121.86, 121.20, 120.90, 113.35, 107.29, 90.96, 18.78, 18.42, 11.86, 11.70, 11.53;

MALDI-TOF (*m/z*): Calcd. for C$_{435}$H$_{447}$IrN$_3$Si$_{12}$: 6243.4, found: 6243.1.

2nd Generation ethynyl Ir(btp)₃ cored polyphenylene dendrimer (4-15)
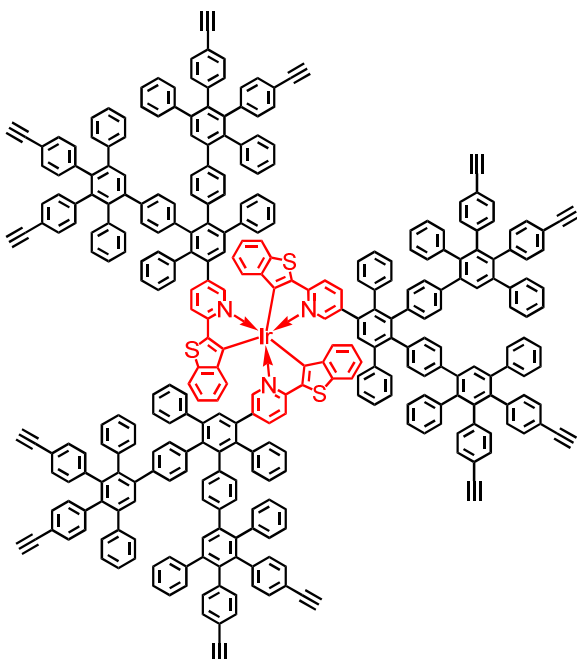
To a solution of 300 mg (0.047 mmol) dendrimer **4-14** in THF (25 mL) was added dropwise a solution of 220 mg (0.842 mmol) TBAF in THF (15 mL). The mixture was stirred at 0 °C for 1 h, then most solvent was distilled and the residue was precipitated in 100 mL MeOH. The solid was dissolved in DCM solution and purified by a short column chromatography using DCM as eluent, affording 160 mg (0.035 mmol) pure product as yellow powder in 75% yield.

^{1}H NMR (500 MHz, CD$_2$Cl$_2$) δ 7.87 – 6.15 (m, 192H, aromatic), 3.02 (d, J = 9.2, 12H);

^{13}C NMR (125 MHz, CD$_2$Cl$_2$) δ 148.16, 142.97, 141.69, 141.13, 139.87, 139.45, 139.13, 139.04, 138.63, 138.13, 137.99, 131.88, 131.16, 130.86, 130.21, 128.88, 128.09, 127.38, 126.89, 126.22, 125.31, 123.80, 119.79, 119.47, 83.79, 77.41;

MALDI-TOF (*m/z*): Calcd. for C$_{333}$H$_{204}$IrN$_3$S$_3$: 4535.6, found 4535.4.

3rd Generation Ir(btp)₃ cored polyphenylene dendrimer (RIrG3):
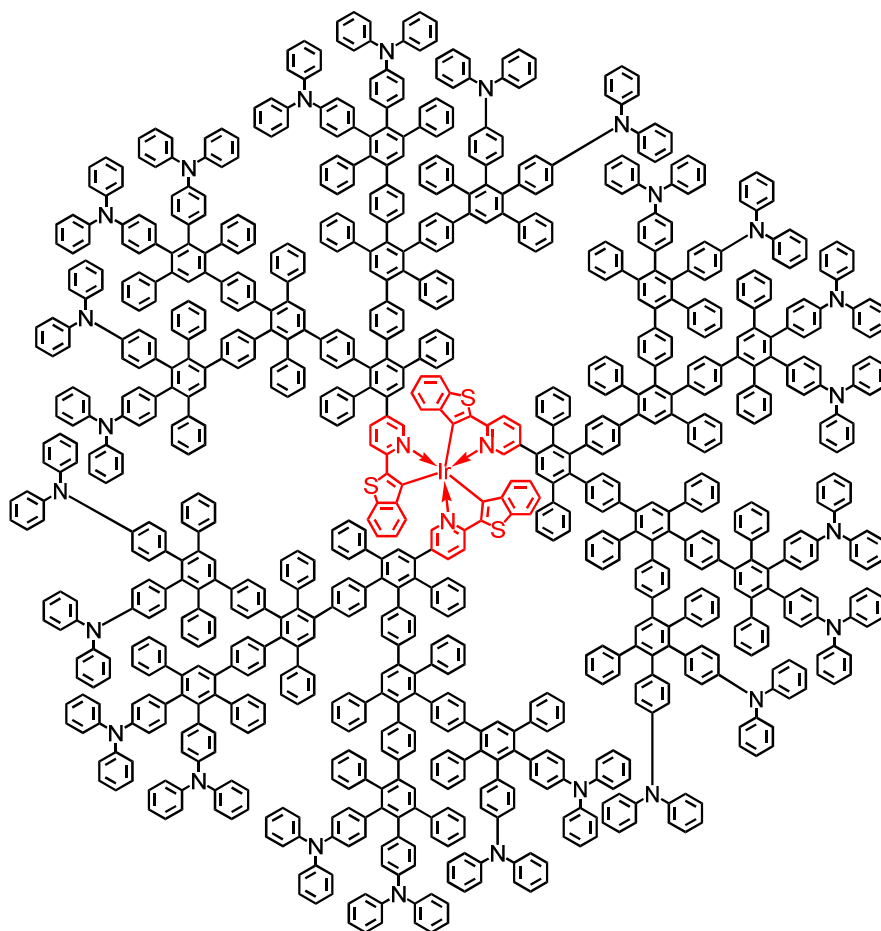
60 mg (0.013 mmol) dendrimer **4-15** and 175 mg (0.234 mmol) end-capping unit **4-9** were dissolved in *o*-xylene (3 mL) in a microwave tube. The argon bubbled mixture was stirred at 170 °C in microwave reactor for 12 h. After cooling to RT, the reaction mixture was precipitated in MeOH, further purified by a GPC column using toluene as the eluent, affording 116 mg (0.009 mmol) pure product as yellow powder in 70% yield.

^{1}H NMR (500 MHz, CD$_2$Cl$_2$) δ 8.18 - 6.17 (m, 660H, aromatic);

^{13}C NMR (125 MHz, CD$_2$Cl$_2$) δ 148.14, 145.75, 145.39, 142.18, 142.10, 141.61, 141.03, 140.50, 139.57, 139.41, 138.71, 136.26, 135.60, 132.94, 132.06, 131.30, 130.42, 129.47, 129.39, 129.00, 128.74, 127.92, 127.23, 126.67, 125.88, 124.00, 123.77, 123.62, 123.37, 122.71, 122.54;

MALDI-TOF (*m/z*): Calcd. for C$_{957}$H$_{660}$IrN$_3$S$_3$: 12816.1, found: 12812.1.
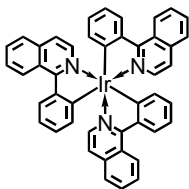
1-Phenylisoquinoline (4-17):
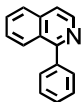
5.0 g (30.7 mmol) 1-chloroisoquinoline and 3.74 g (30.7 mmol) phenylboronic acid were dissolved in 50 mL 2-methoxyethanol and mixed with 25 mL (2M) aqueous sodium carbonate solution. 430 mg (0.37 mmol) Tetrakis(triphenylphosphane)palladium was added to the mixture under argon atmosphere. The mixture was stirred at 80 °C overnight. After cooling to room temperature, the reaction mixture was poured into water and extracted with ethyl acetate. The organic layer was washed with brine several times, and the solvent was then evaporated. The product thus obtained was purified by silica gel column chromatography (hexane/ ethyl acetate, 9:1), affording 5.66 g (27.6 mmol) pure product as white solid in 90 % yield.

^{1}H NMR (250 MHz, CD$_2$Cl$_2$): δ 8.61 (d, J = 5.6 Hz, 1 H), 8.10 (d, J = 8.4 Hz, 1 H), 7.87 (d, J = 8.4 Hz, 1 H), 7.63–7.72 (m, 4 H), 7.49–7.56 (m, 4 H);

^{13}C NMR (75 MHz, CD$_2$Cl$_2$) δ 160.9, 142.4, 139.8, 137.1, 130.2, 130.1, 128.8, 128.6, 127.8, 127.4, 127.2, 126.9, 120.1;

FD-MS (*m/z*): Calcd. for C$_{15}$H$_{11}$N: 205.1, found: 205.1.

Elemental analysis: Calcd. C 87.77%, H 5.40%, N 6.82%, found: C 88.01%, H 5.28%, N 6.54%,

fac-**Tris(1-phenylisoquinolinato)Ir(III) (Ir(piq)$_3$):**

2 g (4.0 mmol) iridium(III) acetylacetonate and 4.08 g (20.0 mmol) 1-chloroisoquinoline (**4-17**) as cyclometalating ligand were dissolved in 100 ml glycerol. The solution was refluxed under argon atmosphere overnight. After completion of the reaction, addition

of 1 M HCl resulted in precipitation of the product, which was filtered, washed with water, and dried at 100 °C in vacuum. The product was further purified by silica gel column chromatography with DCM as an eluent, affording 1.52 g (1.88 mmol) pure product as red solid in 47% yield.

^{1}H NMR (CD$_2$Cl$_2$, 250 MHz) δ 8.96 (m, 3H), 8.18 (d, 3H, J = 7.9 Hz), 7.71 (m, 3H), 7.62 (m, 6H), 7.33 (d, 3H, J = 6.1Hz), 7.09 (d, 3H, J = 6.1Hz), 6.94–6.99 (m, 6H), 6.84 (t, 3H, J = 7.4 Hz).

^{13}C NMR (CD$_2$Cl$_2$, 75 MHz) d (ppm): 168.8, 166.4, 147.4, 141.7, 138.8, 138.6, 132.2, 131.7, 130.9, 129.8, 129.2, 128.7, 128.2, 122.4, 121.2;

FD-MS (*m/z*): Calcd. for C$_{45}$H$_{30}$IrN$_3$: 805.0, found: 805.1.

fac-Tris[1-(3-bromophenyl)isoquinolinato]Ir(III) (4-18):
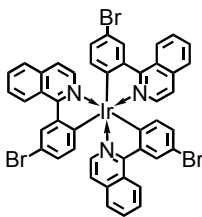

2.67g (15 mmol) N-Bromosuccinimide was added to a solution of 1.21 g (1.5 mmol) **Ir(piq)$_3$** in 400 mL dichloromethane. The mixture was stirred at room temperature under argon for 36 h. The solvent was concentrated to 50 mL and mixed with 500 mL ethanol. The yellow precipitate was collected by filtration and washed with water and ethanol. After it was dried, 1.55 g product was recrystallized in hexane as red crystal in a quantitively yield.

^{1}H NMR (250 MHz, DMSO-d6) δ 8.92 (m, 3H), 8.16 (d, J = 8.0 Hz, 3H), 7.83 (m, 3H), 7.65 (m, 6H), 7.40 (d, J = 5.4 Hz, 3H), 7.02 (d, J = 7.0 Hz, 3H), 6.96 (m, 3H), 6.81 (t, J = 8.0 Hz, 3H);

FDMS (*m/z*): Calcd. for C$_{45}$H$_{27}$Br$_3$IrN$_3$: 1038.9, found: 1039.7.

Elemental analysis: Calcd. C 51.89%, H 2.61%, N 4.03%, found: C 51.63%, H 2.72%, N3.97%

fac-Tris[1-(3-(trimethylsilylethynyl)phenyl)isoquinolinato]Ir(III) (4-19):
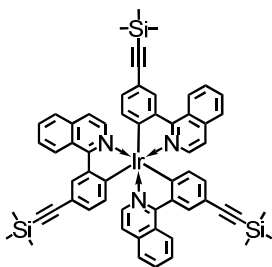
A mixture of 1.50 g (1.44 mmol) complex **4-18** and 3.47 g (8.64 mmol) (tributylstannyl)trimethylsilane were dissolved in 120 mL anhydrate THF in the presence of 125 mg (0.09 mmol) Pd(PPh$_3$)$_2$Cl$_2$ and refluxed for 24 h at 85 °C. After cooling to room temperature, the reaction mixture was extracted with toluene followed by washing with aqueous solution of potassium fluoride to remove extra stannane. The organic phase was dried over MgSO$_4$, and then purified by column chromatography using toluene as the eluent, affording 900 mg (0.82 mmol) pure compound as a red powder in 57% yield.

^{1}H NMR (250 MHz, CD$_2$Cl$_2$) δ 8.93 (m, 3H), 8.29 (d, J = 8.3 Hz, 3H), 7.77 (m, 3H), 7.72 (m, 6H), 7.31 (d, J = 6.2 Hz, 3H), 7.23 (d, J = 6.1Hz, 3H), 6.95 – 6.69 (m, 6H), 0.22 (s, 27H); FDMS (*m/z*): Calcd. for C$_{60}$H$_{54}$IrN$_3$Si$_3$: 1093.3, found: 1093.5.

fac-Tris[1-(3-ethynyl)phenyl)isoquinolinato]Ir(III) (4-20):
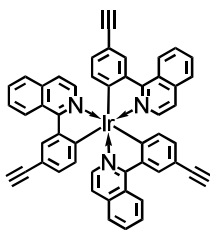
To a solution of 800 mg (0.73 mmol) complex **4-19** in THF (20 mL) was added dropwise a solution of TBAF (860 mg, 3.29 mmol) in THF (10 mL). The reaction was stirred at 0 °C for 1 h and precipitate in 100 mL methanol. The solid was dissolved in DCM and purified by column chromatography using DCM as eluent, affording 520 mg (0.59 mmol) pure product as red powder in 81% yield.

^{1}H NMR (250 MHz, CD$_2$Cl$_2$) δ 8.89 (m, 3H), 8.31 (d, J = 7.6 Hz, 3H), 7.74 (m, 3H), 7.69 (m, 6H), 7.25 (d, J = 6.4 Hz, 3H), 7.19 (d, J = 6.2Hz, 3H), 6.95 – 6.63 (m, 6H), 3.12 (d, J = 2.2 Hz, 3H);

FD-MS (*m/z*): Calcd. for C$_{51}$H$_{30}$IrN$_3$: 877.0, found: 877.2.

1st generation TiPS protected ethynyl Ir(piq)$_3$ cored polyphenylene dendrimer (4-16)
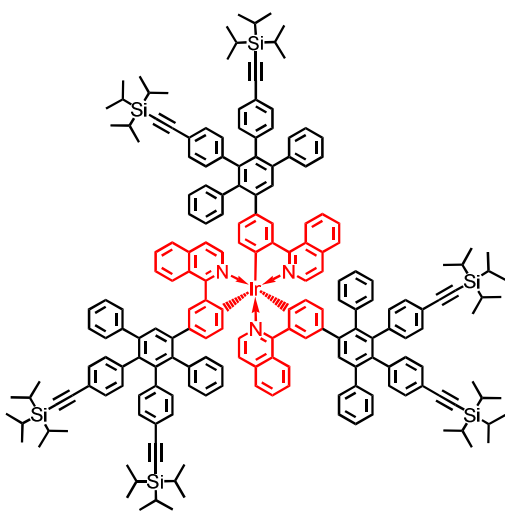
200 mg (0.228 mmol) Ir(btp)$_3$ core **4-20** and 765 mg (1.026 mmol) building unit **4-12** were dissolved in *o*-xylene (2 mL) in a microwave tube under Argon and stirred at 170 °C for 2 h. After cooling to RT, the reaction mixture was precipitated in MeOH, and then further purified by a GPC column chromatography using toluene as eluent, affording 572 mg (0.198 mmol) pure product as red powder in 87% yield.

^{1}H NMR (700 MHz, CD$_2$Cl$_2$) δ 8.29 - 8.09 (m, 3H), 7.83 - 6.62 (m, 81H), 1.09 - 1.07 (m, 126H);

^{13}C NMR (75 MHz, CD$_2$Cl$_2$) δ 145.44, 145.27, 141.55, 141.04, 137.06, 133.10, 132.21, 131.90, 131.03, 130.77, 130.31, 128.00, 127.42, 126.69, 121.08, 120.83, 107.37, 18.77, 11.70.

MALDI-TOF (*m/z*): Calcd. for C$_{201}$H$_{210}$IrN$_3$Si$_6$: 3028.6, found: 3029.3.

Publication

1. **Tianshi Qin**, Gang Zhou, Horst Scheiber, Roland E. Bauer, Martin Baumgarten, Christopher E. Anson, Emil J. W. List, Klaus Müllen. Polytriphenylene Dendrimers: A Unique Design for Blue-Light-Emitting Materials, *Angewandte Chemie International Edition*, 2008, *47*, 8292.

2. **Tianshi Qin**, Junqiao Ding, Lixiang Wang, Martin Baumgarten, Gang Zhou, Klaus Müllen. A Divergent Synthesis of Very Large Polyphenylene Dendrimers with Iridium(III) Cores: Molecular Size Effect on the Performance of Phosphorescent Organic Light-Emitting Diodes, *Journal of American Chemical Society*, 2009, *131*, 14329.

3. An J. J. Ver Heyen, Cédric C. Buron, **Tianshi Qin**, Roland Bauer, Alain M. Jonas, Klaus Müllen, Frans C. De Schryver, Steven De Feyter. Guiding the Self-Assembly of a Second-Generation Polyphenylene Dendrimer into Well-Defined Patterns, *Small*, 2008, *4*, 1160.

4. **Tianshi Qin**, Junqiao Ding, Lixiang Wang, Martin Baumgarten, Gang Zhou, Klaus Müllen. High-effiency Red Phosphorescent Organic Light-Emitting Diodes Based on Polyphenylene Dendrimers with Iridium(III) Cores, In preparation and to be submitted to *Advanced Functional Materials*.

5. Wolfgang Wiedemair, **Tianshi Qin**, Emil J. W. List, Klaus Müllen. High-effiency Blue Organic Light-Emitting Diodes Based on Polytriphenylene Dendrimers with Pyrene Cores In preparation and to be submitted to *Advanced Materials*.
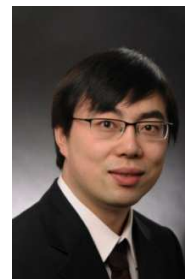
Patent

1. Klaus Müllen, **Tianshi Qin**, Roland Bauer, "*Blue Light Emitting Polytriphenylene Dendrimers, Methods of Preparation and Uses thereof*", *European Patent*, EP17906, 2008-05-09

Curriculum Vitae

Personal Details:

Name:	Tianshi Qin
Date of birth:	Mar. 18th, 1981
Nationalities:	Chinese
Hometown:	Nanjing, P. R. China

Education:

07/2007-Present Max-Planck-Institute for Polymer Research, Mainz, Germany

PhD Candidate, Major: Organic Synthesis and Material Science

Dissertation Topic: New design of polyphenylene dendrimers for full-color light-emitting diodes.

04/2004-06/2007 Martin Luther University, Halle, Germany

Master of Science, Major: Applied Polymer Science

Master thesis: Nitrilotriacetic acid functionalized polyphenylene dendrimers for DNA chelating.

09/1999-06/2003 Department of Chemistry, Nanjing University, Nanjing, China

Bachelor of Science, Major: Chemistry

Honors and fellowship:

First Prize People's Scholarship awarded by Nanjing University (2003)

Max-Planck Fellowship, MPI-P Mainz, (2006-2009)

Chinese Government Award for Outstanding Self-financed Students (2009-2010)